2017-08-22

Platelet Transcriptome Heterogeneity: A Role for RNA Uptake in Vascular Health and Disease

Lauren R. Clancy
University of Massachusetts Medical School

PLATELET TRANSCRIPTOME HETEROGENEITY:

A ROLE FOR RNA UPTAKE IN VASCULAR HEALTH AND DISEASE

A Dissertation Presented

By

LAUREN RUTH CLANCY

Submitted to the Faculty of the

University of Massachusetts Graduate School of Biomedical Sciences, Worcester

in partial fulfillment of the requirements for the degree of

DOCTOR OF PHILOSPHY

August 22, 2017

Translational Sciences

REVIEWER PAGE

PLATELET TRANSCRIPTOME HETEROGENEITY:

A ROLE FOR RNA UPTAKE IN VASCULAR HEALTH AND DISEASE

A Dissertation Presented

By

LAUREN RUTH CLANCY

This work was undertaken in the Graduate School of Biomedical Sciences

Translational Sciences Program

Under the mentorship of

Jane E. Freedman, MD, Thesis Advisor

Eric Mick ScD, Member of Committee

Anastasia Khvorova, PhD, Member of Committee

Evelyn Kurt-Jones, PhD, Member of Committee

Robert Flaumenhaft, MD, PhD, External Member of Committee

John Keaney, MD, Chair of Committee

Anthony Carruthers, Ph.D.,

Dean of the Graduate School of Biomedical Sciences

August 22, 2017

DEDICATION

I would like to dedicate this work to my friends and family.

I love you all more than words can say.

You are and will always be what I am most grateful for in my life.

In loving memory of my grandfather, Ferdinand “Freddie” Martino, 1927-2015

ACKNOWLEDGMENTS

There are many people I would like to thank, who have contributed to the success of this work and my growth throughout graduate school. First I would like to thank the Student Counseling Center at UMMS. The guidance and support I have gained from them has changed the type of person I am profoundly. The lessons I have learned through them have made me a better scientist and better person and I am sure without their services I would not have successfully finished my degree.

I would like to thank the members of all my advisory committees, including Dr. Mary Munson, Dr. John Keaney, Dr. Anastasia Khvorova, Dr. Eric Mick, Dr. Evelyn Kurt-Jones and Dr. Robert Flaumenhaft. I would especially like to thank Drs. Keaney, Khvorova and Mick for serving on all three of my advisory committees and acting as constant guides throughout this entire process.

I would like to thank all the members of my department, the Cardiovascular Medicine division. Though we would have been colleagues no matter what, I am happy to include many of them as friends and deeply appreciate their scientific interest, support and friendship. I have greatly enjoyed working alongside them and look forward to keeping in touch in the future.

I would like to thank all the members of the Freedman lab, past and present, who have given me a home over the last five years. I would specifically like to thank several members: Antonina Risitano, under whom I first began work on the platelet RNA project; Kahraman Tanriverdi, for first educating me in RNA

and for producing the microarray, high throughput gene expression and sequencing data presented here; Heather Corkrey, for being the best baymate a person could ask for - she has not only helped me scientifically but welcomed my loud, often crazy personality into her space for the last two years, and I am thankful for her constant support, upbeat personality and friendship; and Lea Beaulieu, who led the project presented in Chapter 2 and performed the initial platelet subpopulation sorting in Chapter 3 - she first convinced me to rotate in the lab, taught me that “platelets are powerful” and became not only a friend but a true mentor. Finally, Milka Koupenova-Zamor, who is my constant support, sounding board and extra pair of hands. She helped extensively with the *in vivo* experiments outlined in Chapter 3. When I didn’t think I was good enough, she always reminded me I was and then bought me a cookie or spinach “thingie” to cheer me up. Without many of my mornings starting with her and coffee, I would not have survived the last few years. She is and will always be a dear mentor and friend.

A lab is a type of family and ours has a wonderful leader in Jane Freedman. Since the beginning she accepted that I was not your typical “academia-oriented” graduate student. She listened to what I wanted out of my time here and allowed me the freedom to take my career in the direction I chose. She gave me opportunities to grow whenever possible and always listened when I needed her. She has always been a steady presence on this project, calming me when there were unexpected results or mistakes and kicking me in the butt

when I needed it. She has always made lab fun. Whether letting me lock our lab in puzzle rooms or hosting celebratory meals or just treating us to something special, Jane made sure our lab was a home. I want to thank her for being my biggest advocate, my constant source of support, my mentor and my friend.

I have the most wonderful friends and family. Despite the fact that many of them don't have science backgrounds, they have spent the last six years constantly interested in what I do and supporting me any way they can. I have never wanted for a shoulder to cry on or a good laugh and am deeply aware how lucky I am to have each and every one of them. I'd like to thank my brother specifically, for always supporting me any way he can, always knowing how to make me smile and always being willing to be silly and nerdy with me. I'd also like to especially thank Ryan Genga, who decided to go back to grad school at UMMS the same time I did. We have been together in this since day one and through it all he has constantly supported me, whether I needed last minute reagents, a pep talk or a beer. Without his constant support each day, I could not have done this, and without his friendship, I would not be the person I am. There is no better person I could have asked to have beside me.

Finally, I would like to thank my Mom and Dad. They have supported me my whole life and encouraged me to always be who I am and strive for whatever I want. They made sure that throughout this entire experience I never felt alone and have always reminded me to smile, even when I really didn't want to. I am truly grateful to have parents like them. They have always put my brother and me

first and without their constant support, love and direction, I would not be the scientist or person I am today.

To all those above and to anyone I missed who has someone helped me along this path, thank you, from the bottom of my heart.

ABSTRACT

As our understanding of the platelet's systemic role continues to expand beyond hemostasis and thrombosis, interrogation of the platelet's ability to affect diverse biological processes is required. Studies of the platelet's non-traditional roles have focused on developing our understanding of the platelet's relation to specific disease phenotypes as well as elucidation of platelet characteristics, content, and function. The generic content, traditional function and heterogeneity of platelets have long been accepted; more ambiguous and controversial has been how these factors are interrelated.

Investigation of platelet content revealed the presence of biologically functional RNA in anucleated platelets, the correlation of platelet RNA to distinct phenotypes, and the ability of platelets to transfer RNA to other vascular cells; however how these processes occur is unclear. To further interrogate platelet RNA processes, we utilized sorting and RNA sequencing to develop platelet subpopulation transcriptome profiles. We found that platelet heterogeneity extends to the platelet transcriptome: distinct RNA profiles exist dependent on platelet size. We hypothesized that this RNA heterogeneity is the result of RNA transfer between platelets and vascular cells. Using *in vitro* and *in vivo* modeling, we were able to show the novel ability of platelets to take up RNA from vascular cells, correlating to the unique functional profile associated with small platelet transcriptomes. These findings reveal a role for platelet RNA transfer in platelet RNA heterogeneity, with potential correlation to platelet functional diversity

previously proposed. The ability of the platelet to bidirectionally transfer RNA within circulation has implications for vascular health and beyond.

TABLE OF CONTENTS

LIST OF TABLES

LIST OF FIGURES

LIST OF COPYRIGHTED MATERIALS

Chapter I is a combination of original material and excerpts from two published reviews, edited for flow and included with permission.

- *Clancy L, Freedman JE. (2014). New paradigms in thrombosis: novel mediators and biomarkers: Platelet RNA transfer. J Thromb Thrombolysis, 37(1), 12-6*
    - Permission Information: License Number 4151500267613, License Date Jul 17, 2017, Licensed Content Publisher Springer

- *Clancy L, Freedman JE. (2017). Platelets in Thrombotic and Non-Thrombotic Disorders, Pathophysiology, Pharmacology and Therapeutics: an Update, Chapter Title: Implications of Platelet RNA to Vascular Health and Disease, 1st Edition, 2017, 253-261, Gresele, P ed. Springer International Publishing, © 2017, ISBN 9783319474601*
    - Permission Information: With permission of Springer Nature, granted 09 March 2017

Chapter II is adapted from a published manuscript to include supplemental data and is included with permission not required.

- *Beaulieu LM, Clancy L, Tanriverdi K, Benjamin EJ, Kramer CD, Weinberg EO, He X, Mekasha S, Mick E, Ingalls RR, Genco CA, Freedman JE. (2015) Specific Inflammatory Stimuli lead to Distinct Platelet Responses in Mice and Humans. PLoS One. 10(7), e0131688*

Chapter III is adapted from a published manuscript to include supplemental data, included with permission. Chapter IV and Appendices C, E and G also contain excerpts from this same publication.

- *Clancy L, Beaulieu LM, Tanriverdi K, Freedman JE. (2017).The role of RNA uptake in platelet heterogeneity. Thromb Haemost, 117(5), 948-961*
    - Permission Information: Copyright Permission No 116/06/2017

Chapter IV contains a figure adapted from a published manuscript, included with permission.

- *Clancy L, Freedman JE. (2015).The role of circulating platelet transcripts. J Thromb Haemost, 13 Suppl 1, S33-9*
    - Permission Information: License Number 4158990752847, License Date Jul 30, 2017, Licensed Content John Wiley and Sons

Appendix B contains unpublished data from the Freedman Lab. Figure B.1 and corresponding results taken from unpublished manuscript, without permission required.

- *"Platelet activation and miRNA transfer in the regulation of vascular homeostasis"* Lauren Clancy, Antonina Risitano, Kahraman Tanriverdi, David D. McManus, Jesse W. Rowley, Andrew S. Weyrich, Olga Vitseva, Lea M. Beaulieu, Jeffrey J. Rade and Jane E. Freedman

Appendix F is adapted from an unpublished manuscript, to include supplemental data, without permission required.

- *"Viral Micro RNAs are Widely Detected in the Human Circulation"* Milka Koupenova, Eric Mick, Heather A. Corkrey, Tianxiao Huan, Lauren Clancy, Ravi Shah, Emelia J. Benjamin, Daniel Levy, Evelyn A. Kurt-Jones, Kahraman Tanriverdi, and Jane E. Freedman

LIST OF SYMBOLS, ABBREVIATIONS AND NOMENCLATURE

NOTE: For gene abbreviations and descriptions, please see Appendix A.

5-HT	Serotonin; 5'- hydroxytryptoamine
ADP	Adenosine diphosphate
Ago2	Argonaute 2, RISC catalytic component
ANOVA	Analysis of variance
BCR	Breakpoint cluster region
BLV	Bovine leukemia virus
BMI	Body mass index
BP	Blood pressure
BUSM	Boston University School of Medicine
C. pneumoniae / Cp	*Chlamydia pneumoniae*
CAD	Coronary artery disease
CD39	Ectonucleoside triphosphate diphosphohydrolase-1; NTPDase1
CD40LG	CD40 ligand
CD41	Integrin α-IIb
CD42b	Platelet glycoprotein Ib, α polypeptide
CD61	Integrin β-3
CD62P	P-selectin
CD68	CD68 protein
cDNA	Complementary DNA
CFU	Colony forming units
CHD	Coronary heart disease
CLL	Chronic lymphocytic leukemia
C-mpl	Myeloproliferative leukemia protein
CMV	Cytomegaloviruses
COX2	Prostaglandin-endoperoxide synthase 2
Cq	Quantification cycle
CRP	C-reactive protein
Ct	Cycle threshold
Ctrl	Control
CVD	Cardiovascular disease
DAVID	Database for Annotation, Visualization and Integrated Discovery v6.7
DBP	Diastolic BP
ΔCt	Delta Ct (RT-qPCR calculation, difference in threshold between housekeeping and treatment samples)

ΔΔCt	Delta delta Ct (RT-qPCR calculation, difference in threshold between treatment and control samples)
DNA	Deoxyribonucleic acid
EBV	Epstein-Barr virus
EC	Endothelial cell
EDTA	Ethylenediaminetetraacetic acid
EPB41L3	Band 4.1-like protein 3
ES	Enrichment score
ET	Essential thrombocythemia
EU	5'-ethynyl uridine
exRNA	Extracellular RNA
FACS	Fluorescence-activated cell sorting
FDR	False discovery rate
FDR q-val	False discovery rate q-value (FDR adjusted p-value)
FHS	Framingham Heart Study
FITC	Fluorescein isothiocyanate
FPKM	Fragments per kilobase of transcript per million mapped reads
FSC	Forward scatter
GFP	Green fluorescent protein
GO	Gene ontology
GP	Glycoprotein
GP1A/2A	Glycoprotein Ia/IIa complex (integrin $\alpha_2\beta_1$)
GP1B/V/IX	Glycoprotein Ib-IX-V
GP1BB	Glycoprotein Ib, β peptide
GP2B/3A	Glycoprotein IIb/IIIa complex (integrin $\alpha_{IIb}\beta_{3)}$
GPCR	G-protein-coupled receptor
GPS	Gray platelet syndrome
GPVI	Glycoprotein VI
GSEA	Gene Set Enrichment Analysis
GWAS	Genome-wide association study
HBV	Herpes B virus
hCMV	Human cytomegalovirus
HDL	High density lipoprotein
HEK293	Human embryonic kidney cell line
HHV-6A/6B	Human Herpesvirus 6A/6B
HHV-7	Human Herpesvirus 7
HIV	Human immunodeficiency virus
HMEC-1	Human microvascular endothelial cell line
HSC	Hematopoietic stem cells

HSV	Herpes simplex
HSV-1 / HSV1	Herpes simplex virus type 1
HSV-2 / HSV2	Herpes simplex virus type 2
HSV1-KOS	Herpes simplex virus type 1 strain KOS
HUVEC	Human umbilical vein endothelial cells
HVT	Herpesvirus of turkeys
IFN	Interferon
IFU	Infectious unit
IgG	Immunoglobulin G
IGV	Integrative Genomics Viewer (1, 2)
IL1R1	Interleukin 1 receptor, type 1
IL1β	Interleukin 1 beta
IL6	Interleukin 6
ILTV	Infectious laryngotracheitis virus
ITGA2	Integrin alpha-2
KEGG	Kyto Encyclopedia of Genes and Genomes
KSHV	Kaposi's sarcoma herpesvirus
LPS	Lipopolysaccharide
Ly6C	Lymphocyte antigen 6 complex, locus C
Ly6G	Lymphocyte antigen 6 complex, locus G
mCMV	Mouse cytomegalovirus
MCP1	Monocyte chemotactic protein 1
MDV2	Marek's disease virus type 2
MEG-01	Human megakaryoblastic cell line
miRNA	MicroRNA
MMP	Matrix metalloproteinase
mRNA	Messenger RNA
MRP-8/14	Calprotectin (heterodimer of myeloid-related protein 8 and myeloid-related protein 14)
NES	Normalized enrichment score
NET	Neutrophil extracellular trap
NF-kB	Nuclear factor kappa-light-chain-enhancer of activated B cells
Nom p	Nominal p-value
NT	No treatment
NUSE	Normalized Unscaled Standard Error
OPG	Osteoprotegerin
P. gingivalis / Pg	*Porphyromonas gingivalis*
P2Y1	P2Y purinoceptor 1
P2Y12	P2Y purinoceptor 12
PAF	Platelet activating factor

Pam3CSK4	Synthetic triacylated lipopeptide,TLR1/ TLR2 ligand
PAR	Protease-activated receptor
PAR1	Protease-activated receptor 1
PAX5	Paired box protein
PBMC	Peripheral blood mononuclear cell
PCR	Polymerase chain reaction
PDGF	Platelet-derived growth factor
PE-Cy7	Phycoerythrin-cyanine 7 conjugated fluorophore
pfu	Plaque-forming unit
PGE_1	Prostaglandin E_1
piRNA	Piwi-interacting RNA
PLP	Platelet-like particle
PMID	PubMed identifier
PPAR	Peroxisome proliferator-activated receptor
PRP	Platelet rich plasma
PRV	Pseudorabies virus
PTAFR	Platelet activating factor receptor
RIN	RNA integrity number
RISC	RNA-induced silencing complex
rLCV	Rhesus lymphocryptovirus
RLE	Relative Log Expression
RMA	Robust Multiarray Average
RNA	Ribonucleic acid
ROCK	Rho-associated, coiled-coil containing protein kinase
rpm	Reads per million
RQN	RNA quality number
RT	Reactive thrombocytosis
RT-qPCR	Reverse transcription quantitative PCR
S1P	Sphingosine 1-phosphate
S1pr1	Sphingosine 1-phosphate receptor 1
SBP	Systolic BP
SCD	Sickle cell disease
SD	Standard deviation
SELE	E-selectin
sICAM1	Soluble intercellular adhesion molecule 1
SLE	Systemic lupus erythematosus
snoRNA	Small nucleolar RNA
SPIA	Single primer, isothermal linear amplification
SSC	Side scatter
STEMI	ST-elevation myocardial infarction

sTNFR	Soluble tumor necrosis factor receptor
sTNFRII	Soluble tumor necrosis factor receptor II
SuHV1	Suid herpesvirus 1, pseudorabies virus
TFPI	Tissue factor pathway inhibitor
TH1	Type 1 helper cell
THP-1	Human leukemia monocytic cell line
TIMP	Tissue inhibitor of metalloproteinases
TLR	Toll-like receptor
TLR1	Toll-like receptor 1
TLR2	Toll-like receptor 2
TLR4	Toll-like receptor 4
TLR7	Toll-like receptor 7
TNF	Tumor necrosis factor
TPO	Thrombopoietin
tRNA	transfer RNA
UC	Untreated control
u.d.	Undetermined
UMMS	University of Massachusetts Medical School
UTR	Untranslated region
VEGF	Vascular endothelial growth factor
vWF	Von Willebrand Factor
VZV	Varicella-zoster virus
WBC	White blood cell
WT	Wild type
Y-27632	ROCK inhibitor, (1R,4r)-4-((R)-1-aminoethyl)-N-(pyridin-4-yl)cyclohexanecarboxamide
zVAD-FMK	Pan-caspase inhibitor, methyl (3S)-5-fluoro-3-[[(2S)-2-[[(2S)-3-methyl-2-(phenylmethoxycarbonylamino)butanoyl]amino]propanoyl]amino]-4-oxopentanoate

LIST OF MULTIMEDIA OBJECTS OR FILES

Appendix C references a table excerpt from a published manuscript too large to include in the text here, included with permission.

- *Clancy L, Beaulieu LM, Tanriverdi K, Freedman JE. (2017).The role of RNA uptake in platelet heterogeneity. Thromb Haemost, 117(5), 948-961*
    - Permission Information: Copyright Permission No 116/06/2017

File Information

Cuffdiff expression analysis results of sequencing data for large (Ot7226) versus small (Ot7227) platelets.

File available online at www.thrombosis-online.com

(TH117.5_Clancy_Suppl_Table1)

CHAPTER I: INTRODUCTION

Permissions

Chapter I is a combination of original material and excerpts from two published reviews, edited for flow and included with permission.

- *Clancy L, Freedman JE. (2014). New paradigms in thrombosis: novel mediators and biomarkers: Platelet RNA transfer. J Thromb Thrombolysis, 37(1), 12-6*
    - Permission Information: License Number 4151500267613, License Date Jul 17, 2017, Licensed Content Publisher Springer

- *Clancy L, Freedman JE. (2017). Platelets in Thrombotic and Non-Thrombotic Disorders, Pathophysiology, Pharmacology and Therapeutics: an Update, Chapter Title: Implications of Platelet RNA to Vascular Health and Disease, 1st Edition, 2017, 253-261, Gresele, P ed. Springer International Publishing, © 2017, ISBN 9783319474601*
    - Permission Information: With permission of Springer Nature, granted 09 March 2017

Author Contributions

LC performed literature reviews and prepared manuscripts with oversight and editing provided by JEF. Additional editing for original publication in 2017 provided by Hannah Hoffman and Hannah Iafrati.

Summary

Though first observed over 150 years ago, platelets are still a source of constant study today. While these small cellular fragments have now been shown to play integral roles across vast fields of human biology, how these cells act in such important and varied ways is still not fully understand. The more we learn about platelets, what they contain and what they can do, the more amazing it seems that these anucleate fragments control such intricate and delicate mechanistic pathways. Typically hemostatic cells but often referred to as the "barometers of the blood" (3) for their role in infection and immunity, whatever role these tiny cells play, platelets maintain a delicate balance between healing and response. Understanding how cells incapable of transcription can impact so many systemic responses without detrimental effects will not only expand our understanding of disease, but help development of therapeutic and diagnostic approaches in many fields.

Introduction

The Discovery of the Platelet

While some scientific breakthroughs can be easily accredited to a specific researcher or publication, the official "discovery" of the platelet is difficult to ascribe, as it was actually observed by several researchers long before its relevance was understood. The establishment of the platelet as a novel cell type was hampered by a number of obstacles, mainly that initial observations of

platelets were secondary in studies focused on other aspects of hematology and that microscopic techniques sensitive enough to observe platelets were not available in many laboratories and minimally validated and, thus, not publicly accepted (4). Despite these issues, between 1840 and 1886, the further development of the microscope led to an explosion of our understanding of blood components, and eventually the discovery of the platelet. From 1840-1882, there were both written and drawn accounts of what were mostly termed “spherules” or “globules” (4), which can now be attributed to platelets. Some of these observations failed to recognize the significance of these small cells: George Gulliver and William Addison in 1841 and Friedrich Arnold in 1845 all described cellular elements of the same size and functionality as the platelet, but only in passing (4). Other observations recognized the distinct novelty of these structures; however, their hypotheses on their relevance were varied and inevitably incorrect. In 1842, Alfred Donné is credited with first establishing the existence of a third blood element (different from red or white blood cells); however, he believed these small cells were related to chyle globulins (4). While one study focused on the potential of these unknown globules to be related to infection (William Osler, 1873, described them as “peculiar types of bacteria” (4)), the majority focused on platelets as progenitors of other cells. In 1864 Lionel Beale gave a clear account of platelets but firmly stated their germinal nature while Franz Simon in 1842, Gustav Zimmerman in 1846 and George Hayem in 1877 all believed strongly that these small elements were red blood cell

progenitors, Hayem going as far as naming them “haematoblasts” (4, 5). Max Schultze, often credited with the first true description of platelets in 1865, believed them to be derived from leukocyte granules (4). Though he did not go in depth, Schultze was able to point out platelet ubiquity (present in blood samples across numerous studies), size (0.001-0.002 mm) and nature (typically singular though often grouped) (5). Despite the confusion surrounding this third blood component, many illustrations from these studies show accurately what we today call platelets – both in their contributing role to fibrin clot formation and as individual units throughout circulation. Though they had little understanding at the time, even then many of these researchers observed some of the fundamental tenants of platelet biology. Thomas Wharton Jones described platelets present in the masses formed at sites of vessel wall trauma in 1850 (4, 5) and William Osler described how these small elements were singular when observed in circulation but formed masses quickly when blood was removed from the body (4). Max Schultze described how “under some circumstances the appearance is as if rays of finely granular protoplasm emerge from them, similar to the *Amoeba porrecta*…but these appearances are only connected with the coagulation of fibrous material” (5).

Despite initial observations, the man most often credited with the discovery of the platelet is Giulio Bizzozero, who, though undoubtedly not the first to describe platelets, wrote perhaps the first clear and most in-depth description. In 1881 and 1882, Bizzozero published several manuscripts on this third blood

component (5). As his work was first published in Italian, French and German, he called these cells *piastrine* (Italian), *petite plaques* (French) and *Blutplättchen* (German), all of which translate to “small plates” and eventually led to the English word “platelet” (5). Bizzozero described the structure of his “small plates” (“very thin platelets, disc-shaped… round or oval”) (5), size (“diameter two to three times smaller than the diameter or red cells”) (5), and distinct functional ability to form clots (4, 5). He showed what would become one of their most distinct features, their lack of a nucleus, as well as refuted claims of their role as red blood cell progenitors (4, 5). Finally, he established what would be studied over the next century, the role of platelets in thrombosis, or clotting, even describing the initial kinetics of clot formation, with illustrations that are accurate to today (4, 5). Though controversial at the time, Bizzozero’s results were soon confirmed by Curt Schimmelbusch (1885) (4, 5) and publicly supported by Osler (1886) (4), thus, beginning the field of platelet biology. Over the next 100 years, the role platelets play in the cardiovascular system would be established, leading to countless insights and treatments; however, only recently have roles for platelets outside of clotting come to light.

Platelet Biology and Biogenesis

Platelets are the smallest of the human blood cells as well as the second most numerous in the bloodstream. They typically range in size from 1-5 μm and, in their resting state, have a biconvex discoid shape (6). Their unique structural

components include two types of secretory granules (dense and alpha) (7, 8), integral to their function in clotting and hemostasis, and a unique open canalicular membrane system, which allows them to interact with their environment (7). The term platelet specifically refers to mammalian cells, as there is a distinct difference between the mammalian platelet and what are called thrombocytes in other animals (6). While similar in shape, size and function, platelets are lacking one integral feature that thrombocytes and most typical cells possess, a nucleus (6). Standard human platelet counts range from 150,000 - 450,000 platelets/μL (9), with definitive disease states associated with too few (thrombocytopenia) or too many (thrombocytosis, thrombocytothemia) platelets.

The most distinct feature of the platelet, their anucleate nature, is due to their biogenesis. Platelet progenitor cells, megakaryocytes are themselves a unique cell population. Though solely responsible for the production of platelets, they make up a minimal component of the bone marrow (<0.01%) (10-12), and this low cellular count has often hindered their past study. Despite their rarity, megakaryocytes can produce a significant number of platelets, approximately 5000 per megakaryocyte (13), with typically 10^{11} platelets in circulation at any given time (12).

Megakaryocytes develop from hematopoietic stem cells (HSCs), mainly in the bone marrow (though small populations exist in the fetal liver and spleen) (11). As they move from stem cell to early progenitor, they replicate as any other cells would, performing standard cell mitosis. This process is directed by

thrombopoietin (TPO), the primary hormone which drives megakaryocyte and platelet biogenesis (11, 13). Once a cell is fully committed to the megakaryocyte lineage, TPO signaling (through the megakaryocyte-specific receptor c-Mpl) induces the next stage of development, known as megakaryocyte maturation (11, 13). Over the course of the next 4-5 days, megakaryocytes increase in size (up to 100 μm) and prepare for platelet biogenesis by producing excess platelet specific proteins (such as Von Willebrand factor, or vWF) and platelet specific granules (dense and α-granules) (11, 13). This maturation is marked by a shift from a typical mitotic cell cycle to an endomitotic cell cycle, forgoing cell division. During endomitosis, cells go through the typical stages of mitotic development until anaphase B, wherein, instead of continuing on to separation into two cells, telophase and cytokinesis are both aborted, the nuclear envelope reforms and the cell remains singular (6). Megakaryocytes going through endomitosis develop a large cytoplasmic content, full of platelet and cytoskeletal specific proteins, and a multilobed, polyploid nucleus containing nuclear content as high as 128N (6, 11, 13). Maturation is also marked by the development of a specialized membrane system known as the invaginated membrane system (previously referred to as the demarcation membrane system), which is specifically required for platelet production and is believed to provide the phospholipid source material for both the platelet membrane and its open canalicular system (11, 13, 14).

Once megakaryocytes have matured fully, platelet biogenesis begins, as these large megakaryocytes are again stimulated by TPO to extend pseudopodia

into the blood sinuses of the bone marrow, a process known as the “flow model of platelet formation” (11-13). The cytoplasm of the megakaryocytes is extended out into 100-500 μm-long pseudopodia, referred to as “proplatelets” (11-13). Though these proplatelets initially develop in a uniform direction, over the course of 4-10 hours, each proplatelet forms branched extrusions, each 2-4 μm in diameter, at the tip of which platelets can be assembled and released (11-13). This process of proplatelet formation and amplification through branching relies heavily on the cytoskeletal mechanisms within megakaryocytes, specifically on the development of microtubule bundles which run the length of the proplatelets (11-13, 15). Inhibition of microtubule assembly or knock down of tubulin subunits results in thrombocytopenia as well as misshaped and dysfunctional platelets, while inhibition of actin prevents the branching seen during development (11-13, 15-17). While both tubulin and actin dependent mechanisms are clearly required for proper proplatelet formation, they do not solely drive the formation of these structures, as their inhibition does not entirely prevent platelet production (13).

An additional protein, dynein, is also integral to proplatelet and platelet development (13, 18). Dynein directs a mechanism known as microtubule sliding, also essential to platelet production, as its inhibition prevents proplatelet formation (13, 18). Microtubules, formed from polymerization of α and β tubulin dimers and concurrent proteins, not only help establish the overall structure of the proplatelet, but also act as the “highways” through which materials from the cytoplasm are specifically sorted to the platelet assembly regions (13, 19).

Granules and organelles travel along the microtubules (aided by additional proteins and microtubule sliding) and eventually gather in the tips of the proplatelets (13, 18, 19). Additionally, specific RNAs and proteins are sorted into these regions as well, for inclusion in nascent platelets (13, 20). As the proplatelets continue to develop (at an average rate of 0.85 μm/min), the entire cytoplasm of the megakaryocyte is converted into these 250-500 μm tubes, leaving the nuclear material to be compressed and degraded (13, 21, 22).

After formation of the proplatelets, the next step in platelet biogenesis is release into the bloodstream. Proplatelets squeeze through the vascular lining and enter the blood sinuses and, as blood passes through the sinus, multiple forces act on the pseudopodia to encourage platelet release (11, 13). Historically, little has been known about the process of both elongation through the vascular lining and platelet release into the vasculature. Platelet release was believed only to occur through the effects of shear force, specifically, as blood passed the extended pseudopodia, the flow caused the ends to break off, forming new platelets (11-13). Though this mechanism is an essential form of platelet release, new studies have elucidated additional methods of release as well as more details on how proplatelets initially end up in the blood sinuses. Most recently, it has been shown that interaction between a high concentration blood protein (sphingosine 1 phosphate -S1P) and its receptor on megakaryocytes (S1pr1) not only results in release of proplatelets into circulation but is integral for the directional growth of the proplatelets into the sinusoidal space in the first place

(lack of S1pr1 signaling results in extravascular proplatelet and platelet development) (11, 23). Additionally, studies have revealed that actin-rich regions of the platelet plasma membrane, termed podosomes, pave the way for proplatelet protrusions through the sinus lining through degradation of the extracellular matrix (11, 24). Taken together, these recent studies have started to elucidate how precisely these protrusions get from the parental cell into the sinuses and begin to give a clearer image of this important step in platelet production.

Once proplatelets are inside the sinuses, segments are released into the blood stream to produce the heterogeneous platelet population. While some of the proplatelet extrusions release fragments of typical mature platelet size and shape, others can break off into larger, less typical fragments. Sometimes an entire proplatelet is fragmented and enters the bloodstream (11-13). Once in the circulation, proplatelets form a distinct barbell structure, with platelet assembly regions at each end (11, 12, 25). These barbell structures will eventually split into smaller mature platelets in the circulation (11, 12, 25). Other times a structure known as a preplatelet may break off (11, 21). Preplatelets are 2-10 μm in diameter and can revert back to the structure of the circulating proplatelet and similarly create mature platelets in circulation (11, 26). This phenomenon of proplatelet reversion and mature platelet formation within the circulation appears microtubule dependent and results in very uniform sized platelets (11, 21, 27).

Additionally, as this process occurs within the circulation, it can result in platelet production far away from the bone marrow, such as in the lung (11).

Though a historically controversial topic, many platelet biologists agree that even beyond the presence of the proplatelets and preplatelets in the bloodstream, the mature platelet population is heterogeneous (28). A number of studies in the 1970s and 1980s focused on defining the overall scope of this heterogeneity with contradicting results (28). These studies were not well standardized and used multiple model organisms and modes of isolation. Subsequently, results were extremely varied, especially when an association between platelet subpopulations and platelet circulating age was addressed. It was clear however that most studies agreed on the heterogeneous range of sizes and densities within a typical platelet population. Some conclusions focused on platelet size have become accepted in platelet biology. The association between platelet size and reactivity is now well established, with larger platelets having more prothrombotic tendencies than smaller platelets. Mean platelet volume positively correlates to platelet aggregation, higher expression of adhesion molecules and elevated associations with cardiovascular risk (11, 29-33). Some work has focused on the connection between platelet volume and gene expression, with the most recent findings suggesting a role for ITGA2 in determining platelet volume and, thus, reactivity (11, 34, 35). An additional large scale GWAS study by Gieger et al has associated 70 genes with platelet volume (11, 36). Understanding the heterogenic nature of the platelet

population will have implications not only on how we view the platelet's traditional role in cardiovascular disease, but in its connections to non-vascular phenotypes and platelet therapies.

Platelets Role in Hemostasis and Thrombosis

As described, the historic role of platelets in clot formation was identified as early as the 1800s. Clinically, this function is both beneficial (hemostasis, the prevention of blood loss) and detrimental (thrombosis, the formation of clots within the vasculature), and thus requires delicate regulation with minor perturbations having catastrophic consequences. Once platelets enter the bloodstream, they circulate over the next 7-10 days (7, 8), responding to the microenvironment present in the sinuses. One of the best known responses is in the setting of exposed subendothelium at sites of vascular injury (37, 38). This hemostatic response is carefully regulated by a number of signaling events and feedback loops which can be loosely grouped into two phases, primary and secondary hemostasis; and described as platelet adhesion, platelet secretion and platelet aggregation (7, 8, 38).

In primary hemostasis, platelets first identify vessel wall damage and begin adhesion to the injury site (7, 8, 38). This process occurs through a number of different signaling cascades and is significantly dependent on glycoproteins (GPs) expressed on the platelet surface (7, 8, 38). The inhibitory methods of intact endothelium (specifically production of prostacyclin and nitric oxide and

expression of CD39) are decreased upon vessel damage and extracellular matrix proteins, such as collagen, are exposed to the open circulation (7, 8). Platelet adhesion, or initial binding of platelets to the site, depends on the level of shear in circulation and can be dependent on binding of either plasma-derived von Willebrand factor (vWF, high shear) or platelet-expressed GP1A/2A (low shear) to this exposed collagen (7, 8, 38). vWF binding results in its own conformational change allowing platelet binding via GP1B/V/IX, resulting in platelets rolling along the exposed endothelium and interacting in a reversible manner (7, 8, 38). This interaction decreases platelet velocity allowing for the additional low shear interactions described, as well as interaction between platelet-expressed GPVI and collagen (7, 8, 38). These initial interactions and resultant platelet adhesion may lead to activation and a number of distinct physiological changes within the platelets themselves. The platelet cytoskeleton changes as activated platelets no longer hold their resting discoid shape, but instead transform to extend numerous pseudopodia further into the injury site and circulation (7, 8, 38). Platelet granular secretion occurs, with both dense and α-granules releasing a number of procoagulatory, platelet activating factors, as well as increasing platelet-GP surface expression (notably GP2B/3A, which binds fibrinogen and induces additional granule secretion) (7, 8, 38). Additional proteins can be activated as well and, taken together these events prime the platelets for eventual stable clot formation that characterizes secondary hemostasis.

In secondary hemostasis, the factors released from platelet granules, most importantly adenosine diphosphate (ADP) and serotonin (5-hydroxytryptoamine, 5-HT), amplify the initial platelet signal, resulting in continued activation of platelets and induction of the coagulation cascade (7, 8, 38). ADP specifically interacts with two platelet-expressed receptors, P2Y1 and P2Y12 (7, 8, 38). P2Y1 activation results in continued platelet shape change and reversible platelet aggregation while P2Y12 activation results in additional granule secretion and activation of GP2B/3A (7, 8, 38). While resting platelets express GP2B/3A on their surface, in its lower concentration and inactivated form, this receptor does not easily bind soluble ligands (7, 8, 38). However, once activated, GP2B/3A is primed to interact with soluble ligands and play an integral role in stable clot production (7, 8, 38).

As changes occur within the platelets themselves, the original injury and platelet adhesion and activation also induce the initiation of the coagulation cascade. The coagulation cascade is a series of signaling events that occur in the circulation resulting in the formation of a stable blood clot (7, 8, 38). This cascade is triggered by a number of factors, some from the exposure at the site of injury and some through platelet activation. Release of procoagulatory factors into circulation, such as tissue factor from the exposed endothelium or Factors V, VII, XI and XIII from granule secretion, sets off and propagates this signaling cascade, resulting in the production of thrombin from its precursor prothrombin (7, 8, 38). Thrombin is also produced in response to the exposure of negatively

charged phospholipids on the activated platelet membrane (8). Thrombin is a serine protease that then can cleave soluble fibrinogen to produce insoluble strands of fibrin, an important building block, which combined with the presence of activated GP2B/3A on platelets leads to the formation a cross-linked stable fibrin-platelet clot at the site of injury (7, 8). This form of clot is irreversible, creating a hemostatic plug, and is regulated by a distinct feedback loop through a number of coagulation factors (specifically inhibition of Factor VII, thrombin and Factors V and VIII by tissue factor pathway inhibitor, TFPI, antithrombin and active protein C, respectively) (6-8). The formation of this hemostatic plug stably prevents blood loss and promotes wound healing at the site of injury.

While the immediate and irreversible response of platelets to sites of injury is essential for prevention of blood loss and proper wound healing, if incorrectly regulated, it can have detrimental effects on cardiovascular health. If clot formation is left unchecked, thrombosis can occur, resulting in occlusion of the vessel, decrease of blood flow and cellular death, a paradigm that occurs in the setting of myocardial infarction and stroke. During atherosclerosis, i.e. vessel wall disease characterized by development of fatty plaques within arteries which causes narrowing of the sinuses, even characteristic ”normal” clot formation can result in vessel occlusion, and acute cardiac ischemia (6). Accordingly, it is imperative that platelet regulation is not only location specific but tightly controlled, to provide the balance required for proper cardiovascular health.

Alternative Platelet Functions throughout the Circulation

Platelets' traditional role in hemostasis and their role in the chronic inflammatory disease atherosclerosis illustrate the link between platelets and inflammation and have been studied extensively. However, our understanding of platelets and their varied functions has increased alongside our knowledge of platelets' roles in the body's systemic responses. Deeper connections between local inflammation, infection and cancer progression were revealed by more recent studies of platelet biology. Patients with rheumatoid arthritis possess hyperactive platelet microparticles in their joint fluid, linking platelets to development of local inflammation (39-44). Similarly, platelets have been associated with the systemic response to infection, both viral and bacterial, through their expression of toll like receptors (TLRs), especially toll like receptor 4 (TLR4) and toll like receptor 7 (TLR7) (3, 45-57). The expression of both these TLRs on platelets allows platelets to act as sentinels in the blood – early sensors detecting foreign pathogens (lipopolysaccharide expressed on Gram-negative bacteria in the case of TLR4 (3, 50, 58) and single-stranded RNA viruses in the case of TLR7 (55)). Activation of these receptors allows platelets to induce a number of immune responses, including neutrophil recruitment and bacterial removal, neutrophil extracellular trap (NET) formation and heterotypic aggregate development (3, 54, 55, 59).

Studies have found a number of links between platelets, coagulation and cancer. It has been shown that tumors themselves can have a distinct effect on

coagulation through formation and release of a number of prothrombotic factors (such as tissue factor expression on the surface of cancer cells) (60-63), corresponding to data which shows select oncology patients suffer from coagulation disorders throughout their disease progression (64). These individuals subsequently face a greater risk both of thrombotic events, such as pulmonary embolism and deep vein thrombosis, and of platelet alterations in platelet counts and volume (65, 66). A variety of proangiogenic platelet factors, such as vascular endothelial growth factor (VEGF) and platelet-derived growth factor (PDGF), have been correlated to the required physiological processes for tumor metastasis, such as angiogenesis and chemotaxis (67-70). These correlations, along with the existence of activated platelets in tumor vasculature, suggest that platelets play a role in developing the essential blood supply for tumor growth (71, 72) and furthering tumor cell metastasis (potentially through concealing tumor development from systemic inflammatory reactions) (73). An inverse relationship between platelet inhibition and thrombotic events and tumor growth further supports the role of platelets in tumor development (74-77). As our understanding of platelet capability expanded from its function in hemostasis to one in moderating systemic inflammation, immune response, and cancer progression, one uncertainty that emerged was how the anucleate platelet is capable of such versatile functions.

Platelet Content

As described, platelet biogenesis occurs through the manual fragmentation of megakaryocytes, and thus, platelets do not contain nuclei and are incapable of transcription. Evaluation of platelet contents however revealed that platelets contain all the components required for signal-dependent translation including functional ribosomes, signaling proteins, messenger RNAs (mRNAs), and microRNAs (miRNAs) (78-80). The mechanism of platelet biogenesis combined with their lack of transcriptional ability implied that the platelet profile reflected that of their parental cells and was, therefore, inherently invariable; however, further analysis of this concept questions this assumption. Megakaryocytes are capable of transcription and altering their own transcriptome, allowing for the potential to similarly produce diverse platelets under different circumstances. Additionally, it was found that megakaryocytes specifically sorted and packaged material into platelets in the final stages of thrombopoiesis (20). A study of matrix metalloproteinases (MMPs) and their tissue inhibitors (TIMPs) revealed that, though megakaryocytes expressed 10 MMP family members at the mRNA level, only 7 of these were found in platelets (20). Additionally, one of these transcripts not found in platelets, *MMP2*, was expressed at the protein level in platelets (20). This suggests that megakaryocytes can selectively sort mRNAs into platelets during platelet biogenesis (20). Therefore, although platelet contents at the time of biogenesis are derived from megakaryocytes, it may not directly reflect the entire profile of the parental megakaryocytes. These findings suggested an expansive evaluation of the platelet transcriptome and proteome was necessary

to better understand the functional capabilities of platelets, especially under specific physiological settings where an altered platelet profile might be present.

Initial microarray-based studies estimated only 1500-4000 transcripts in healthy human platelets (81, 82); however the development of deep sequencing allowed for full detection of 9500 mRNA transcripts (80, 83-85). Platelets also contain various forms of small RNAs, with microRNAs (miRNAs) accounting for 80% of the small RNA expressed (86). MiRNAs, 19 to 24-nucleotide (nt) non-coding RNAs, regulate mRNA translation through sequence-specific recognition of non-coding regions in the 3' untranslated region (UTR) of target mRNAs (87) . miRNAs can regulate several targets at once and thus can have a profound effect on cellular environments with minimal material. The presence of megakaryocyte derived precursor and mature miRNAs as well as the presence of the machinery necessary to perform pre-miRNA processing in platelets led to complementary research evaluating the platelet miRNA profile (86, 88). This profiling of platelets identified 532 miRNAs in healthy patient platelets, 40 of which were novel miRNAs, with members of the let-7 family being the most represented (86).

Platelet RNA Content and Disease Associations

While initial studies focused on healthy platelet profiling, follow up focused on correlating platelet RNA profiling to platelet reactivity, species variability and disease modeling. Differential expression analysis of healthy patient miRNA

profiles revealed a correlation between platelet reactivity and miRNA and mRNA expression (89, 90). 74 miRNAs were differentially expressed in platelets, with the majority showing increased expression in hyper-reactive platelets (89). This corresponded to an increased differential expression of mRNAs in hyporeactive platelets (89). Analysis of their findings in hyper-reactive platelets to identify differentially expressed increased miRNAs with corresponding decreased target mRNAs revealed 12 miRNA-mRNA pairs, establishing a role for miRNA regulation of mRNA (and thus protein) expression in platelet reactivity (89). Examples of miRNA links to platelet reactivity in the context of cardiovascular disease are also abundant (91-94).

Similarly, an early comparison study between human and mouse platelets, evaluated potential roles RNA may play in platelet functional diversity (80). This study identified a large amount of conservation (approximately 4990 transcripts) between species, with 58% of human platelet transcripts conserved in the mouse platelet profile, and 83% of the mouse profile found in the human profile; however, it also revealed distinct expression variants between the two species which reflected previously described functional differences between human and mouse platelets (80). Specifically, expression of protease-activated receptor (PAR) transcripts in human and mouse platelets directly reflected previously known information about human and mouse platelet signaling (80). This study found the transcript for PAR1, the primary thrombin receptor in human platelets, was expressed in human platelets at 13.5 times the level it is in mouse platelets,

and mouse platelets expressed an alternative PAR transcript, *PAR3* (80, 95-97). This corresponds to and explains previous data showing knockdown of *PAR1* in mice having no effect on the mouse platelet thrombin response (80, 95, 96). Similarly, previous studies showing differential response to platelet activating factor (PAF) in human and mouse platelets (human platelets responded, mouse platelets did not), is explained by the presence of platelet activating factor receptor (PTAFR) transcript in only human platelets, not mouse platelets (80, 98, 99). Finally, the presence of CD68 transcript in human platelets and not mouse platelets, correlates to CD68 platelet protein expression (80). Taken together, these studies demonstrate the functional relevance of platelet RNA to platelet reactivity.

The ability of megakaryocytes to alter their transcriptome and preferentially sort platelets led to further evaluation of platelet RNA profiles under various physiological conditions. An abundant amount of correlations exist between platelet RNA expression and physical phenotypes and pathologies. Studies have identified specific differential profiles associated with patient age (129 mRNAs and 15 miRNAs), patient gender (54 mRNAs and 9 miRNAs) and patient race (100, 101). Body mass index was significantly ($P<0.005$) linked to higher expression of 11 of 48 transcripts analyzed in platelets from the Framingham Heart Study (FHS), highlighting differential expression of platelet inflammatory transcripts such as intercellular adhesion molecule 1 (*ICAM1*),

S100 calcium-binding protein A9 (*S100A9*), interleukin 6 (*IL6*), interleukin 1 receptor 1 (*IL1R1*) and *TLR2* (53).

Similar differential profiles exist under various pathologies as well. Systemic lupus erythematosus (SLE) patients' platelets displayed the type 1 interferon (IFN) gene signature, with increased expression of type 1 IFN related transcripts (*PRKRA, IFITM1, SELP* and/or *CD69*), especially in patients with a history of vascular disease, myocardial infarction, or arterial or venous thrombosis (42, 102). This correlates to known interferon secretion by platelets post immune cell activation, which plays a role in SLE development (42, 43). A characterization of sickle cell disease (SCD) shows an increased risk of cardiovascular complications specifically linked to increased endothelial damage, inflammation and platelet activation (103). Increased platelet activation directly affects SCD progression through a number of mechanisms, such as creation of microparticles and increased plasma expression of pro-coagulation and adhesion factors (103). Coinciding with previous reports linking platelet reactivity to distinct miRNA profiles, a study identified 40 differentially expressed miRNAs (16 upregulated, 24 downregulated) in SCD patient platelets and correlated these patterns to specific miRNA families and resulting regulation of SCD platelet mRNA (103).

Unsurprisingly, platelet RNA expression correlations exist for cardiovascular and platelet related disease as well. RNA comparison of platelets from acute ST-elevation myocardial infarction (STEMI) patients and stable

coronary artery disease (CAD) patients revealed 54 differentially expressed RNA, 29 increased and 25 decreased in STEMI patients, with the most significantly increased transcripts being *CD69* and *MRP-14* (104). Increased platelet transcript expression of *MRP-14* correlated to plasma protein levels of MRP-8/14 and a prospective case study utilizing the Women's Healthy Study correlated MRP-8/14 plasma protein levels to incidence of female patients experiencing an initial cardiovascular event (104). Additional studies comparing the transcriptomes of non-STEMI patient platelets to STEMI patient platelets similarly revealed distinct differential expression between the two patient subtypes (105). Thrombocytosis, high platelets counts in the blood, can be differentiated in to different classes, specifically essential thrombocythemia (ET), a myeloproliferative disorder, and reactive thrombocytosis (RT) (106). Definitive diagnosis of the etiology of thrombocytosis is often difficult and as the two types' prognoses and associated complications differ, this lack of clear differentiation can impede treatment (106). RNA sequencing of thrombocytotic patients identified unique RNA profiles of the two phenotypes of thrombocytosis and allowed for selection of an 11 transcript biomarker set which can be used to differentiate RT, ET and normal patients (106). Additional studies by the same group identified a 21-miRNA biomarker set for distinguishing ET patients from normal patients, which could be narrowed to a 3 miRNA subset (miR-10a, miR-148a and miR-490-5p) using statistical analyses (107). The identification of these unique mRNA and miRNA signatures to the forms of thrombocytosis may allow

for better detection, diagnosis and treatment in patients. With the presence of unique platelet RNA expression profiles associated with such widespread clinical phenotypes in the realms of disease and inflammation, the study of the functional roles of platelet RNA has developed into an increasingly relevant field of research.

Roles for Platelet RNA

Translational Capacity of Platelet RNA

Initial assumptions centered on platelet RNA being integral to platelet protein production and subsequent platelet function alteration in response to their microenvironment. Platelets have the capacity to execute both pre-mRNA processing and protein translation in a signal-dependent manner (78, 88, 108). Lipopolysaccharide (LPS) signaling in platelets catalyzes a number of reactions, resulting in the upregulation of mature IL1β protein. Platelet LPS stimulation results in the processing of stored *pro-IL1β* mRNA; intronic regions are spliced to form the mature mRNA form of the precursor protein. LPS also stimulates translation of the newly formed mature mRNA and cleavage of the precursor protein to form functional, mature Il1β protein, affecting platelet response to bacterial infection (88, 109-111). Additionally, platelets possess the ability to process pre-miRNA to mature miRNA, allowing for platelet miRNA regulation of platelet mRNA expression (88); this is demonstrated in studies where the existence of a miRNA network affects expression of the P2Y12 receptor within

platelets and alters the ability of the platelet to aggregate (90). Despite these findings, analysis and comparison of the platelet transcriptome to the platelet proteome revealed that the platelet transcriptome was not completely represented at the proteome level, with estimates ranging from 70-90% coverage (108, 112, 113).

Platelet RNA Transfer

Platelets utilize many types of cell-to-cell communication, including direct – moving through the platelet canalicular membrane system that allows passage of small molecules out of the cell – and indirect – discharging microvesicles and exosomes– methods (114-119). The possibility of a functional role of platelet RNA being platelet-cell communication was hypothesized due to the existence of these cellular communication capabilities and the presence of the unexplained fraction of platelet RNA post transcriptome-proteome correlation studies. This hypothesis has been investigated by several different labs, resulting in several publications on the topic (Table 1.1), with the ability of the platelet to transfer its RNA to other cells first being described by our lab.

Table 1.1: Summary of studies demonstrating definitive platelet RNA transfer.

Title	Journal Information	Transfer Shown	Cell Effect	Authors
Platelets and platelet-like particles mediate intercellular RNA transfer.(114)	Blood, 2012 Jun 28; 119(26): 6288-95.	mRNA	Platelet-like particles can transfer active mRNA to endothelial cells *in vitro* and *in vivo.*	Risitano, A. et al
Platelets activated during myocardial infarction release functional miRNA, which can be taken up by endothelial cells and regulate ICAM1 expression. (120)	Blood, 2013 May 9; 121(19): 3908-17	miRNA	miRNA released from platelets during myocardial infarction can regulate ICAM1 expression in endothelial cells.	Gidlöf, O. et al
Activated platelets can deliver mRNA regulatory Ago2·microRNA complexes to endothelial cells via microparticles. (121)	Blood, 2013 May 7 [Epub ahead of print]	miRNA	miR-223 is shed from activated platelets into microparticles in Ago2·miR-223 complexes. These microparticles are taken up by endothelial cells and actively affect gene expression.	Laffont, B. et al
MicroRNA-223 delivered by platelet-derived microvesicles promotes lung cancer cell invasion via targeting tumor suppressor EPB41L3.(122)	Mol Cancer, 2015 Mar 11; 14-58	miRNA	Transfer of miR-223, typically overexpressed in platelets of non-small cell lung cancer patients, from platelet-derived microvesicles regulated EPB41L3 expression, resulting in increased tumor cell invasion.	Liang, H, et al

Horizontal RNA transfer mediates platelet-induced hepatocyte proliferation. (123)	Blood, 2015 Aug 6: 126(6):798-806	mRNA	Inhibition of platelet and platelet-like particle internalization and RNA transfer blocks hepatocyte proliferation	Kirschbaum, M, et al
Platelet microparticles reprogram macrophage gene expression and function. (124)	Thromb Haemost, 2016 Jan; 115(2): 311-23	miRNA	Delivery of platelet-derived miR-126-3p to macrophages resulted in significant differential gene expression and increased phagocytic phenotypes.	Laffont, B. et al
Platelet microparticles infiltrating solid tumors transfer miRNAs that suppress tumor growth. (125)	Blood, 2017 May 12 [Epub ahead of print]	miRNA	Delivery of platelet-derived miR-24 impacts tumor growth	Michael, JV, et al

Initially, in order to investigate the possibility of platelet RNA transfer, we created an *in vitro* modeling system using cultured cell lines to mimic the vascular environment (114). By treating MEG-01 cells, a human megakaryocyte cell line, with thrombopoietin (TPO), a megakaryocyte maturation hormone that induces thrombopoiesis *in vivo* (13), we created platelet-like particles (PLPs). PLPs are structures similar to platelets but with some phenotypic differences (126). These PLPs allowed us to observe how platelets interact with vascular cells *in vitro* and to monitor platelet RNA during these interactions. In this study, PLPs containing fluorescent RNA were created by nucleofecting MEG-01 cells before TPO stimulation (114). Upon incubation of these fluorescently labeled PLPs with either

human umbilical vein endothelial cells (HUVEC), or a monocyte cell line, THP-1, we observed RNA transfer to both types of target cells, using both flow cytometry and fluorescence microscopy for analysis (114). Additionally, using microarray analysis, cells treated with non-labeled PLPs had specific transcript expression increases, the most prevalent of which were globins (114). Upon infusion of wild type platelets into *Tlr2 -/-* mice and aggregation induced by lipopolysaccharide, the Tlr2 transcript was observed in the monocytes of *Tlr2 -/-* host animals, confirming the *in vitro* phenomenon *in vivo* (114). Additional studies utilizing *in vitro* co-incubation modeling support the transfer of a range of platelet mRNA (notably, platelet marker transcripts) from human platelets to cells (unpublished data, Appendix B, Table B.1). Taken together, these studies support the transfer of platelet RNA from platelets to vascular cells, specifically endothelial cells and monocytes.

Initially, additional platelet RNA transfer studies focused on the transfer of platelet miRNA to recipient cells, as the miRNA's mode of regulation could result in profound and broad effects on other cells of the vascular system. Gidlöf et al. looked at the role miRNAs play in platelets during myocardial infarction (120). During myocardial infarction, blood flow is disturbed by thrombosis and oxygen supply to cardiac tissue is blocked, resulting in damage or death to the myocardium. In this setting, there is activation of platelets at the site of injury, thus, Gidlöf et al. hypothesized that miRNA content of platelets and the release and subsequent uptake of these miRNA played a role in the evolution of

myocardial injury (120). Initial studies focused on identifying if ST elevation myocardial infarction (STEMI) patients possessed a unique miRNA profile as compared to healthy subjects (120). In this study, STEMI patients had 9 miRNAs with significantly different expression levels as compared to controls (120). In addition, 8 miRNAs were significantly downregulated in patients while miR-320a was upregulated (120). Since the majority of differentially expressed miRNAs decreased in platelets in STEMI patients, Gidlöf hypothesized that this was due to platelet release of miRNAs upon aggregation (120). They choose 4 candidate miRNAs from the 8 described above (based on the relevance of their possible targets to cardiovascular disease) and showed that post thrombin stimulation of platelets, these miRNAs significantly increased in the supernatant (120). This insight was confirmed through further analysis of healthy donor platelets, STEMI patient peripheral blood platelet and STEMI patient platelets from the site of occlusion (120). Platelets from the actual thrombus showed decreased levels of these 4 miRNAs as compared to both healthy individuals and STEMI peripheral platelets (120). They further investigated whether these miRNAs released from platelets during aggregation transferred to endothelial cells (120). By transfecting platelets with a synthetic exogenous miRNA, as well as a synthetic fluorescently labeled miRNA, they showed transfer from platelets to HMEC-1 cells in a time and activation dependent manner (120).

Several reports have shown microparticle dependent miRNA transfer between cells (115, 117-119, 127). Platelets have also been shown to release

microparticles (0.1 – 1 μm) into the bloodstream upon activation (116). Based on these reports as well as the initial findings described above, Gidlöf investigated the role microparticles potentially play in platelet RNA transfer. Preliminary studies by Gidlöf focused on monitoring fluorescent synthetic miRNA transfer to platelet microparticles as well as blocking microparticle production using Brefeldin A (120). Gidlöf demonstrated significant enrichment of the fluorescent miRNA in platelet derived microparticles post thrombin activation (120). This enrichment was abated with pretreatment with Brefeldin A to block microparticle formation (120). He additionally showed that blocking platelet microparticle production significantly decreased transfer of a fluorescently labeled miRNA from platelets to HMEC-1 cells upon coincubation (120).

Laffont, et al. further investigated the role of platelet miRNA in transfer and the role microparticles may play (121). Laffont was able to show that miR-223, a miRNA highly expressed in platelets, was shed post platelet thrombin activation (121). Thrombin induced activation results in over a 60 fold increase in miR-223 expression in platelet derived microvesicles (121). The shed miR-223 is complexed with Ago2 protein in microvesicles and is functional in RISC activity assays (121). Laffont also showed platelet-derived microparticle uptake into HUVEC cells, with the microparticle persisting for 48 hours within cells before slowly diffusing (121). Follow up studies utilizing the same approach focused on an additional miRNA highly expressed in platelets, miR-126-3p. They showed

similar uptake and enrichment, this time in macrophages, independent of the macrophage-dependent transcription (124).

The relevance of platelet RNA transfer strongly depends on the functionality of the transferred RNA in the target cells. Several labs have demonstrated the functional relevance of platelet RNA transfer. Risitano, et al. demonstrated RNA functionality through transfer of a GFP labeled vector from platelets to recipient HUVEC and THP-1 cells (114). Kirschbaum, et al. showed the first endogenous example of functional platelet mRNA transfer (123). Platelets were shown to be internalized and localized to the perinuclear region of hepatocytes, while labeled platelets-like particle (PLP) RNA was shown to accumulate in the hepatocyte cytoplasm (123). The ability of the platelet to stimulate hepatocyte proliferation proved dependent on functional RNA transfer from platelets to hepatocytes (123). Interestingly, Kirschbaum also noted that this phenomenon was not seen if only platelet-derived microvesicles were used, suggesting a potential microparticle-independent mechanism of transfer (123). Gidlöf demonstrated transfer of functional miRNAs from platelets to endothelial cells (120). Gidlöf introduced luciferase reporter constructs designed with the 3'-UTRs of the predicted targets of their 4 miRNAs of interest (miRNAs 22, 185, 320b and 423-5p, mRNA targets *ICAM-1, eNOS, VEGFA* and *VEGFB*, respectively) into target HEK293 cells in culture (120). After incubation with thrombin-activated platelets, the *ICAM1* reporter signal was quenched compared to a scrambled pre-miRNA introduced supporting the transfer of functional miR-

22 and miR-320b (120). Additionally, HMEC-1 cells incubated with platelet releasate after thrombin activation showed *ICAM1* downregulation by 30%, confirming the construct results (120). Upon knockdown of endogenous miR-320b, platelet releasate could rescue miR-320b induced *ICAM1* degradation (120). These experiments were confirmed with direct miRNA overexpression of miR-320b in HMEC-1 cells (120). Similarly, Laffont et al. showed miRNA-Ago2 complexes present in platelets were functional post transfer from thrombin activated platelets to HUVEC cells (121). Transfected reporter constructs in HUVEC cells showed 44% degradation post platelet coincubation and thrombin activation (121). Additionally, endogenous mRNA targets of miR-223 in HUVECs showed >50% degradation post platelet microparticle incubation (121). Follow up studies by Laffont revealed that similar transfer of platelet-derived miR-126 to macrophages resulted in functional gene regulation (124). Utilizing a similar approach to Gidlöf, transfection of a reporter construct in macrophages showed that uptake of platelet microparticle-derived miR-126-3p resulted in functional regulation, with a 23% decrease in construct expression (124). Exposure and uptake of platelet-derived microparticles also resulted in significant transcriptome-wide expression changes (66 miRNAs and 653 RNAs) and altered functional capacity of macrophages (increased phagocytic phenotype) (124). Most recently, Liang et al. and Michael, et al. showed that impact of platelet microparticle miRNA transfer on cancer progression, though their results show opposite impact on tumor development. Liang et al. demonstrated that miR-223,

one of the most abundant miRNAs in platelets, is increased in the platelets of patients with non-small cell lung cancer (122). Evaluation of the role platelet-derived miR-223 may play in cancer progression revealed its transfer from platelet-derived microvesicles to cancer cells, resulting in downregulation of tumor suppressor EPB4L13 and concurrent increase in tumor cell invasion (122). Alternatively, Michael et al. showed that transfer of platelet-derived miR-24 to solid tumor cells resulted in disrupted mitochondrial function, resulting in tumor cell death and proliferation decline (125). All these studies support the hypothesis that platelet RNA may affect vascular cell function through cell-cell communication and RNA regulation.

Potential Platelet RNA Disease Relevance and Research Applications

As previously outlined, correlations exist between specific platelet profiles and several physiological and disease states. The response of megakaryocytes to their acute environment and pathophysiological alterations in the body may influence the type of platelet produced during thrombopoiesis, with specific platelet transcripts reflecting the overlying condition. New diagnostic and therapeutic tools could arise if the function that these specific transcripts have in the disease state were more fully understood. If these transcripts are specifically sorted by megakaryocytes into platelets in response to a systemic stimulant, it may suggest a role for the transcript in platelet function and disease development which could shed light on the disease itself (such as sorting of a specific

signaling transcript into platelets to allow for platelets to respond to a particular form of infection or inflammation occurring systemically). An example of research development through platelet RNA profiling involves gray platelet syndrome (GPS), or platelet alpha-granule deficiency, a bleeding disorder associated with platelets lacking alpha granules (128). GPS platelet RNA sequencing showed abnormal results for a specific transcript, *NBEAL2* (128). Further analysis revealed mutations in this gene resulted in abnormal pre-mRNA processing, defective protein sorting in megakaryocytes and impaired alpha granule biogenesis in platelets, causally linking *NBEAL2* expression to disease development (128-132).

Alternatively, the presence of a specific transcript in platelets under certain conditions or during a disease state may not reflect a role in platelet function and disease development; instead, it may simply represent the upregulation of these transcripts by megakaryocytes responding to stimuli and the subsequent increase in platelet expression due to subsequent platelet release. Though not causally linked to disease development, this scenario still poses advantages to researchers, as platelet transcripts could be used as biomarkers. Conventional biomarker research concentrates on identifying protein biomarkers, but given the availability and accessibility of platelets and the correlation of distinct platelet mRNA and miRNA profiles to physiological conditions, platelet RNA-based biomarkers could be utilized to identify disease states, aid research and develop therapeutic targets. Examples of therapeutic monitoring already exist; as

described, specific platelet RNA profiling can be used in differentiating the classical phenotypes associated with thrombocytosis. Additionally, as connections between platelets and cancer were explored, associations between tumor RNA and platelets were also discovered. Several studies have shown association between tumor-derived RNAs and platelets in liquid biopsies, supporting an additional role for platelet RNA analysis in biomarker diagnostics (133-136). Further identification of platelet biomarkers and their correlation to disease states may allow for future development of disease screening, especially relevant for diseases that are difficult to diagnose or characterize.

Full elucidation of systemic platelet capabilities depends on our clear comprehension of platelet RNA function. If platelet transcripts directly impact platelet and vascular function through either translational control or RNA transfer, realizing how these transcripts influence disease development will shed light upon both the given disease and possible treatments. For example, as described, the correlation between increased presence of MRP-8/14 protein (and the corresponding increase in *MRP-14* transcript) and future cardiovascular events in women (104), not only reveals information about the development of cardiovascular disease in women but also potential diagnostic and therapeutic targets. Furthermore, the ability of platelets to transfer RNA to vascular cells has possible therapeutic implications. Recent studies have utilized platelet membranes to improve nanoparticle drug delivery (137) and, once the mechanism and relevance of platelet RNA transfer and its subsequent effect on

recipient cells is fully understood, there may be potential to develop platelet RNA transfer via an individualized therapeutic delivery system.

Conclusions

The systemic relevance of platelets is no longer limited to their conventional roles in hemostasis and thrombosis; our understanding of platelet biology has broadened to include correlations and connections to physiological states, diseases and cellular communication. These additional connections and links between platelets and diverse systemic responses suggest the potential impact of platelets on vascular cell phenotypes, disease, and therapeutic development. Accordingly, greater comprehension of platelet RNA transcripts bolsters our understanding of both platelets' conventional thrombotic functions and their non-conventional roles, potentially having extensive implications in a variety of diseases and research areas. As we begin to understand how the platelet RNA transcriptome varies both over time and within a set population, we may be able to better understand how this anucleate cell has such broad systemic impact.

CHAPTER TWO: PLATELET TRANSCRIPTOME DIFFERENTIAL EXPRESSION IN RESPONSE TO INFECTION

Permissions

Chapter II is adapted from a published manuscript to include supplemental data and is included with permission not required.

- *Beaulieu LM, Clancy L, Tanriverdi K, Benjamin EJ, Kramer CD, Weinberg EO, He X, Mekasha S, Mick E, Ingalls RR, Genco CA, Freedman JE. (2015) Specific Inflammatory Stimuli lead to Distinct Platelet Responses in Mice and Humans. PLoS One. 10(7), e0131688*

Author Contributions

Beaulieu LM, et al: Conceived and designed the experiments: LMB LC CDK EOW XH SM RRI CAG JEF. Performed the experiments: LMB LC KT CDK EOW XH SM. Analyzed the data: LMB LC KT CDK EOW EM. Contributed reagents/materials/analysis tools: EJB EM RRI CAG JEF. Wrote the paper: LMB LC KT EJB CDK EOW XH EM RRI CAG JEF.

Preface

As described in Chapter 1, the platelet's role in immunity and infection has been elucidated in recent years. An explanation for the platelet's ability to play such diverse systemic roles could lie in better clarification of the intersection between platelets and their RNA. Platelets' integral roles in immune detection, as well as their capacity for translational regulation, suggest that the mechanism by which platelets adapt to disease and infection could depend on how platelet RNA changes throughout its' life span and in response to environmental stimuli. To better comprehend these interactions, we need to understand not only the role of the platelet in these responses, but how the overall platelet RNA content changes in response to the distinct phenotypic microenvironments.

Summary

Diverse and multi-factorial processes contribute to the progression of cardiovascular disease. These processes affect cells involved in the development of this disease in varying ways, ultimately leading to atherothrombosis. The goal of our study was to compare the differential effects of specific stimuli - two bacterial infections and a Western diet - on platelet responses in *ApoE*-/- mice, specifically examining inflammatory function and gene expression. Results from murine studies were verified using platelets from participants of the Framingham Heart Study (FHS; n = 1819 participants). Blood and spleen samples were collected at weeks 1 and 9 from *ApoE*-/- mice infected

with *Porphyromonas gingivalis* or *Chlamydia pneumoniae* and from mice fed a Western diet for 9 weeks. Transcripts based on data from a Western diet in *ApoE*-/- mice were measured in platelet samples from FHS using high throughput RT-qPCR. At week 1, both bacterial infections increased circulating platelet-neutrophil aggregates. At week 9, these cells individually localized to the spleen, while Western diet resulted in increased platelet-neutrophil aggregates in the spleen only. Microarray analysis of platelet RNA from infected or Western diet-fed mice at week 1 and 9 showed differential profiles. Genes, such *as Serpina1a, Ttr, Fgg, Rpl21*, and *Alb*, were uniquely affected by infection and diet. Results were reinforced in platelets obtained from participants of the FHS. Using both human studies and animal models, results demonstrate that variable sources of inflammatory stimuli have the ability to influence the platelet phenotype in distinct ways, indicative of the diverse function of platelets in thrombosis, hemostasis, and immunity.

Introduction

Cardiovascular disease (CVD) is a chronic inflammatory process with multiple etiologies, including genetic and environmental factors. Bacterial infections and obesity are two known pro-inflammatory contributors to the development of CVD. The effects of these inflammatory stimuli on vascular cells have been extensively studied, with the exception for the second most abundant cell in circulation, the platelet. Particularly, in light of work which shows the relationship between

platelet transcripts and CVD in FHS (53, 138) and their new role in inflammation (139-141), questions still remain as to how platelets contribute to the development of CVD. The goals of our study were to characterize the differential effects of two common bacterial infections and a Western diet on platelet inflammatory function and gene transcripts in *ApoE*$^{-/-}$ mice and in human samples. These results will help to better understand the connections between inflammatory stimuli, cardiovascular disease, and platelets.

One bacterium associated with CVD is the gram-negative oral pathogen *Porphyromonas gingivalis* (*P. gingivalis*), which induces low-grade chronic inflammation associated with oral bone loss, clinically known as periodontal disease. This bacterium expresses several outer membrane proteins which are recognized by the innate immune system through Toll-like receptor 2 (TLR2). In ApoE$^{-/-}$ mice, *P. gingivalis* accelerates atherosclerotic plaque size (142-144), with accumulation of lipids, T cells, and macrophages compared to uninfected mice (143). Plaque collagen and elastin content is also altered with infection, suggesting that *P. gingivalis* infection affects the stability of atherosclerotic plaques (143). In humans, *P. gingivalis* is detected in atherosclerotic plaques (145, 146) and is associated with the development of carotid artery atherosclerosis (147).

Another bacterium associated with CVD is the obligate intracellular gram-negative bacterium, *Chlamydia pneumoniae* (*C. pneumoniae*). It is associated with atypical pneumonia, as well as pharyngitis, bronchitis, and sinusitis in

humans. This bacterium is also recognized in part by TLR2 on innate immune cells. It has also been demonstrated to increase atherosclerotic plaque size, lipid content, and dendritic cells in *ApoE*$^{-/-}$ mice compared to uninfected mice (148). In humans, *C. pneumoniae* antibody seropositivity is associated with the progression of coronary artery calcification (149) and risk of coronary heart disease and myocardial infarction (150). *C. pneumoniae* has also been identified through PCR methodology in atherosclerotic plaques in humans (151, 152).

Obesity, having a body mass index (BMI) ≥30 kg/m^2, is another key risk factor associated with CVD. In the US, 35% of adults are considered obese (153). For individuals ≥20 years of age surveyed between 2009 and 2010, 35.8% were obese and 72.5% had a health score of 0-1, classifying them in poor cardiovascular health (153). Consistent with the importance of weight and diet, in animal models of atherosclerosis, feeding animals a high fat diet increases atherosclerotic plaque size, number, and severity (154-156).

We have previously demonstrated that in human and mouse platelets, *P. gingivalis* is recognized by TLR2 and induces aggregation (157) and heterotypic aggregate formation (139, 140). *C. pneumoniae* also binds to platelets to induce aggregation and P-selectin expression (158). A Western diet in C57BL/6J mice increases thrombin-induced platelet adhesion (139). The goal of this study was to characterize the differential effects of these two common bacterial infections and a Western diet on platelet inflammatory function and gene transcripts at different timepoints in a well-established atherosclerosis murine model prior to the

formation of plaques. These results were also correlated with recent observations from aortic tissue following exposure to the same inflammatory stimuli (159). Our results suggest that both inflammatory stimuli and the kinetics of the response differentially influence platelet transcripts and inflammatory function. Furthermore, our results were corroborated in human studies and provide insight into how platelets alter the development of CVD.

Materials and Methods

Animals

Mice were cared for at the Boston University School of Medicine (BUSM) Vivarium. All work was approved by BUSM Institutional Animal Care and Use Committee. Mice were housed in a 12 hour light cycle at constant temperature and humidity with free access to food and water. During procedures, mice were monitored and removed if exhibiting signs of distress. *P. gingivalis* strain 381 and *C. pneumoniae* strain AO3 were grown and purified as previously described (160, 161). One set of *ApoE*$^{-/-}$ male mice (Jackson Laboratories) were treated with 4% sulfamethoxazole in their drinking water for 10 days to clear normal oral microflora (159). These mice were then challenged 5 times per week for 3 weeks on the buccal surface of their maxilla with $1x10^9$ CFU *P. gingivalis* in 2% carboxymethyl cellulose. An additional set of *ApoE*$^{-/-}$ male mice were challenged intranasally once per week for three weeks with $2x10^6$ IFU *C. pneumoniae* suspended in sucrose-phosphate-glutamate buffer while under light anesthesia

of ketamine and xylazine (159). Mice were sacrificed by CO_2 asphyxiation followed by cervical dislocation at an early timepoint 1 day after the last *P. gingivalis* challenge (~9 weeks of age at start) and 4 days after the last *C. pneumoniae* exposure (~9 weeks of age at start), with n=3 for each group (159). Another group was sacrificed 9 weeks later (~6 weeks of age at start for both groups), with n=3 for each group, prior to the formation of overt aortic plaque formation as seen at later timepoints with these stimuli (143, 148, 159, 162). A final group of *ApoE*$^{-/-}$ male mice (~16 weeks of age at start) were fed a Western diet (17.3% protein, 48.5% carbohydrates, 1.2% fat, and 0.2% cholesterol; Teklad Harlan) for 9 weeks and then sacrificed with n=6 for the Western diet (159). Analysis was performed on samples collected from mice at each timepoint.

Whole Blood Cell and Platelet Counts

Blood collected from each mouse was analyzed for white blood cell (WBC) and platelet content using a COULTER® A$^{C.}$T Series Analyzer (Becton Dickinson) (139).

Heterotypic Aggregate Formation

A sample of whole blood from each mouse was dual stained with anti-mouse CD41 FITC-conjugated and anti-mouse Ly6G PE-Cy7-conjugated antibodies and appropriate isotype controls (eBioscience; Cat# 11-0411 and 25-5931, respectively). The percent of platelet-positive neutrophils was determined using a

FACSCalibur Flow Cytometer with Cell Quest Software (BD Bioscience) (139, 140).

Spleen Sectioning and Staining

Frozen spleen sections were stained with anti-mouse CD41 (Abcam; Cat# ab63983) and anti-mouse Ly6G and Ly6C (BD Bioscience; Cat# 553123) antibodies and appropriate isotype controls, followed by anti-rabbit IgG Alexa Fluor 405-conjugated and anti-rat Texas Red ®-X secondary antibodies (Life Technologies; Cat# A-31556 and T-6392, respectively). Samples were visualized using Leica TCS SP5 II Confocal Microscope with Leica Application Suite Advanced Fluorescence Version 2.6.0.7266 software then analyzed with ImageJ (v1.46r) and Adobe Photoshop CS3 (v13.0.1).

Platelet RNA Isolation

Platelets were isolated from blood samples using a series of centrifugation steps. Briefly, samples were centrifuged at 450*xg* for 7 minutes. The top layer consisting of platelet rich plasma (PRP) was removed and diluted 2.33X with platelet wash buffer (10 mM sodium citrate, 150 mM sodium chloride, 1 mM EDTA, 1% dextrose, pH 7.4) and 1:10000 prostaglandin E_1 (Calbiochem). Samples were centrifuged at 300*xg* for 4 minutes to remove any contaminating WBC. The supernatant was further diluted 3X with platelet wash buffer and

PGE_1, then centrifuged at 3500*xg* for 10 minutes (139). The resulting platelet pellet was lysed and RNA was isolated using the miRNeasy Kit (Qiagen).

RNA Microarray and Analysis

RNA from each mouse in each condition was pooled to generate at least 50 ng of RNA per sample. Samples were reverse transcribed using Ovation Pico WTA System V2 (Nugen) and purified using Agencourt RNA Clean XP Purification Beads. After SPIA amplification and purification, samples were labeled using the Encore Biotin Module (Nugen) and hybridized to the GenChip Mouse Gene 1.0 ST Array (Affymetrix), stained, and scanned using an Affymetrix GeneArray Scanner 3000 7G Plus. All procedures were performed by the Microarray Resource Facility at Boston University. Affymetrix CEL files were normalized to produce gene-level expression values using the Robust Multiarray Average (RMA) (163) in the Affymetrix Bioconductor (v1.28.1) (164) and an Entrez Gene-specific probe set (v14.0.0) mapping from the Molecular Behavioral Neuroscience Institute at the University of Michigan (http://brainarray.mbni.med.umich.edu/ Brainarray/Database/CustomCDF) (165). Array quality was assessed by computing Relative Log Expression (RLE) and Normalized Unscaled Standard Error (NUSE) using the AffyPLM Bioconductor (v1.26.1) (166). All microarray analyses were performed using the R environment (v2.15.1) for statistical computing. Gene Set Enrichment Analysis (GSEA; v2.0.13) (167) was used to identify biological terms, pathways, and processes.

By using the normalized enrichment score (NES) of ≥2/-2, the false discovery rate (FDR) of <0.05, and the nominal *p*-value (Nom *p*) of <0.05, we identified gene sets that were significantly enriched for and would have been affected the most by treatment. The Entrez Gene identifiers of the mouse homologs of the genes (as determined using HomoloGene v65 (168)) were ranked according to the log2-transformed fold change computed for each comparison; in cases where a given mouse gene mapped to more than one human gene, one homolog was randomly chosen. These ranked lists were then used to perform pre-ranked GSEA analyses (default parameters with random seed 1234) using Entrez Gene versions of the Biocarts, KEGG, Reactome, and Gene Ontology (GO) gene sets obtained from the Molecular Signature Database (MsigDB; v3.0) (169). Post analysis information on transcript alternative names and functions were determined using genecard.org and ncbi.nlm.nih.gov. Original publication heatmaps were created using MeV v4.9.0 (170). Heatmaps presented here created using Microsoft Excel 2010.

RT-qPCR Verification

Isolated RNA was converted to cDNA using High-Capacity cDNA Reverse Transcription Kit (Life Technologies), followed by pre-amplification using TaqMan® PreAmp Master Mix (Life Technologies). RT-qPCR was performed on the Applied Biosystems 7900 HT Fast Real-Time PCR System with SDS 2.2.2 Software (Life Technologies) using primers and probes for the following genes

(Life Technologies): microfibrillar-associated protein 1a (*MFAP1A*), glyceraldehyde-3-phosphate dehydrogenase (*GAPDH*), β-actin (*ACTB*), and β2-microglobulin (*B2M*). Analysis included correcting by the mean of the three housekeeping genes (ΔCt) – *GAPDH, ACTB*, and *B2M* – followed by calculating the difference between treatment and untreated controls (ΔΔCt). Fold change (graphed) was then determined by calculating $2^{-\Delta\Delta Ct}$.

Framingham Heart Study

As previously described (53, 138, 139), platelet RNA was isolated from 1819 participants of the FHS Offspring Cohort Examination 8 using miRNeasy kit (Qiagen) and converted to cDNA. Pre-amplification was performed using TaqMan® PreAmp Master Mix (Life Technologies). Quantitative RT-PCR was performed using the BioMark™ System (Fluidigm) with primers and probes from Life Technologies. Results were compared to data collected from the medical history and physical examination of each participant. Individuals were categorized as having hypertension if they had systolic blood pressure ≥140 mm Hg, diastolic blood pressure ≥90 mm Hg, or were receiving treatment for hypertension. They were categorized as having diabetes if their fasting blood glucose was ≥126 mg/dL, their non-fasting blood glucose was ≥200 mg/dL, or were being treated with insulin or hypoglycemic drugs. Finally, individuals were categorized as smokers if they had smoked 1 cigarette a day in the year prior to examination. All of this work with the FHS was approved by the University of

Massachusetts Medical School and Boston University Medical Center Institutional Review Boards and all participants gave written informed consent (53, 138, 139). Interleukin 6 (IL6) and C-reactive protein (CRP) levels were measured as previously described (138).

Statistics

Data from *ApoE*$^{-/-}$ mouse studies were reported as the mean ± the standard deviation. In some cases, the percent compared to untreated controls, which was set to 100%, was reported. All data were analyzed by ANOVA followed by Tukey's Multiple Comparison Test using GraphPad Prism 5 software. Data were considered normally distributed, with a two-sided $p<0.05$ being significant.
For the FHS, descriptive statistics were reported as the mean ± standard deviation for continuous variable or the count (percent) for binary variables. Quantitative RT-PCR cycle threshold (Ct) values were corrected (ΔCT) by the geometric mean of three housekeeping genes – *GAPDH, ACTB,* and *B2M*. Genes not expressed and failing to report a Ct value within a set period were assigned the maximum Ct value allowed in our procedure (28 cycles). Multivariable linear regression models for gene expression (ΔCt) were fitted adjusting for the following confounders – BMI, smoking status, total cholesterol, HDL cholesterol, triglycerides, systolic blood pressure, diastolic blood pressure, glucose levels, diabetes, coronary heart disease [angina pectoris, coronary insufficiency, myocardial infarction adjudicated by a review panel], lipid-lowering

therapy, hormone replacement therapy, antihypertensive therapy, and regular aspirin therapy (at least 3 times a week). All statistical analysis was performed using Stata 12.0 software (53, 138, 139). Statistical significance was assessed using two-sided *p*-value, with those <0.05 being considered statistically significant.

Results

Differential platelet gene expression in *ApoE*$^{-/-}$ mice infected with bacteria or fed a Western diet

ApoE$^{-/-}$ mice (n = 3) were infected orally with *P. gingivalis* or intranasally with *C. pneumoniae*. One day after the last oral infection with *P. gingivalis* and 4 days after the last intranasal infection with *C. pneumoniae* (week 1), platelet RNA was isolated and pooled to generate a sufficient amount of RNA per condition for microarray analysis. Due to the small sample size, only genes up- or downregulated 2-fold or greater and pathways with a normalized enrichment score (NES) ≥ ~2/-2, nominal *p*-value (Nom *p*) <0.05, and a false discovery rate (FDR *q*) <0.05 were considered. Additionally, this data was intended to generate hypotheses on how platelets and platelet transcripts are affected by different inflammatory stimuli over time. During Week 1, we observed increased expression of 129 genes and decreased expression in 59 genes following *P. gingivalis* infection compared to untreated controls (Figure 2.1). The top five upregulated genes with known function were *Serpina1a* (27.09-fold), *Alb* (17.83-

fold), *Ttr* (15.84-fold), *Apoa2* (15.08-fold), and *Kng1* (13.01-fold). The top 5 downregulated genes were *Stard6* (-5.49-fold), *Spic* (-5.42-fold), *Hmox1* (-4.60-fold), *Igk-v21-4* (-3.08-fold), and *Rassf4* (-2.89-fold). Using Gene Set Enrichment Analysis (GSEA), we identified gene sets with increased expression following *P. gingivalis* infection with an NES ≥2, a Nom p <0.05, and an FDR q <0.05. These gene sets included coagulation, lipids, signaling pathways, RNA/gene expression, and inflammation (Table 2.1). Gene sets, which exhibited decreased expression, included those involved in enzyme activity, differentiation, metabolism, extracellular matrix related, signaling, and cytoskeleton pathways; however, these gene sets were not significant (NES >-2, FDR q >0.05; Table 2.2).In *ApoE*$^{-/-}$ mice infected with *C. pneumoniae* at week 1, there were 87 platelet transcripts increased and 70 transcripts decreased 2-fold or more compared to untreated control (Figure 2.1). The top 5 genes that exhibited an increase in expression were *Serpina1a* (13.17-fold), *Alb* (7.75-fold), *Serpina3k* (6.47-fold), *Ttr* (6.20-fold), and *Kng1* (5.14-fold). The top 5 genes that exhibited a decrease in expression were *Nono* (-10.89-fold), *Spic* (-6.92-fold), *Hmox1* (-5.15-fold), *Pcdhgb7* (-4.09-fold), and *Stard6* (-4.09-fold). GSEA identified the following positively enriched gene sets: coagulation, lipids, metabolism, signaling pathways, cytoskeleton, and RNA/gene expression (NES ≥2, Nom p <0.05, FDR q <0.05; Table 2.3). As seen with *P. gingivalis*, negatively enriched genes, including those involved in enzyme activity, signaling, and extracellular matrix, were affected but not significantly (NES >-2, FDR q >0.05; Table 2.4).

Figure 2.1: Genes upregulated and downregulated at week 1 in *ApoE*$^{-/-}$ mice with bacterial infection. Heatmap shows the transcripts identified through microarray as upregulated or downregulated 2-fold or more with either *P. gingivalis* (Pg) or *C. pneumoniae* (Cp) infection compared to untreated control in the *ApoE*$^{-/-}$ mice. Each condition represents RNA from 3 mice pooled.

Week 1			Week 1			Week 1			Week 1			Week 1		
Pg	Cp		Pg	Cp		Pg	Cp		Pg	Cp		Pg	Cp	
27.09	13.17	Serpina1a	2.82	2.37	Fga	2.03	2.19	Naa10	-1.07	-2.12	Mrgpra5	-2.09	-1.73	4930520O04Rik
17.83	7.79	Alb	2.77	1.42	Gm 7225	2.02	1.65	Olfr441	-1.07	-2.19	A630055G03Rik	-2.09	-1.48	Tbc1d8b
15.84	6.26	Ttr	2.76	1.65	Rab5b	2.01	2.28	Cd3d	-1.08	2.17	Olfr344	-2.09	1.20	Hsp90aa1
15.08	4.41	Apoa2	2.70	2.08	Acsf2	2.01	-1.10	Gm 5413	-1.09	3.52	A530064D06Rik	-2.10	-1.72	Retnla
13.01	5.26	Kng1	2.67	1.35	Sesn3	2.01	1.34	LOC 100048057	-1.09	2.53	Traj49	-2.11	-2.68	Sms
12.46	4.55	Serpina1c	2.62	-1.00	Apoc4	2.01	2.03	Trim 59	-1.10	-2.40	Ifi205	-2.11	-1.49	Pcdha6
11.18	5.14	Ahsg	2.62	1.06	Apoc2	2.01	1.78	Cd79b	-1.11	4.29	AI747699	-2.11	-2.56	Ifitm 6
10.80	4.67	Gc	2.61	1.78	Igl-J1	2.01	-1.56	Gstm 1	-1.12	-2.02	Rsph3a	-2.13	-1.26	Akr1b10
9.36	5.47	Serpina3k	2.59	1.12	Mrto4	2.00	1.74	Zfp422	-1.13	-2.51	Apol10a	-2.14	-1.43	Hspd1
9.28	4.16	Apoa1	2.57	2.22	Oxct2b	1.94	2.61	Obox2	-1.14	-2.13	Gpx4	-2.15	-2.97	S100a8
5.11	3.82	Mup3	2.57	1.15	Crm3	1.91	2.22	5430413K10Rik	-1.15	-2.20	S100a4	-2.15	1.28	BC094916
8.85	3.07	Rdh7	2.57	1.10	Cyp4a10	1.89	2.02	Naa50	-1.15	-2.78	Gpr137b-ps	-2.15	-1.81	Hist2h2ab
6.71	2.48	Fgg	2.52	1.62	Kng2	1.85	2.90	Zfp825	-1.20	-2.46	Prelp	-2.16	-1.72	Fcgr3
8.01	2.40	Fzp	2.51	1.96	0610010O12Rik	1.79	2.39	Igk-V8-16	-1.20	2.83	4933426I21Rik	-2.17	-2.51	Cyp3a44
7.49	3.36	Serpina1d	2.50	-1.17	Gm 8909	1.78	2.49	Gm 5292	-1.22	2.29	Pcdha1	-2.17	-1.86	Gm 13139
7.42	1.96	Fgb	2.50	-1.48	4921524J17Rik	1.76	3.25	Trdv4	-1.23	-2.22	4930433N12Rik	-2.18	-1.53	Ccr2
7.19	3.41	Fetub	2.47	2.64	Prh1	1.75	2.44	Igkv1-117	-1.25	-2.66	Mgp	-2.18	-2.41	Hrnr
7.08	2.09	Igh-2	2.47	1.15	Serping1	1.69	2.20	Olfr541	-1.30	-3.64	Gm 14420	-2.19	1.02	Ifi204
6.88	-1.13	Hamp	2.46	2.83	Ugt2b36	1.68	2.94	Mir700	-1.32	2.16	Plp-ps2b	-2.19	2.22	Vmn2r69
6.46	2.69	Apoc1	2.45	2.66	Pcdha5	1.65	2.10	Zswim1	-1.32	2.16	Immp1l	-2.20	-1.73	Gnrh1
6.00	1.43	Ambp	2.43	1.18	Grap	1.65	2.60	Vmn1r196	-1.34	-2.56	Saxb1	-2.25	-2.25	Gm 3643
5.90	1.68	Fabp1	2.43	2.69	Npm 3-ps1	1.62	-2.67	Gm 6252	-1.34	-2.57	1700019G17Rik	-2.26	-2.32	Ccl6
5.79	1.64	F2	2.39	1.94	Gm 5571	1.61	2.09	BC003331	-1.34	-2.15	Gm 5959	-2.26	-1.68	Gm 10336
5.74	1.76	Mug1	2.39	1.59	BC002059	1.56	2.02	Gpbp1l1	-1.36	-2.07	Rbm4b	-2.26	-2.59	Pcdha12
5.70	1.44	Itih4	2.38	1.38	Apoh	1.55	2.20	Mir31	-1.36	2.86	Gm 10651	-2.27	-1.26	U2af1
5.31	1.31	Cyp3a11	2.37	2.08	Npm 1	1.50	2.03	1110012L19Rik	-1.37	-2.11	Try10	-2.30	-2.51	Cd209f
5.35	2.64	Vtn	2.36	1.75	Klhdc5	1.48	2.02	Igk-C2	-1.40	-2.17	Vmn1r213	-2.31	-2.13	Gm 5629
5.33	2.75	Mgat1	2.35	1.28	2010001M09Rik	1.48	2.12	Tcrg-C4	-1.46	-2.10	Gm 6570	-2.31	1.18	X76971
5.12	2.23	Es31	2.33	-1.00	Mettl7b	1.48	2.15	Gpx2	-1.49	-2.25	Rai12	-2.34	-2.08	Gm 10035
5.05	2.61	Ugt2b5	2.33	2.50	Gm 4964	1.47	2.14	Rlpl2	-1.52	-2.33	Trim 34	-2.39	-1.71	Cnn1
5.06	4.85	Serpina1b	2.33	-1.42	Olfr23-ps1	1.46	3.24	Gm 13034	-1.52	-2.22	Cd5l	-2.39	-3.41	Il1b
4.83	2.45	Trf	2.32	1.48	Cyp1a2	1.45	2.16	Copa6	-1.53	-2.38	2010107H07Rik	-2.40	-1.63	1810009J06Rik
4.74	1.65	Plg	2.28	1.20	Igl-C1	1.41	2.37	Olfr521	-1.55	-2.13	Mfap5	-2.43	-1.03	Olfr744
4.74	1.60	Ugt1a6b	2.28	1.39	Pigr	1.40	2.29	Elovl2	-1.58	-2.56	2810405K02Rik	-2.43	-1.42	Apol9b
4.73	2.38	Cyp2f2	2.26	1.86	Gemin8	1.40	2.72	Gm 4478	-1.59	-2.25	Tmx2	-2.43	-1.50	Man1b1
4.42	1.07	Fgl1	2.26	1.21	Igkv12-44	1.40	2.99	LOC 100044509	-1.66	-2.02	Tcrd-C	-2.46	-1.51	Gm 16527
4.38	1.08	Serpinc1	2.26	2.48	4833413D08Rik	1.39	2.07	Gm 10029	-1.66	-2.30	Hist1h2ab	-2.46	-2.45	Ms4a6c
4.09	-1.04	Gm 9740	2.24	1.67	Angptl3	1.37	2.29	Gm 189	-1.68	-2.01	Nptxr	-2.47	-1.50	Hdc
4.08	1.49	Rbp4	2.24	-1.16	Cbx6	1.36	2.19	Plekhf1	-1.69	-2.12	Gm 1418	-2.49	1.03	Gm 4889
4.04	3.01	Gm 8290	2.23	1.90	Set	1.36	2.12	Chchd1	-1.69	-2.10	Wdr53	-2.49	-2.09	Olfr1170
3.98	2.08	Hpx	2.22	1.33	Bank1	1.35	2.16	1190002N15Rik	-1.70	-2.11	Siglece	-2.49	-2.88	Emr1
3.93	1.77	Ces3	2.21	1.54	Cyp3a59	1.35	2.74	Bhmt	-1.70	-2.12	Hebp1	-2.52	-2.02	Nutf2
3.87	1.69	Rpl21	2.20	1.25	Olfr1303	1.32	2.07	Hnrpdl	-1.71	-3.45	Gnpda1	-2.54	-3.03	Hbq1
3.64	1.40	Gm 13212	2.19	1.44	Gkap1	1.32	2.42	Car3	-1.71	-2.42	Mageb16	-2.57	-4.09	Pcdhgb7
3.53	1.62	Uevld	2.18	1.12	C3	1.30	2.16	Olfr224	-1.72	-2.29	Kl101	-2.62	-2.41	Zc4h2
3.49	1.93	Lyrm 7	2.17	1.38	Apof	1.29	2.55	Prps1	-1.78	-2.04	C1qb	-2.63	-2.86	Trgj4
3.45	-1.53	Gm 10878	2.15	1.45	Zfp787	1.29	2.01	Gm ap9	-1.78	-2.03	Gm 5081	-2.66	-3.74	Gm 11428
3.44	1.64	Hp	2.15	1.62	Ly86	1.28	2.48	Higd1a	-1.79	-2.24	Gda	-2.67	-1.62	1110002L01Rik
3.42	1.50	Ahcy	2.15	2.26	C8b	1.27	-2.73	Gm 4459	-1.85	-2.96	Rhox4g	-2.67	-2.65	Mnd1
3.42	1.47	Cyp2e1	2.14	-1.01	Mir712	1.26	2.05	Sco2	-1.87	-2.16	Hist1h4b	-2.75	-1.42	Bckdk
3.35	3.60	Gm 10880	2.13	1.45	Apoa5	1.26	-2.27	Ass1	-1.90	-2.23	Marco	-2.80	-1.97	A630098A13Rik
3.32	1.99	Gm 4738	2.13	1.40	Serpinb9f	1.25	2.11	Fads1	-1.93	-2.27	Acp5	-2.81	-1.98	AU019823
3.24	1.40	Apob	2.12	-1.10	Gm 16519	1.24	-2.02	Gm 9232	-1.94	-2.29	Olfr205	-2.82	-10.89	Nono
3.24	2.16	Cpamd8	2.12	1.34	Srsf3	1.18	2.66	Cxcl2	-1.97	-2.12	Clec4a3	-2.85	-3.84	Aif1
3.23	-1.05	H2-Q8	2.12	1.20	Polr2k	1.16	-2.21	Gm 5154	-1.97	-3.97	Mt2	-2.86	-2.86	Stfa2l1
3.20	1.11	Gsta3	2.12	1.34	Kmo	1.14	-2.25	Chn3	-2.00	-1.42	Phf11	-2.89	-2.89	Rassf4
3.19	2.42	Apoc3	2.11	1.12	N6amt2	1.12	2.39	Zfp456	-2.03	1.37	Nsfl1c	-3.07	-1.45	AA792892
3.18	2.04	Gm 6749	2.10	1.72	Snora73a	1.09	2.04	B3gnt8	-2.03	-1.43	Trappc2	-3.08	-1.42	Igk-V21-4
3.09	1.13	Pcdhga1	2.10	1.13	Dzgt1b	1.08	2.11	Taar7a	-2.03	1.01	Vault rc5	-3.09	-3.97	Gm 7188
3.06	1.47	Hrg	2.10	2.61	Olfr403	1.05	-2.05	1100001G20Rik	-2.03	-1.31	Gtpbp8	-3.48	-2.50	Gm 4759
3.06	2.40	Olfr1418	2.10	1.43	Stap1	1.03	2.51	Gm 7015	-2.03	-2.92	Nfil3	-3.66	-3.66	Gm 9756
3.05	1.53	Mat1a	2.09	1.21	Cp	1.02	2.17	4930524N10Rik	-2.05	-1.94	Cdkn1a	-3.71	-1.06	Gm 5331
3.02	1.90	Gm 7582	2.09	1.53	Cd79a	1.01	-2.21	Gm 6969	-2.05	-1.65	Pram 1	-4.58	-3.85	Gm 5476
3.01	2.39	Snord104	2.09	1.16	Arhgef1	-1.01	-2.19	Prp2	-2.05	-1.22	Zfp882	-4.60	-5.15	Hmox1
3.00	1.43	Es1	2.07	-1.05	Tbc1d22b	-1.01	2.02	Vmn2r12	-2.06	-1.55	Pygl	-5.42	-6.92	Spic
2.99	1.83	Azgp1	2.07	1.08	Rnase4	-1.01	2.78	Tlr13	-2.08	-1.30	Rhox4f	-5.49	-4.09	Stard6
2.86	2.08	Igkv10-96	2.06	1.09	Scd1	-1.02	2.89	AI324046	-2.08	-1.20	H2-T22	-8.01	-16.57	Gm 11710
2.85	1.20	Orm 1	2.06	1.52	Vmn1r175	-1.02	2.08	Snora28	-2.08	-1.78	E030030I06Rik			
2.85	3.09	Aph1a	2.05	1.26	Spib	-1.02	2.19	LOC 100038947	-2.09	-1.63	Gpn2			
2.84	2.17	Aadac	2.05	1.40	Olfr1148	-1.04	-2.08	Tgfbi	-2.09	-2.87	S100a9			

-5 0 5

Table 2.1: Positively enriched gene sets in platelets from *ApoE*$^{-/-}$ mice infected with *P. gingivalis* compared to untreated control – at Week 1.

NAME	SIZE	ES	NES	NOM *p*-val	FDR *q*-val
PLATELET DEGRANULATION	80	0.731	2.302	<0.001	<0.001
LIPOPROTEIN METABOLISM	26	0.888	2.272	<0.001	<0.001
INTRINSIC PATHWAY	23	0.903	2.249	<0.001	<0.001
COMPLEMENT AND COAGULATION CASCADES	62	0.744	2.232	<0.001	<0.001
REGULATION OF GENE EXPRESSION IN BETA CELLS	56	0.732	2.149	<0.001	<0.001
PEPTIDE CHAIN ELONGATION	38	0.763	2.093	<0.001	<0.001
FORMATION OF FIBRIN CLOT CLOTTING CASCADE	31	0.798	2.104	<0.001	<0.001
REGULATION OF BETA CELL DEVELOPMENT	69	0.683	2.070	<0.001	<0.001
CHYLOMICRON MEDIATED LIPID TRANSPORT	17	0.885	2.104	<0.001	<0.001
GENE EXPRESSION	357	0.553	2.074	<0.001	<0.001
RIBOSOME	39	0.743	2.079	<0.001	<0.001
AMI PATHWAY	19	0.890	2.109	<0.001	<0.001
INFLUENZA LIFE CYCLE	87	0.659	2.080	<0.001	<0.001
INFLUENZA VIRAL RNA TRANSCRIPTION AND REPLICATION	54	0.703	2.086	<0.001	<0.001
VIRAL MRNA TRANSLATION	39	0.757	2.114	<0.001	<0.001
FORMATION OF A POOL OF FREE 40S SUBUNITS	49	0.737	2.114	<0.001	<0.001
RNA BINDING	195	0.580	2.051	<0.001	<0.001
STRUCTURAL CONSTITUENT OF RIBOSOME	44	0.726	2.033	<0.001	0.001
LIPID TRANSPORT	26	0.788	2.023	<0.001	0.001
REACTOME GTP HYDROLYSIS AND JOINING OF THE 60S RIBOSOMAL SUBUNIT	58	0.679	1.995	<0.001	0.002
HIV1 TRANSCRIPTION ELONGATION	37	0.713	1.991	<0.001	0.002
PLATELET ACTIVATION	158	0.571	1.978	<0.001	0.003
PLATELET AGGREGATION PLUG FORMATION	26	0.779	1.981	<0.001	0.003
PROTEIN HETERODIMERIZATION ACTIVITY	71	0.639	1.982	<0.001	0.003
GRB2 SOS LINKAGE TO MAPK	15	0.884	1.976	<0.001	0.003

SIGNALING TO INTERGRINS					
TRANSLATION	71	0.643	1.983	<0.001	0.003
NEGATIVE REGULATION OF MULTICELLULAR ORGANISMAL PROCESS	28	0.741	1.959	<0.001	0.003
INTEGRIN αIIB β3 SIGNALING	23	0.794	1.957	<0.001	0.003
EXTRACELLULAR SPACE	209	0.545	1.938	<0.001	0.004
FORMATION OF PLATELET PLUG	177	0.556	1.936	<0.001	0.004
P130CAS LINKAGE TO MAPK SIGNALING FOR INTEGRINS	15	0.851	1.930	<0.001	0.005
TRANSLATION INITIATION COMPLEX FORMATION	38	0.689	1.927	0.002	0.005
REGULATION OF PROTEIN STABILITY	18	0.811	1.924	<0.001	0.005
TAT MEDIATED HIV1 ELONGATION ARREST, RECOVERY	27	0.739	1.901	<0.001	0.007
RIBONUCLEOPROTEIN COMPLEX BIOGENESIS, ASSEMBLY	71	0.628	1.903	<0.001	0.007
CYTOKINE SECRETION	15	0.848	1.905	<0.001	0.007
NUCLEOLUS	105	0.572	1.893	<0.001	0.007
INTEGRIN CELL SURFACE INTERACTIONS	80	0.606	1.896	<0.001	0.007
FORMATION OF TERNARY COMPLEX AND 43S COMPLEX	32	0.720	1.893	<0.001	0.007
INSULIN SYNTHESIS AND SECRETION	81	0.600	1.882	<0.001	0.009
TRANSCRIPTION OF THE HIV GENOME	55	0.639	1.881	<0.001	0.009
OXYGEN BINDING	19	0.799	1.874	<0.001	0.010
PEPTIDYL TYROSINE MODIFICATION	27	0.723	1.875	<0.001	0.010
FORMATION AND MATURATION OF mRNA TRANSCRIPT	137	0.551	1.868	<0.001	0.011
IMMUNE EFFECTOR PROCESS	33	0.700	1.859	0.002	0.012
RNA POLII CTD PHOSPHORYLATION AND INTERACTION WITH CE	24	0.744	1.854	0.002	0.013
HIV LIFE CYCLE	94	0.573	1.850	<0.001	0.013
LATE PHASE OF HIV LIFE CYCLE	82	0.597	1.851	<0.001	0.013

LIPID TRANSPORTER ACTIVITY	23	0.729	1.847	<0.001	0.013
ELONGATION, PROCESSING OF CAPPED TRANSCRIPTS	119	0.552	1.845	<0.001	0.014
HEMOSTASIS	262	0.505	1.839	<0.001	0.014
PEPTIDYL TYROSINE PHOSPHORYLATION	25	0.724	1.831	<0.001	0.016
ATP DEPENDENT HELICASE ACTIVITY	24	0.736	1.826	0.002	0.017
PPAR SIGNALING PATHWAY	67	0.596	1.819	<0.001	0.018
mRNA PROCESSING	30	0.695	1.816	0.002	0.019
RNA POLYMERASE II TRANSCRIPTION	84	0.569	1.808	0.002	0.020
REGULATION OF HYDROLASE ACTIVITY	65	0.599	1.810	<0.001	0.020
ANTIGEN BINDING	16	0.766	1.787	0.004	0.027
METABOLISM OF XENOBIOTICS BY CYTOCHROME P450	52	0.615	1.783	<0.001	0.028
PHASE II CONJUGATION	44	0.617	1.772	0.004	0.031
LIPID BINDING	73	0.586	1.773	<0.001	0.032
FURTHER PLATELET RELEASATE	19	0.756	1.774	<0.001	0.032
tRNA AMINOACYLATION	40	0.631	1.766	0.002	0.034
STEROID BINDING	17	0.755	1.754	0.006	0.036
FORMATION OF THE EARLY ELONGATION COMPLEX	29	0.673	1.758	0.004	0.036
INTRINSIC PATHWAY	17	0.745	1.759	0.002	0.036
PROTEIN RNA COMPLEX ASSEMBLY	56	0.604	1.757	0.002	0.036
RHO PROTEIN SIGNAL TRANSDUCTION	34	0.645	1.760	<0.001	0.036
REGULATION OF CELL MIGRATION	26	0.693	1.754	0.006	0.036
MAINTENANCE OF LOCALIZATION	19	0.733	1.752	0.004	0.036
RNA POLYMERASE I TRANSCRIPTION TERMINATION	19	0.732	1.754	0.006	0.037
miRNA BIOGENESIS	17	0.750	1.748	0.010	0.038
PD1 SIGNALING	18	0.740	1.744	0.002	0.039
PPARα PATHWAY	56	0.583	1.737	<0.001	0.042
IMMUNE RESPONSE	205	0.486	1.733	<0.001	0.042
PROCESSING OF CAPPED INTRON CONTAINING PRE	123	0.521	1.736	<0.001	0.043

MRNA					
mRNA SPLICING	95	0.549	1.733	<0.001	0.043
REGULATION OF SECRETION	36	0.631	1.733	0.004	0.043
REGULATION OF PROTEIN SECRETION	18	0.724	1.721	0.006	0.048
DOWNSTREAM TCR SIGNALING	36	0.638	1.722	0.005	0.048
EXTRACELLULAR REGION PART	297	0.471	1.718	<0.001	0.048
RNA PROCESSING	146	0.502	1.716	<0.001	0.049
MEDIATOR COMPLEX	18	0.730	1.713	0.004	0.050

SIZE – Number of genes; ES – Enrichment Score; NES – Normalized Enrichment Score; NOM *p*-val – Nominal *p*-value; FDR *q*-val – False Discovery Rate.

Table 2.2: Negatively enriched gene sets in platelets from *ApoE*-/- mice infected with *P. gingivalis* compared to untreated control – at Week 1.

NAME	SIZE	ES	NES	NOM *p*-val	FDR *q*-val
METALLOPEPTIDASE ACTIVITY	49	-0.505	-1.541	0.016	0.834
ACTIVATION OF NMDA RECEPTOR UPON GLUTAMATE BINDING AND POSTSYNAPTIC EVENTS	33	-0.547	-1.547	0.020	0.860
β-ALANINE METABOLISM	22	-0.613	-1.553	0.029	0.897
TRAFFICKING OF AMPA RECEPTORS	29	-0.555	-1.503	0.029	0.979
CONTRACTILE FIBER	21	-0.591	-1.512	0.052	0.982
MUSCLE DEVELOPMENT	90	-0.434	-1.493	0.007	0.994
EXTRACELLULAR MATRIX STRUCTURAL CONSTITUENT	24	-0.608	-1.553	0.029	0.996
THIOLESTER HYDROLASE ACTIVITY	16	-0.676	-1.612	0.022	1.000
MEIOTIC CELL CYCLE	33	-0.567	-1.593	0.020	1.000
LYSOSOME	116	-0.453	-1.589	0.002	1.000
OTHER GLYCAN DEGRADATION	16	-0.681	-1.577	0.022	1.000
EXOPEPTIDASE ACTIVITY	30	-0.578	-1.563	0.014	1.000
PROPANOATE METABOLISM	29	-0.588	-1.559	0.025	1.000
SMOOTH MUSCLE CONTRACTION	17	-0.638	-1.558	0.025	1.000
CALCIUM ION BINDING	88	-0.460	-1.555	0.002	1.000
MUSCLE CELL DIFFERENTIATION	21	-0.585	-1.477	0.049	1.000
SYNAPTIC VESICLE	15	-0.634	-1.457	0.054	1.000
AMINO SUGAR AND NUCLEOTIDE SUGAR METABOLISM	43	-0.489	-1.452	0.034	1.000
GLYCOPROTEIN METABOLIC PROCESS	81	-0.435	-1.451	0.013	1.000
MEIOSIS I	20	-0.574	-1.450	0.056	1.000

SIZE – Number of genes; ES – Enrichment Score; NES – Normalized Enrichment Score; NOM *p*-val – Nominal *p*-value; FDR *q*-val – False Discovery Rate.

Table 2.3: Positively enriched gene sets in platelets from *ApoE*$^{-/-}$ mice infected with *C. pneumoniae* compared to untreated control – at Week 1.

NAME	SIZE	ES	NES	NOM *p*-val	FDR *q*-val
LIPOPROTEIN METABOLISM	26	0.775	2.083	<0.001	0.008
LIPID TRANSPORT	26	0.738	1.986	<0.001	0.015
PLATELET DEGRANULATION	80	0.597	1.994	<0.001	0.017
AMI PATHWAY	19	0.780	1.924	<0.001	0.026
ORGANELLE LOCALIZATION	24	0.731	1.893	0.002	0.027
INTRINSIC PATHWAY	23	0.731	1.909	<0.001	0.030
MAINTENANCE OF LOCALIZATION	19	0.758	1.895	<0.001	0.030
COMPLEMENT AND COAGULATION CASCADES	62	0.610	1.925	<0.001	0.032
CHYLOMICRON MEDIATED LIPID TRANSPORT	17	0.769	1.898	0.002	0.032
PROTEIN HETERODIMERIZATION ACTIVITY	71	0.569	1.871	<0.001	0.034
TRANSCRIPTION OF THE HIV GENOME	55	0.594	1.855	<0.001	0.040
P130CAS LINKAGE TO MAPK SIGNALING FOR INTEGRINS	15	0.777	1.837	0.002	0.043
RESPONSE TO NUTRIENT LEVELS	28	0.688	1.839	<0.001	0.046
STEROID BINDING	17	0.744	1.802	<0.001	0.065
HELICASE ACTIVITY	46	0.595	1.779	<0.001	0.065
REGULATION OF PROTEIN STABILITY	18	0.732	1.794	<0.001	0.067
GRB2 SOS PROVIDES LINKAGE TO MAPK SIGNALING FOR INTERGRINS	15	0.771	1.788	0.002	0.067
CYTOKINE SECRETION	15	0.762	1.779	0.004	0.068
FORMATION AND MATURATION OF MRNA TRANSCRIPT	137	0.493	1.781	<0.001	0.070
SELENOAMINO ACID METABOLISM	26	0.662	1.766	0.006	0.075

SIZE – Number of genes; ES – Enrichment Score; NES – Normalized Enrichment Score; NOM *p*-val – Nominal *p*-value; FDR *q*-val – False Discovery Rate.

Table 2.4: Negatively enriched gene sets in platelets from *ApoE*$^{-/-}$ mice infected with *C. pneumoniae* compared to untreated control – at Week 1.

NAME	SIZE	ES	NES	NOM *p*-val	FDR *q*-val
CALCIUM ION BINDING	88	-0.535	-1.789	<0.001	0.256
MITOCHONDRIAL RIBOSOME	20	-0.699	-1.742	0.002	0.260
IL1R PATHWAY	32	-0.658	-1.834	<0.001	0.266
EXTRACELLULAR MATRIX STRUCTURAL CONSTITUENT	24	-0.709	-1.803	<0.001	0.282
ORGANELLAR RIBOSOME	20	-0.699	-1.745	0.008	0.290
TOLL PATHWAY	36	-0.616	-1.758	<0.001	0.296
GSK3 PATHWAY	27	-0.636	-1.689	0.004	0.422
GLYCOSAMINOGLYCAN DEGRADATION	21	-0.742	-1.848	<0.001	0.424
RIBOSOMAL SUBUNIT	18	-0.690	-1.679	0.008	0.426
RIBOSOME	30	-0.598	-1.651	0.008	0.468
ACETYLCHOLINE BINDING	17	-0.688	-1.631	0.013	0.475
LYSOSOME	116	-0.465	-1.614	0.004	0.486
LEISHMANIA INFECTION	61	-0.512	-1.637	0.002	0.487
NTHI PATHWAY	23	-0.640	-1.654	0.008	0.498
NEGATIVE REGULATION OF CELL DIFFERENTIATION	25	-0.611	-1.602	0.022	0.505
REGULATION OF CELL DIFFERENTIATION	55	-0.524	-1.617	0.004	0.508
REGULATION OF MYELOID CELL DIFFERENTIATION	16	-0.670	-1.586	0.015	0.555
DIGESTION	36	-0.566	-1.579	0.017	0.556
CATION BINDING	188	-0.423	-1.560	<0.001	0.624
NFκB PATHWAY	23	-0.604	-1.549	0.023	0.653

SIZE – Number of genes; ES – Enrichment Score; NES – Normalized Enrichment Score; NOM *p*-val – Nominal *p*-value; FDR *q*-val – False Discovery Rate.

Nine weeks following the last infection with *P. gingivalis*, *C. pneumoniae*, or 9 weeks of feeding a Western diet, *ApoE*$^{-/-}$ mice were sacrificed in order to understand the changes in platelet transcripts before the formation of overt plaques. Following *P. gingivalis* infection, only 41 genes were increased and 32 were decreased (Figure 2.2). The top 5 genes that exhibited increased expression were *Mfap1a* (5.31-fold), *Trbv4* (4.21-fold), *Polr2c* (3.99-fold), *Cidec* (3.97-fold), and *Sms* (3.75-fold). Top 5 genes that exhibited decreased expression were *S100a8* (-4.15-fold), *S100a9* (-4.08-fold), *Olfr135* (-3.45-fold), *Fcf1* (-3.26-fold), and *Agk* (-3.01-fold). GSEA identified numerous gene sets positively enriched, including coagulation and signaling pathways; however, these gene sets were not significantly altered by *P. gingivalis* infection (NES >-2, FDR q >0.05; Table 2.5). It was the negatively enriched gene sets that were more significantly affected, including RNA/gene expression (NES ≤-2, Nom p <0.05, FDR q <0.05; Table 2.6).

Figure 2.2: Genes upregulated and downregulated at week 9 in *ApoE*$^{-/-}$ mice with bacterial infection or a Western diet. Heatmap shows the transcripts identified through microarray as upregulated or downregulated 2-fold or more by infection with *P. gingivalis* (Pg), *C. pneumoniae* (Cp), or fed a Western diet (WD) compared to untreated control in the *ApoE*$^{-/-}$ Mice. Each condition represents RNA from 3 mice pooled.

Week 9			
WD	Pg	Cp	
7.18	4.21	1.59	Trbv4
5.78	1.13	1.06	LOC100038947
5.09	2.89	2.37	2410018L13Rik
4.54	1.54	-1.51	Gm14118
4.22	-1.06	-2.56	Gm4964
3.90	2.60	4.34	Trav13-3
3.74	1.28	4.16	Tmx2
3.71	2.57	1.50	Gm8698
3.46	2.40	3.76	Gm5637
3.36	-1.09	-1.76	Gm10885
3.14	3.75	1.94	Sms
3.10	1.02	-1.13	E330020D12Rik
3.03	-1.04	1.91	Grpnat1
3.05	-1.48	-1.62	Igkv1-117
3.00	2.33	3.52	Rpl21
2.97	1.11	-1.49	Gm10878
2.96	1.84	1.28	Gm6749
2.95	-1.00	1.11	Gm5431
2.90	2.70	3.81	Nup62-ps1
2.82	1.18	1.27	Igkv14-111
2.76	-1.27	-1.14	Ahcy
2.75	-1.18	-1.02	Igh-1b
2.75	1.57	1.33	Ugt1a5
2.71	1.55	1.73	Serpina3l
2.71	1.84	1.09	5830417I10Rik
2.66	1.88	1.65	Olfr97
2.66	2.36	1.36	Gm189
2.64	1.46	1.24	Sfn
2.64	1.48	-1.17	Catspergl
2.63	1.79	1.35	Cd3d
2.60	1.20	1.16	Gsdmc3
2.58	2.24	-1.45	Trim34
2.55	-1.10	-1.29	Ear2
2.53	-1.33	-1.13	Ubiqp1
2.54	-1.19	1.02	Gm5416
2.53	1.10	1.40	Olfr612
2.53	2.19	1.89	IgLV2
2.52	2.11	1.90	Gm5965
2.50	1.19	1.43	2810055G20Rik
2.50	2.17	3.00	Gm7188
2.49	2.59	-1.71	Dppa3
2.48	1.36	1.78	Cd53
2.47	-1.15	-1.09	Cyp4a10
2.42	1.17	1.66	Gm14851
2.41	-2.18	-1.60	Gm1524
2.40	-1.59	-1.11	Col3
2.37	1.62	-1.08	Gm5476
2.35	-2.08	-1.61	Gm11710
2.35	2.01	1.46	Fcer2a
2.33	1.52	1.85	Tsnax
2.31	1.17	1.51	Gpraspl
2.30	-1.48	1.27	Gstm2
2.29	2.17	-1.09	Igkv12-44
2.29	1.03	1.20	Degs1
2.29	1.31	3.35	2fp59
2.27	1.30	1.27	Bin3
2.23	1.31	1.51	Lancl3
2.23	1.12	1.25	Sho1
2.23	2.52	1.10	H2-DMb1
2.24	1.05	-1.30	C330018D20Rik
2.23	1.25	1.27	Sstxb1
2.21	-1.25	-1.10	Ms4a6b
2.20	-1.30	-1.55	Pstm4
2.20	1.89	1.55	Mir540
2.19	2.01	-1.09	Mrpl22
2.19	1.07	1.71	Hist1h3a
2.18	-1.00	-1.05	Vmn2r84
2.18	-1.17	-1.10	Gm10883
2.18	1.27	2.28	Zfp617
2.18	1.47	1.72	Cenpq
2.18	1.21	-1.13	Gm8995
2.16	-1.91	-2.55	Npm1
2.16	1.65	2.07	6230400D17Rik
2.14	1.48	-1.04	Rbm12b
2.14	1.08	1.22	Sall
2.14	-1.01	1.17	Slc9a5
2.14	1.55	1.88	Med29
2.13	-1.53	-1.06	Ube2n
2.12	-1.83	-1.49	Trac
2.09	1.33	1.41	Dnm3os
2.09	1.85	-1.00	Trdjf
2.09	1.73	-1.03	Nt5c3l
2.08	1.86	1.40	Gm2666
2.07	1.65	1.07	Fxyd3
2.06	1.24	1.11	Ifi3
2.05	1.08	1.86	Pstmd10
2.04	1.43	1.61	H2-T10
2.04	-1.27	2.44	Mrto4
2.03	1.02	-1.00	Gpnmb
2.03	1.30	1.24	Grap

Week 9			
WD	Pg	Cp	
2.02	1.13	1.25	Il30
2.01	-1.11	1.49	Isl2
2.01	3.31	2.67	Mfap1a
1.95	1.48	3.35	Sat
1.93	3.53	4.28	Gm4459
1.91	2.32	1.45	Klrc2
1.89	2.09	1.30	Gm8909
1.88	2.54	3.72	6720489N17Rik
1.87	1.07	-2.08	Gm7362
1.86	1.69	2.62	Gm5168
1.80	-1.06	2.03	Aga
1.80	2.93	1.68	Podhgb5
1.77	-1.59	-2.20	Gngt2
1.72	2.05	1.40	Gm9803
1.71	2.37	1.71	Ndufs3
1.71	3.99	2.92	Pdlr2c
1.68	2.08	1.97	Podhia6
1.68	-2.29	-1.12	Igh-5
1.66	2.13	1.41	Olfr403
1.62	2.11	2.66	H3f3a
1.60	-1.26	-2.13	Gm9740
1.57	1.80	2.02	Gm10029
1.52	1.30	2.04	Gm13213
1.49	2.67	1.53	Il205
1.49	1.18	2.01	Gmeb1
1.48	2.24	1.40	Snora41
1.47	1.36	-4.01	Snora35b
1.45	-1.12	-2.13	Dock2
1.45	1.55	2.16	Igkv7-2
1.43	-1.32	-2.49	Nudt21
1.43	-2.16	1.19	Trim12
1.43	-1.47	-2.15	Samhd1
1.42	-1.65	-2.40	Rps24
1.40	2.65	1.82	Zcwpw2
1.40	2.91	1.30	Cldn22
1.39	4.21	3.99	Gm5154
1.36	-1.23	-2.84	Iqcf3
1.35	-1.03	2.64	Pfgdh
1.35	1.57	2.12	Podhec2
1.34	1.05	-2.83	Psmb3
1.33	1.26	2.82	Tymp
1.32	1.04	2.01	Olfr638
1.32	-1.46	-2.26	S100a4
1.30	3.54	1.10	Mageb16
1.28	-1.71	-2.87	Ass1
1.28	2.38	1.33	Dcakd
1.28	-1.38	-2.17	Lcp1
1.26	-1.54	-2.21	Cysp
1.25	1.68	2.77	C130026I21Rik
1.24	-1.00	-2.64	Eif2s1
1.23	-2.10	-3.04	Rps25
1.22	-1.44	-2.00	Fam111a
1.22	-1.82	-2.45	Sfn2
1.20	2.13	1.87	1700034H14Rik
1.20	-1.23	-3.01	Hnrl
1.19	1.65	2.86	Gm10767
1.19	1.23	2.08	D630032N06Rik
1.18	-3.26	-1.08	Fcrl1
1.16	2.88	-1.01	X76971
1.16	-1.00	-2.26	Scd1
1.14	-1.49	-2.37	Il27ra
1.12	-1.49	-2.56	Sfpi1
1.12	1.18	-2.04	Igk-C1
1.12	2.52	1.41	Fdps
1.11	1.41	2.24	Cda
1.11	1.49	2.48	BC061237
1.09	-1.17	-2.35	Srm 2
1.09	1.27	2.02	6530418L21Rik
1.07	1.34	2.09	Kiaa1109
1.06	-2.98	1.14	Gm15417
1.05	2.78	-1.28	Mfap5
1.05	-2.29	-2.14	Ugt2a2
1.04	1.25	2.05	L2hgdh
1.04	-1.17	-2.26	Mgp
1.04	-1.89	-3.72	Rangrf
1.03	-1.44	-2.19	Nmi
1.02	-1.62	-2.14	Nedd9
1.02	-1.00	-2.58	Dapl1
1.02	-1.92	-2.37	Il203
1.01	2.21	1.07	Olfr399
-1.00	2.48	-1.18	Lypla2
-1.00	-1.07	2.09	Rbp2
-1.00	-1.31	-2.00	Cd2ap
-1.00	-1.34	-2.02	Znhit1
-1.00	-1.00	-2.05	Eif4h
-1.00	-1.00	-2.22	4930562F07Rik
-1.00	-1.02	-2.30	Lsm2
-1.00	-1.00	-2.97	Snrpd3
-1.00	2.40	1.01	Rnu3a
-1.02	1.41	2.29	Dstn12

Week 9			
WD	Pg	Cp	
-1.02	-1.30	-2.43	Mrps28
-1.02	2.33	3.49	Aph1a
-1.04	-2.94	-2.56	Sfrs1
-1.05	-1.12	2.09	Gm5941
-1.05	-1.19	2.35	Fam136a
-1.06	1.43	2.01	Dpy19l3
-1.06	-1.14	-2.39	Ighg1
-1.06	-4.48	-1.56	9030624G23Rik
-1.07	-1.29	-2.25	Ifitm 6
-1.09	-1.30	-2.33	Csnk2a1
-1.10	-1.36	-2.40	Gm15210
-1.10	2.50	-1.07	4921509C19Rik
-1.10	-1.87	-2.67	Gstm1
-1.11	-1.79	-2.05	Snx20
-1.11	-1.53	-4.54	Gm11428
-1.11	-1.54	-2.18	Amc10
-1.12	1.11	-2.07	C3
-1.12	-1.82	-2.69	S100a6
-1.12	-2.56	1.46	LOC100048057
-1.13	-3.01	-1.44	Agk
-1.14	-1.46	-2.31	Rps27l
-1.16	-1.48	-2.53	Rgs2
-1.16	2.24	-1.17	Rdh7
-1.17	-1.22	-2.09	Cd3g
-1.17	-2.14	-2.34	Sfla31
-1.17	-2.14	-2.34	Sfla31
-1.17	-1.49	-2.04	Sfla3
-1.19	-2.05	-1.10	Plb
-1.19	2.58	-1.32	1110028F11Rik
-1.19	-1.00	-2.55	Gm5413
-1.21	-2.00	-1.34	Manea
-1.21	-1.77	-2.66	Pfkp
-1.22	-2.17	-1.31	Olfr441
-1.22	-2.08	-1.02	2400001E08Rik
-1.22	-1.51	-2.13	Gm9781
-1.23	-1.39	-2.03	Mrpl33
-1.24	2.51	1.60	1700034J23Rik
-1.26	-1.34	-2.19	Fkbp4
-1.27	-1.77	-2.34	Mrpl42
-1.28	3.97	-1.00	Cdkc
-1.28	-1.62	-2.32	Il28b
-1.28	-1.22	-2.27	Igl-V1
-1.29	-2.01	1.34	Loe1i
-1.30	-1.30	-2.14	Stpr1
-1.30	2.42	-1.63	Cyp2e1
-1.31	3.03	-1.74	Serpina1d
-1.33	-1.48	-2.00	Rwdd1
-1.33	-1.45	-2.24	Eif4a2
-1.35	-2.23	-1.43	Diablo
-1.37	-1.40	-6.79	Nono
-1.39	-2.35	-3.44	Gm6894
-1.39	-1.63	-2.01	Ddx28
-1.41	-2.14	-2.06	Rassf4
-1.42	-1.24	2.10	Pdlr3g
-1.44	-1.22	-2.57	Gbx1
-1.46	-1.95	-2.86	G3bp1
-1.47	-1.64	-2.97	Olfr3
-1.47	-1.63	-2.01	Tfam
-1.48	-2.10	-2.50	Igh-3
-1.50	-1.78	-2.32	Igkv12-46
-1.52	-2.13	-1.67	Gm10884
-1.53	-2.37	-1.33	Zcchc17
-1.53	-2.04	-1.56	Polh
-1.55	-2.33	-2.29	Ifitm 1
-1.55	1.97	-2.09	Podhia5
-1.56	-1.96	-2.88	Mndal
-1.56	1.18	-2.34	Cyp2d10
-1.57	-3.45	-3.10	Olfr135
-1.57	-2.01	1.20	Gm6712
-1.60	1.19	-4.12	Ly6c1
-1.62	2.08	-1.88	Apoc3
-1.67	-2.01	-1.35	Exosc7
-1.67	-1.13	-2.77	Gm7015
-1.69	-2.22	1.36	Podhga10
-1.73	-3.33	-2.34	1830127L07Rik
-1.74	-4.15	-9.38	S100a8
-1.77	1.08	-2.07	Gm6252
-1.77	-2.01	-1.36	Igk-V21-12
-1.80	-1.19	-4.41	Rpl18a
-1.80	-4.08	-9.38	S100a9
-1.83	-2.07	-1.83	Car1
-1.87	-1.49	-2.01	Mad4
-1.87	-2.19	-2.25	Prp
-1.90	-2.34	-1.83	Igk-V19-20
-1.90	-1.27	-2.10	Olfr1337
-1.94	-1.82	-4.11	Gm13212
-1.98	-1.25	-2.11	Cdo1
-2.00	1.14	-1.08	0610010O12Rik
-2.00	-1.24	-1.51	Mir1
-2.01	-1.03	1.05	Olfr57

Week 9			
WD	Pg	Cp	
-2.02	1.10	-1.10	Snord104
-2.02	-1.11	-1.52	Lrgf
-2.03	-1.58	-1.67	Thrsp
-2.03	-1.97	-3.01	Gm10651
-2.04	-1.16	-1.07	St3gal6
-2.04	-1.17	1.45	Gm8973
-2.05	-1.81	-1.81	Gm129
-2.05	-2.09	-1.07	Gm13931
-2.06	-1.37	-1.63	Gm10643
-2.06	-4.12	-1.30	9330159H04Rik
-2.06	1.09	-2.05	Vtn
-2.07	-2.73	-2.07	Olfr205
-2.07	1.44	-2.41	Prnt
-2.08	1.54	-2.94	Fgb
-2.08	-1.61	-1.08	Gm5321
-2.09	-1.41	-1.24	Krt8
-2.09	-1.50	-1.43	Apol10a
-2.10	1.28	-1.14	Olfr1162
-2.14	-1.11	-1.42	Gm6981
-2.14	-1.50	-1.18	C87977
-2.17	-1.32	-1.42	Igkv1-69
-2.18	-1.27	-1.41	Ptpn5
-2.18	-1.25	-1.32	Zfp580
-2.20	-1.35	-1.34	Olfr1371
-2.22	1.28	1.05	Podhia8
-2.22	-1.53	-1.12	Rbm xrt
-2.24	-1.18	-1.19	Mrgpra3
-2.24	-1.18	-1.23	Gm4943
-2.24	-2.29	-3.02	Mrps18a
-2.25	1.59	-1.46	Hamp
-2.26	-1.84	-1.35	Tmem 159
-2.26	-1.95	-1.95	2310034G01Rik
-2.27	-1.16	-1.02	Mir700
-2.28	-1.56	-1.56	Zfp623
-2.30	-2.38	-1.30	Acot9
-2.31	-1.66	-1.67	Gm8096
-2.31	3.58	-3.69	Serpina1c
-2.32	-1.49	-3.14	Mrps26
-2.33	-1.55	-1.99	Mt2
-2.33	1.46	-1.16	5830417G23Rik
-2.36	1.06	-1.08	Hp
-2.37	1.67	-3.11	Apoc1
-2.39	1.15	-2.10	Gnpda1
-2.41	1.38	-1.59	Cetn4
-2.45	-1.39	-1.28	Olfr1077-ps1
-2.45	-1.53	-1.77	Klrc1
-2.55	1.52	-2.12	Mgst1
-2.56	-1.91	-1.62	Gm10455
-2.57	-2.63	-2.34	Vmn2r66
-2.58	-1.52	-1.52	Hsd17b7
-2.59	-1.16	-2.65	Fabp5
-2.62	2.90	-1.49	Cfd
-2.66	-1.49	-1.38	Rbpj
-2.68	-1.01	-1.48	Snora73b
-2.70	-1.02	-2.36	Ahsg
-2.71	-1.00	-1.84	Bgn
-2.71	-1.94	-1.10	Hist1h4f
-2.77	1.37	-1.14	Es31
-2.83	1.27	-2.61	Pzp
-2.84	1.80	-1.77	Ambp
-2.90	1.31	-2.82	Trf
-2.91	-1.67	-2.02	Olfr406-ps
-2.97	1.70	-2.98	Gc
-3.08	-1.17	-1.38	Nutf2
-3.15	-3.75	-2.21	Gm5514
-3.32	-2.47	-1.99	Loe1c
-3.39	-1.59	-3.73	Rhps1
-3.64	-1.34	-1.06	Ugt1a2
-3.69	2.29	-3.03	Car3
-3.74	-1.24	-1.42	Krt81
-3.86	1.75	-3.11	Fgg
-3.91	1.38	-3.55	Mup3
-4.26	1.24	-4.06	Apoa1
-4.35	1.93	-4.25	Serpina3k
-4.55	1.66	-3.42	Apoa2
-4.95	1.46	-4.63	Serpina1b
-4.97	-2.02	-1.19	Gm11937
-5.51	1.68	-5.46	Ttr
-6.89	2.75	-3.98	Fabp1
-18.34	1.81	-15.46	Alb

Table 2.5: Positively enriched gene sets in platelets from *ApoE*$^{-/-}$ Mice infected with *P. gingivalis* compared to untreated control – at Week 9.

NAME	SIZE	ES	NES	NOM *p*-val	FDR *q*-val
NEUROPEPTIDE RECEPTOR ACTIVITY	21	0.750	1.912	0.002	0.052
COMPLEMENT AND COAGULATION CASCADES	62	0.623	1.942	<0.001	0.060
NEUROPEPTIDE BINDING	22	0.721	1.821	0.002	0.093
PEPTIDE RECEPTOR ACTIVITY	48	0.605	1.802	<0.001	0.100
GLUCONEOGENESIS	28	0.685	1.822	0.002	0.116
PLATELET DEGRANULATION	80	0.560	1.836	<0.001	0.128
COMPLEMENT CASCADE	18	0.727	1.752	0.018	0.172
RESPONSE TO NUTRIENT	16	0.738	1.738	0.009	0.180
AMI PATHWAY	19	0.702	1.709	0.007	0.227
RESPONSE TO EXTRACELLULAR STIMULUS	32	0.585	1.636	0.011	0.248
COMP PATHWAY	16	0.708	1.666	0.006	0.252
G-PROTEIN COUPLED RECEPTOR ACTIVITY	172	0.448	1.651	<0.001	0.255
METABOLISM OF BILE ACIDS AND BILE SALTS	26	0.613	1.638	0.016	0.256
RESPONSE TO NUTRIENT LEVELS	28	0.622	1.658	0.009	0.257
PROTEIN SECRETION	28	0.620	1.678	0.004	0.262
INTRINSIC PATHWAY	23	0.648	1.669	0.007	0.265
PEPTIDE BINDING	79	0.500	1.639	0.002	0.268
RHODOPSIN LIKE RECEPTOR ACTIVITY	123	0.480	1.682	<0.001	0.276
DETECTION OF CHEMICAL STIMULUS	15	0.706	1.608	0.027	0.309
STRUCTURAL CONSTITUENT OF MUSCLE	26	0.603	1.598	0.015	0.324

SIZE – Number of genes; ES – Enrichment Score; NES – Normalized Enrichment Score; NOM *p*-val – Nominal *p*-value; FDR *q*-val – False Discovery Rate.

Table 2.6: Negatively enriched gene sets in platelets from *ApoE*$^{-/-}$ mice infected with *P. gingivalis* compared to untreated control – at Week 9.

NAME	SIZE	ES	NES	NOM *p*-val	FDR *q*-val
TRANSPORT OF MATURE mRNA DERIVED FROM AN INTRON CONTAINING TRANSCRIPT	45	-0.641	-1.847	<0.001	0.036
TRANSPORT OF THE SLBP INDEPENDENT MATURE mRNA	29	-0.701	-1.840	<0.001	0.036
SPLICEOSOME	108	-0.579	-1.911	<0.001	0.038
FORMATION OF THE TERNARY COMPLEX, 43S COMPLEX	32	-0.709	-1.887	<0.001	0.038
FORMATION OF A POOL OF FREE 40S SUBUNITS	49	-0.641	-1.831	<0.001	0.038
ATP DEPENDENT RNA HELICASE ACTIVITY	15	-0.807	-1.854	<0.001	0.039
TRANSLATION INITIATION COMPLEX FORMATION	38	-0.669	-1.872	<0.001	0.042
GTP HYDROLYSIS, JOINING OF 60S RIBOSOMAL SUBUNIT	58	-0.626	-1.859	<0.001	0.043
RNA HELICASE ACTIVITY	22	-0.776	-1.926	<0.001	0.055
RNA DEPENDENT ATPASE ACTIVITY	16	-0.779	-1.789	0.002	0.060
ATP DEPENDENT HELICASE ACTIVITY	24	-0.705	-1.793	0.002	0.061
ACTIVATION OF NFκB TRANSCRIPTION FACTOR	18	-0.752	-1.798	0.004	0.062
SPLICEOSOME	38	-0.642	-1.782	0.002	0.062
RNA SPLICING	76	-0.572	-1.776	<0.001	0.064
GENE EXPRESSION	357	-0.468	-1.759	<0.001	0.067
RNA BINDING	195	-0.495	-1.765	<0.001	0.070
POSITIVE REGULATION OF TRANSCRIPTION FACTOR ACTIVITY	24	-0.694	-1.759	0.006	0.070
tRNA METABOLIC PROCESS	18	-0.735	-1.738	0.004	0.080
ANTIGEN PROCESSING AND PRESENTATION	49	-0.604	-1.741	<0.001	0.081
POSITIVE REGULATION OF BINDING	28	-0.655	-1.734	0.002	0.081

SIZE – Number of genes; ES – Enrichment Score; NES – Normalized Enrichment Score; NOM *p*-val – Nominal *p*-value; FDR *q*-val – False Discovery Rate.

Nine weeks following the last infections with *C.pneumoniae*, there was differential effects on gene expression profiles as compared to that observed early after infection. Twenty-seven genes were increased and 109 decreased at week 9 compared to untreated control (Figure 2.2). The top 5 genes with increased expression at week 9 were *Rpl21* (5.52-fold), *Trav13-3* (4.34-fold), *Tmx2* (4.16-fold), *Nup62-il4i1* (3.81-fold), and *Aph1a* (3.48-fold). The top 5 genes with decreased expression at week 9 were *Alb* (-16.46-fold), *S100a9* (-9.38-fold), *S100a8* (-9.38-fold), *Nono* (-6.79-fold), and *Ttr* (-5.46-fold). Similarly to *P. gingivalis* at week 9, GSEA identified numerous gene sets positively enriched but that were not significantly affected by *C. pneumoniae* (Table 2.7). Gene sets negatively enriched at week 9 were significant, including coagulation, RNA/gene expression, and inflammation (NES <-2, Nom p <0.01, FDR q <0.05 Table 2.8).

In mice fed a Western diet for 9 weeks, there were 67 genes increased and 67 genes decreased (Figure 2.2). The top 5 genes that exhibited increased expression as a result of a Western diet were *Trbv4* (7.14-fold), *Trav13-3* (3.90-fold), *Tmx2* (3.74-fold), *Sms* (3.14-fold), and *Gnpnat1* (3.05-fold). The top 5 genes with decreased expression with a Western diet were *Alb* (-18.34-fold), *Fabp1* (-6.89-fold), *Ttr* (-5.51-fold), *Serpina1b* (-4.95-fold), and *Apoa2* (-4.95-fold). Numerous gene sets were positively enriched, including those associated with DNA/proliferation, inflammation, RNA/gene expression, and signaling (NES >2, Nom p <0.05, FDR q <0.05; Table 2.9). Only a few gene sets were negatively enriched, including those involved in coagulation and lipid (NES <-2, Nom p

<0.01, FDR *q* <0.05; Table 2.10). As a way to verify these results, RT-qPCR was run on week 9 samples for *MFAP1A*. As seen in Figure 2.3, there is an increase in its expression with *P. gingivalis* infection that is greater than the increase with *C. pneumoniae* infection or a Western diet, similar to the findings in the microarray.

Table 2.7: Positively enriched gene sets in platelets from *ApoE*$^{-/-}$ mice infected with *C. pneumoniae* compared to untreated control – at Week 9.

NAME	SIZE	ES	NES	NOM *p*-val	FDR *q*-val
NEUROTRANSMITTER RECEPTOR ACTIVITY	49	0.658	2.007	<0.001	0.017
NEUROPEPTIDE RECEPTOR ACTIVITY	21	0.771	1.966	<0.001	0.018
NEUROTRANSMITTER BINDING	52	0.604	1.848	0.003	0.058
NEUROPEPTIDE BINDING	22	0.737	1.849	<0.001	0.073
APICAL PART OF CELL	17	0.764	1.850	<0.001	0.094
PEPTIDE RECEPTOR ACTIVITY	48	0.587	1.771	<0.001	0.139
ACETYLCHOLINE BINDING	17	0.738	1.737	<0.001	0.160
ANION CATION SYMPORTER ACTIVITY	15	0.737	1.745	0.009	0.164
RESPONSE TO NUTRIENT	16	0.725	1.711	0.012	0.197
PHOSPHOLIPASE C ACTIVITY	15	0.719	1.675	0.010	0.261
STRUCTURAL CONSTITUENT OF MUSCLE	26	0.617	1.642	0.005	0.306
SYNAPTIC VESICLE	15	0.701	1.648	0.017	0.311
NEGATIVE REGULATION OF DNA METABOLIC PROCESS	16	0.685	1.611	0.020	0.385
SECRETORY GRANULE	17	0.648	1.578	0.032	0.424
SYMPORTER ACTIVITY	30	0.576	1.590	0.010	0.432
RHODOPSIN LIKE RECEPTOR ACTIVITY	123	0.445	1.581	0.004	0.440
TRANS GOLGI NETWORK	18	0.647	1.541	0.030	0.464
SECONDARY ACTIVE TRANSMEMBRANE TRANSPORTER ACTIVITY	44	0.509	1.544	0.019	0.477
LYSOSOME	116	0.437	1.545	0.007	0.500
REGULATION OF PEPTIDYL TYROSINE PHOSPHORYLATION	16	0.653	1.547	0.031	0.520

SIZE – Number of genes; ES – Enrichment Score; NES – Normalized Enrichment Score; NOM *p*-val – Nominal *p*-value; FDR *q*-val – False Discovery Rate.

Table 2.8: Negatively enriched gene sets in platelets from *ApoE*$^{-/-}$ mice infected with *C. pneumoniae* compared to untreated control – at Week 9.

NAME	SIZE	ES	NES	NOM *p*-val	FDR *q*-val
TRANSLATION	71	-0.753	-2.207	<0.001	<0.001
GTP HYDROLYSIS, JOINING OF 60S RIBOSOMAL SUBUNIT	58	-0.780	-2.194	<0.001	<0.001
PEPTIDE CHAIN ELONGATION	38	-0.819	-2.169	<0.001	<0.001
FORMATION OF A POOL OF FREE 40S SUBUNITS	49	-0.798	-2.155	<0.001	<0.001
VIRAL MRNA TRANSLATION	39	-0.801	-2.135	<0.001	<0.001
RIBOSOME	39	-0.807	-2.115	<0.001	<0.001
REGULATION OF GENE EXPRESSION IN BETA CELLS	56	-0.741	-2.095	<0.001	<0.001
SPLICEOSOME	108	-0.660	-2.065	<0.001	<0.001
STRUCTURAL CONSTITUENT OF RIBOSOME	44	-0.758	-2.042	<0.001	<0.001
TRANSLATION INITIATION COMPLEX FORMATION	38	-0.770	-2.052	<0.001	<0.001
RNA SPLICING	76	-0.689	-2.021	<0.001	<0.001
REGULATION OF BETA CELL DEVELOPMENT	69	-0.700	-2.033	<0.001	<0.001
PLATELET DEGRANULATION	80	-0.675	-1.997	<0.001	0.001
FORMATION OF THE TERNARY COMPLEX, 43S COMPLEX	32	-0.787	-1.998	<0.001	0.001
RNA BINDING	195	-0.600	-1.986	<0.001	0.001
RNA HELICASE ACTIVITY	22	-0.836	-1.982	<0.001	0.001
ANTIGEN PROCESSING AND PRESENTATION	49	-0.724	-1.986	<0.001	0.001
INFLUENZA LIFE CYCLE	87	-0.652	-1.967	<0.001	0.001
ATP DEPENDENT HELICASE ACTIVITY	24	-0.811	-1.968	<0.001	0.001
REGULATION OF LIPID METABOLISM BY PPARα	60	-0.688	-1.954	<0.001	0.001
GENE EXPRESSION	357	-0.563	-1.955	<0.001	0.001
PPAR SIGNALING PATHWAY	67	-0.679	-1.956	<0.001	0.001
INFLUENZA VIRAL RNA TRANSCRIPTION, REPLICATION	54	-0.689	-1.958	<0.001	0.001
RNA PROCESSING	146	-0.607	-1.944	<0.001	0.001
LIPOPROTEIN METABOLISM	26	-0.783	-1.937	<0.001	0.002
PPARα PATHWAY	56	-0.680	-1.928	<0.001	0.002

SIZE – Number of genes; ES – Enrichment Score; NES – Normalized Enrichment Score; NOM *p*-val – Nominal *p*-value; FDR *q*-val – False Discovery Rate.

Table 2.9: Positively enriched gene sets in platelets from *ApoE*$^{-/-}$ mice on a Western diet compared to untreated control – at Week 9.

NAME	SIZE	ES	NES	NOM *p*-val	FDR *q*-val
M-G1 TRANSITION	59	0.678	2.125	<0.001	<0.001
ORC1 REMOVAL FROM CHROMATIN	61	0.665	2.084	<0.001	0.001
CDT1 ASSOCIATION WITH THE CDC6 ORC ORIGIN COMPLEX	50	0.687	2.072	<0.001	0.001
P53-INDEPENDENT DNA DAMAGE RESPONSE	41	0.727	2.096	<0.001	0.001
HOST INTERACTIONS OF HIV FACTORS	108	0.590	2.033	<0.001	0.001
DNA REPLICATION PRE INITIATION	73	0.631	2.041	<0.001	0.001
PD1 SIGNALING	18	0.843	2.045	<0.001	0.001
STABILIZATION OF P53	44	0.715	2.056	<0.001	0.001
VIF MEDIATED DEGRADATION OF APOBEC3G	43	0.718	2.096	<0.001	0.002
SIGNALING BY WNT	56	0.639	1.995	<0.001	0.002
DOWNSTREAM TCR SIGNALING	36	0.711	1.979	<0.001	0.003
REGULATION OF ORNITHINE DECARBOXYLASE	46	0.667	1.961	<0.001	0.003
PROTEASOME	42	0.675	1.965	<0.001	0.003
AUTODEGRADATION OF CDH1 BY CDH1 APC	54	0.642	1.963	<0.001	0.003
SYNTHESIS OF DNA	86	0.594	1.966	<0.001	0.004
SCF β TRCP MEDIATED DEGRADATION OF EMI1	46	0.660	1.927	<0.001	0.005
TRANSLATION INITIATION COMPLEX FORMATION	38	0.660	1.909	0.002	0.006
TCR SIGNALING	52	0.627	1.911	<0.001	0.007
CDC20 PHOSPHO-APC MEDIATED DEGRADATION OF CYCLIN A	60	0.613	1.897	<0.001	0.009
FORMATION OF THE TERNARY COMPLEX, 43S COMPLEX	32	0.686	1.875	<0.001	0.012
PHOSPHORYLATION OF CD3 AND TCR ζ CHAINS	15	0.803	1.869	<0.001	0.013
REGULATION OF APC ACTIVATORS BETWEEN G1-S, EARLY ANAPHASE	67	0.580	1.857	<0.001	0.015
T CELL ACTIVATION	42	0.633	1.846	0.002	0.017
SCF SKP2 MEDIATED DEGRADATION OF P27 P21	50	0.615	1.847	<0.001	0.017
PREFOLDIN MEDIATED TRANSFER	25	0.686	1.842	<0.001	0.018

OF SUBSTRATE TO CCT TRIC					
GENERATION OF SECOND MESSENGER MOLECULES	25	0.715	1.833	<0.001	0.019
DNA DAMAGE RESPONSE SIGNAL TRANSDUCTION	33	0.665	1.821	<0.001	0.021
TRANSLATION	71	0.567	1.816	<0.001	0.022
ASTHMA	21	0.706	1.807	0.002	0.024
GTPASE REGULATOR ACTIVITY	55	0.583	1.802	<0.001	0.024
REGULATION OF ACTION POTENTIAL	16	0.768	1.808	0.004	0.024
REACTOME S PHASE	100	0.532	1.804	<0.001	0.024
MITOSIS	80	0.546	1.797	<0.001	0.025
CELL CYCLE CHECKPOINTS	105	0.530	1.788	<0.001	0.027
RAS GUANYL NUCLEOTIDE EXCHANGE FACTOR ACTIVITY	17	0.749	1.768	0.006	0.032
M PHASE OF MITOTIC CELL CYCLE	82	0.540	1.766	<0.001	0.033
HEMATOPOIETIC CELL LINEAGE	73	0.553	1.772	<0.001	0.033
CYCLIN E ASSOCIATED EVENTS DURING G1-S TRANSITION	56	0.577	1.768	0.002	0.033
HIV INFECTION	168	0.496	1.770	<0.001	0.033
INFLUENZA VIRAL RNA TRANSCRIPTION AND REPLICATION	54	0.570	1.757	<0.001	0.036
MITOTIC M M-G1 PHASES	151	0.494	1.754	<0.001	0.037
PROTEIN MODIFICATION BY SMALL PROTEIN CONJUGATION	41	0.596	1.750	0.002	0.038
B CELL RECEPTOR SIGNALING PATHWAY	73	0.534	1.739	<0.001	0.041
CHAPERONIN MEDIATED PROTEIN FOLDING	46	0.575	1.741	<0.001	0.042
UBIQUITIN CYCLE	46	0.595	1.739	<0.001	0.042
METABOLISM OF PROTEINS	162	0.482	1.735	<0.001	0.042
CYSTEINE TYPE ENDOPEPTIDASE ACTIVITY	37	0.615	1.730	<0.001	0.045
M PHASE	109	0.510	1.727	<0.001	0.046

SIZE – Number of genes; ES – Enrichment Score; NES – Normalized Enrichment Score; NOM *p*-val – Nominal *p*-value; FDR *q*-val – False Discovery Rate.

Table 2.10: Negatively enriched gene set in platelets from *ApoE*$^{-/-}$ mice on a Western diet compared to untreated control – at Week 9.

NAME	SIZE	ES	NES	NOM *p*-val	FDR *q*-val
PLATELET DEGRANULATION	80	-0.665	-2.147	<0.001	0.001
LIPOPROTEIN METABOLISM	26	-0.749	-1.971	<0.001	0.021
OXYGEN BINDING	19	-0.776	-1.951	<0.001	0.022
P130 CAS LINKAGE TO MAPK SIGNALING FOR INTEGRINS	15	-0.778	-1.791	0.004	0.069
CYTOKINE SECRETION	15	-0.768	-1.774	0.006	0.074
REGULATION OF PROTEIN SECRETION	18	-0.733	-1.791	0.002	0.075
AMI PATHWAY	19	-0.748	-1.797	<0.001	0.076
PPAR SIGNALING PATHWAY	67	-0.591	-1.860	<0.001	0.080
PPARα PATHWAY	56	-0.601	-1.844	<0.001	0.080
IMMUNE EFFECTOR PROCESS	33	-0.664	-1.820	<0.001	0.080
ANTIGEN BINDING	16	-0.771	-1.774	0.004	0.080
REGULATION OF PROTEIN STABILITY	18	-0.749	-1.800	0.002	0.082
COMPLEMENT AND COAGULATION CASCADES	62	-0.581	-1.807	0.002	0.085
LIPID TRANSPORT	26	-0.695	-1.824	<0.001	0.089
GAP JUNCTION ASSEMBLY	17	-0.747	-1.744	0.004	0.100
PROTEIN SECRETION	28	-0.643	-1.732	<0.001	0.109
COLLAGEN	23	-0.676	-1.720	<0.001	0.112
METABOLISM OF BILE ACIDS AND BILE SALTS	26	-0.641	-1.721	0.006	0.117
REGULATION OF MAP3K CASCADE	17	-0.718	-1.709	0.010	0.120
REGULATION OF HEART CONTRACTION	22	-0.664	-1.704	0.008	0.121

SIZE – Number of genes; ES – Enrichment Score; NES – Normalized Enrichment Score; NOM *p*-val – Nominal *p*-value; FDR *q*-val – False Discovery Rate.

Figure 2.3: Verification of microarray analysis through RT-qPCR. Gene expression for *Mfap1a* at Week 9 identified through the microarray were verified using RT-qPCR. Each condition represents RNA from 3 mice pooled.

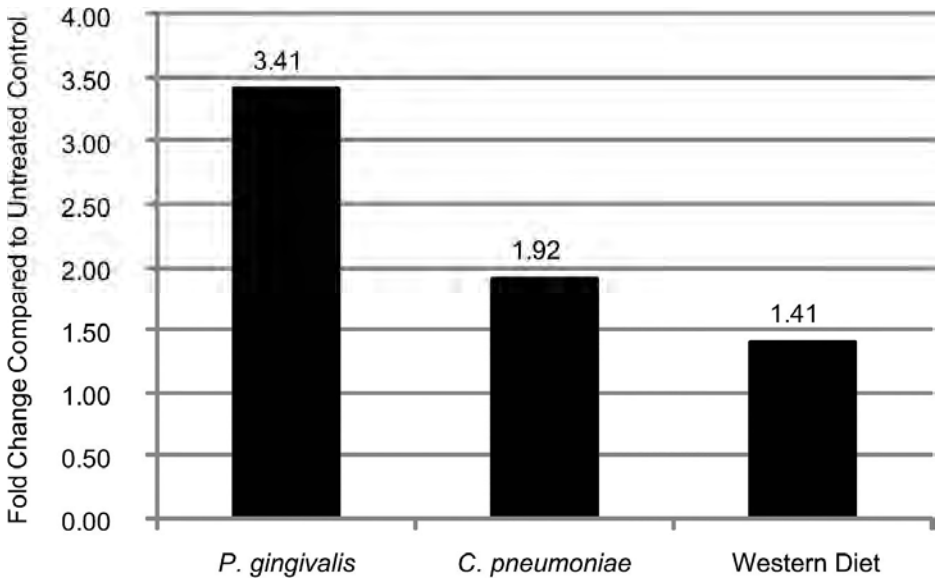

Differential physiological effects of bacterial infections or a Western diet in *ApoE*$^{-/-}$ mice

There were no changes in body mass (Figure 2.4), or increases in white blood cell (WBC) counts (Figure 2.5*a*) at week 1 in *ApoE*$^{-/-}$ mice infected with either *P. gingivalis* or *C. pneumoniae*. Only *C. pneumoniae* altered platelet counts (Figure 2.5*b*) compared to untreated control, although not significantly, suggesting this bacterial infection altered megakaryocyte maturation and platelet production and/or platelet clearance. Circulating heterotypic aggregates (platelet-neutrophil aggregates) were significantly increased in *C. pneumoniae* infected mice at week 1 (Figure 2.6); however, there were inconsistencies with the *P. gingivalis*-infected

ApoE$^{-/-}$ mice, but the data suggest that there was an increase in aggregate formation as well. Analysis of spleen sections from *P. gingivalis* or *C. pneumoniae* infected mice revealed increased CD41 levels, a platelet marker, and Ly6G levels, a neutrophil marker (Figure 2.7*a-c*; IgG controls in Figure 2.8). However, there were no heterotypic aggregates as indicated by the lack of overlap between the two signals when merged (Figure 2.7*a,d*).

Figure 2.4: Change in *ApoE*$^{-/-}$ mouse body mass with infection and diet.
Mass was measured on Week 1, which was 24 h after the last *P. gingivalis* challenge and 4 days after *C. pneumoniae* exposure (n = 3 for each group), and on Week 9 (n = 3 for Untreated Control, *P. gingivalis*-Infected, and *C. pneumoniae*-Infected; n = 6 for Western diet). Data is normally distributed and analyzed using an ANOVA.

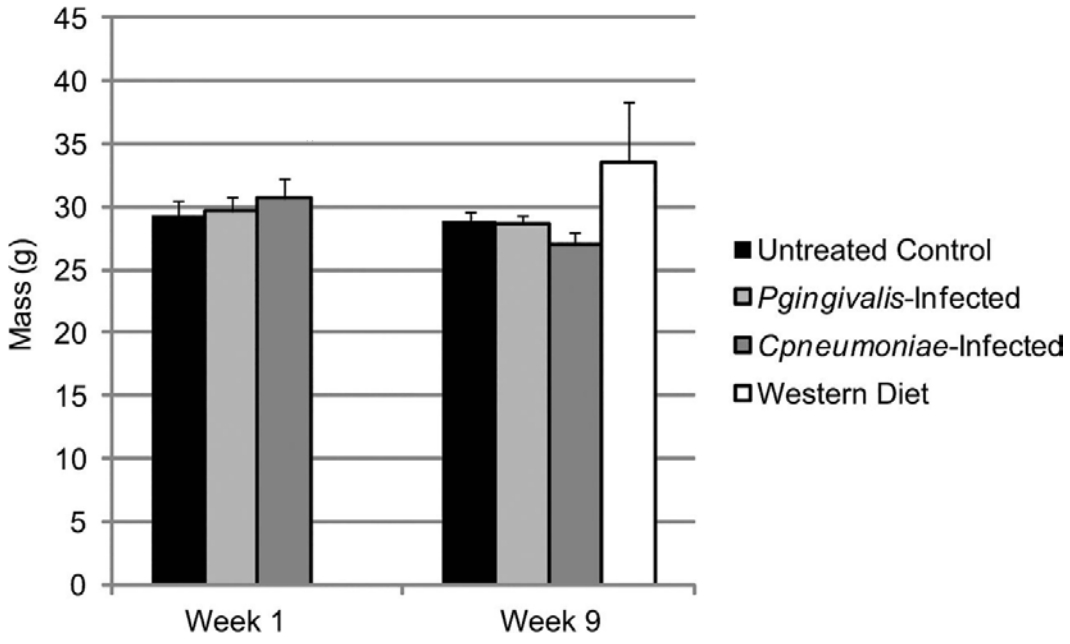

Figure 2.5: WBC and platelet count changes with infection and diet in the *ApoE*$^{-/-}$ mice. Whole blood cell counts were assessed to determine the number of WBC and platelets. Measurements were performed on Week 1, which was 24 h after the last *P. gingivalis* challenge and 4 days after exposure to *C. pneumoniae* (n = 3 for each group), and on Week 9 (n = 3 for untreated control, *P. gingivalis*-Infected, and *C. pneumoniae*-Infected; n = 6 for Western diet). Data is normally distributed and analyzed using an ANOVA.

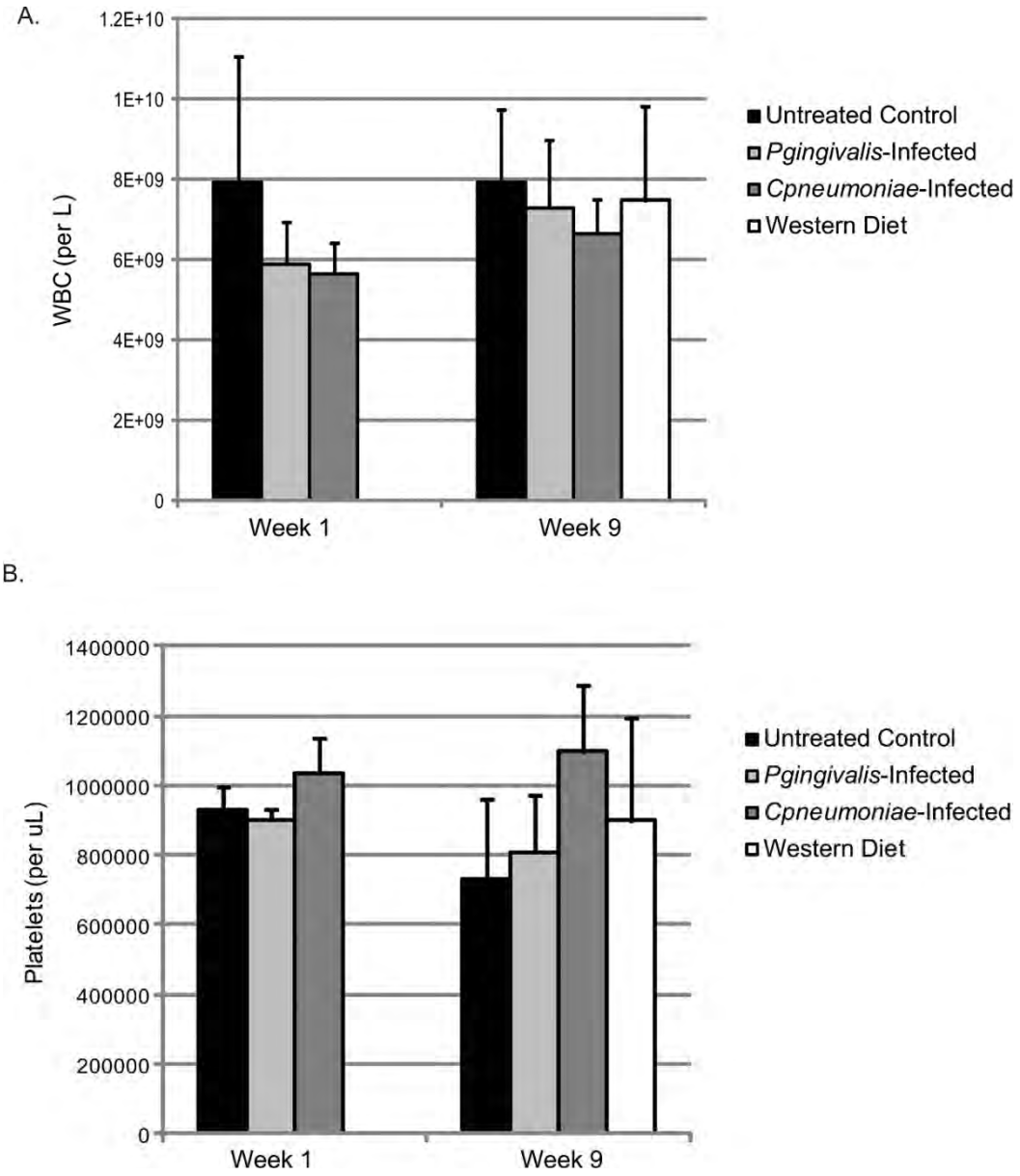

Figure 2.6: Heterotypic aggregate formation in *ApoE*$^{-/-}$ mice with infection and diet. Whole blood samples taken on Week 1 (24 h after the last *P. gingivalis* challenge and 4 days after exposure to *C. pneumoniae*; n = 3 for each group) and on Week 9 (n = 3 for each group) and dual stained for platelet marker (CD41) and neutrophil marker (Ly6G). The percent of platelet-positive neutrophils were determined through flow cytometry and normalized to untreated control at each timepoint. Data is normally distributed and analyzed using an ANOVA. *p<0.05 compared to untreated control at Week 1.

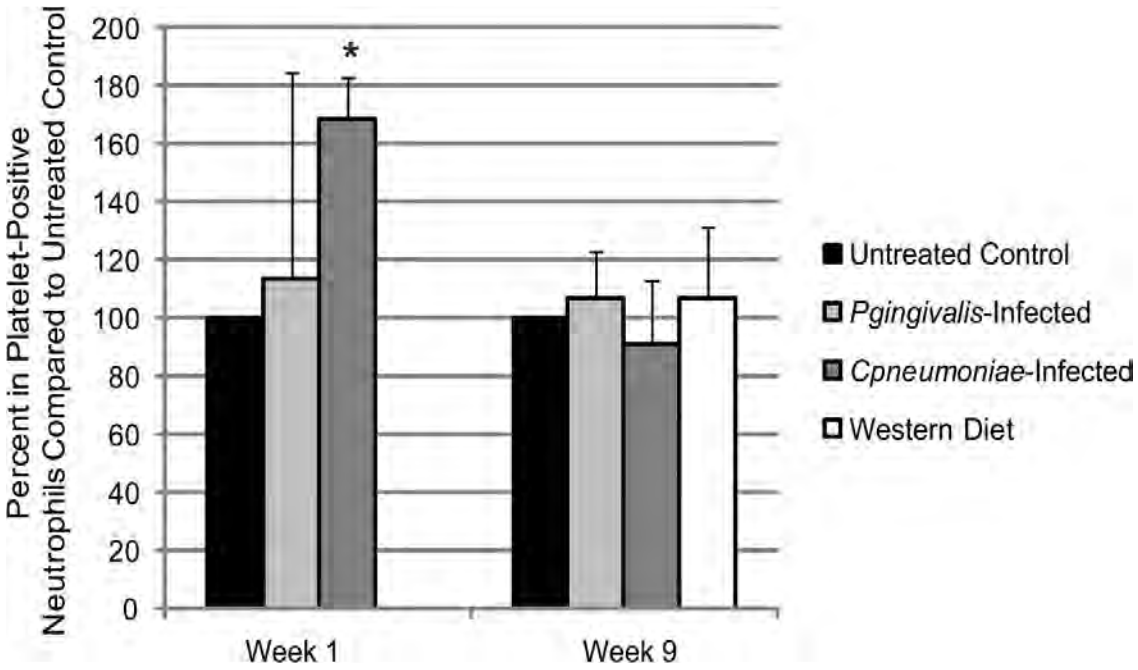

Figure 2.7: Platelet and neutrophil content in spleens in *ApoE*$^{-/-}$ mice with infection and diet. (A) Spleen sections from *ApoE*$^{-/-}$ mice at week 1 and week 9 were stained for CD41 (platelet marker; Alexa Fluor 405) and Ly6G (neutrophils; Texas Red) and visualized by confocal microscopy at 63X. The amount of CD41 staining (area; B), Ly6G staining (area; C), and the overlap of each signal (% pixels with overlapping signal); (D) were quantified. Data is normally distributed and analyzed using an ANOVA. n = 3 for each condition; ***p<0.001 compared to untreated control. Scale Bar in merged images = 50.0 µm.

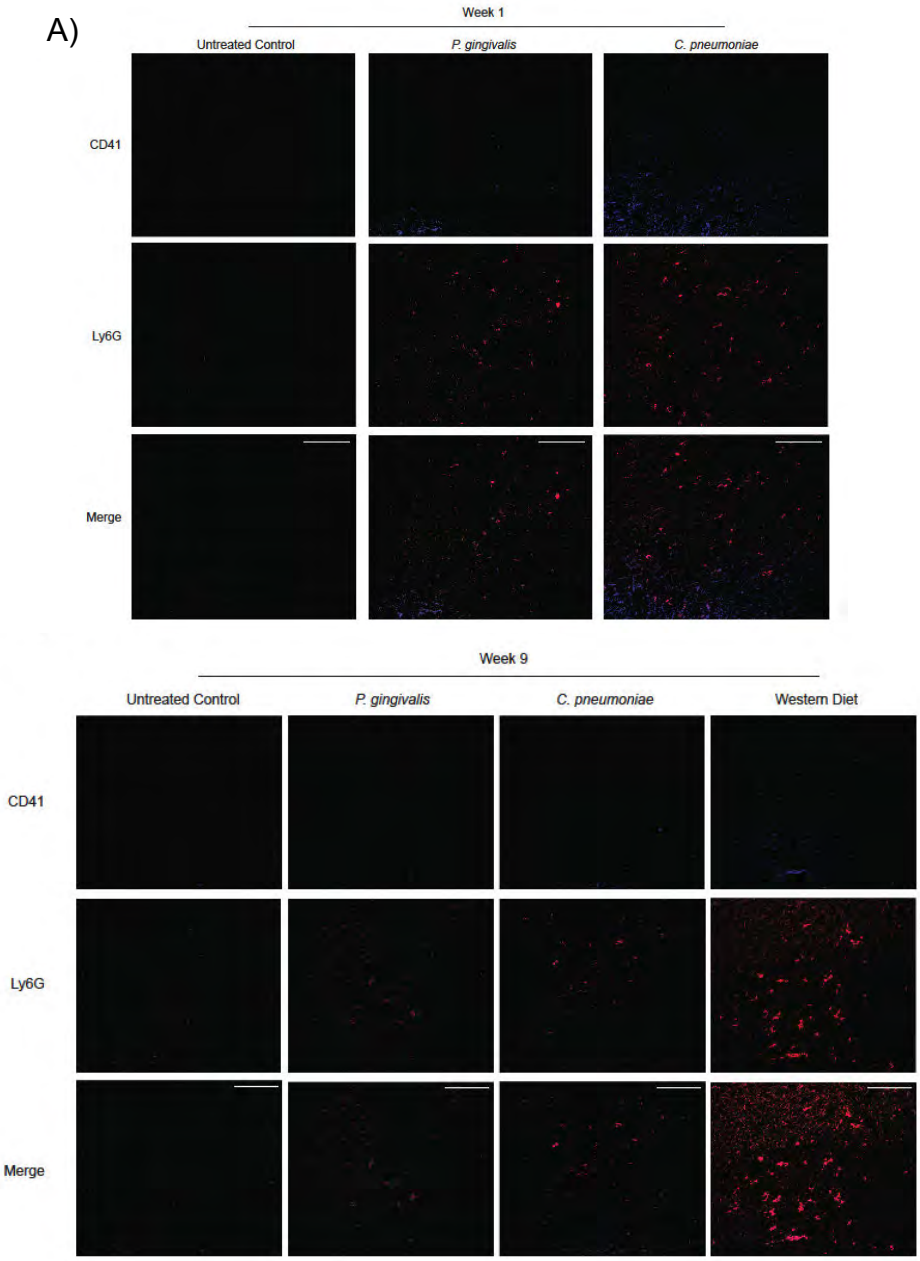

B)

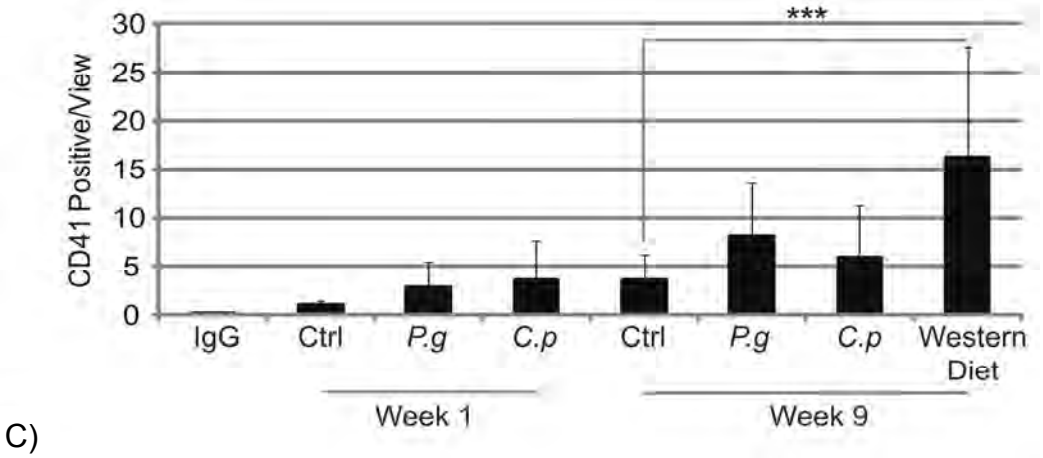
***
CD41 Positive/View
30
25
20
15
10
5
0
IgG
Ctrl
P.g
C.p
Ctrl
P.g
C.p
Western Diet
Week 1
Week 9

C)

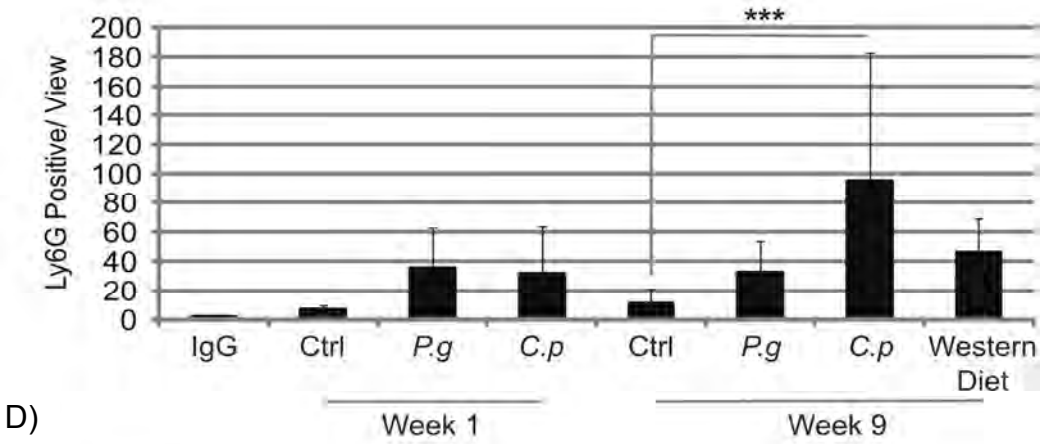
***
Ly6G Positive/ View
200
180
160
140
120
100
80
60
40
20
0
IgG
Ctrl
P.g
C.p
Ctrl
P.g
C.p
Western Diet
Week 1
Week 9

D)

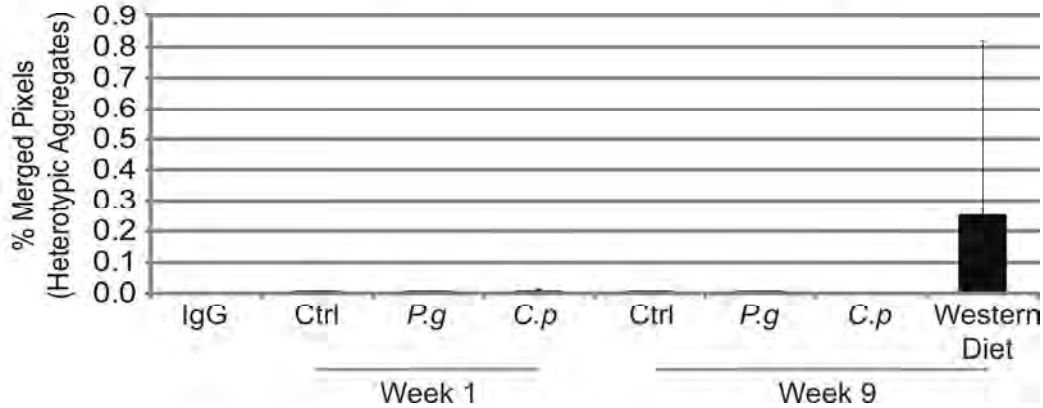
% Merged Pixels
(Heterotypic Aggregates)
0.9
0.8
0.7
0.6
0.5
0.4
0.3
0.2
0.1
0.0
IgG
Ctrl
P.g
C.p
Ctrl
P.g
C.p
Western Diet
Week 1
Week 9

Figure 2.8: IgG staining for spleen sections. Spleen sections from *ApoE*-/- mice stained with corresponding isotype control antibodies for CD41 and Ly6G antibodies, followed by fluorescent secondary antibodies. Samples visualized using a confocal microscope at 63X. Scale bar in merged image = 50.0 µm.

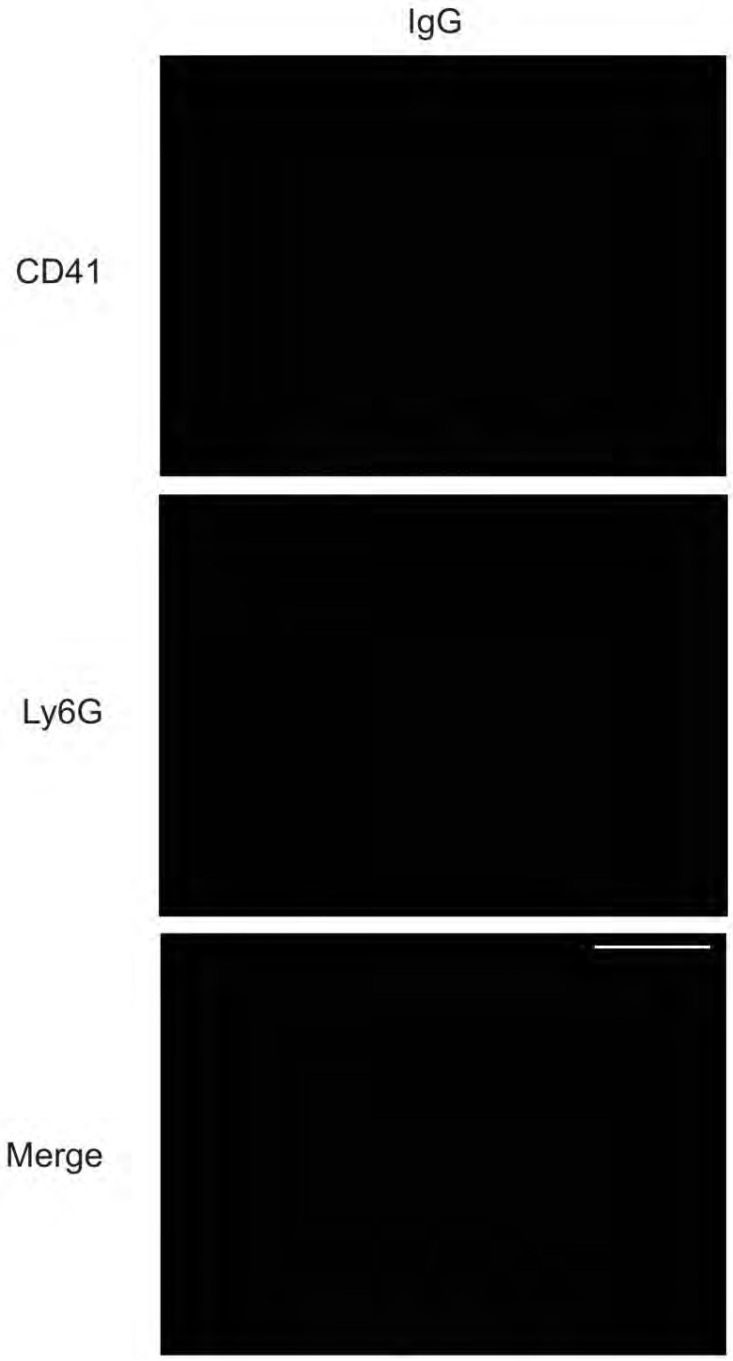

At week 9, *P. gingivalis* or *C. pneumoniae* infections did not alter *ApoE*$^{-/-}$ mouse body mass (Figure 2.4). However, in mice fed a Western diet, there was an increase in body mass by 5.2g. There was no effect on WBC counts at week 9 with either bacteria or a Western diet (Figure 2.5*a*). Platelet counts were still elevated following *C. pneumoniae* infection (Figure 2.5*b*). The increased circulating heterotypic aggregates seen with bacterial infections at week 1 were gone by week 9 (Figure 2.6). There were a greater number of platelets in the spleen sections from *P. gingivalis* or *C. pneumoniae* infected mice at week 9 as compared to week 1 (Figure 2.7*a,b*). *P. gingivalis* infection maintained the same amount of neutrophils in the spleen from week 1 to 9 (Figure 2.7*a,c*). For *C. pneumoniae*, there was a significantly greater number of neutrophils compared to untreated control at week 9 than that observed at week 1 (Figure 2.7*a,c*). A Western diet at week 9 did not increase circulating heterotypic aggregate formation. There was a significant increase in platelets in the spleens of mice fed a Western diet (Figure 2.7*a,b*) and a non-significant increase in neutrophils (Figure 2.7*a,c*). Unlike that observed following bacterial infections, there were heterotypic aggregates present in the spleens of mice fed a Western diet (Figure 2.7*a,d*).

Changes in platelet transcripts due to diet in participants of the Framingham Heart Study

To verify the relevance of the *in vivo* mouse observations, select platelet transcripts altered by a Western diet in the *ApoE*$^{-/-}$ mice were measured in participants of the FHS (n = 1819; Table 2.11). These genes were either increased or decreased in the *ApoE*$^{-/-}$ mice fed a Western diet, including albumin (*Alb*), α-1-microglobulin (*Ambp*), chemokine ligand 3 (*Ccl3*), CD3 antigen (*Cd3d*), CD53 antigen (*Cd53*), fatty acid binding protein 1 (*Fabp1*), fatty acid binding protein 5 (*Fabp5*), fibrinogen γ chain (*Fgg*), mitochondrial ribosomal protein S26 (*Mrps26*), nuclear receptor subfamily 2 (*Nr2f6*), ribosomal protein L21 (*Rpl21*), α-1-antitrypsin (*Serpina1*), and vitronectin (*Vtn*). These genes encompass various functional groups identified in the microarray, including coagulation, gene expression, inflammation, and lipids. These transcripts were compared to variables measured in the FHS that were associated with increased obesity (53, 171) and a Western diet (162, 172) in prior publications, including cholesterol, BMI, lipids, and triglyceride levels. A complete list of genes and their relationship with all studied clinical variables is found in Table 2.12.

Table 2.11 Framingham Heart Study Offspring Cohort Examination 8 characteristics.

Variables	Mean ± Standard Deviation/Number (%)
Sample Size	1819
Women	993 (51)
Age (y)	67±9
BMI (kg/m^2)	28.3±5.3
Systolic Blood Pressure (mm Hg)	129±17
Diastolic Blood Pressure (mm Hg)	73±10
Lipid Treatment	798 (44)
Total Cholesterol/HDL Ratio (mg/100 mL)	3.5±1.1
Triglycerides (mg/100 mL)	116±67
Glucose (mg/dL)	107±25
Antihypertensive Treatment	919 (51)
Aspirin (3 times/week)	823 (45)
Current Hormone Replacement Therapy	104 (6)
Diabetes mellitus	255 (14)
Prevalent Coronary Heart Disease	199 (11)
Smoker	155 (8.5)

Table 2.12: Relations between gene expression and clinical variables in FHS.

Gene Symbol	FHS Clinical Variable	Fold Change[1]	*p*-value	Regression Coefficient	Lower 95% CI	Upper 95% CI
ALB	Men	1.356	0.01	-0.439	-0.752	-0.127
ALB	Triglycerides	0.895	0.03	0.003	<0.001	0.006
ALB	Aspirin 3X/Week	1.276	0.03	-0.352	-0.664	-0.040
AMBP	Men	0.661	<0.01	0.598	0.254	0.943
AMBP	Antilipid R_x	0.675	<0.01	0.567	0.202	0.932
AMBP	BMI	0.874	0.02	0.039	0.007	0.071
AMBP	Aspirin 3X/Week	1.318	0.02	-0.398	-0.741	-0.054
CCL3	Age	1.182	<0.01	-0.024	-0.040	-0.008
CCL3	Men	1.245	0.01	-0.316	-0.561	-0.070
CCL3	Antihypertensive R_x	1.231	0.02	-0.299	-0.557	-0.042
CCL3	Diabetes	1.318	0.03	-0.398	-0.748	-0.048
CD3D	Men	1.940	<0.01	-0.956	-1.212	-0.699
CD3D	BMI	1.097	0.03	-0.027	-0.051	-0.003
CD3D	Diabetes	1.307	0.04	-0.386	-0.751	-0.022
CD53	Men	1.747	<0.01	-0.805	-1.047	-0.562
CD53	Total Cholesterol:HDL Ratio	1.127	0.02	-0.172	-0.316	-0.028
CD53	Triglycerides	0.923	0.04	0.002	<0.001	0.005
FABP1	Men	0.684	<0.01	0.547	0.221	0.873
FABP1	Antilipid R_x	0.679	<0.01	0.559	0.214	0.904
FABP5	Total Cholesterol:HDL Ratio	1.148	<0.01	-0.200	-0.337	-0.062
FABP5	Men	1.244	0.01	-0.315	-0.547	-0.084
FABP5	Age	1.129	0.02	-0.018	-0.033	-0.002
FABP5	Diabetes	1.276	0.04	-0.352	-0.682	-0.022
FABP5	Diastolic Bp	0.906	0.04	0.014	<0.001	0.028
FGG	Men	0.656	<0.01	0.608	0.277	0.940
FGG	Antilipid R_x	0.679	<0.01	0.560	0.208	0.911
FGG	BMI	0.870	0.01	0.040	0.009	0.071
FGG	Aspirin 3X/Week	1.324	0.02	-0.405	-0.735	-0.074
MRPS26	Men	1.607	<0.01	-0.684	-0.920	-0.448
NR2F6	Men	1.692	<0.01	-0.759	-1.001	-0.516
NR2F6	BMI	1.112	0.01	-0.031	-0.053	-0.008
NR2F6	Total Cholesterol:HDL Ratio	1.151	0.01	-0.203	-0.347	-0.060
NR2F6	Diastolic Bp	0.895	0.03	0.016	0.002	0.030
NR2F6	Triglycerides	0.921	0.04	0.002	<0.001	0.005
RPL21	Men	1.709	<0.01	-0.773	-1.000	-0.547

RPL21	BMI	1.106	0.01	-0.029	-0.050	-0.008
RPL21	Diastolic Bp	0.899	0.02	0.015	0.002	0.029
RPL21	Diabetes	1.258	0.04	-0.331	-0.653	-0.009
SERPINA1	Men	1.360	<0.01	-0.444	-0.712	-0.176
SERPINA1	BMI	1.131	0.01	-0.036	-0.061	-0.010
SERPINA1	Age	1.160	0.02	-0.021	-0.039	-0.004
SERPINA1	Diastolic Bp	0.886	0.03	0.017	0.002	0.033
VTN	Aspirin 3X/Week	1.382	<0.01	-0.467	-0.764	-0.171
VTN	Triglycerides	0.872	<0.01	0.004	0.001	0.007

[1]Fold Change for FHS – regression coefficient transformed ($2^{-\beta}$) to express fold change in gene expression associated with 1 unit change in clinical covariate, with the exception in triglycerides (50 points), systolic and diastolic blood pressure (10 points), age (10 years), and BMI (5 points).

Abbreviations – BMI – Body Mass Index, BP – Blood Pressure, CI – Confidence Interval, HDL – High Density Lipoprotein, R_x - Medication

Of the genes decreased in *ApoE*$^{-/-}$ mice fed a Western diet, 4 out of the 7 (*ALB, AMBP, FGG*, and *VTN*) were also significantly decreased with a higher mean BMI or triglycerides in the FHS (Table 2.13 and Table 2.12). *FABP1* was not associated with cholesterol, BMI, or triglycerides, while *FABP5* and *SERPINA1* were increased with a higher mean in cholesterol or BMI. As for the genes that increased with a Western diet in the *ApoE*$^{-/-}$ mice, 4 of the 5 (*CD3D, CD53, NR2F6,* and *RPL21*) were also increased significantly with a higher mean BMI, triglycerides, and/or cholesterol (Table 2.13 and Table 2.12). *CD53* and *NR2F6* were increased significantly with an increased mean total cholesterol:HDL ratio and BMI but decreased significantly with increased mean triglyceride levels. One transcript, *CCL3*, although increased in the mice, was not increased in individuals in the FHS with these variables but was associated with other factors, such as diabetes (Table 2.12).

Table 2.13:The relation between gene expression, clinical variables, and inflammatory markers in the FHS.

			FHS Fold Change (95% Conference Interval)				
Gene	**Gene Function**	**Mouse Microarray Data (Fold Change Compared to UC)**	**Total Cholesterol: HDL[1]**	**Triglycerides[1]**	**BMI[2]**	**CRP[2]**	**IL6[2]**
ALB	Fatty Acid Transport	0.055	--	0.90 (0.81, 0.99)*	--	--	--
FABP1	Fatty Acid Transport/ Metabolism	0.15	--	--	--	0.82 (0.74, 0.91)***	0.71 (0.60, 0.83)***
SERPINA1	Inflammation	0.20	--	--	1.13 (1.04, 1.23)**	1.29 (1.19, 1.40)***	1.50 (1.32, 1.72)***
FGG	Coagulation	0.26	--	--	0.87 (0.78, 0.97)*	0.83 (0.74, 0.92)***	0.68 (0.58, 0.80)***
AMBP	Coagulation	0.35	--	--	0.87 (0.78, 0.98)*	0.80 (0.72, 0.89)***	0.68 (0.57, 0.81)***
FABP5	Fatty Acid Transport/ Metabolism	0.39	1.15 (1.04, 1.26)**	--	--	1.10 (1.02, 1.18)*	1.12 (1.00, 1.26)*
MRPS26	Gene Expression- Mitoribosomes	0.43	--	--	--	1.14 (1.05, 1.22)***	1.22 (1.09, 1.38)***
VTN	Coagulation	0.49	--	0.87 (0.79, 0.96)**	--	--	0.85 (0.73, 0.99)*
CCL3	Inflammation	2.40	--	--	--	1.14 (1.05, 1.23)**	1.27 (1.13, 1.44)***

CD53	Inflammation	2.48	1.13 (1.02, 1.24)*	0.92 (0.85, 1.00)*	1.08 (1.00, 1.17)*	1.14 (1.05, 1.23)***	1.24 (1.10, 1.40)***
NR2F6	Gene Expression – Inflammation	2.55	1.15 (1.04, 1.27)**	0.92 (0.85, 1.00)*	1.11 (1.03, 1.20)**	1.17 (1.09, 1.26)***	1.26 (1.12, 1.42)***
CD3D	Inflammation	2.63	--	--	1.10 (1.01, 1.19)*	1.14 (1.05, 1.24)**	1.21 (1.07, 1.38)**
RPL21	Translation	3.00	--	--	1.11 (1.03, 1.19)**	1.12 (1.04, 1.20)**	1.21 (1.08, 1.35)**

[1]Fold Change for FHS: Total Cholesterol:HDL, BMI, Triglycerides – regression coefficient transformed ($2^{-\beta}$) to express fold change in gene expression associated with 1 unit change in clinical covariate, with the exception in BMI (5 points) and triglycerides (50 points). *p<0.05, **p<0.01, ***p<0.001.

[2] Fold Change for FHS: CRP and IL6 – regression coefficient transformed ($2^{-\beta}$) to express fold change in gene expression associated with $\log_e$-CRP or $\log_e$-IL6 serum levels adjusted for multiple covariates. *p<0.05, **p<0.01, ***p<0.001.

Abbreviations: BMI – Body mass index, CRP – C-reactive protein, FHS – Framingham Heart Study, HDL – High density lipoprotein, IL6 – Interleukin 6, Total Cholesterol:HDL – Ratio between total and HDL cholesterol, UC – untreated control.

Transcripts altered by a Western diet that were examined in FHS were also compared to circulating levels of CRP and IL6 (Table 2.13), inflammatory markers shown to be increased in individuals with CVD (173, 174), obesity (171, 175), and a Western diet (172, 176, 177). As previously shown, these cytokines also associated significantly with inflammatory-related transcripts from platelets in FHS (138). All but one transcript was significantly associated with higher mean levels of CRP and/or IL6. *AMBP, FABP1, FGG*, and *VTN* levels decreased with a higher mean level of CRP and/or IL6, which were all decreased in *ApoE*$^{-/-}$ mice fed a Western diet and some in the FHS. *CCL3, CD3D, CD53, FABP5, MRPS26, NR2F6, RPL21*, and *SERPINA1* were increased significantly with a higher mean CRP and/or IL6, which the majority were also increased in either FHS or in *ApoE*$^{-/-}$ mice fed a Western diet. Only expression of *ALB* was not significantly associated with either of these cytokines.

Discussion

The goal of the study was to characterize the effects of inflammatory stimuli – bacterial infections and a Western diet – on platelet transcripts and inflammatory function over time in a murine model of CVD. Similar effects on platelets were observed following infection with *P. gingivalis* and *C. pneumoniae* early after infection as determined by both transcriptional profiles and heterotypic aggregate formation. However, at a later timepoint (week 9), their effects on transcription diverged, with *C. pneumoniae* infection affecting platelets more

similarly to a Western diet. The effects of a Western diet on platelet transcripts were confirmed in platelet samples from FHS.

Platelet transcripts and inflammatory function were measured at week 1 following either *P. gingivalis* or *C. pneumoniae* infection to establish the early responses to each bacterium in *ApoE*$^{-/-}$ mice. Platelet transcripts were affected similarly by each bacterial infection, which suggests that each stimuli was activating through common pathways, most likely the TLR2-NFκB pathway via the megakaryocyte, which we previously published on (178). It is hypothesized that bacteria are recognized by megakaryocytes through their innate immune receptors. This hypothesis has been explored using Pam3CSK4, a TLR2 synthetic agonist, in human and mouse megakaryocytes, showing upregulation of inflammatory and coagulation related transcripts (178). Genes associated with RNA/gene expression and molecular transport, were also increased in platelets following infection with *P. gingivalis* and *C. pneumonia*. It is hypothesized the increase in gene expression correlates to an increase in mRNA translation within the platelets, as has been seen with platelets in response to cytokines (110, 138). Additionally, the increased number of transcripts in both of these groups could be transferred to other vascular cells, such as endothelial cells or monocytes (114), to increase translation in these cells in response to infection. We hypothesized transcriptional changes would be reflective with functional modifications in the platelets. As seen at week 1, there was an increase in circulating heterotypic aggregates and positive enrichment of inflammatory gene

sets (i.e., complement cascade). Not only is platelet production affected but so is platelet response. As previously shown, platelets respond to Pam3CSK4, *P. gingivalis* (139, 140), and *C. pneumoniae* (data not shown) through TLR2 and IL1R1. This results in platelets binding to neutrophils to form heterotypic aggregates, as well as increased P-selectin surface expression, and adhesion to collagen, increasing the risk of thrombosis as seen in human studies (158, 179).

At week 9, following *P. gingivalis* and *C. pneumoniae* infections, before overt plaque formation had yet to occur in the aorta, alterations in both platelet transcripts and inflammatory function are still occurring. Although not directly measured in our study, previous work by our group and others has shown that each bacterium is still present in the systems of these mice. An increase in circulating *P. gingivalis*-specific IgG has been detected through 13 weeks post infection (180) and by 24 weeks, this bacterium is identified in aorta, heart, and liver tissue (181). As for *C. pneumoniae*, there is a measurable serum IgG level up to 16 weeks, with bacteria detected in the lungs, aorta, heart, and spleen (182). Overall, both bacteria upregulated fewer genes at the later timepoint compared than observed at week 1 (Figure 2.9).

Figure 2.9: Comparison of genes affected by both bacterial infections at week 1 and week 9. Heatmap shows the transcripts identified through microarray as upregulated or downregulated 2-fold or more with either *P. gingivalis* (Pg) or *C. pneumoniae* (Cp) infection compared to untreated control in the *ApoE*$^{-/-}$ mice at week 1 and 9. Each condition represents RNA from 3 mice pooled.

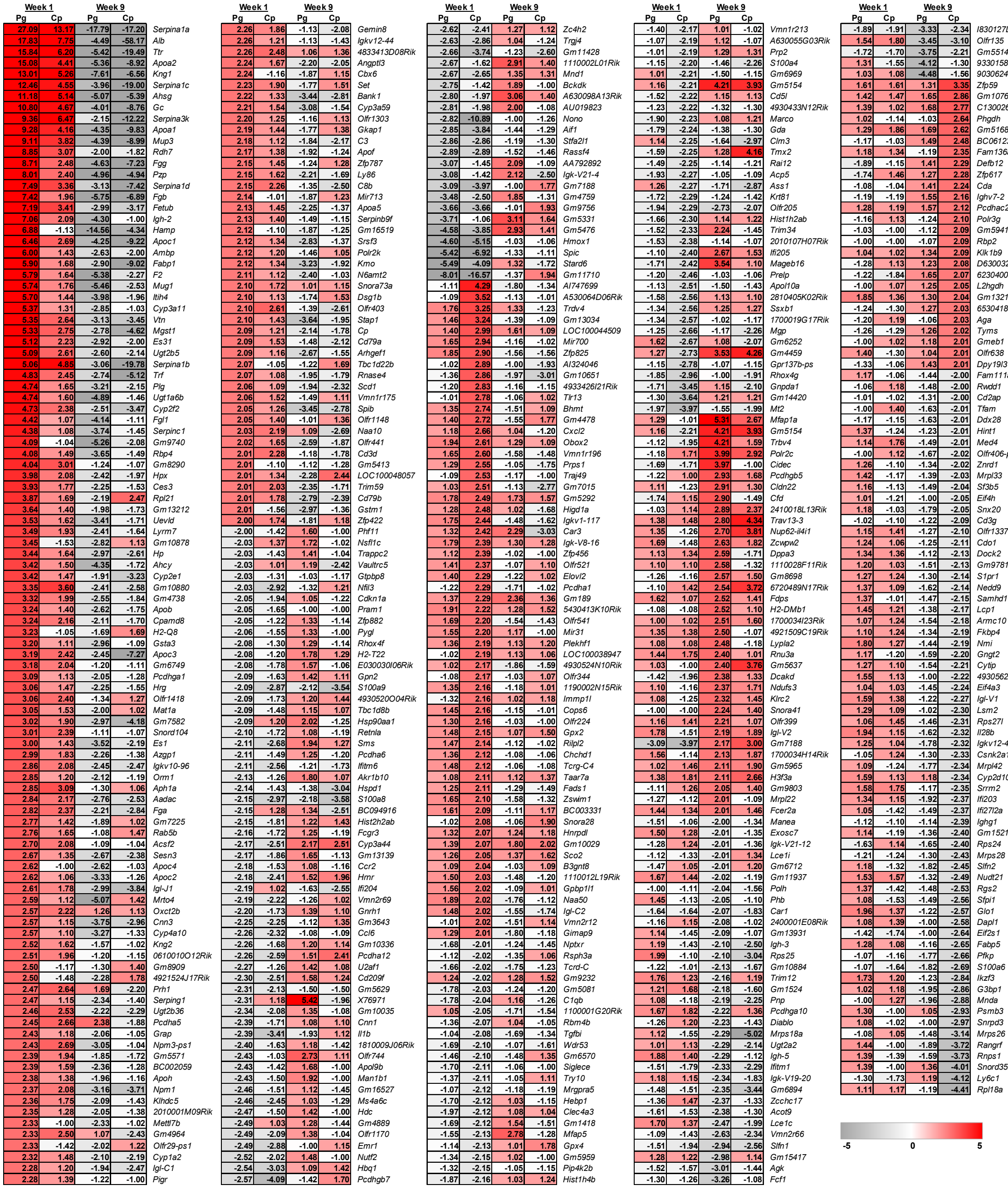

Week 1		Week 9		
Pg	Cp	Pg	Cp	
27.09	13.17	-17.79	-17.20	*Serpina1a*
17.83	7.75	-4.49	-58.17	*Alb*
15.84	6.20	-5.42	-19.49	*Ttr*
15.08	4.41	-5.36	-8.92	*Apoa2*
13.01	5.26	-7.61	-6.56	*Kng1*
12.46	4.55	-3.96	-19.00	*Serpina1c*
11.18	5.14	-5.07	-5.39	*Ahsg*
10.80	4.67	-4.01	-8.76	*Gc*
9.36	6.47	-2.15	-12.22	*Serpina3k*
9.28	4.16	-4.35	-9.83	*Apoa1*
9.11	3.82	-4.39	-8.99	*Mup3*
8.85	3.07	-2.00	-1.82	*Rdh7*
8.71	2.48	-4.63	-7.23	*Fgg*
8.01	2.40	-4.96	-4.94	*Pzp*
7.49	3.36	-3.13	-7.42	*Serpina1d*
7.42	1.96	-5.75	-6.89	*Fgb*
7.19	3.41	-2.99	-3.17	*Fetub*
7.06	2.09	-4.30	-1.00	*Igh-2*
6.88	-1.13	-14.56	-4.34	*Hamp*
6.46	2.69	-4.25	-9.22	*Apoc1*
6.00	1.43	-2.63	-2.00	*Ambp*
5.90	1.68	-2.90	-9.02	*Fabp1*
5.79	1.64	-5.38	-2.27	*F2*
5.74	1.76	-5.46	-2.53	*Mug1*
5.70	1.44	-3.98	-1.96	*Itih4*
5.37	1.31	-2.85	-1.03	*Cyp3a11*
5.35	2.64	-3.13	-3.45	*Vtn*
5.33	2.75	-2.78	-4.62	*Mgst1*
5.12	2.23	-2.92	-2.00	*Es31*
5.09	2.61	-2.60	-2.14	*Ugt2b5*
5.06	4.85	-3.06	-19.78	*Serpina1b*
4.83	2.45	-2.74	-5.12	*Trf*
4.74	1.65	-3.21	-2.15	*Plg*
4.74	1.60	-4.89	-1.46	*Ugt1a6b*
4.73	2.38	-2.51	-3.47	*Cyp2f2*
4.42	1.07	-4.14	-1.11	*Fgl1*
4.38	1.08	-3.74	-1.45	*Serpinc1*
4.09	-1.04	-5.26	-2.08	*Gm9740*
4.08	1.49	-3.65	-1.49	*Rbp4*
4.04	3.01	-1.24	-1.07	*Gm8290*
3.98	2.08	-2.42	-1.97	*Hpx*
3.93	1.77	-2.25	-1.53	*Ces3*
3.87	1.69	-2.19	2.47	*Rpl21*
3.64	1.40	-1.98	-1.73	*Gm13212*
3.53	1.62	-3.41	-1.71	*Uevld*
3.49	1.93	-2.41	-1.64	*Lyrm7*
3.45	-1.53	-2.82	1.13	*Gm10878*
3.44	1.64	-2.97	-2.61	*Hp*
3.42	1.50	-4.35	-1.72	*Ahcy*
3.42	1.47	-1.91	-3.23	*Cyp2e1*
3.35	3.60	-2.41	-2.58	*Gm10880*
3.32	1.99	-2.55	-1.84	*Gm4738*
3.24	1.40	-2.62	-1.75	*Apob*
3.24	2.16	-2.11	-1.70	*Cpamd8*
3.23	-1.05	-1.69	1.69	*H2-Q8*
3.20	1.11	-2.96	-1.09	*Gsta3*
3.19	2.42	-2.45	-7.27	*Apoc3*
3.18	2.04	-1.20	-1.11	*Gm6749*
3.09	1.13	-2.05	-1.28	*Pcdhga1*
3.06	1.47	-2.25	-1.55	*Hrg*
3.06	2.40	-1.34	1.27	*Olfr1418*
3.05	1.53	-2.00	1.02	*Mat1a*
3.02	1.90	-2.97	-4.18	*Gm7582*
3.01	2.39	-1.11	-1.07	*Snord104*
3.00	1.43	-3.52	-2.19	*Es1*
2.99	1.83	-2.26	-1.38	*Azgp1*
2.86	2.08	-2.45	-2.47	*Igkv10-96*
2.85	1.20	-2.12	-1.19	*Orm1*
2.85	3.09	-1.30	1.06	*Aph1a*
2.84	2.17	-2.76	-2.53	*Aadac*
2.82	2.37	-2.21	-2.84	*Fga*
2.77	1.42	-1.89	1.02	*Gm7225*
2.76	1.65	-1.08	1.47	*Rab5b*
2.70	2.08	-1.09	-1.04	*Acsf2*
2.67	1.35	-2.67	-2.38	*Sesn3*
2.62	-1.00	-2.62	-1.03	*Apoc4*
2.62	1.06	-3.33	-1.26	*Apoc2*
2.61	1.78	-2.99	-3.84	*Igl-J1*
2.59	1.12	-5.07	1.42	*Mrto4*
2.57	2.22	1.26	1.13	*Oxct2b*
2.57	1.15	-3.75	-2.96	*Cnn3*
2.57	1.10	-3.27	-1.33	*Cyp4a10*
2.52	1.62	-1.57	-1.02	*Kng2*
2.51	1.96	-1.20	-1.15	*0610010O12Rik*
2.50	-1.17	-1.30	1.40	*Gm8909*
2.50	-1.48	-2.28	1.78	*4921524J17Rik*
2.47	2.64	1.69	-2.20	*Prh1*
2.47	1.15	-2.34	-1.40	*Serping1*
2.46	2.53	-2.22	-2.29	*Ugt2b36*
2.45	2.66	2.38	-1.88	*Pcdha5*
2.43	1.18	-2.06	-1.05	*Grap*
2.43	2.69	-3.05	-1.04	*Npm3-ps1*
2.39	1.94	-1.85	-1.72	*Gm5571*
2.39	1.59	-2.36	-1.28	*BC002059*
2.38	1.38	-1.96	-1.16	*Apoh*
2.37	2.08	-3.16	-3.71	*Npm1*
2.36	1.75	-2.09	-1.43	*Klhdc5*
2.35	1.28	-2.05	-1.38	*2010001M09Rik*
2.33	-1.00	-2.33	-1.02	*Mettl7b*
2.33	2.50	1.07	-2.43	*Gm4964*
2.33	-1.42	-2.02	1.22	*Olfr29-ps1*
2.32	1.48	-2.10	-2.19	*Cyp1a2*
2.28	1.20	-1.94	-2.47	*Igl-C1*
2.28	1.39	-1.22	-1.00	*Pigr*

Week 1		Week 9		
Pg	Cp	Pg	Cp	
2.26	1.86	-1.13	-2.08	*Gemin8*
2.26	1.21	-1.13	-1.43	*Igkv12-44*
2.26	2.48	1.06	1.36	*4833413D08Rik*
2.24	1.67	-2.20	-2.05	*Angptl3*
2.24	-1.16	-1.87	1.15	*Cbx6*
2.23	1.90	-1.77	1.51	*Set*
2.22	1.33	-3.44	-2.81	*Bank1*
2.21	1.54	-3.08	-1.54	*Cyp3a59*
2.20	1.25	-1.16	1.13	*Olfr1303*
2.19	1.44	-1.77	1.38	*Gkap1*
2.18	1.12	-1.84	-2.17	*C3*
2.17	1.38	-1.92	-1.24	*Apof*
2.15	1.45	-1.24	1.28	*Zfp787*
2.15	1.62	-2.21	-1.69	*Ly86*
2.15	2.26	-1.35	-2.50	*C8b*
2.14	-1.01	-1.87	1.23	*Mir713*
2.13	1.45	-2.25	-1.37	*Apoa5*
2.13	1.40	-1.49	-1.15	*Serpinb9f*
2.12	-1.10	-1.87	-1.25	*Gm16519*
2.12	1.34	-2.83	-1.37	*Srsf3*
2.12	1.20	-1.46	1.05	*Polr2k*
2.12	1.34	-3.23	-1.92	*Kmo*
2.11	1.12	-2.40	-1.03	*N6amt2*
2.10	1.72	1.01	1.15	*Snora73a*
2.10	1.13	-1.74	1.53	*Dsg1b*
2.10	2.61	-1.39	-2.61	*Olfr403*
2.10	1.43	-3.64	-1.95	*Stap1*
2.09	1.21	-2.14	-1.78	*Cp*
2.09	1.53	-1.48	-2.12	*Cd79a*
2.09	1.16	-2.67	-1.55	*Arhgef1*
2.07	-1.05	-1.22	1.69	*Tbc1d22b*
2.07	1.08	-1.95	-1.79	*Rnase4*
2.06	1.09	-1.94	-2.32	*Scd1*
2.06	1.52	-1.49	1.11	*Vmn1r175*
2.05	1.26	-3.45	-2.78	*Spib*
2.05	1.40	-1.01	1.36	*Olfr1148*
2.03	2.19	1.09	-2.69	*Naa10*
2.02	1.65	-2.59	-1.87	*Olfr441*
2.01	2.28	-1.18	-1.78	*Cd3d*
2.01	-1.10	-1.12	-1.28	*Gm5413*
2.01	1.34	-2.28	2.44	*LOC100048057*
2.01	2.03	-2.35	-1.71	*Trim59*
2.01	1.78	-2.79	-2.39	*Cd79b*
2.01	-1.56	-2.97	-1.36	*Gstm1*
2.00	1.74	-1.81	1.18	*Zfp422*
-2.00	-1.42	1.60	-1.00	*Phf11*
-2.03	1.37	1.72	-1.02	*Nsfl1c*
-2.03	-1.43	1.41	-1.04	*Trappc2*
-2.03	1.01	1.19	-2.42	*Vaultrc5*
-2.03	-1.31	-1.03	-1.17	*Gtpbp8*
-2.03	-2.92	-1.32	1.21	*Nfil3*
-2.05	-1.94	1.05	-1.22	*Cdkn1a*
-2.05	-1.65	-1.00	-1.00	*Pram1*
-2.05	-1.22	1.33	-1.14	*Zfp882*
-2.06	-1.55	1.33	-1.00	*Pygl*
-2.08	-1.30	1.29	-1.14	*Rhox4f*
-2.08	-1.20	1.78	1.29	*H2-T22*
-2.08	-1.78	1.57	-1.06	*E030030I06Rik*
-2.09	-1.63	1.42	1.11	*Gpn2*
-2.09	-2.87	-2.12	-3.54	*S100a9*
-2.09	-1.73	1.20	1.44	*4930520O04Rik*
-2.09	-1.48	1.15	1.07	*Tbc1d8b*
-2.09	1.20	2.02	-1.25	*Hsp90aa1*
-2.10	-1.72	1.08	-1.19	*Retnla*
-2.11	-2.68	1.94	1.27	*Sms*
-2.11	-1.49	1.25	-1.20	*Pcdha6*
-2.11	-2.56	-1.21	-1.73	*Ifitm6*
-2.13	-1.26	1.80	1.07	*Akr1b10*
-2.14	-1.43	-1.38	-3.04	*Hspd1*
-2.15	-2.97	-2.18	-3.58	*S100a8*
-2.15	1.28	1.34	-2.51	*BC094916*
-2.15	-1.81	1.22	1.43	*Hist2h2ab*
-2.16	-1.72	1.25	-1.19	*Fcgr3*
-2.17	-2.51	2.17	2.51	*Cyp3a44*
-2.17	-1.86	1.65	-1.13	*Gm13139*
-2.18	-1.53	1.08	-1.16	*Ccr2*
-2.18	-2.41	1.52	1.96	*Hrnr*
-2.19	1.02	-1.63	-2.55	*Ifi204*
-2.19	-2.22	-1.26	1.02	*Vmn2r69*
-2.20	-1.73	1.39	1.10	*Gnrh1*
-2.25	-2.25	-1.12	1.35	*Gm3643*
-2.26	-2.32	-1.08	-1.09	*Ccl6*
-2.26	-1.68	1.20	1.14	*Gm10336*
-2.26	-2.59	1.51	2.41	*Pcdha12*
-2.27	-1.26	1.42	1.08	*U2af1*
-2.30	-2.51	1.58	1.24	*Cd209f*
-2.31	-2.13	-1.50	-1.50	*Gm5629*
-2.31	1.18	5.42	-1.96	*X76971*
-2.34	-2.08	1.35	-1.08	*Gm10035*
-2.39	-1.71	1.08	1.10	*Cnn1*
-2.39	-3.41	-1.93	1.12	*Il1b*
-2.40	-1.63	1.18	-1.42	*1810009J06Rik*
-2.43	-1.03	2.73	1.11	*Olfr744*
-2.43	-1.42	1.68	-1.00	*Apol9b*
-2.43	-1.50	1.92	-1.00	*Man1b1*
-2.46	-1.51	1.12	-1.45	*Gm16527*
-2.46	-2.45	1.03	-1.29	*Ms4a6c*
-2.47	-1.50	1.42	-1.00	*Hdc*
-2.49	1.03	1.28	-1.44	*Gm4889*
-2.49	-2.09	1.38	-1.04	*Olfr1170*
-2.49	-2.88	-1.00	1.15	*Emr1*
-2.52	-2.02	1.48	-1.00	*Nutf2*
-2.54	-3.03	1.09	1.42	*Hbq1*
-2.57	-4.09	-1.42	1.70	*Pcdhgb7*

Week 1		Week 9		
Pg	Cp	Pg	Cp	
-2.62	-2.41	1.27	1.12	*Zc4h2*
-2.63	-2.86	1.04	-1.24	*Trgj4*
-2.66	-3.74	-1.23	-2.60	*Gm11428*
-2.67	-1.62	2.91	1.40	*1110002L01Rik*
-2.67	-2.65	1.35	1.31	*Mnd1*
-2.75	-1.42	1.89	-1.00	*Bckdk*
-2.80	-1.97	3.06	1.40	*A630098A13Rik*
-2.81	-1.98	2.00	-1.08	*AU019823*
-2.82	-10.89	-1.00	-1.26	*Nono*
-2.85	-3.84	-1.44	-1.29	*Aif1*
-2.86	-2.86	-1.19	-1.30	*Stfa2l1*
-2.89	-2.89	-1.52	-1.46	*Rassf4*
-3.07	-1.45	2.09	-1.09	*AA792892*
-3.08	-1.42	2.12	-2.50	*Igk-V21-4*
-3.09	-3.97	-1.00	1.77	*Gm7188*
-3.48	-2.50	1.85	-1.31	*Gm4759*
-3.66	-3.66	-1.01	1.93	*Gm9756*
-3.71	-1.06	3.11	1.64	*Gm5331*
-4.58	-3.85	2.93	1.41	*Gm5476*
-4.60	-5.15	-1.03	-1.06	*Hmox1*
-5.42	-6.92	-1.33	-1.11	*Spic*
-5.49	-4.09	1.32	-1.72	*Stard6*
-8.01	-16.57	-1.37	1.94	*Gm11710*
-1.11	4.29	-1.80	-1.34	*AI747699*
-1.09	3.52	-1.13	-1.01	*A530064D06Rik*
1.76	3.25	1.33	-1.23	*Trdv4*
1.46	3.24	-1.39	-1.09	*Gm13034*
1.40	2.99	1.61	1.09	*LOC100044509*
1.65	2.94	-1.16	-1.02	*Mir700*
1.85	2.90	-1.56	-1.56	*Zfp825*
-1.02	2.89	-1.00	-1.93	*AI324046*
-1.36	2.86	-1.97	-3.01	*Gm10651*
-1.20	2.83	-1.16	-1.15	*4933426I21Rik*
-1.01	2.78	-1.06	1.02	*Tlr13*
1.35	2.74	-1.51	1.09	*Bhmt*
1.40	2.72	-1.55	1.77	*Gm4478*
1.18	2.66	1.04	-1.20	*Cxcl2*
1.94	2.61	1.29	1.09	*Obox2*
1.65	2.60	-1.58	-1.48	*Vmn1r196*
1.29	2.55	-1.05	-1.75	*Prps1*
-1.09	2.53	-1.17	-1.00	*Traj49*
1.03	2.51	-1.13	-2.77	*Gm7015*
1.78	2.49	1.73	1.57	*Gm5292*
1.28	2.48	1.02	-1.68	*Higd1a*
1.75	2.44	-1.48	-1.62	*Igkv1-117*
1.32	2.42	2.29	-3.03	*Car3*
1.79	2.39	1.30	1.28	*Igk-V8-16*
1.12	2.39	-1.02	-1.00	*Zfp456*
1.41	2.37	-1.07	1.10	*Olfr521*
1.40	2.29	-1.22	1.02	*Elovl2*
-1.22	2.29	-1.71	-1.02	*Pcdha1*
1.37	2.29	2.36	1.36	*Gm189*
1.91	2.22	1.28	1.52	*5430413K10Rik*
1.69	2.20	-1.54	-1.43	*Olfr541*
1.55	2.20	1.17	-1.00	*Mir31*
1.36	2.19	1.13	1.20	*Plekhf1*
-1.02	2.19	1.13	1.06	*LOC100038947*
1.02	2.17	-1.86	-1.59	*4930524N10Rik*
-1.08	2.17	-1.03	1.07	*Olfr344*
1.35	2.16	-1.18	1.01	*1190002N15Rik*
-1.32	2.16	1.02	1.18	*Immp1l*
1.45	2.16	-1.15	-1.01	*Cops6*
1.30	2.16	-1.03	-1.00	*Olfr224*
1.48	2.15	1.07	1.50	*Gpx2*
1.47	2.14	-1.12	-1.02	*Rilpl2*
1.36	2.12	-1.08	-1.06	*Chchd1*
1.48	2.12	-1.06	-1.08	*Tcrg-C4*
1.08	2.11	1.12	1.37	*Taar7a*
1.25	2.11	-1.29	-1.49	*Fads1*
1.65	2.10	-1.58	-1.32	*Zswim1*
1.61	2.09	-1.11	1.17	*BC003331*
-1.02	2.08	-1.06	1.90	*Snora28*
1.32	2.07	1.24	1.18	*Hnrpdl*
1.39	2.07	1.80	2.02	*Gm10029*
1.26	2.05	1.37	1.62	*Sco2*
1.09	2.04	-1.03	1.09	*B3gnt8*
1.50	2.03	-1.48	-1.20	*1110012L19Rik*
1.56	2.02	-1.09	1.01	*Gpbp1l1*
1.89	2.02	-1.76	-1.12	*Naa50*
1.48	2.02	-1.55	-1.74	*Igl-C2*
-1.01	2.02	-1.51	1.14	*Vmn2r12*
1.29	2.01	-1.80	-1.18	*Gimap9*
-1.68	-2.01	-1.24	-1.45	*Nptxr*
-1.12	-2.02	-1.35	1.06	*Rsph3a*
-1.66	-2.02	-1.75	-1.23	*Tcrd-C*
1.24	-2.02	1.28	1.52	*Gm9232*
-1.78	-2.03	-1.24	-1.20	*Gm5081*
-1.78	-2.04	1.16	-1.26	*C1qb*
1.05	-2.05	-1.71	-1.54	*1100001G20Rik*
-1.36	-2.07	1.04	-1.05	*Rbm4b*
-1.04	-2.08	-1.69	-1.34	*Tgfbi*
-1.69	-2.10	-1.07	-1.61	*Wdr53*
-1.46	-2.10	-1.48	1.35	*Gm6570*
-1.70	-2.11	-1.06	-1.00	*Siglece*
-1.37	-2.11	-1.05	1.11	*Try10*
-1.07	-2.12	-1.18	-1.19	*Mrgpra5*
-1.70	-2.12	1.03	-1.15	*Hebp1*
-1.97	-2.12	1.08	1.04	*Clec4a3*
-1.69	-2.12	1.54	-1.51	*Gm1418*
-1.55	-2.13	2.78	-1.28	*Mfap5*
-1.14	-2.13	1.01	1.78	*Gpx4*
-1.34	-2.15	1.02	-1.00	*Gm5959*
-1.32	-2.15	-1.05	-1.15	*Pip4k2b*
-1.87	-2.16	1.03	1.24	*Hist1h4b*

Week 1		Week 9		
Pg	Cp	Pg	Cp	
-1.40	-2.17	1.01	-1.02	*Vmn1r213*
-1.07	-2.19	1.12	-1.07	*A630055G03Rik*
-1.01	-2.19	1.29	1.31	*Prp2*
-1.15	-2.20	-1.46	-2.26	*S100a4*
1.01	-2.21	-1.50	-1.15	*Gm6969*
1.16	-2.21	4.21	3.93	*Gm5154*
-1.52	-2.22	1.15	1.13	*Cd5l*
-1.23	-2.22	-1.32	-1.30	*4930433N12Rik*
-1.90	-2.23	1.08	1.21	*Marco*
-1.79	-2.24	-1.38	-1.30	*Gda*
1.14	-2.25	-1.64	-2.97	*Clm3*
-1.59	-2.25	1.28	4.16	*Tmx2*
-1.49	-2.25	-1.14	-1.21	*Rai12*
-1.93	-2.27	-1.05	-1.09	*Acp5*
1.26	-2.27	-1.71	-2.87	*Ass1*
-1.72	-2.29	-1.24	-1.42	*Krt81*
-1.94	-2.29	-2.73	-2.07	*Olfr205*
-1.66	-2.30	1.14	1.22	*Hist1h2ab*
-1.52	-2.33	2.24	-1.45	*Trim34*
-1.53	-2.38	-1.14	-1.07	*2010107H07Rik*
-1.10	-2.40	2.67	1.53	*Ifi205*
-1.71	-2.42	3.54	1.10	*Mageb16*
-1.20	-2.46	-1.03	-1.06	*Prelp*
-1.13	-2.51	-1.50	-1.43	*Apol10a*
-1.58	-2.56	1.13	1.10	*2810405K02Rik*
-1.34	-2.56	1.25	1.27	*Ssxb1*
-1.34	-2.57	-1.02	-1.17	*1700019G17Rik*
-1.25	-2.66	-1.17	-2.26	*Mgp*
1.62	-2.67	1.08	-2.07	*Gm6252*
1.27	-2.73	3.53	4.26	*Gm4459*
-1.15	-2.78	-1.07	-1.15	*Gpr137b-ps*
-1.85	-2.96	-1.00	-1.91	*Rhox4g*
-1.71	-3.45	1.15	-2.10	*Gnpda1*
-1.30	-3.64	1.21	1.21	*Gm14420*
-1.97	-3.97	-1.55	-1.99	*Mt2*
1.29	-1.01	5.31	2.67	*Mfap1a*
1.16	-2.21	4.21	3.93	*Gm5154*
-1.12	-1.95	4.21	1.59	*Trbv4*
-1.18	1.71	3.99	2.92	*Polr2c*
-1.69	-1.71	3.97	-1.00	*Cidec*
-1.22	1.00	2.93	1.68	*Pcdhgb5*
1.11	-1.23	2.91	1.30	*Cldn22*
-1.74	1.15	2.90	-1.49	*Cfd*
-1.03	1.14	2.89	2.37	*2410018L13Rik*
1.38	1.48	2.80	4.34	*Trav13-3*
1.35	-1.26	2.70	3.81	*Nup62-il4i1*
1.69	-1.48	2.63	1.82	*Zcwpw2*
1.13	1.34	2.59	-1.71	*Dppa3*
1.10	1.10	2.58	-1.32	*1110028F11Rik*
-1.26	-1.16	2.57	1.50	*Gm8698*
-1.10	1.42	2.54	3.72	*6720489N17Rik*
1.62	1.07	2.52	1.41	*Fdps*
-1.08	-1.08	2.52	1.10	*H2-DMb1*
1.00	1.02	2.51	1.60	*1700034I23Rik*
1.35	1.38	2.50	-1.07	*4921509C19Rik*
1.08	1.08	2.48	-1.18	*Lypla2*
1.44	1.75	2.40	1.01	*Rnu3a*
1.03	-1.00	2.40	3.76	*Gm5637*
-1.42	-1.96	2.38	1.33	*Dcakd*
1.10	-1.16	2.37	1.71	*Ndufs3*
1.08	-1.25	2.32	1.45	*Klrc2*
-1.00	-1.00	2.24	1.40	*Snora41*
1.16	1.41	2.21	1.07	*Olfr399*
1.78	-1.51	2.19	1.89	*Igl-V2*
-3.09	-3.97	2.17	3.00	*Gm7188*
1.56	-1.14	2.13	1.87	*1700034H14Rik*
1.02	1.46	2.11	1.90	*Gm5965*
1.38	1.81	2.11	2.66	*H3f3a*
-1.11	1.26	2.05	1.40	*Gm9803*
-1.27	-1.12	2.01	-1.09	*Mrpl22*
1.44	1.34	2.01	1.46	*Fcer2a*
-1.51	-1.06	-2.00	-1.34	*Manea*
1.50	1.28	-2.01	-1.35	*Exosc7*
-1.28	1.24	-2.01	-1.36	*Igk-V21-12*
-1.12	-1.33	-2.01	1.34	*Lce1i*
-1.47	1.05	-2.01	1.20	*Gm6712*
1.67	1.44	-2.02	-1.19	*Gm11937*
-1.00	-1.11	-2.04	-1.56	*Polh*
1.45	-1.13	-2.05	-1.10	*Phb*
-1.64	-1.64	-2.07	-1.83	*Car1*
-1.16	1.15	-2.08	-1.02	*2400001E08Rik*
1.14	-1.45	-2.09	-1.07	*Gm13931*
1.19	-1.43	-2.10	-2.50	*Igh-3*
1.99	-1.10	-2.10	-3.04	*Rps25*
-1.22	-1.01	-2.13	-1.67	*Gm10884*
1.76	1.23	-2.16	1.19	*Trim12*
1.21	1.68	-2.18	-1.60	*Gm1524*
1.08	-1.18	-2.19	-2.25	*Pnp*
1.67	1.82	-2.22	1.36	*Pcdhga10*
-1.26	1.20	-2.23	-1.43	*Diablo*
1.12	-1.55	-2.29	-5.02	*Mrps18a*
1.01	1.13	-2.29	-2.14	*Ugt2a2*
1.88	1.40	-2.29	-1.12	*Igh-5*
-1.51	-1.79	-2.33	-2.29	*Ifitm1*
1.18	1.15	-2.34	-1.83	*Igk-V19-20*
-1.48	-1.51	-2.35	-3.44	*Gm6894*
-1.36	1.47	-2.37	-1.33	*Zcchc17*
-1.61	-1.53	-2.38	-1.30	*Acot9*
1.70	1.37	-2.47	-1.99	*Lce1c*
-1.09	-1.43	-2.63	-2.34	*Vmn2r66*
-1.51	-1.94	-2.94	-2.56	*Slfn1*
1.28	1.22	-2.98	1.14	*Gm15417*
-1.52	-1.57	-3.01	-1.44	*Agk*
-1.30	-1.26	-3.26	-1.08	*Fcf1*

Week 1		Week 9		
Pg	Cp	Pg	Cp	
-1.89	-1.91	-3.33	-2.34	*I830127L07Rik*
1.54	1.80	-3.45	-3.10	*Olfr135*
-1.72	-1.70	-3.75	-2.21	*Gm5514*
1.31	-1.55	-4.12	-1.30	*9330158H04Rik*
1.03	1.08	-4.48	-1.56	*9030624G23Rik*
1.61	1.61	1.31	3.35	*Zfp59*
1.42	1.47	1.65	2.86	*Gm10767*
1.39	1.02	1.68	2.77	*C130026I21Rik*
1.02	-1.14	-1.03	2.64	*Phgdh*
1.29	1.86	1.69	2.62	*Gm5168*
-1.17	-1.03	1.49	2.48	*BC061237*
1.18	1.34	-1.19	2.35	*Fam136a*
-1.89	-1.15	1.41	2.29	*Defb12*
-1.74	1.46	1.27	2.28	*Zfp617*
-1.08	-1.04	1.41	2.24	*Cda*
-1.19	-1.19	1.55	2.16	*Ighv7-2*
1.28	1.19	1.57	2.12	*Pcdhac2*
-1.16	1.13	-1.24	2.10	*Polr3g*
-1.03	-1.00	-1.12	2.09	*Gm5941*
-1.00	-1.00	-1.07	2.09	*Rbp2*
1.04	1.02	1.34	2.09	*Klk1b9*
-1.28	1.13	1.23	2.08	*D630032N06Rik*
-1.22	-1.84	1.65	2.07	*6230400D17Rik*
-1.00	1.07	1.25	2.05	*L2hgdh*
1.85	1.36	1.30	2.04	*Gm13213*
-1.24	-1.30	1.27	2.03	*6530418L21Rik*
-1.20	1.19	-1.06	2.03	*Aga*
-1.26	-1.29	1.26	2.02	*Tyms*
-1.00	1.02	1.18	2.01	*Gmeb1*
1.40	-1.30	1.04	2.01	*Olfr638*
-1.33	-1.06	1.43	2.01	*Dpy19l3*
1.17	-1.06	-1.44	-2.00	*Fam111a*
-1.06	1.18	-1.48	-2.00	*Rwdd1*
-1.01	-1.02	-1.31	-2.00	*Cd2ap*
-1.00	1.40	-1.63	-2.01	*Tfam*
-1.17	-1.15	-1.63	-2.01	*Ddx28*
1.37	-1.24	-1.23	-2.01	*Hint1*
1.14	1.76	-1.49	-2.01	*Med4*
-1.00	1.12	-1.67	-2.02	*Olfr406-ps*
1.26	-1.10	-1.34	-2.02	*Znrd1*
1.42	-1.17	-1.39	-2.03	*Mrpl33*
1.16	-1.13	-1.49	-2.04	*Sf3b5*
1.01	-1.21	-1.00	-2.05	*Eif4h*
1.18	-1.03	-1.79	-2.05	*Snx20*
-1.02	-1.10	-1.22	-2.09	*Cd3g*
1.15	1.41	-1.27	-2.10	*Olfr1337*
1.24	1.06	-1.25	-2.11	*Cdo1*
1.34	1.36	-1.12	-2.13	*Dock2*
1.20	1.03	-1.51	-2.13	*Gm9781*
1.27	1.24	-1.30	-2.14	*S1pr1*
1.37	1.09	-1.62	-2.14	*Nedd9*
1.37	-1.01	-1.47	-2.15	*Samhd1*
1.45	1.21	-1.38	-2.17	*Lcp1*
1.07	1.24	-1.54	-2.18	*Armc10*
1.10	1.24	-1.34	-2.19	*Fkbp4*
1.80	1.27	-1.44	-2.19	*Nmi*
1.17	-1.20	-1.59	-2.20	*Gngt2*
1.27	1.10	-1.54	-2.21	*Cytip*
1.55	1.13	-1.00	-2.22	*4930562F07Rik*
1.04	1.03	-1.45	-2.24	*Eif4a3*
1.59	1.38	-1.22	-2.27	*Igl-V1*
1.29	1.09	-1.02	-2.30	*Lsm2*
1.06	1.45	-1.46	-2.31	*Rps27l*
1.94	1.15	-1.62	-2.32	*Il28b*
1.25	1.04	-1.78	-2.32	*Igkv12-46*
-1.05	1.24	-1.30	-2.33	*Csnk2a1*
1.09	-1.24	-1.77	-2.34	*Mrpl42*
1.59	1.13	1.18	-2.34	*Cyp2d10*
1.58	1.75	-1.17	-2.35	*Srrm2*
1.34	1.15	-1.92	-2.37	*Ifi203*
1.05	-1.42	-1.49	-2.37	*Ifi27l2a*
-1.12	-1.10	-1.14	-2.39	*Ighg1*
1.14	-1.19	-1.36	-2.40	*Gm15210*
-1.63	1.14	-1.65	-2.40	*Rps24*
-1.21	-1.24	-1.30	-2.43	*Mrps28*
1.18	-1.32	-1.82	-2.45	*Slfn2*
1.53	1.57	-1.32	-2.49	*Nudt21*
1.37	-1.42	-1.48	-2.53	*Rgs2*
1.08	-1.53	-1.49	-2.56	*Sfpi1*
1.96	1.37	-1.22	-2.57	*Glo1*
1.08	1.39	-1.00	-2.58	*Dapl1*
-1.42	-1.74	-1.00	-2.64	*Eif2s1*
1.28	1.08	-1.16	-2.65	*Fabp5*
-1.07	-1.16	-1.77	-2.66	*Pfkp*
-1.07	-1.64	-1.82	-2.69	*S100a6*
1.73	1.20	-1.23	-2.84	*Ikzf3*
1.02	1.18	-1.95	-2.86	*G3bp1*
-1.00	1.27	-1.96	-2.88	*Mnda*
1.30	-1.00	1.05	-2.93	*Psmb3*
1.08	-1.02	-1.00	-2.97	*Snrpd3*
-1.08	1.05	-1.48	-3.14	*Mrps26*
1.44	-1.00	-1.89	-3.72	*Rangrf*
1.39	-1.39	-1.59	-3.73	*Rnps1*
1.39	-1.00	1.36	-4.01	*Snord35b*
-1.30	-1.73	1.19	-4.12	*Ly6c1*
1.11	1.17	-1.19	-4.41	*Rpl18a*

Infection with *C. pneumoniae* resulted in more downregulation in gene expression, which was further supported by GSEA, showing significant negative enrichment in gene sets. Unlike with *C. pneumoniae*, *P. gingivalis* infection alterations in gene transcript changes were diminished at week 9. It is hypothesized that over the course of the infection, megakaryocytes are slowly returning to baseline in terms of the types of RNA produced, with fewer genes and gene groups being altered. Further, changes in transcripts are also reflective of platelet function. Platelet-neutrophil aggregates are no longer in circulation at week 9. The cells were individually present in the spleens obtained from these mice. It is possible that we no longer see these cells as aggregates even in the spleens because the interaction between the platelets and neutrophils is transient, a brief interaction that results in activation of either/both cells and transfer of information on the current environment. With more platelets in the spleen, it is expected that there would be a decrease in circulating platelet levels. Instead, the platelet concentrations stay steady if not increase. This data suggest megakaryocytes are still responding to the infection, directly or indirectly.

With a Western diet, it was expected that lipid associated genes would be upregulated in platelets, but instead, as seen in FHS (53, 138, 139), there was an increase in inflammatory related transcripts, as well as signaling and proliferation. As previously seen with the FHS (53), the changes associated with a Western diet on platelets can either be due to the diet, change in body weight, or the proinflammatory setting. Further work is needed to understand this relationship.

Interestingly, many genes and/or gene function groups altered by a Western diet were also altered following a *C. pneumoniae* infection. Genes downregulated following a Western diet or *C. pneumoniae* infection included *Ttr, Gc, Alb, Apoa2,* and *Fabp1*. Functionally, the Western diet did not produce circulating heterotypic aggregates but did promote the formation of aggregates to the vessel wall, as seen in the spleens. It is hypothesized that a Western diet, promotes platelets adhesion to the blood vessels, which promotes adhesion of immune cells as well, leading to the formation of atherosclerosis (183).

The effects of a Western diet in the *ApoE*$^{-/-}$ mice were verified using platelet transcripts from the FHS. Thirteen genes were identified from the microarray data, including *ALB, AMBP, CCL3, CD3D, CD53, FABP1, FABP5, FGG, MRPS26, NR2F6, RPL21, SERPINA1*, and *VTN*. Twelve out of the 13 genes had altered gene expression that correlated to one or more clinical variables associated with adiposity, including BMI, triglycerides, and cholesterol. Additionally, inflammatory related cytokines, CRP and IL6, which are increased with CVD and associate significantly with inflammatory related transcripts from platelets in FHS (138), were associated with changes in 12 of the 13 identified transcripts, again, supporting the notion that platelets react with an inflammatory stimuli resembles their reaction to a Western diet.

In conjunction with the analysis of platelets in these *ApoE*$^{-/-}$ mice, aortic tissue, consisting of endothelial cells, immune cells, and smooth muscle cells, were also examined by microarray. At week 1, *P. gingivalis* infection had little

effect on gene expression in the aortic tissue. *C. pneumoniae* infection upregulated genes associated with GPCR signaling, viral myocarditis, antigen processing/presentation, and membranes in the entire aortic tissue (159), which is in contrast to what is shown here in platelets. When comparing the platelet data to the results from the aortic tissue at week 9, we see there are no gene sets similarly affected with either bacterial infection (159). In fact, two pathways positively enriched in aortic tissue, PPAR signaling and peptide chain formation, are negatively enriched in platelets. As for a Western diet, there were only 4 similarities found in the positively enriched gene sets, which consisted of B cell receptor signaling pathways, host interactions of HIV factors, cell cycle checkpoints, and M-G1 transition.

Strengths and Limitations

Our study has substantial advantages including a translational breadth with experimental and epidemiological data relating transcripts from mouse and human platelets and mouse platelet function, human lipid, adiposity, and inflammatory data from FHS. However, we note the following caveats in our study. Our bacterial and Western diet exposure data were conducted in 3 mice, so we may have been underpowered to detect modest effect sizes. We could not verify any confounding attributions due to antibiotic pre-treatment with the *P. gingivalis* group for all genes identified; however, we were able to show in a couple of genes they were not altered by antibiotics (sham treatment) compared

to untreated control in C57BL/6J mice (Figure 2.10). Additionally, there are discrepancies between human and mouse data due to species differences (80). Our FHS data were observational and cross-sectional–we cannot rule out residual confounding or establish the temporality or causal nature of the associations we report. In addition, our cohort was constituted of largely middle-aged to older adults of European ancestry; we cannot determine the generalizability of our findings to younger individuals or other races/ethnicities. Finally, it should be noted that we did not correct for the number of statistical comparisons made when examining the relationships between each gene and clinical covariates in the FHS samples. To reduce the probability of type I error, we focused interpretation on only those covariates of most relevance given the mouse experiments examining a Western diet.

Figure 2.10: Effects of antibiotics (sham) on gene expression in C57BL/6J. Comparison of gene expression of *Tmx2* and *Mfap1a* between untreated control and sham (with 4% sulfamethoxazole in their drinking water for 10 days to clear normal oral microflora) in C57BL/6J mice. Each condition consists of n=3 mice with RNA pooled.

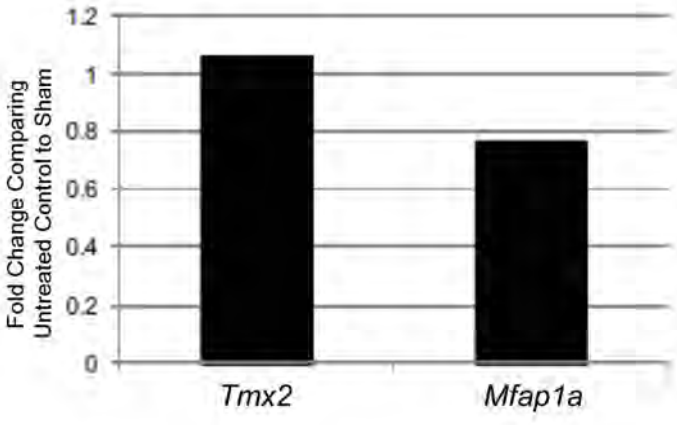

Conclusions

Overall, as has been seen with other immune cells, platelets respond differentially to distinct inflammatory etiologies. Platelets early response to an infection with an oral bacterium or a respiratory bacterium, both associated with CVD, were similar; however, over time, the effects on platelets by each bacterium diverge. Interestingly, *C. pneumoniae* alters platelet transcripts similarly to a Western diet at week 9. In conclusion, the inflammatory-induced transcriptional and functional changes measured in platelets appear to reflect systemic changes occurring with disease development, and provides insight into progression and regression.

CHAPTER III: THE ROLE OF RNA UPTAKE IN PLATELET HETEROGENEITY

Permissions

Chapter III is adapted from a published manuscript to include supplemental data, included with permission.

- *Clancy L, Beaulieu LM, Tanriverdi K, Freedman JE. (2017).The role of RNA uptake in platelet heterogeneity. Thromb Haemost, 117(5), 948-961*
    - Permission Information: Copyright Permission No 116/06/2017

Author Contributions

L.C. performed all experiments and analyses unless noted below. L.C. wrote manuscript. J.E.F. oversaw overall project development and coordination. L.M.B performed initial platelet sorting experiments. K.T. performed high throughput gene expression analyses. All authors commented on the interpretation of results, and reviewed and approved the manuscript.

Summary

The role of platelets in regulating vascular homeostasis has expanded beyond mediation of hemostasis and thrombosis. The discovery of platelet RNA and the presence of subpopulations of platelets containing varying amounts of RNA suggest a role for platelet transcripts in vascular function. As the RNA in anucleated platelets is biologically functional and may transfer to other vascular cells, we hypothesized that platelet RNA diminishes over the lifespan of the platelet with diminishing platelet size due to horizontal cellular transfer. The purpose of this study is to determine if platelet RNA variance is the result of horizontal cellular transfer between platelets and other vascular cells. Utilizing platelet sorting and RNA sequencing, we found that smaller platelets contained a more diverse set of transcripts than larger platelets. Further investigation using fluorescence imaging, gene expression analyses and *in vitro* and *in vivo* modeling revealed that platelets take up RNA from other vascular cells in a complex manner, revealing a dynamic role for platelets in modulating vascular homeostasis through bidirectional RNA transfer. The resultant RNA profile heterogeneity suggests unique functional roles for platelets dependent on size and complexity.

This study expands our basic understanding of platelet function and heterogeneity and is the first to evaluate endogenous vascular RNA uptake and its relation to platelet processes. Our findings describe a novel endogenous phenomenon that can help elucidate the platelet's role in these non-thrombotic

and hemostatic fields, as well as present potential for diagnostic and therapeutic development.

Introduction

Platelets, anucleate blood borne cells generated from megakaryocytes, play a central role in the regulation of vascular homeostasis. Recent studies have expanded the functional roles of the platelet to several non-hemostatic/thrombotic fields, including immune response, tumor progression, tumor metastasis, and other non-vascular diseases (184). As described in Chapter 1, as our understanding of the diverse functional capacity of platelets expanded, so did the need to understand the platelet's content fully. The elucidation of the standard platelet RNA profile, as well as correlations between platelet RNA and specific disease states, fueled our interest in the role this RNA plays in various functional settings. Initial investigation into the role of RNA in platelets focused on the platelet's translational capacity. Platelets contain all of the components necessary to perform pre-mRNA processing and signal-dependent translation (88, 109-111); however, this translational capacity of platelets appears limited (78, 79), the stability of platelet mRNA transient (185), and the correlation to the platelet proteome partial and controversial (113). As an alternative explanation for the presence of RNA in platelets, several studies have recently shown that platelets have the ability to transfer their RNA to other

vascular cells, where these transcripts are both intact and functional (114, 120, 124).

In this study, by analyzing platelet RNA content, we aimed to investigate which transcripts are actively transferred by platelets and how this transfer may affect vascular homeostasis. Canonically, platelets range in size: new platelets recently released to the bloodstream, or “reticulated”, are larger while those that have been in circulation for some time are smaller (186, 187). Historically, this size difference has been used to demonstrate bone marrow response in the setting of thrombocytopenia; the presence of reticulated platelets marks the repopulation of platelets after depletion (187). There is evidence, however, that larger platelets can become smaller after release through the process of budding (13). Though the connections between platelet size and age remain controversial (28), it is generally accepted that larger, presumably younger, platelets contain more RNA content as compared to smaller, presumably older, platelets (186). We hypothesized that the difference in size and RNA content between platelet populations coincides with the observation that platelets transfer RNA to other vascular cells. Whether due to age, budding or RNA transfer, it stands to reason that the smaller platelet RNA transcriptome would be a subset of the larger platelet profile; those transcripts missing from the smaller platelet profile would represent either the transferred transcripts or those degraded during the platelet’s 7-10 day lifespan (37). Surprisingly, our initial RNA sequencing analysis revealed that instead of smaller platelet RNA profiles reflecting a subset of the

larger platelet profile, smaller platelets contained a unique and more expansive transcriptome than larger platelets, specifically containing diverse transcripts of unknown origin. Based on this finding and our previous work showing that platelets can transfer RNA to vascular cells, we hypothesized that platelets can also take up mRNA from vascular cells. Here, we report for the first time that platelets are capable of taking up RNA from other vascular cells in a complex and multifaceted manner and this results in distinct platelet subpopulations with divergent RNA profiles. This novel RNA uptake function expands our understanding of platelet RNA transfer to a bidirectional phenomenon and implies that platelets could play a much broader systemic role in the vasculature than previously understood.

Materials and Methods

Cell cultures

Human umbilical vein endothelial cells (HUVECs; #CC-2519, Lonza, Walkersville, MD, USA), were cultured in endothelial growth medium (#CC-3124, Lonza) and used between second and eighth passages. THP-1 cells (#TIB-202, ATCC, Manassas, VA, USA) were grown in suspension in RPMI 1640 supplemented with L-glutamine, 10% heat-inactivated fetal bovine serum, and 1% antibiotic/antimycotic (#11875-093, Life Technologies, Grand Island, NY, USA).

Animals

C57BL/6J (wild type -WT) and B6.129-Tlr2^{tm1Kir}/J (*TLR2*$^{-/-}$) mice were purchased from The Jackson Laboratory (#000664; #004650, Bar Harbor, ME, USA) and housed in the animal facility at the University of Massachusetts Medical School (UMMS). All methods for mouse work were approved by UMMS Institutional Animal Care and Use Committee.

Platelet isolation

Human platelets were isolated from freshly drawn venous blood collected in ACD SolutionA tubes (#364606, BD, Franklin Lakes, NJ, USA) from healthy donors taking no medication. All work was approved by the Institutional Review Board of UMMS and all participants gave informed consent. Blood samples were centrifuged at 150*g* for 15 minutes with no brake. Upper layer (platelet rich plasma) was isolated and diluted 1:1 times the volume with platelet wash buffer (10 mmol/L sodium citrate, 150 mmol/L sodium chloride, 1mmol/L EDTA, and 1% dextrose, pH 7.4) with prostaglandin E1 (PGE1- 1:10,000, #538903-1MG, EMD Millipore, Billerica, MA, USA). Samples were centrifuged at 750*g* for 15 minutes on low brake. The resulting pellet contains platelets. Washed platelets were resuspended in HEPES buffer (140 mmol/L NaCl, 6.1 mmol/L KCl, 2.4 mmol/L $MgSO_4.7H_20$, 1.7 mmol/L Na_2HPO_4, 5.8 mmol/L sodium HEPES, supplemented with 0.35% BSA and 0.1% dextrose) when noted. Mouse platelets were similarly processed from whole blood collected from cardiac puncture into tubes

containing citrate-phosphate-dextrose solution (15.6 mmol/L citric acid anhydrous, 89.4 mmol/L sodium citrate, 18.5 mmol/L sodium phosphate, and 2.56% dextrose, pH 7.35). Samples were centrifuged at 250*g* for 10 minutes with no brake. Samples were checked for platelet count and purification using Coulter ® A$^{C.}$T Series Analyzer (BD). If additional wash was required, platelets were diluted 2.33x with platelet wash buffer (10 mmol/L sodium citrate, 150 mmol/L sodium chloride, 1mmol/L EDTA, and 1% dextrose, pH 7.4) with PGE1 (1:10,000). Samples were centrifuged at 250*g* for 15 minutes with no brake. The resulting supernatant was removed and centrifuged at 3500*g* for 10 minutes with a low brake to concentrate platelets in pellet.

Platelet Population Sorting

Initial Sorting for Sequencing Run: Whole blood was obtained from 2 healthy, male donors (one under the age of 35, one over the age of 35) and platelets were individually sorted directly from whole blood into two populations: larger, RNA rich ("large/young platelet population") and smaller, RNA poor ("small/old platelet population") using initial red blood cell lysis, followed by staining and positive selection, negative selection and size and complexity gating using FACSAria with FACSDiva v6.1.3 software (BD Biosciences). Whole blood from fresh donors was obtained and red blood cells were lysed using RBC lysis solution (#11814389001, Roche, Basel, Switzerland). Using both negative (Vybrant DyeCycle Violet Stain for DNA –#V35003, Life Technologies, Grand

Island, NY, USA; CD62P activated platelet population –#555524, BD Biosciences) and positive (CD61, platelet marker –#130-098-578, Miltenyi Biotec, San Diego, CA, USA) selection, the resting platelet population was identified. This resting platelet population was further analyzed based on size staining (Calcein AM –#C3100-MP, Life Technologies,) and complexity (side scatter). Corresponding IC controls were used for all antibodies. The smallest 10% ("small/old platelet population", ~1-2 μm diameter based on flow cytometry bead comparison) and the largest 10% ("large/young platelet population", ~ 6 μm diameter based on flow cytometry bead comparison) of the resting population were collected and used for population specific RNA isolation. Experiment 1 yielded 17.4 x 10^6 small platelets and 16.4 x 10^6 large platelets. Experiment 2 yielded 18.8 x 10^6 small platelets and 17.1 x 10^6 large platelets.

Sorting for follow up qPCR: Whole blood was obtained from two healthy males (one <35 years old, one >35 years old) and two healthy females (one <35 years old, one >35 years old) and sorted as described above. The 10% smallest and 10% largest platelets were sorted and isolated for further analysis. The yield of each of these additional sorts was: 3.5 x 10^6, 3.0 x 10^6, 2.6 x 10^6 and 1.7 x 10^6 small platelets and 3.1 x 10^6, 2.8 x 10^6, 2.0 x 10^6 and 1.5 x 10^6 large platelets. All sorting was performed in conjunction with the UMMS Flow Cytometry Core.

RNA Isolation

Total RNA was isolated from cells and platelets using the miRNeasy Mini kit with on column DNase1 digest (#217004, Qiagen, Germantown, MD, USA) according to the manufacturer's directions unless noted in methods.

Sequencing: Total RNA was extracted from platelet sorting samples as described in “RNA Isolation.” After RNA isolation, large platelet RNA and small platelet RNA from individual sortings was combined together to create one large platelet RNA sample (8.4 ng) and one small platelet RNA sample (5.6 ng). Both samples were submitted to Otogenetics Corporation (Norcross, GA, USA) for RNA-Seq assays. Briefly, the integrity and purity of total RNA were assessed using Agilent Bioanalyzer (RNA Integrity Numbers – RIN – calculated to be 6.4 for the large platelet sample and 6.0 for the small platelet sample) and OD260/280 and 1-2 µg of cDNA was generated using Clontech SMARTer PCR cDNA kit (Cat# 634925, Clontech Laboratories, Inc., Mountain View, CA). cDNA was fragmented using Covaris (Covaris, Inc., Woburn, MA), profiled using Agilent Bioanalyzer, and subjected to Illumina library preparation using NEBNext reagents (Cat# E6040, New England Biolabs, Ipswich, MA). The quality, quantity and the size distribution of the Illumina libraries were determined using an Agilent Bioanalyzer 2100. The libraries were then submitted for Illumina HiSeq2000 sequencing according to the standard operation. Paired-end 90 or 100 nucleotide (nt) reads were generated and checked for data quality using FASTQC (Babraham Institute, Cambridge, UK). The small platelet library generated 13.6 million reads

while the large platelet library generated 19.1 million reads. The data were then subjected to data analysis using the platform provided by DNAnexus (DNAnexus, Inc, Mountain View, CA) or the platform provided by Center for Biotechnology and Computational Biology (University of Maryland, College Park, MD) as previously described (*Nature Protocols* **7**:562-578, 2012). Sequencing data analysis was performed using Tophat (v2.0.5) against reference assembly USCS hg19 (downloaded from Illumina iGenome) (transcript mapping) and Culllinks.cuffdiff (v.2.0.2) defined by the annotation file genes.gtf (from Illumina iGenome) (expression level calculation). For sequencing data, see Appendix C.

DAVID Analysis

The Database for Annotation, Visualization and Integrated Discovery (DAVID) v6.7 was used to analyze the functional relevance of young versus old platelet sequencing data. Differential gene expression files were obtained from Otogenetics (see “Sequencing”) and genes were selected for analysis first based on Cuffdiff output (NOTEST, HIDATA, LOWDATA and FAIL results were excluded) and then based on expression changes between samples. Specifically, genes were determined to be young or old platelet specific if they were expressed at < 0.1 FPKM in 1 population and > 1 FPKM in the other population. This cutoff was based on a 0.3 FPKM expression threshold used in a previous platelet RNA sequencing study(80).

In Vivo TLR2 (Pam3CSK4) stimulation experiment

C57BL/6J (WT) mice were injected intraperitoneally with either sterile saline or Pam3CSK4 (4 mg/kg; #tlrl-pms, Invivogen, San Diego, CA, USA). After 3 hour incubation time, blood was harvested via cardiac puncture into citrate-phosphate-dextrose solution. Platelets were isolated from whole blood by centrifugation as described in "Platelet Isolation". Isolated platelets were processed for RNA isolation, cDNA preparation, and RT-qPCR by high throughput gene expression analysis as described.

In vivo platelet RNA transfer

Peripheral blood mononuclear cells (PBMCs) from WT and *TLR2*$^{-/-}$ mice were isolated using LymphoPrep (#AXS-1114544, Stem Cell Technologies, Vancouver, BC, Canada) and SepMate (#15415, Stem Cell Technologies) protocols. In brief, whole blood was collected as described above. Samples were diluted 1:1 in 1x PBS with 2% FBS and layered on top of LymphoPrep media in SepMate conicals. Samples were centrifuged at 1200*g* for 10 minutes with brake. The top layer of plasma above the interphase was removed and the remaining interphase portion above the SepMate barrier was poured into a separate conical. Interphase samples were diluted by 1:1 in 1x PBS, 2% fetal bovine serum (FBS) and centrifuged at 150*g* for 10 minutes, with no brake. The resultant pellet was additionally washed in 1x PBS/2% FBS and recentrifuged at *150g* for 10 minutes. The resulting pellet contains PBMCs. Approximately 2×10^6 PBMCs

were resuspended in sterile saline solution and injected into each *TLR2*$^{-/-}$ mice via tail-vein injection (total volume, 200 µL). After 1 hour, *TLR2*$^{-/-}$ mice were intraperitoneally injected with 5 µg/g lipopolysaccharide (LPS; #tlrl-3pelps, InvivoGen) or saline. Blood samples were collected via cardiac puncture as above 3 hours after LPS injection. Platelets were isolated as previously described in "Platelet isolation" and processed for RNA isolation, cDNA preparation, and RT- qPCR as described. Taqman gene expression assay for *TLR2* detection: Mm00442346_m1.

Isolation of platelet fraction post in vivo control experiment

Control experiment was run to check the purity of platelet fractions isolated from whole blood post *in vivo* experimentation. C57BL/6J (WT) mice were intraperitoneally injected with 5 µg/g lipopolysaccharide (LPS; #tlrl-3pelps, InvivoGen) or saline. Blood samples were collected via cardiac puncture 3 hours after LPS injection, as in "*In vivo* platelet RNA transfer". Platelets were isolated as previously described in "Platelet isolation" and checked by flow cytometry for size (FSC), complexity (SSC) and CD41 expression (CD41–#17-0411, ThermoFisher Scientific (Affymetrix/eBioscience), Waltham, MA, USA).

In Vitro Simulated Clot Experiments

In vitro simulated clot experiments were conducted in 6 well culture plates at 37C, 5% CO2. For all experiments, HUVECs were plated at 5000 cells/cm^2 and

cultured as described until >85% confluent. Platelets were isolated as described in “Platelet Isolation”. Cells were washed one time with 1x phosphate buffered saline (PBS)(#10010-049, Life Technologies) and put in low phenol red endothelial cell medium (#CC-3129, Lonza, Walkersville, MD, USA). Cells were pretreated with or without thrombin stimulation (1 hr, 0.1U/mL; #HT-1002a, Enzyme Research Laboratories, South Bend, IN, USA), washed and co-incubated for 2 hours with resting platelets or thrombin-stimulated (0.1 U/mL) platelets. After co-incubation, platelets were removed from wells, pelleted and resuspended in Qiazol for RNA isolation. HUVECs were washed 2x in PBS and then resuspended in Qiazol for RNA isolation. Transcription shutdown *in vitro* simulated clot experiments followed the same protocol as above with additional α-amanitin pretreatment of HUVECs before thrombin stimulation. Cells were pre-treated with either α-amanitin (4 hours, 10 µg/mL; #129741-1MG, EMD Millipore), thrombin (1 hr, 0.1U/mL), both (4 hour alpha-amanitin treatment with thrombin bolus after 3 hours) or neither. Transcription shutdown in HUVECs treated with α-amanitin was confirmed with Click-iT® RNA AlexaFluor 488 Imaging Kit (#C10329, Life Technologies). Brefeldin A inhibition simulated clot experiments followed same protocol as above with two exceptions: co-incubation time was 10 minutes and HUVECs were pretreated with brefeldin A (10 µg/mL, #00-4506-51, eBioscience, San Diego, CA) or methanol control. Pretreatment was 2 hours long with thrombus stimulation 1 hour post inhibitor addition. Conditioned media experiments followed a similar protocol to above. HUVECs were plated at 5000

cells/cm^2 and cultured as described until >85% confluent. Platelets were isolated as described in “Platelet isolation”. Cells were washed one time with 1x PBS and put in low phenol red endothelial cell medium. Cells were pretreated with or without thrombin stimulation (1 hr, 0.1U/mL), after which conditioned media was moved to a new 6-well plate. Conditioned media was combined with either additional media or with resting platelets or thrombin-stimulated (0.1 U/mL) platelets and incubated for 2 hours at 37C, 5% CO2. After co-incubation, media and platelets were removed from wells, pelleted and resuspended in Qiazol for RNA isolation. HUVECs were washed 2x in PBS and then resuspended in Qiazol for RNA isolation. Control experiments to check cellular contamination in isolated platelet fractions followed the same protocol as initial clot experiments listed above, followed by flow cytometric analysis of platelets for size (FSC), complexity (SSC) and CD42b expression (CD42b – #11-0429, ThermoFisher Scientific (Affymetrix/eBioscience), Waltham, MA, USA).

Click-iT® Simulated Clot Experiments

Click-iT® RNA Capture kit (#C10365, Life Technologies) was used to label cellular-RNA prior to incubation. Cells were first treated with 5’-ethynyl uridine (5’-EU) at 0.2 mmol/L overnight then stimulated with either thrombin (HUVEC, 0.1U/mL) or Pam3CSK4 (THP1, 10 µg/mL) for 1 hour, resulting in all nascent cellular RNA incorporating this unique nucleotide. Cells were washed twice with PBS and incubated with platelet rich plasma (PRP) as described in *“In Vitro*

Simulated Clot Experiments. Post incubation, platelet fraction was separated from cellular fraction (HUVEC experiments - removed platelets manually, THP1 - separated through centrifugation at 750*g* for 15 minutes with low brake). Once platelet fraction was obtained, performed RNA Capture was performed according to manufacturer's method to isolate cellular-derived RNA. RNA was converted to cDNA as described in "cDNA Reaction". Gene expression was assessed using the TaqMan Gene Expression Platform as described in "RT-qPCR" and "High-Throughput RT-qPCR".

cDNA Reaction

RNA was converted to cDNA with the High-Capacity cDNA Reverse Transcription kit (#4368813, Life Technologies). cDNA was preamplified prior to real time (RT)-qPCR reaction using TaqMan PreAmp Master Mix (#4391128, Life Technologies) and TaqMan Gene Expression assays (#4331182, #4351372, Life Technologies) according to the manufacturer's protocol.

RT-qPCR

Gene expression was assessed using TaqMan Gene Expression assays with Real Time PCR instrument (Applied Biosystems 7900 HT Fast Real-Time PCR System with SDS Version 2.2.2 software; Life Technologies) or via High-Throughput RT-qPCR (see "High-Throughput RT-qPCR"). RT-qPCR results were calculated using the ΔΔCt method, with background cycle threshold (Ct) set to

35. Platelet RT-qPCR array results were normalized using housekeeping genes glyceraldehyde 3-phosphate dehydrogenase (*GAPDH*), glucose-6-phosphate isomerase (*GPI*) and/or vesicle associated membrane protein 3 (*VAMP3*) as noted in individual results. HUVEC RT-qPCR array results were normalized using *CD63* and *CD81*. These genes were selected for normalization using the geNorm analysis module of qbase+ software version 2.6 (www.qbaseplus.com, Biogazelle, Zwijnaarde, Belgium). The software is based on the qBase quantification model(188) and contains the geNorm module for identification of stably expressed reference genes(189). *In vivo* mouse experiment RT-qPCRs were normalized to beta-actin (*β-actin*) or *GAPDH* as noted with results.

High-Throughput RT-qPCR

TaqMan gene expression assays and TaqMan Gene Expression Master Mix (#4369542, Life Technologies) were used to run Dynamic Array 96.96 chips (Fluidigm, South San Francisco, CA) on BioMark System (Fluidigm) for high-throughput gene expression analysis. Differential expression analysis and statistical analysis performed using the RT^2 Profiler PCR Array Data Analysis tool version 3.5 (http://pcrdataanalysis.sabiosciences.com/pcr/arrayanalysis.php, Qiagen). Normalization performed using housekeeping genes as described in "RT-qPCR" in the Online Methods.

Fluorescent RNA transfer in flow adhesion model

HUVEC RNA was stained using SYTO® RNASelect™ fluorescent green stain (#S32703, Life Technologies) at 1:125 dilution for 1 hour in serum free media. After incubation, stain was removed and cells were washed twice with 1x PBS. Cells were then used in the flow adhesion model (55). Human platelets, isolated from whole blood, as described, were run over cells for noted time at 3 mL/min in 1x PBS, pH 7.4. After the run was complete, platelets were recovered from buffer, concentrated, fixed in IC fixative buffer (#00-8222-49, eBioscience, San Diego, CA, USA) and mounted on slides using ProLong Gold (#P36930, Life Technologies). HUVECs were washed once with PBS, pH 7.4, fixed with cold methanol and mounted on slides using ProLong Gold. For indirect transfer experiment, PBS pH 7.4 alone was flowed over HUVECs under designated sample conditions. Buffer was then recovered and incubated with platelets with or without stimulation for a specified time. Platelets were then recovered and analyzed as described.

Whole Blood Counts

Blood collected from each mouse was analyzed for white blood cell (WBC) and platelet content using a Coulter ® A$^{C\cdot}$T Series Analyzer (BD).

Confocal microscopy

Fluorescent imaging samples were analyzed by confocal microscopy. Imaging was performed on TCS SP5II confocal microscope and captured using Leica

Confocal Version 2.5 software (Leica Microsystems; Buffalo Grove, IL, USA). Image quantification was performed by selecting individual cells across the field (*n*=20) per sample and using Image J (1.48V) software to measure mean fluorescence.

Flow cytometry

Flow cytometry was performed on a BD LSRII using BD FACSDiva v6.2 software (BD) and analyzed using FlowJo Version X.

Fragment analysis

Fragment analysis and RNA integrity number (RIN) calculation of sequencing samples performed by Otogenetics as described in “Sequencing”. Fragment analysis and RNA quality number (RQN) calculation of additional sorting samples used for RT-qPCR analysis performed via the UMMS DNA Fragment Analysis Service using an Advanced Analytical instrument with a Total RNA assay, running PROSize 2.0 analysis software.

Data analysis

All values are expressed as the mean (SD) of at least 3 different experiments. RT-qPCR fold changes were calculated using ΔΔCt method. Statistical analyses were performed using Prism software (GraphPad Prism v6; La Jolla, CA, USA). Individual statistical analysis tests noted in figure legends. Statistical analyses of

samples examined with RT^2 Profiler PCR Array Data Analysis tool version 3.5 analyzed by student's t-test of the replicate 2^ (-ΔΔCt) with $p<0.05$. For additional statistical tests not included in original text, please see Appendix D.

Results

Size differentiated platelet subpopulations show distinct RNA profiles with diverse functionalities

To interrogate the impact of platelet size on RNA content, we identified and isolated large and small platelet subpopulations from human whole blood using flow cytometry. Removal of cells through lysis, negative selection, positive selection and gating based on size and cellular complexity allowed for isolation of the 10% largest and 10% smallest resting platelet populations (Figure 3.1).

Figure 3.1: Workflow of fluorescence-activated cell sorting (FACS) of large and small platelet populations. Large and small platelets were separated by FACS and analyzed for RNA content via RNA sequencing. (A) FACS sorting approach to isolate larger platelet and smaller platelet subpopulations. Representative images of sorting technique show selection of CD61+, DNA-, CD62P- population to obtain resting platelet population. This was followed by CD61+ confirmation and FSC/SSC gating to isolate 10% smallest and 10% largest platelet subpopulations. Events in representative flow cytometry images color-coded for convenience: resting platelets (red/pink), 10% smallest platelets (blue), 10% largest platelets (orange).

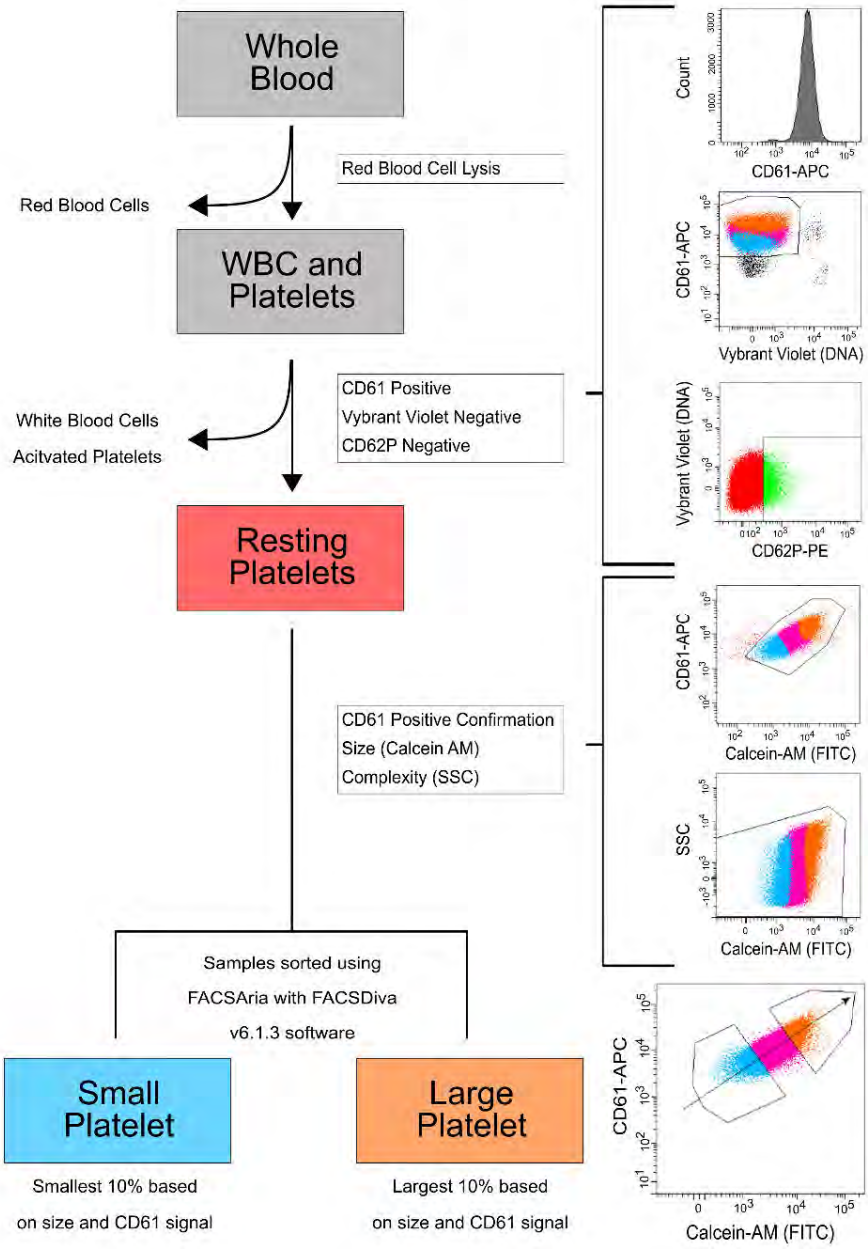

RNA sequencing of these specific subpopulations revealed that, although the majority of RNA transcripts identified were shared by both populations, each subpopulation had a distinct set of platelet transcripts unique to itself. Cuffdiff analysis of RNA sequencing results identified 7500 successfully mapped transcripts (Appendix C), of which 5027 were present in both populations, 378 were specific to the younger, larger platelet population and 2314 were specific to the older, smaller platelet population (Figure 3.2).

Figure 3.2: Differential RNA expression in large and small platelet populations. Large and small platelets were separated by FACS and analyzed for RNA content via RNA sequencing. (B) Venn diagram of DAVID analysis results of large versus small platelet RNA sequencing data.

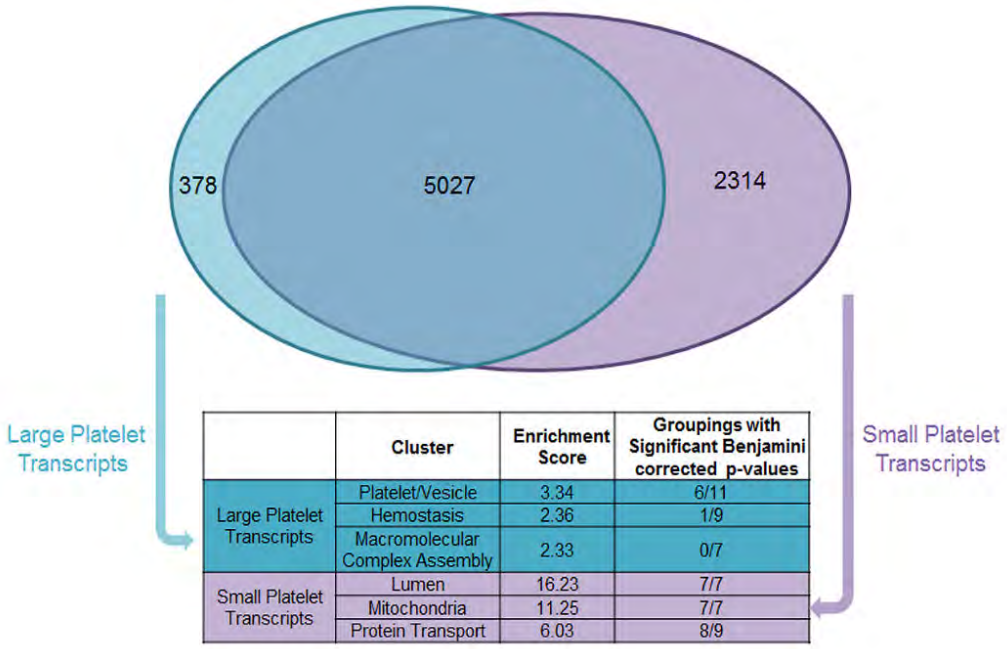

	Cluster	Enrichment Score	Groupings with Significant Benjamini corrected p-values
Large Platelet Transcripts	Platelet/Vesicle	3.34	6/11
	Hemostasis	2.36	1/9
	Macromolecular Complex Assembly	2.33	0/7
Small Platelet Transcripts	Lumen	16.23	7/7
	Mitochondria	11.25	7/7
	Protein Transport	6.03	8/9

Contrary to our anticipated results, the transcripts specific to the smaller platelet population represented a distinctly different and more varied transcript profile than larger platelets. DAVID (Database for Annotation, Visualization and Integrated Discovery v6.7) functional annotation analysis of the two subpopulations' transcriptomes showed distinct functional association differences between the two groups. While the 378 transcripts present only in larger platelets were loosely associated with 129 functional clusters, they were only enriched (enrichment score > 3) in 1 (platelet/vesicle association) (Figure 3.2). Larger platelet transcripts were associated with 142 gene ontology (GO) terms, with 8 terms correlated with a Benjamini corrected $p<0.05$ (Table 3.1).

Table 3.1: DAVID Gene Ontology (GO) functional analysis of small and large platelet RNA profiles. Overall representation of GO categories and associated terms for large and small platelet RNA DAVID analysis.

Platelet Population	Gene Ontology Category	Associated Terms	Individual terms with Benjamini correction of p-value <0.05
Small	Biological Process (BP)	281	33
	Cellular Compartment (CC)	90	31
	Molecular Function (MF)	98	27
	Total	469	91
Large	Biological Process (BP)	83	0
	Cellular Compartment (CC)	38	8
	Molecular Function (MF)	21	0
	Total	142	8

The smaller platelet specific transcripts were associated with 451 functional clusters and enriched in 16 of them, the most enriched of which included protein transport and mitochondrial function (Figure 3.2). Smaller platelet transcripts were associated with 469 GO terms, with 91 terms with a Benjamini corrected $p<0.05$ (Table 3.1). In-depth analysis of the biological processes associated with individual platelet populations also revealed a distinct trend: while the larger platelet profile included typical platelet-associated functions, such as platelet activation, hemostasis and wound healing, these functions were not associated with the smaller platelet profile (Appendix E). The smaller platelet profile, in turn, had a number of functions distinctly associated with vascular cell function, such as T cell, lymphocyte and B cell activation, proliferation, differentiation and/or apoptosis (Appendix E). We repeated this initial sorting experiment, performing four additional rounds of sorting, to validate the results comparing small and large platelet specific RNA profiles using real time quantitative polymerase chain reaction (RT-qPCR). Several targets covering a span of expression levels in initial RNA sequencing were validated by RT-qPCR, including those genes typically considered stable in cells (such as *β-actin*, *B2M*, and *GAPDH*, though these genes are notably differentially expressed here), those equally expressed in initial sequencing results (such as *GUK1, LSP1, NFKBIA* and *SELL*) and those with higher expression in large platelet RNA than in small platelet RNA (such as *BCL2L1, PF4, CD40* and *SELP*) (Figure 3.3, Table 3.2).

Figure 3.3: RT-qPCR validation and analysis of platelet subpopulation RNA profiles. RT-qPCR validation of RNA from small and large platelet subpopulation sorting. Raw Cq values for *n*=4 biological replicates, error bars representing mean (SD). Black bars represent small platelet RNA results, gray represent large platelet RNA results. *P*-values calculated by unpaired two-tailed T-test with p<0.05 (**P*<0.05, ***P*<0.01, ****P*<0.001, *****P*<0.0001).

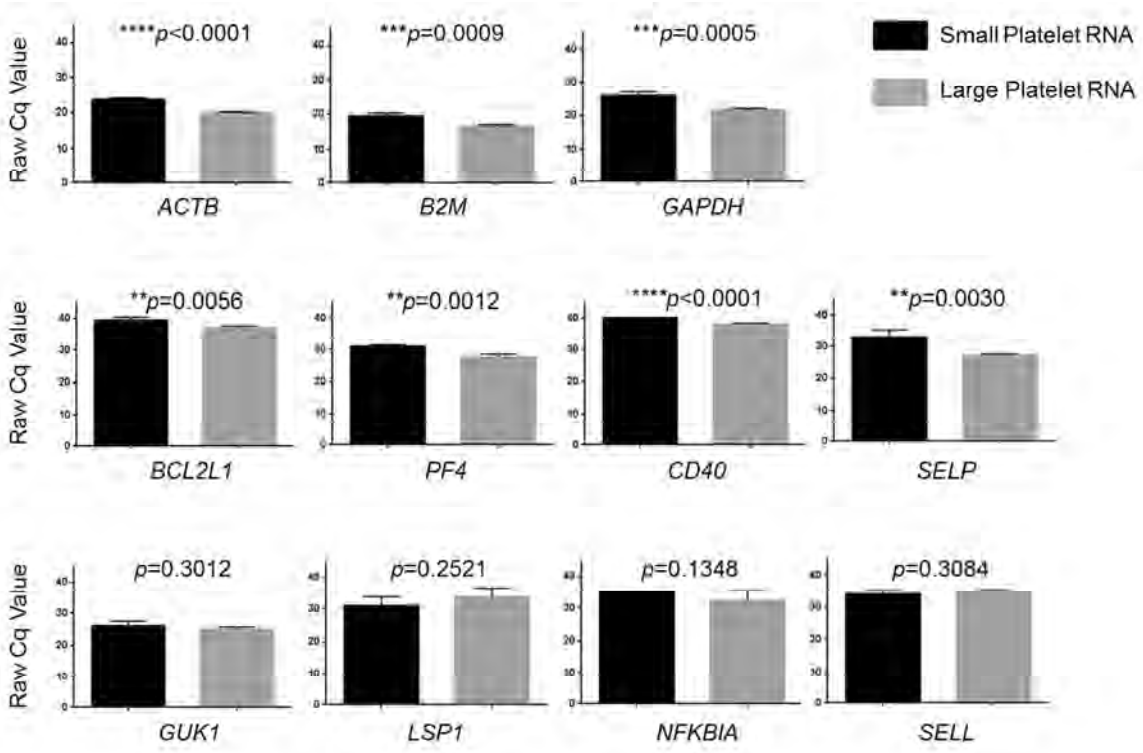

Table 3.2: Sequencing results for select targets validated using RT-qPCR. Sequencing FPKM (fragments per kilobase of transcript per million mapped reads) (and RPKM – reads per kilobase of transcript per million mapped reads) for targets selected for RT-qPCR validation.

Display Name	Name	Rowley (RPKM)	Clancy Large Platelet (FPKM)	Clancy Small Platelet (FPKM)
NM_001101	*ACTB*	3482.0	5197.9	2399.6
NM_004048	*B2M*	20654.6	38185.9	12039.4
NM_002046	*GAPDH*	259.3	404.5	157.3
NM_003005	*SELP*	125.5	8.2	0.7
NM_001191	*BCL2L1*	238.1	41.9	12.9
NM_002619	*PF4*	7223.1	8775.9	359.9
NM_001250	*CD40*	6.5	12.5	0
NM_152854		n/a	0	1.6
NM_00159391	*GUK1*	52.3	181.2	178.3
NM_001013255	*LSP1*	15.8	0	30.6
NM_002339		n/a	94.8	49.6
NM_020529	*NFKBIA*	13.2	489.2	454.7
NM_000655	*SELL*	n/a	92.6	165.6
NR_029467		10.2	51.4	3.1

Analysis of the coverage tracks of these targets from initial sequencing revealed similar coverage patterns between platelet subpopulations (Figure 3.4, panels 1-3).

Figure 3.4: Integrative Genomics Viewer (IGV) analysis of platelet subpopulation RNA profiles. IGV (1, 2) coverage tracks for select gene targets analyzed during RT-qPCR validation. Blue trace represents larger platelet RNA, pink trace represents small platelet RNA, and black trace represents gene reference sequence.

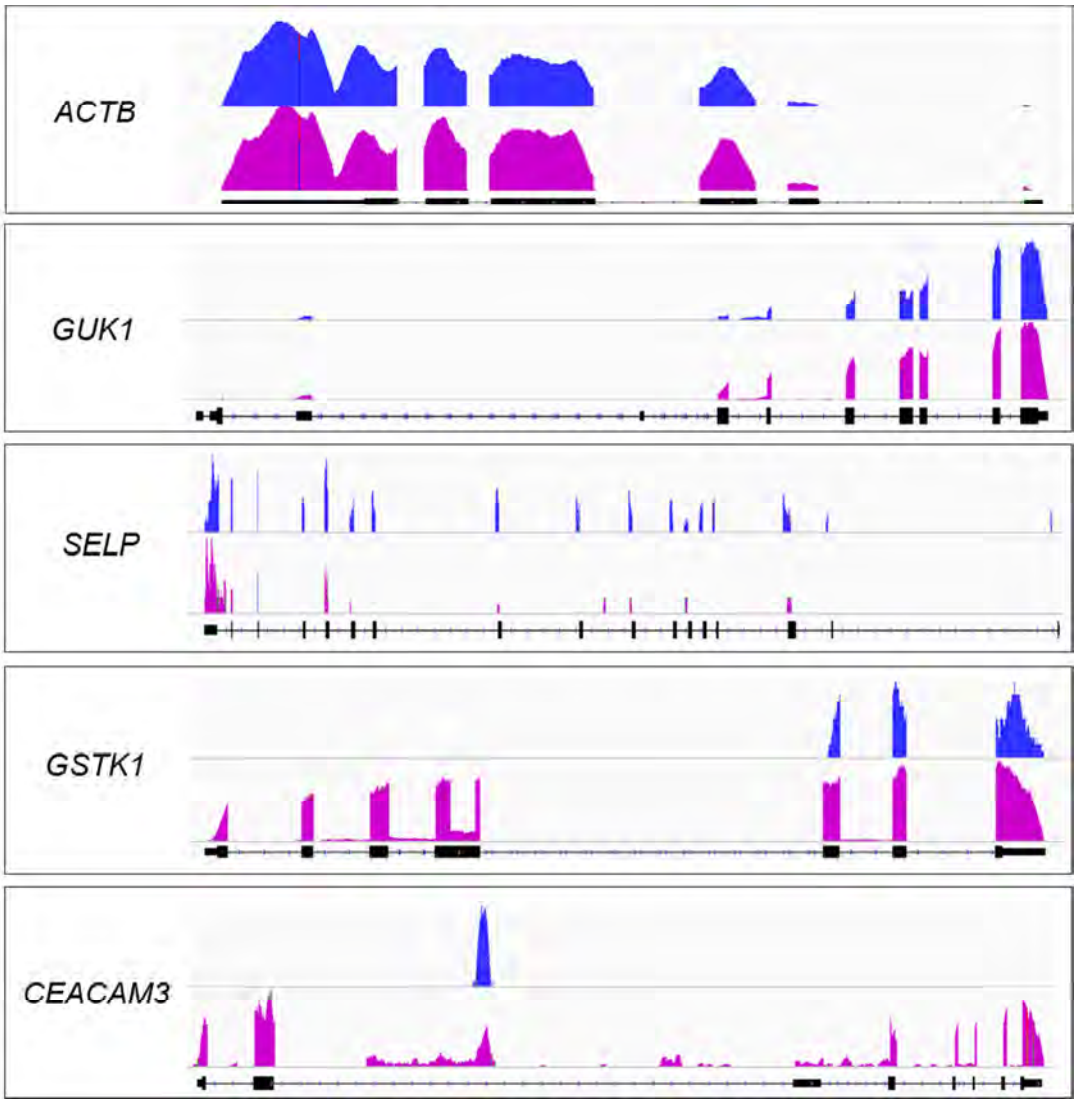

Interestingly, validation of targets with higher expression values in smaller platelet RNA was not possible by RT-qPCR. Analysis of the coverage tracks of these genes revealed that these targets showed significantly different coverage between platelet subpopulations, with the smaller platelet sample often covering more of the overall transcript than the large (Figure 3.4, panels 4-5). Despite these coverage differences, targeted RT-qPCR did not validate sequencing results (data not shown). Interestingly, analysis of the overall RNA quality of the original sequencing samples as well as the validation samples (either through calculation of RNA integrity (RIN) or RNA quality (RQN) number) revealed a distinct pattern – the smaller platelet subpopulation RNA was always of lesser quality than the larger platelet population (Table 3.3).

Table 3.3: Fragment analysis results for sequencing and RT-qPCR validation of FACS samples. RNA integrity number (RIN) (sequencing sample) or RNA quality number (RQN) for samples from platelet subpopulation study. ǂ denotes sample with particularly low concentration which we believe resulted in false negative RQN.

Experiment	Small Platelet	Large Platelet
Sequencing	6.0	6.4
Validation Sorts	1.0	3.1
	0.0	1.4
	1.0	0.0ǂ
	0.0	4.4

This suggests RT-qPCR validation was unsuccessful due to the fragmented nature of the smaller platelet RNA. These findings support that small and large

platelet subpopulations show distinct transcript diversity associated with discrete functionalities, as well as differing RNA quality, which may reflect novel functional differences between these subpopulations.

Stimulation of vascular cell interaction leads to increased platelet transcript uptake *in vivo.*

Based on the observations of increased transcript diversity in the smaller platelet population, the lack of transcription in platelets, and previous work on the uptake of microvesicles by platelets (133, 135, 190), we investigated whether platelets take up RNA from other cells throughout the vasculature *in vivo*. To study this question, we induced platelet and white blood cell (WBC) interaction in C57BL/6J mice by treating them with Pam3CSK4, a toll-like receptor 1/toll-like receptor 2 (TLR1/TLR2) ligand (114, 140, 191, 192). Post stimulation, platelets were harvested and analyzed for RNA content for various adhesion and inflammatory transcripts. Several transcripts showed distinct increases post Pam3CSK4 treatment (Figure 3.5).

Figure 3.5: Increased transcript expression in platelets post *in vivo* stimulation. Significant (* *P*<0.05; ** *P*< 0.01) transcript fold changes (expressed as $2^{-\Delta\Delta Ct}$) in wild type platelet transcript expression levels post Pam3CSK4 stimulation. All samples were normalized to *β-actin* with *n*=3 mice per group, values expressed as mean (SD). *P*-values calculated using individual unpaired t-test

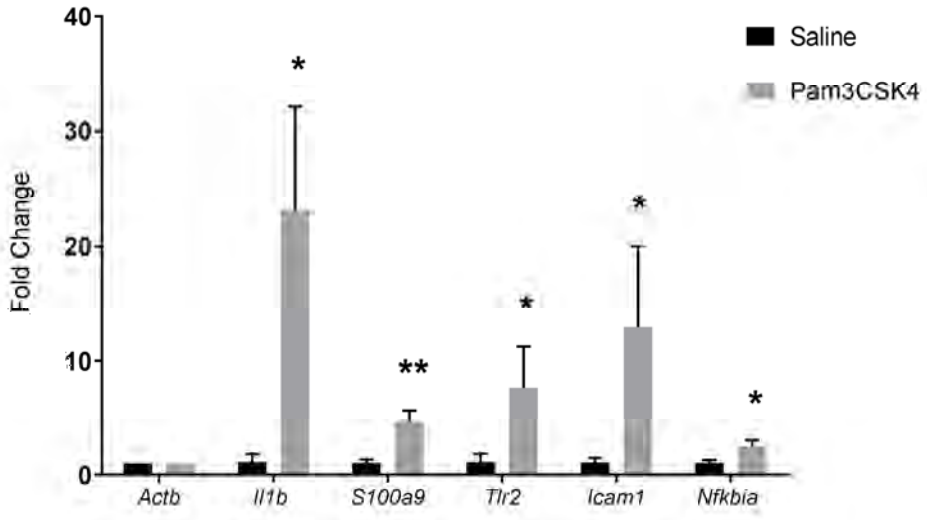

The increase in interleukin 1 beta (IL1β) mRNA post stimulation draws a parallel to previous publications that show *pro-IL1β* is processed in toll-like receptor 4 (TLR4)-stimulated platelets (88, 109-111). As there is no evidence for a similar phenomenon based on TLR2 signaling or with these other targets, the increase of these transcripts supports the hypothesis that, under appropriate stimulation, platelets can take up transcripts from other vascular cells.

To confirm that these transcripts come from other vascular cells and not through platelet internal RNA processing, we developed an infusion model to better track transcript origin, allowing us to monitor expression of *Tlr2* after platelet stimulation. Peripheral blood mononuclear cells (PBMCs) were isolated

from C57BL/6J mice. These PBMCs were then infused into *Tlr2*$^{-/-}$ mice. After stimulation of WBC and platelet interaction with lipopolysaccharide (LPS) (114), platelets were isolated from mice and analyzed for RNA content. The presence of wild type *Tlr2* transcript in platelets from *Tlr2*$^{-/-}$ mice post infusion and stimulation supports the transfer of RNA *in vivo* from the wild type PBMCs to platelets in response to inflammation (Figure 3.6).

Figure 3.6: Increased transcript expression in platelets post platelet transfusion and *in vivo* stimulation. Presence of wild type *Tlr2* in platelets from transfused mice. *Tlr2* fold changes (expressed as $2^{-\Delta\Delta Ct}$) in platelets. All samples were normalized against *GAPDH with n=3 mice per group, values expressed as mean (SD)*. The transfer of *Tlr2* mRNA from PBMCs to platelets under LPS stimulation was significant compared to control infusions (**P* =0.023, assessed by one-way ANOVA with Tukey's multiple comparisons test post analysis, α = 0.05).

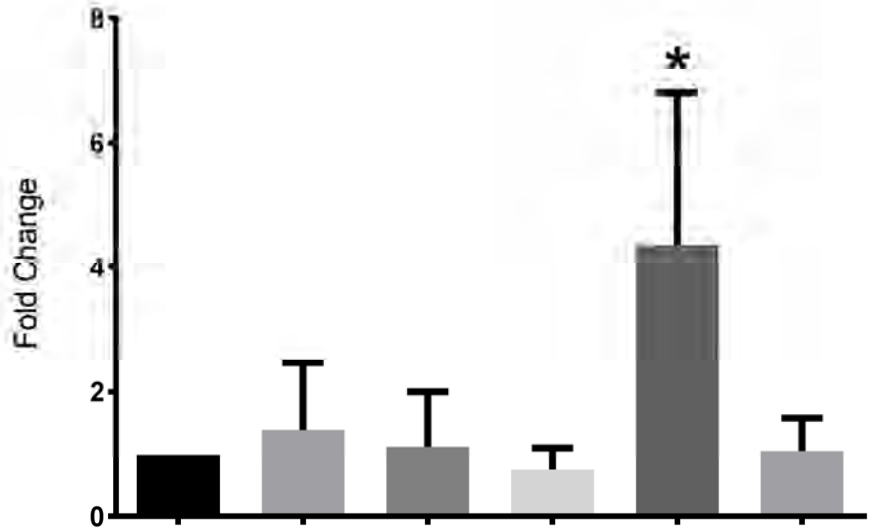

PBMCs Background	n/a	C57BL/6J	*Tlr2-/-*	n/a	C57BL/6J	*Tlr2-/-*
LPS Treatment	-	-	-	+	+	+

As a control, we performed additional rounds of this experiment and platelet isolation to analyze isolated platelet fractions for potential cellular contamination. Flow cytometry analyses revealed the main population isolated was CD41 positive with no significant shift in size or complexity due to treatment (Figure 3.7, panels 1-2). There was a slight decrease in CD41 expression between saline and LPS treated mice (Figure 3.7, panel 3); however, with no significant shift in population, this suggests shedding of CD41 in response to stimulation, as previously seen with other platelet markers (193).

Figure 3.7: Confirmation of platelet isolation during *in vivo* stimulation experiments. Flow cytometric analysis of isolated platelet population post *in vivo* stimulation. Mice were treated and samples isolated as performed in *Tlr2-/-* experiments. Samples were then stained for CD41 and analyzed by flow cytometry for changes in complexity (SSC), size (FSC) and CD41 expression. A) Percentage of total events within designated platelet gate. B) Percentage of events within designated gate which were CD41 positive. C) Geometric mean of fluorescence corresponding to CD41 expression of events within designated gate. All results were analyzed using unpaired t-test ($p<0.05$). Error bars represent mean (SD) of $n=5$ for each group.

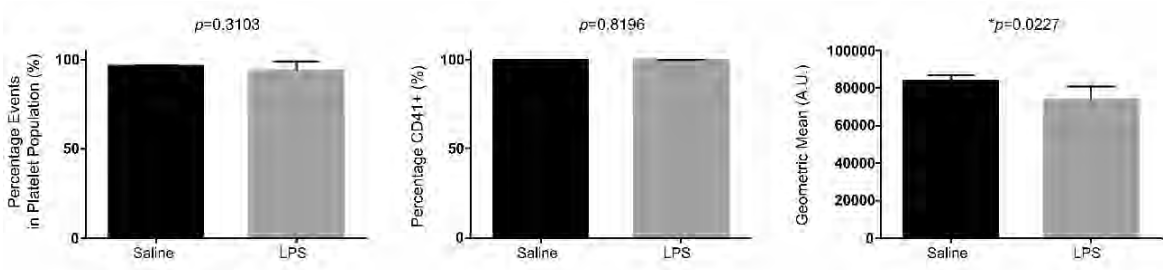

Taken together, these results confirm the novel ability of platelets to take up cellular RNA from endothelial cells and leukocytes and suggest potential for platelet based communication throughout the vasculature.

Platelet transcript levels are increased after *in vitro* co-incubation with endothelial cells

To further study the phenomenon of platelet RNA transfer, we co-incubated resting or activated human platelets with human umbilical vein endothelial cells (HUVECs) under various conditions and measured platelet transcript levels by RT-qPCR post incubation. To mimic a clot environment, we combined HUVEC and platelets under low-dose thrombin stimulation. We analyzed ninety-six inflammatory and adhesion transcripts in platelets under four conditions: platelets with and without stimulation, alone or in the presence of HUVECs. Table 3.4 highlights the 38 transcripts that showed notable increases in expression levels when comparing platelets alone to platelets post incubation with endothelial cells. Sixteen genes were increased in platelets solely upon incubation with HUVECs with a less than 10% increase in expression with stimulation (Table 3.4*a*). The remaining 22 genes, showed increased expression with HUVEC incubation and an even greater fold change when stimulated (Table 3.4*a*). Additionally, 18 transcripts showed fold regulation changes that were statistically significant when compared to platelet expression levels alone (noted in red, Table 3.4*a*).

Table 3.4: Differential gene expression in platelets after *in vitro* simulated clot experiments. RT-qPCR results for genes that show upregulation in platelets after incubation with unstimulated or stimulated endothelial cells (ECs) under normal conditions (A) or with pretreatment transcription shutdown in ECs through α-amanitin treatment (B). RT-qPCR results were normalized to three housekeeping genes (*GAPDH, GPI* and *VAMP3*) with platelet alone samples set as experimental controls. Gray color coding denotes magnitude of fold regulation across samples for a given gene. Cells and genes in red text signify $P < 0.05$ (based on a Student's t-test of the replicate $2^{(-\Delta\Delta Ct)}$ values for each gene in the control group and treatment groups) for given value. Legend below table describes sample setup conditions. A) Results represent n=6 experiments. B) Results represent n=3 experiments.

Magnitude of Fold Regulation

Min Max

A)	Platelets Alone	Stimulated Platelets	Unstimulated Platelets Post ECs Incubation	Stimulated Platelets Post Stimulated ECs Incubation
CXADR	1.0	-1.0	**2709.8**	**2264.3**
COL18A1	1.0	-1.7	**950.4**	**1251.7**
SELE	1.0	-1.0	566.8	**9080.5**
ICAM1	1.0	-2.9	**401.1**	**918.4**
ITGA5	1.0	3.1	**160.7**	**186.5**
TLR3	1.0	-3.1	**115.1**	79.5
CXCL1	1.0	-1.5	67.1	**230.1**
CXCL12	1.0	5.6	57.0	45.8
TLR4	1.0	-1.1	**33.9**	**40.5**
KIAA1462	1.0	-2.7	**27.6**	**25.9**
CX3CL1	1.0	-10.8	27.2	155.1
IL6	1.0	2.3	21.5	43.5
VCAM1	1.0	-2.3	19.5	508.4
CD81	1.0	-3.3	**18.1**	**22.2**
CXCL2	1.0	23.8	17.6	59.2
EIF4G1	1.0	2.1	**15.2**	**17.4**
TNFSF10	1.0	2.7	12.8	**12.0**
CALR	1.0	-1.3	**12.2**	**13.9**
ASGR1	1.0	-1.0	11.7	12.3
VEGFA	1.0	-1.6	8.1	17.1
IL8	1.0	4.6	6.2	16.3
SIRPA	1.0	-2.9	5.3	5.1
VEGFB	1.0	-1.0	**5.0**	**5.2**
VAMP5	1.0	-3.2	5.0	**4.7**
VIP	1.0	-1.5	4.8	6.5
CRP	1.0	-1.0	4.8	15.3
IFNA1	1.0	-1.0	4.4	15.3
TNFRSF1B	1.0	-1.2	4.2	4.3
CCL7	1.0	3.1	3.8	3.0
NFKBIA	1.0	1.4	3.1	**5.3**
CD63	1.0	-1.2	**2.8**	**2.9**
SELENBP1	1.0	-3.4	2.7	1.5
DICER1	1.0	2.7	2.6	2.8
KIAA0232	1.0	-1.2	2.6	2.2
IFITM3	1.0	1.1	2.3	2.0
MAP4K4	1.0	-1.1	2.2	**2.8**
CXCL6	1.0	-6.4	2.1	18.8
VEGFC	1.0	1.0	1.8	2.0

Platelets	+	+	+	+
Platelet Thrombin Stimulation	-	+	-	+
EC Incubation	-	-	+	+
EC Transcription Shutdown	-	-	-	-
EC Thrombin Stimulation	-	-	-	+

B)	Platelets Alone	Stimulated Platelets	Unstimulated Platelets Post EC Incubation	Stimulated Platelets Post Stimulated ECs Incubation
CXADR	1.0	-1.3	**5361.9**	12880.0
COL18A1	1.0	-2.7	**251.2**	477.3
SELE	1.0	-1.3	266.3	10342.8
ICAM1	1.0	-8.8	570.9	**2625.8**
ITGA5	1.0	1.2	**52.4**	**88.5**
TLR3	1.0	-11.3	1.7	2.3
CXCL1	1.0	-9.4	7.0	24.2
CXCL12	1.0	1.4	1.9	35.5
TLR4	1.0	-1.8	14.9	21.6
KIAA1462	1.0	-15.3	**4.3**	**7.8**
CX3CL1	1.0	-139.6	14.4	19.6
IL6	1.0	-2.8	1.1	38.0
VCAM1	1.0	1.1	**196.3**	33.6
CD81	1.0	-1.3	16.0	30.3
CXCL2	1.0	88.1	156.3	380.4
EIF4G1	1.0	-1.2	**3.5**	**5.6**
TNFSF10	1.0	-1.4	3.2	4.7
CALR	1.0	1.0	**9.5**	**14.9**
ASGR1	1.0	-1.3	-1.3	49.2
VEGFA	1.0	-2.3	**7.3**	8.2
IL8	1.0	22.7	21.4	205.8
SIRPA	1.0	-1.0	**10.2**	13.6
VEGFB	1.0	1.2	**6.7**	**7.5**
VAMP5	1.0	-1.0	**3.9**	**6.7**
VIP	1.0	14.4	29.8	54.2
CRP	1.0	-1.3	-1.3	-1.8
IFNA1	1.0	-1.3	8.2	9.3
TNFRSF1B	1.0	1.1	3.2	2.6
CCL7	1.0	-1.3	-1.3	4.9
NFKBIA	1.0	1.2	4.0	4.9
CD63	1.0	-1.2	1.9	2.8
SELENBP1	1.0	1.1	-1.1	-1.3
DICER1	1.0	-1.2	-1	-1.2
KIAA0232	1.0	-1.1	-1	-1
IFITM3	1.0	1.1	2.4	2.8
MAP4K4	1.0	-1.2	1.8	2.6
CXCL6	1.0	-7.2	1.3	-3.4
VEGFC	1.0	-1.1	2.2	2.2
Platelets	+	+	+	+
Platelet Thrombin Stimulation	-	+	-	+
EC Incubation	-	-	+	+
EC Transcription Shutdown	-	-	+	+
EC Thrombin Stimulation	-	-	-	+

To ensure our platelet isolation approach resulted in minimal cell contamination post co-incubation, we performed control experiments analyzing the resultant platelet fractions from both conditioned media alone and platelet co-incubation setups. Analysis of total event count and CD42b+ expression via flow cytometry found minimal contribution of endothelial microparticles in the platelet fraction as prepared (Figure 3.8, Figure 3.9). These results highlight the increase of specific transcripts in platelets after interaction with endothelial cells and suggest that the increase in platelet RNA may be transcript specific.

Figure 3.8: Contribution of microvesicles to isolated platelet fraction during *in vitro* simulated clot experiments. Flow cytometric analysis of isolated platelet fraction post co-incubation *in vitro* with HUVEC. Co-incubation experiments were conducted as described. Post co-incubation, platelet fractions from conditioned media alone and co-incubation wells were analyzed for total number of events and total number of CD42b+ events. Percentage of total events which were CD42b+. Comparison was only performed using unstimulated samples due to known shedding of CD42b+ by platelets in response to stimulation (194). Results analyzed using unpaired two tailed t-test ($p<0.05$). Error bars represent mean (SD) of n=3.

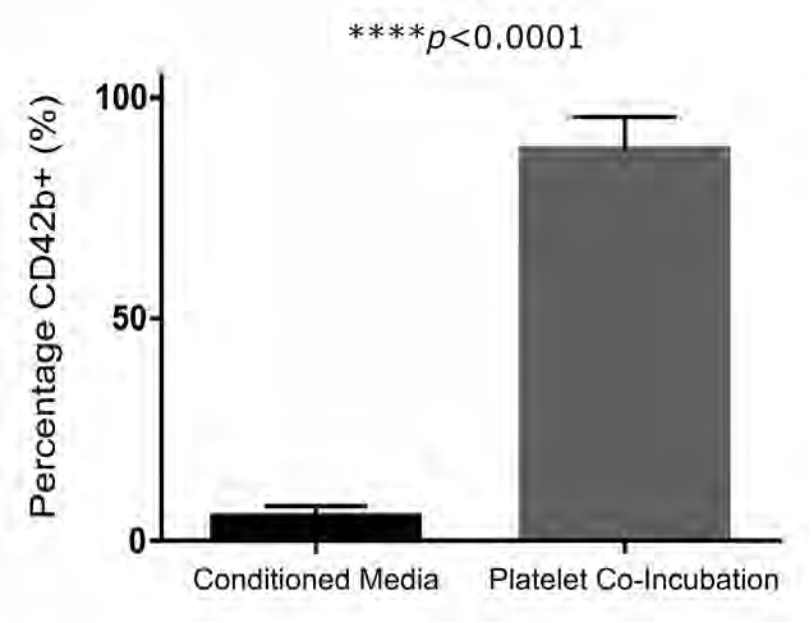

Figure 3.9: Contribution of microvesicles to isolated platelet fraction total cell count during *in vitro* simulated clot experiments. Flow cytometric analysis of isolated platelet fraction post co-incubation *in vitro* with HUVEC. Co-incubation experiments were conducted as described. Post co-incubation, platelet fractions from conditioned media alone and co-incubation wells were analyzed for total number of events and total number of CD42b+ events. Fold change of event concentration as compared to unstimulated platelet co-incubation sample. Total events, total run time and constant flow rate of flow cytometer was used to calculate events/mL for each sample. Fold change was then calculated using unstimulated platelet co-incubation sample as control (set to 1). Results analyzed using ordinary one-way ANOVA with Tukey's multiple comparison test post analysis (**P*<0.05, ****P*<0.001, *****P*<0.0001).

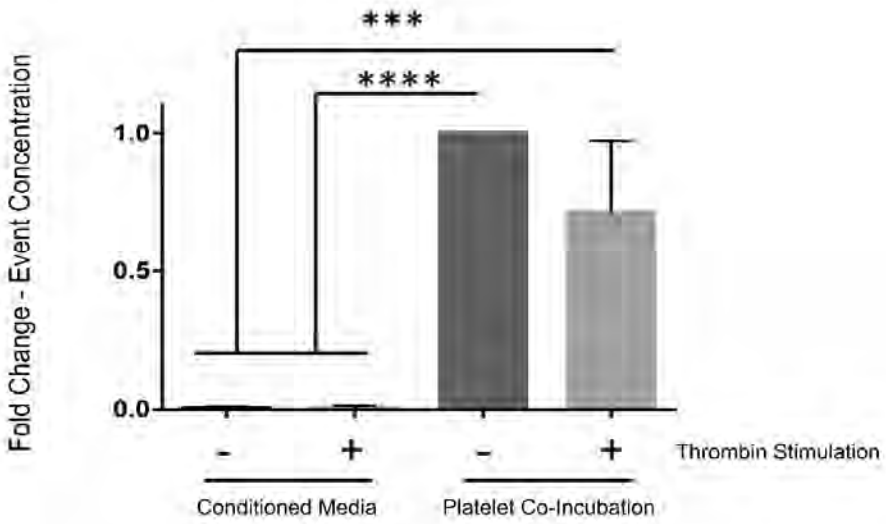

Next we sought to investigate if the increases in platelet transcript levels were dependent on HUVECs being transcriptionally active. We repeated the simulated clot experiments using HUVECs that had been treated with α-amanitin to halt transcription. Of the 38 transcripts, 25 transcripts held the patterns seen with active transcription; however 13 transcripts showed altered expression patterns with cessation of HUVEC transcription, 9 showing almost complete attenuation of expression in all conditions (Table 3.4*b*). 10 of the transcripts which initially showed significant expression changes post incubation were no

longer significant while 3 alternative transcripts now showed significant changes (significant genes and samples noted in red, Table 3.4*b*). These data suggest that the impact of HUVEC transcription on the increase in RNA expression in platelets post co-incubation is transcript dependent.

Transcripts present in platelets post incubation with vascular cells are of cellular origin

Though platelets cannot transcribe new mRNAs, they are capable of performing pre-mRNA processing (78, 79, 88, 109-111). After observing transcript increases in platelets post incubation with endothelial cells, we wanted to confirm that these transcripts were of endothelial origin. We performed simulated clot experiments utilizing Click-iT® technology to pre-label HUVEC RNA. After co-incubation, the platelet and HUVEC fractions were separated and the Click-iT® capture technology was used to isolate out only HUVEC-RNA from the platelet RNA fraction. Of the 96 targets analyzed, 78 showed expression of HUVEC-RNA in platelets post incubation; this was denoted by a decrease in raw Cq value when comparing platelets alone to platelets post Click-iT® labeled HUVEC incubation. 29 of these transcripts had raw Cq value decreases with $p<0.005$ (data not shown) with12 of these transcripts' significance $p<0.0001$ (Figure 3.10*a,* Table 3.5*a*). Because platelets could interact with other vascular cells *in vivo*, this experiment was repeated using a monocyte cell line, THP1, as the donor cell and Pam3CSK4 stimulation, previously shown to result in platelet-monocyte

activation (114, 140, 191, 192). Results showed 62 THP1-derived transcripts present in platelets post incubation, 19 of the transcripts with a significance of p<0.005 (data not shown), 12 of which with a significance *p*<0.0001. (Figure 3.10*b*, Table 3.5*b*). This suggests the transfer of multiple vascular cell-derived transcripts into platelets post interaction.

Figure 3.10: Gene expression levels of cell-derived RNA in platelets post incubation with cells. Endothelial cell (EC) or monocyte cell RNA was labeled with 5'-ethynyl uridine (EU) and, post incubation with platelets, the platelet fraction was isolated and cell specific RNA captured using the Click-iT® RNA capture method. 96 transcripts were investigated by high throughput RT-qPCR. Results given as raw Cq values. Results show transcripts with *P* <0.0001(****) for unpaired t-test using Sidak-Bonferroni method (α = 0.05) comparing stimulated platelets alone to stimulated platelets after incubation with cells A) Endothelial cell, B) Monocyte cell. Toll-like receptor 9 (*TLR9*) in A) and vesicle associated membrane protein 5 (*VAMP5*) in B) representative examples of non-significant genes (‡). Error bars represent mean (SD) of *n*=4 experiments.

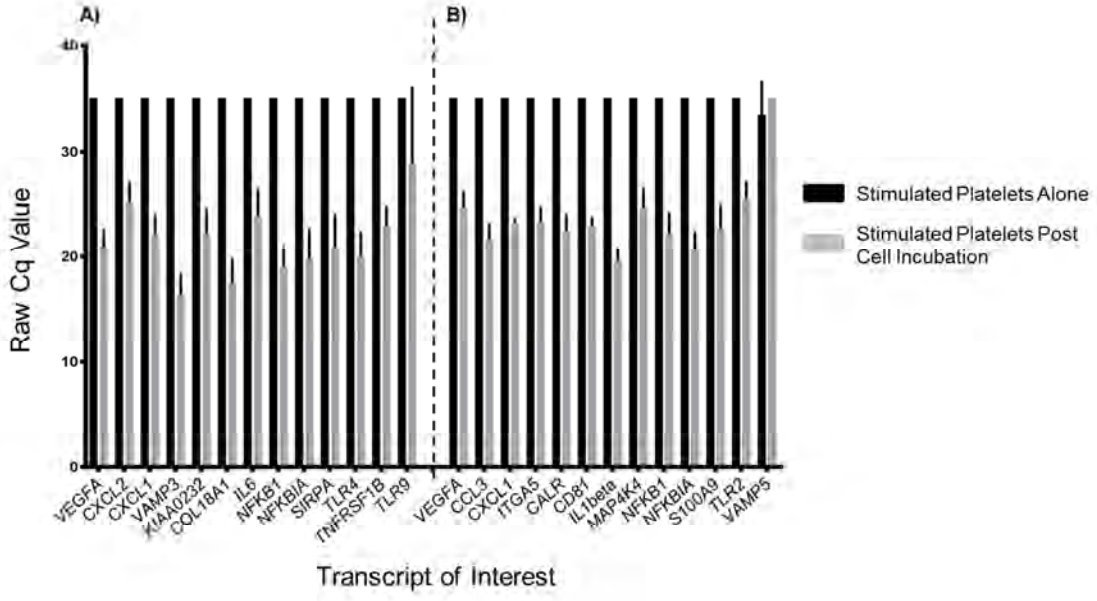

Table 3.5: Gene expression levels of cell-derived RNA in platelets and cells post incubation. Corresponding data to Figure 3.10. Given as raw Cq values ± SD. A) Endothelial cell experiment results. B) Monocyte cell experiment results. *P* value calculated using unpaired individual t-test with Sidak-Bonferroni method (α=0.05).

	Platelets			Cells		
A)	Stimulated Platelets Alone	Stimulated Platelets Post Stimulated Cell Incubation	P Value	Stimulated ECs Alone	Stimulated ECs Post Stimulated Platelet Incubation	P value
VEGFA	35±0	21±1.6	1.853E-06	20±1.9	20.4±1.6	0.710759
CXCL2	35±0	25.1±1.9	4.271E-05	20.5±2	22.4±1	0.130826
CXCL1	35±0	22.1±1.9	8.64E-06	18.5±2.2	19.7±1.3	0.419857
VAMP3	35±0	16.3±2	1.41E-06	14.7±2.2	15.6±1.4	0.540878
KIAA0232	35±0	22.2±2.3	3.137E-05	21.1±2	22.2±1.2	0.363746
COL18A1	35±0	17.5±2.3	4.526E-06	15.7±2	16.1±1	0.737166
IL6	35±0	23.9±2.4	9.188E-05	22±2.8	25.7±6.2	0.321157
NFKB1	35±0	19±2	3.448E-06	17.6±2.4	18.1±1.2	0.707888
NFKBIA	35±0	19.8±2.8	3.603E-05	17.3±1.6	17.5±0.8	0.817402
SIRPA	35±0	20.9±3.1	9.748E-05	17.8±2.3	18.2±1.3	0.743477
TLR4	35±0	20±2.3	1.274E-05	19.1±2.7	19.9±1.9	0.664009
TNFRSF1B	35±0	22.9±1.8	1.106E-05	20.3±1.7	20.7±0.9	0.640854
TLR9	35±0	28.8±7.2	0.134268	25.4±6.4	23.7±1.2	0.608435

B)	Stimulated Platelets Alone	Stimulated Platelets Post Stimulated Cell Incubation	P Value	Stimulated THP1 Cells Alone	Stimulated THP1 Cells Post Stimulated Platelet Incubation	P value
VEGFA	35±0	24.7±1.4	6.248E-06	18.5±2.2	18.4±0.5	0.947354
CCL3	35±0	21.7±1.4	1.467E-06	15.4±1.2	15±1.1	0.640623
CXCL1	35±0	23.2±0.3	6.662E-10	17.7±1.1	17.3±0.6	0.553204
ITGA5	35±0	23.3±1.3	2.167E-06	18.3±2.2	18.1±0.6	0.889952
CALR	35±0	22.4±1.5	3.412E-06	16.4±2	16.3±0.5	0.922571
CD81	35±0	22.9±0.8	8.562E-08	17.7±1.4	17.9±0.5	0.803036
IL1beta	35±0	19.6±1.2	2.231E-07	14±1.6	13.8±0.6	0.807309
MAP4K4	35±0	24.6±1.8	2.325E-05	21±2.2	19.9±0.8	0.387366
NFKB1	35±0	22.2±1.89	1.031E-05	16.1±1.8	15.5±0.7	0.556131
NFKBIA	35±0	20.6±1.8	3.861E-06	14.9±1.8	14.6±0.4	0.788136
S100A9	35±0	22.6±2.2	3.087E-05	18.5±1.9	18.3±0.1	0.810029
TLR2	35±0	25.4±1.6	1.759E-05	20.2±2.9	19±0.6	0.443895
VAMP5	33.5±3	35±0	0.355918	30.2±5.7	25.9±1.7	0.205488

Transcript level increases in platelets occur under both static and flow conditions

To visualize the transfer of mRNA from cells to platelets, we used SYTO® RNASelect™, a RNA specific fluorescent dye, to label HUVEC total RNA. Platelets were then incubated with the labeled HUVECs, with and without thrombin stimulation. Post static incubation, platelets showed fluorescence expression by flow cytometry (Figure 3.11).

Figure 3.11: Platelet RNA uptake from endothelial cells under static conditions via flow cytometry. A) Unstimulated or stimulated human platelets post static incubation with RNASelect-treated endothelial cells analyzed by flow cytometry (*n*=3). Legend denotes experimental conditions for each sample, error bars represent mean (SD). B) Representative flow cytometry images of each sample setup. Y axis: SSC (complexity); X axis: RNASelect (FITC) expression (denotes HUVEC-derived RNA within platelets). Panels in order of legend in A) from left to right.

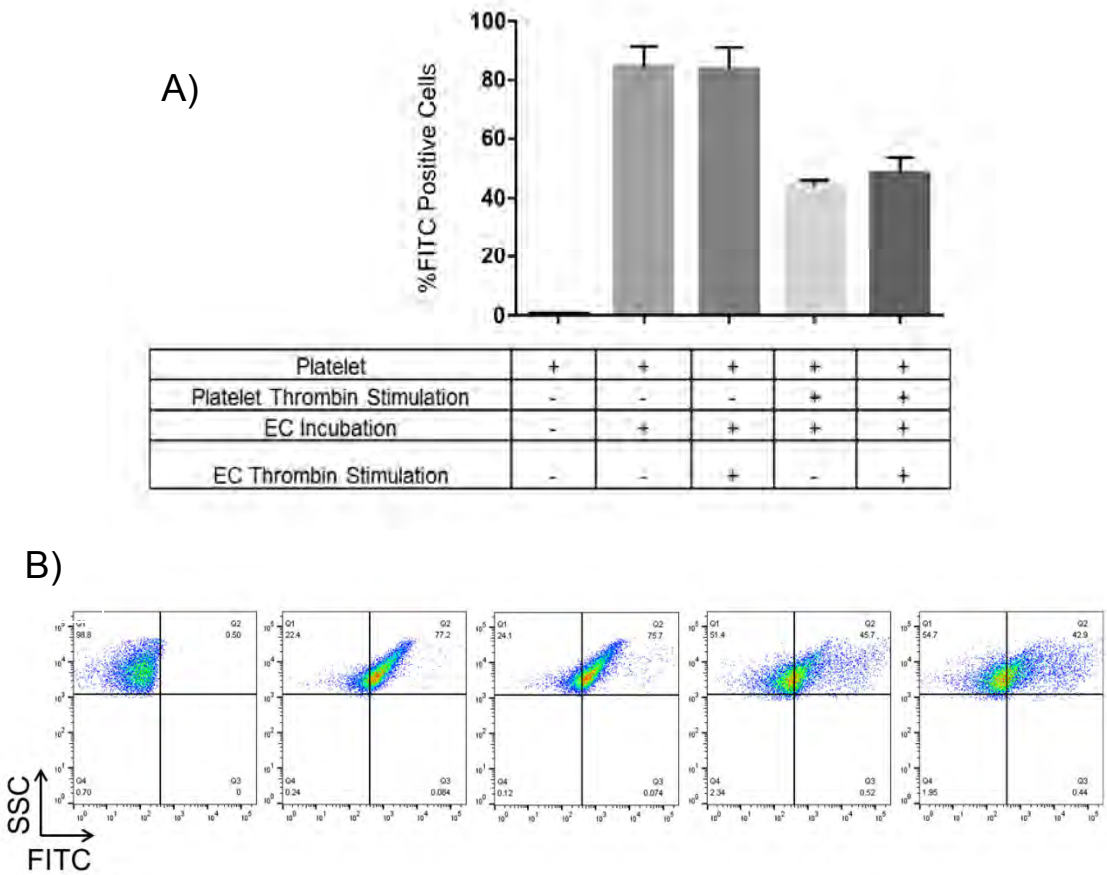

We expanded this study to look at RNA transfer under flow conditions, better reflecting what occurs *in vivo*. SYTO® RNASelect™ labeled HUVECs were grown on slides and platelets were flowed over the slides, with or without thrombin stimulation. We recovered these platelets and analyzed them for fluorescent RNA expression using confocal microscopy. At 10 minutes, unstimulated platelets showed minimal, but evident, fluorescence expression,

while there was a distinct increase in fluorescence under stimulation (Figure 3.12-i, ii). At 30 minutes, both unstimulated and stimulated conditions showed fluorescence expression but the visible spike seen at 10 minutes with stimulation was diminished (Figure 3.12-iii, iv). Quantification of the fluorescent mean of individual cell from these images highlights the upsurge at 10 minutes with stimulation (significantly higher than all other samples) and reveals that at 30 minutes with stimulation there is also a significant increase over unstained and unstimulated controls (Figure 3.13). Confocal Z-axis profiling supports the internalization of HUVEC-derived RNA within these platelets (Figure 3.14).These trends were consistent across several biological replications. Though inter-individual platelet reactivity most likely accounts for the variance in expression spike, these data support the transfer of distinct HUVEC RNA into platelets under the minimal, but necessary, contact achieved during flow conditions.

Figure 3.12: RNA transfer from endothelial cells to platelets via fluorescence imaging. Endothelial cell RNA was labeled with SYTO® RNASelect™ green fluorescent cell stain. Unstimulated (i, iii) or stimulated (ii, iv) human platelets were flowed over RNASelect-treated endothelial cells for noted time. After incubation, platelets were recovered for analysis by confocal microscopy. Scale bar denotes 25 µm. Panels are representative of one experiment from *n*=5-6 experiments generated from different donors, and show fluorescent image top panel, DIC-Pol image bottom panel for each conditions.

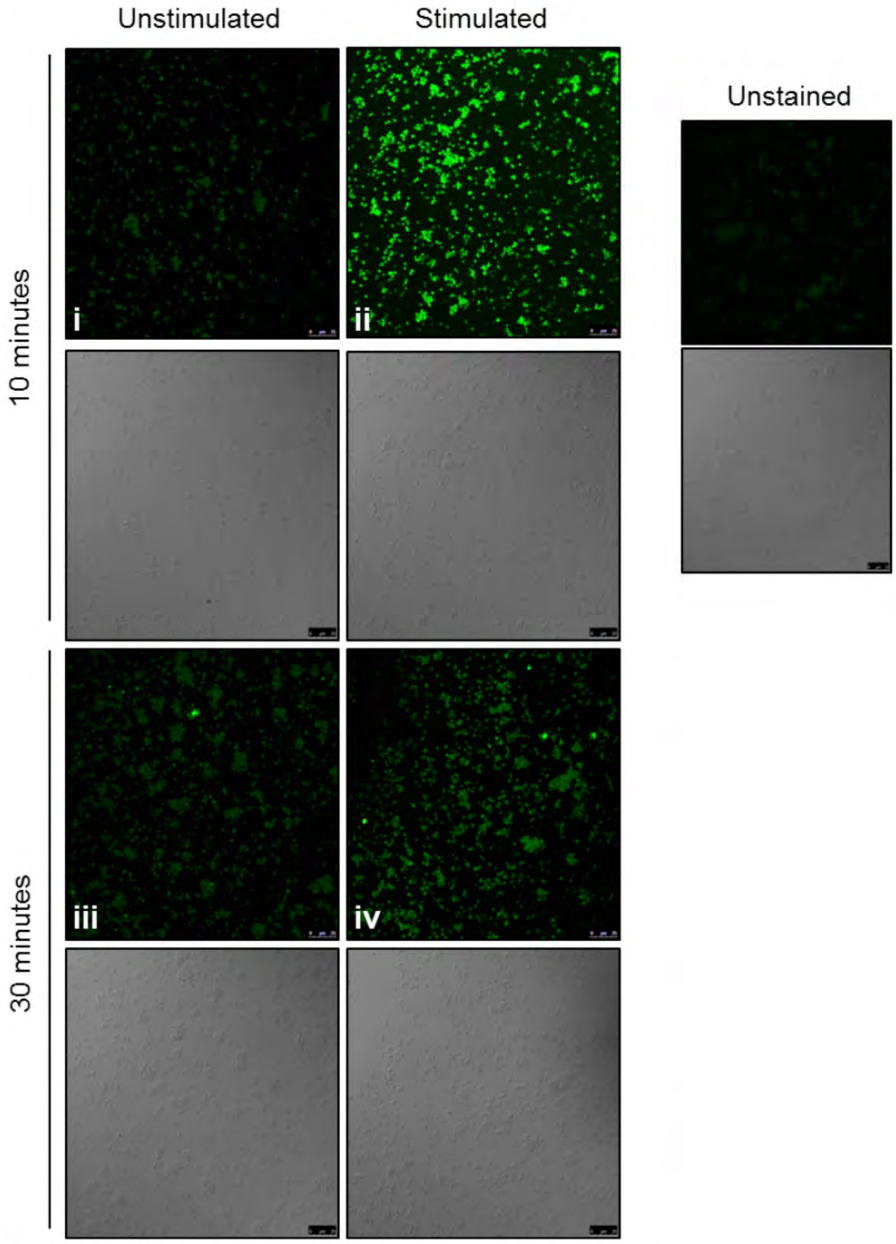

Figure 3.13: Quantification of RNA transfer from endothelial cells to platelets via fluorescence imaging. Endothelial cell RNA was labeled with SYTO® RNASelect™ green fluorescent cell stain. Quantification of images from Figure 3.12. Image quantification was performed using Image J (1.48V) software to measure mean fluorescence. Values represent mean (SD) of *n*=20 individual cells from each image. Analysis of results by one-way ANOVA with Tukey's multiple comparisons test post analysis (α = 0.05): Overall *p*<0.0001. Additional significant comparisons noted in figure legend (* *P*<0.05; ** *P*< 0.01; ***P<0.01; ****P<0.001).

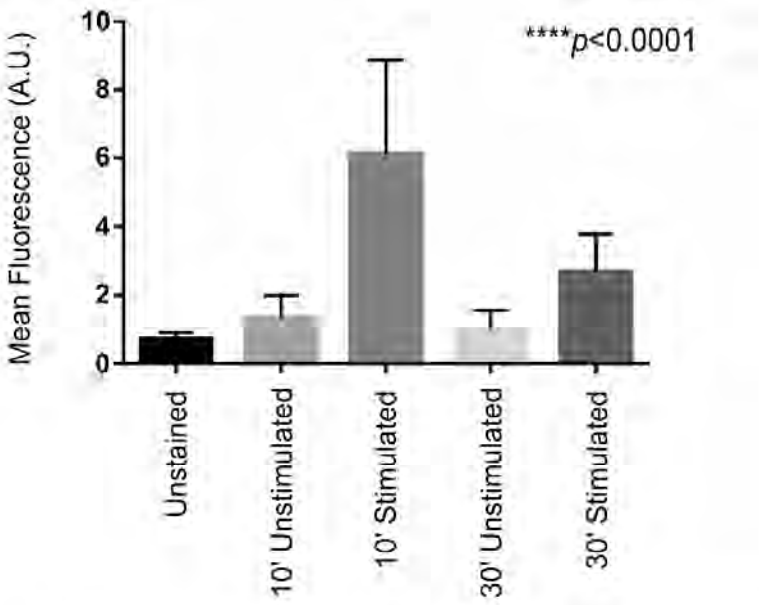

		Unstained	10'		30'	
			Unstimulated	Stimulated	Unstimulated	Stimulated
10'	Unstimulated	ns	-	-	-	-
	Stimulated	****	****	-	-	-
30'	Unstimulated	ns	ns	****	-	-
	Stimulated	***	*	****	**	-

Figure 3.14: Uptake and internalization of RNA from endothelial cells by platelets via fluorescence imaging. Endothelial cell RNA was labeled with SYTO® RNASelect™ green fluorescent cell stain. Confocal Z-axis profile (created using ImageJ) of representative image from flow adhesion experiment. Confocal stack images taken from 1 µm below and 1 µm above center of cell (set to 0.0 µm), with each z-step equal to 0.15 µm.

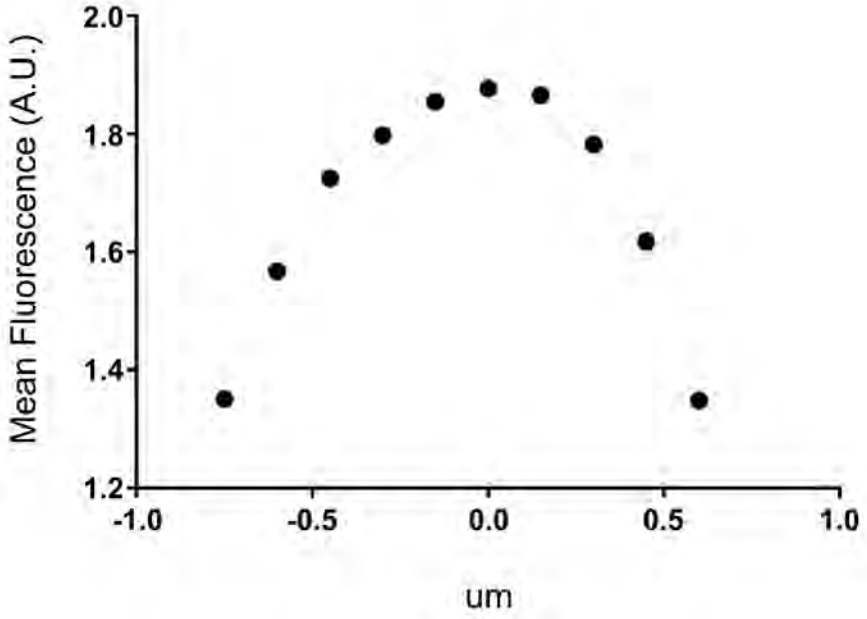

Platelet transcript uptake is a complex, multifaceted process

Upon confirmation of the presence of cellular-derived mRNAs in platelets as well as the occurrence of this phenomenon under flow conditions, we aimed to investigate the mechanism of uptake. It is known that vascular cells and platelets release microvesicles, especially in response to stimulation (116, 195). There is also evidence to support microvesicle-based miRNA transfer from platelets to cells (120, 124), as well as platelet-microvesicle interaction and uptake (133, 135, 190). Based on this, we hypothesized that platelet uptake may occur via a microparticle dependent mechanism. Initial experiments adapting our

fluorescence flow adhesion experiments to see if transfer could occur indirectly revealed similar results as seen in our direct model, with the exception of attenuation of the spike seen at 10 minutes under stimulation. These initial findings suggested that uptake is partially occurring through microparticles; however, the expression and uptake increases seen *in vitro* with stimulation are either dependent on direct platelet-endothelial cell interaction or the microenvironment normally present in the vasculature.

To further tease apart the mechanism of platelet RNA uptake, we developed two adaptations of our *in vitro* simulated clot experiments to investigate the role microparticles may play in this phenomenon. The first set of experiments utilized brefeldin A, a microparticle inhibitor previously demonstrated to impact exosome-like vesicle regulation as well as platelet miRNA transfer to endothelial cells (120, 196). Experiments were conducted with 10 minute co-incubation periods to try and capture the transfer spike identified in fluorescence experiments. Expression of E-selectin (*SELE*) mRNA, previously shown increased in platelets post endothelial cell incubation (Table 3.4) was significantly decreased in platelets after incubation with brefeldin A/thrombin treated endothelial cells as controlled to methanol/thrombin treated HUVECs (Figure 3.15).

Figure 3.15: The effects of endothelial cell microparticle production on differential gene expression in platelets post incubation. Analysis of the ability of endothelial-derived microparticles to impact E-selectin expression in platelets post incubation. RT-qPCR results for e-selectin (*SELE*) expression in platelets after incubation with unstimulated or stimulated endothelial cells (ECs) pretreated with brefeldin A or control methanol. RT-qPCR results (expressed as $2^{-\Delta\Delta Ct}$) were normalized to *β-actin* and controlled against individual platelet background expression, with error bars representing *n*=3, mean (SD). *P*-values calculated using one-way ANOVA with Tukey's multiple comparison test post analysis (**P*<0.05, ****P*<0.001, *****P*<0.0001).

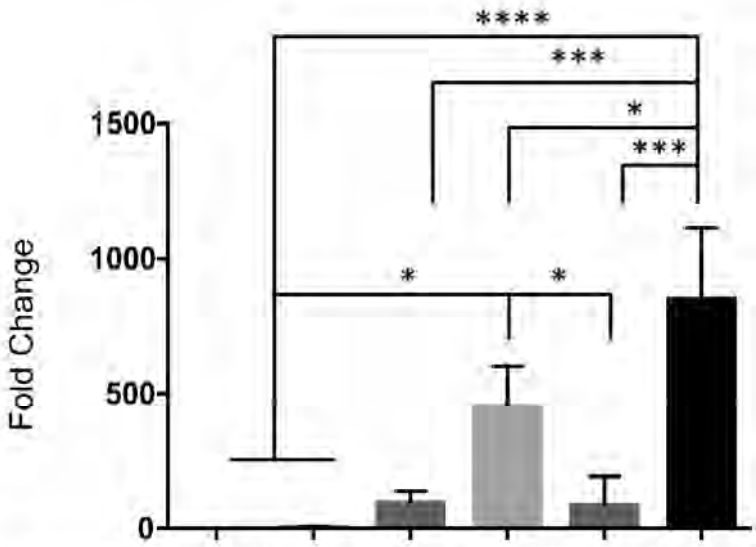

Platelet	+	+	+	+	+	+
Platelet Thrombin Stimulation	-	+	-	+	-	+
EC Pretreatment	-	-	Brefeldin	Brefeldin	Methanol	Methanol
EC Incubation	-	-	+	+	+	+
EC Thrombin Stimulation	-	-	-	+	-	+

Interestingly, HUVEC brefeldin treatment did not reduce expression levels completely to basal level, but instead to an intermediate expression level. Additional analysis of another mRNA, *COL18A1* (collagen type XVIII, Alpha 1), identified in Table 3.4 did not show a significant expression difference when comparing incubation with brefeldin-treated HUVECs and methanol-treated HUVECs (data not shown). Similar experiments with alternative microparticle

inhibitors (Y-27632, a ROCK inhibitor, and zVAD-FMK, a pan caspase inhibitor) did not show significant effects on platelet *SELE* expression post incubation (data not shown). Taken together, these data suggest a role for exosome vesicular secretion in platelet RNA uptake, as well as an aspect of transcript specificity to what is taken up.

The second set of adapted experiments addressed the ability of microparticles alone to cause expression changes in platelets, as well as the potential issue of cell contamination in co-incubation studies. Instead of direct incubation with cells, platelets were co-incubated with conditioned media from endothelial cells treated under the same conditions as the co-incubation experiments. Samples were isolated from both co-incubation wells as well as conditioned media only wells and *SELE* expression was again analyzed. qPCR results confirmed that, though there is a percentage of expression change in the platelet fraction that may be due to endothelial microparticles, the expression change with platelets present was significantly higher (Figure 3.16). Taken together, these results suggest that platelet uptake from vascular cells can occur through microparticle transfer and that this may be a multifaceted process, dependent on exosome secretion and transcript specificity.

Figure 3.16: The effects of endothelial cell microparticle exposure on differential gene expression in platelets post incubation. Analysis of the ability of endothelial-derived microparticles to impact E-selectin expression in platelets post incubation. RT-qPCR results for *SELE* expression in platelet isolated fractions from either conditioned media alone wells (columns 3 and 4) or co-incubation wells (columns 5 and 6). RT-qPCR results were normalized to *GAPDH* and controlled against individual platelet background expression (column 1) (expressed as $2^{-\Delta\Delta Ct}$). Error bars represent *n*=4 experimental replicates using the same individual's platelets, mean ± SD. An additional 3 biological replicates support this finding. *P*-values calculated using one-way ANOVA with Tukey's multiple comparison test post analysis (**P*<0.05, ***P*<0.01, ****P*<0.001, *****P*<0.0001), overall *P*=0.0001.

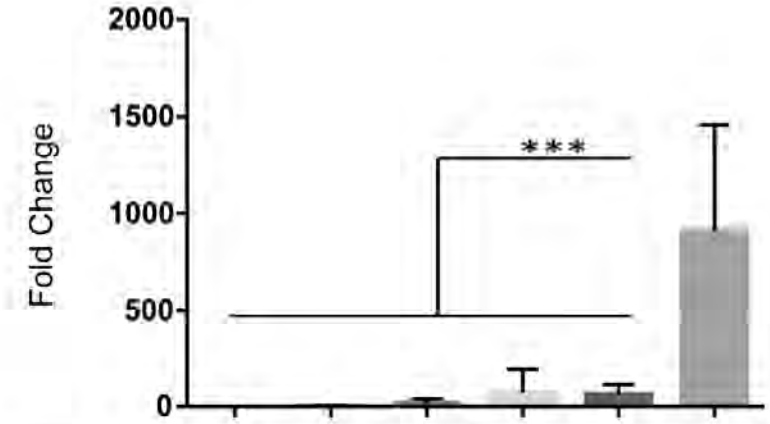

Platelet	+	+	-	-	+	+
Platelet Thrombin Stimulation	-	+	-	+	-	+
EC Thrombin Stimulation	-	-	-	+	-	+
EC - Platelet Incubation	-	-	-	-	+	+

Platelet transcript uptake results in changes to the apoptotic signature of platelets

Analysis of the smaller platelet RNA profile revealed a number of functional connections to apoptosis and cell death regulation (Appendix E*b*). Based on these findings, we hypothesized that one functional role for platelet RNA uptake may be to clean up debris being released into circulation by dying or dead

vascular cells. To address this hypothesis, we reanalyzed samples from the direct *in vitro* simulated clot experiments, the Pam3CSK4 *in vivo* experiments, as well as the conditioned media simulated clot experiments for changes in known apoptotic mRNAs. Interestingly, for the conditioned media and Pam3CSK4 experiments, though there seemed to be some changes in apoptotic mRNA expression, none of the results were significant (data not shown); however, for the traditional *in vitro* direct incubation experiments, two targets, *BCL2*-Like 11 (*BCL2L11* or *BIM*) and *BCL2* Associated X Protein (*BAX*), both pro-apoptotic mRNAs, showed significant expression increases in platelets after incubation with endothelial cells (Figure 3.17).

Figure 3.17: The effect of platelet co-incubation with endothelial cells on the platelet apoptotic profile. RT-qPCR results (expressed as $2^{-\Delta\Delta Ct}$) for *BIM* and *BAX* expression in platelets after incubation with unstimulated or stimulated endothelial cells. RT-qPCR results were normalized to *GAPDH* and controlled against average individual platelet background expression (column 1). Error bars represent *n*=4 experimental replicates using the same individual's platelets, mean ± SD. An additional 5 biological replicates support this finding. *P*-values calculated using two-way ANOVA with Tukey's multiple comparison test post analysis (**P*<0.05, ***P*<0.01, ****P*<0.001, *****P*<0.0001).

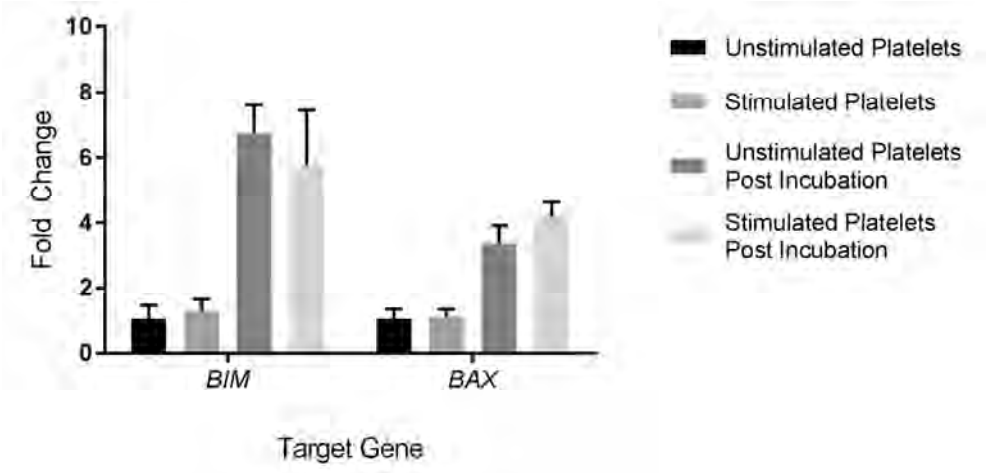

Both *BIM* and *BAX* have previously been linked to platelet clearance and vascular cell apoptosis, though the extent of the role they play is not fully understood (197-201). The increase in these transcripts in platelets post incubation, as well as the findings suggesting increased fragmentation in small platelet RNA, reveals a potential role for platelets as “housekeepers” in the blood, though further analysis needs to be performed to understand the total impact of these target expression changes to the platelets themselves as well as to the vasculature overall.

Discussion

The presence of large and small platelet subpopulations and the potential correlation to platelet age and RNA content has been established (186, 187). As an explanation for the importance of platelet RNA, we and others have demonstrated platelet RNA transfer to vascular cells (114, 120, 124) and assumed that this observation, coupled with RNA degradation, explains the decrease of platelet RNA in the older, smaller platelet subpopulation. Upon investigation of which transcripts are actively transferred by platelets, we uncovered that, despite their decreased RNA content, the smaller platelet population contains a diverse transcript profile. In nucleated cells, this observation would not be that surprising due to active transcription; however, as platelets are anucleated and cannot alter their own transcriptome, the origin of these transcripts before this study was unknown. This data led us to hypothesize

that platelets' RNA transfer capability is actually bidirectional: the deposition of RNA to vascular cells, coupled with RNA uptake from vascular cells would explain the decreased amount of total RNA with increased variability in smaller platelets. Supportive of our hypothesis, there are several studies that demonstrated the ability of platelets to sequester tumor-derived RNA biomarkers from tumor microvesicles (133, 135); however, none of these studies adequately described this phenomenon in platelets. Though our initial platelet subpopulation analysis was performed on a small sample size, a potential limitation to our study, follow up experiments supported not only the RNA heterogeneity of platelet subpopulations but also the ability of platelets to take up RNA from other cells in a dynamic manner. This is the first focused evaluation showing the uptake of endogenous cellular transcripts *in vitro* and *in vivo* from vascular cells to platelets. Thus, these findings expand our understanding of platelet RNA transfer to a dynamic bidirectional process between platelets and vascular cells. Here, we report that platelets can uptake RNA from endothelial and WBCs and this ability not only results in distinct platelets subpopulations but also presents a novel mechanism by which platelets may regulate vascular homeostasis and systemic responses during infection or inflammation.

Taken in light of platelets' canonical roles in thrombosis and hemostasis, the ability of platelets to take up RNA from other cells may suggest additional mechanisms for regulating thrombotic events beyond the release of miRNA (120, 124). We can hypothesize three potential functional roles for platelet RNA

uptake: the manipulation of the platelet protein profile, a bidirectional communication system in the vasculature, or a debris cleaning mechanism allowing for the fine tuning of vascular cell responses to stimuli.

As previously described, though capable of protein production, platelet translational capacity is modest and signal-dependent (78, 79). We observed platelet mRNA expression changes post cellular co-incubation even in the absence of stimulation, suggesting that platelet protein regulation may not fully explain the functional relevance of platelet RNA. Additionally, we further analyzed our findings to determine if the transcripts we identified as being involved in platelet RNA uptake had previously been linked to the platelet transcriptome or platelet proteome. We compared the 38 transcripts noted to transfer from HUVECs in *in vitro* simulated clot experiments to the PlateletWeb resource (202). This revealed that the transcripts of interest were divided: 18 transcripts were present in platelets either at the transcriptome level, the proteome level or both while 20 associated transcripts had not been detected in the platelet at any expression level (data not shown). PlateletWeb analysis of the top 100 large versus 100 small platelet transcripts from our sequencing analysis also revealed an interesting pattern; while both populations contained about 50 transcripts with no protein representation in platelets at all, the larger platelet transcripts' associated proteins were evenly divided in representation among the transcriptome and proteome level (14 transcriptome, 18 proteome, 21 both) while the smaller platelet transcripts were heavily represented at the proteome level (3

transcriptome, 28 proteome, 8 both) (202). This comparison of our transcripts of interest to the PlateletWeb resources is complicated - it does not take endogenous platelet protein production or protein uptake into account. Moreover, the evaluation of the small versus large platelets expression levels may have allowed for genes which are usually overshadowed in large heterogeneous populations to be identified. However, it is clear that not all transcripts identified here as present in platelets either in post transfer experiments or in subpopulations correlate to proteome changes. The heterogeneity of platelet subpopulation mRNA expression may help explain previous difficulties in correlating the platelet transcriptome to the platelet proteome (113).

Our previous publication showed the functional relevance of platelet mRNA transfer to vascular cells and has since been validated by several other publications focusing on the miRNA and mRNA transfer of platelet to cells (120, 123, 124). Further analysis of the functional capabilities of smaller platelet RNA revealed a large number of associations with distinct vascular cell applications, ranging from T cell and B cell activation, to lymphocyte and erythrocyte differentiation to apoptosis and cell death (Appendix E*b*). Taken in combination, the presence of these widely diverse functional transcripts in platelets, and the ability of platelets to transfer RNA to other vascular cells creates the potential for a new cell-cell communication pathway to allow for RNA transfer across the vasculature. The platelet would present a unique communication vehicle both

due to its universal access as well as due to its clear connections to varying systemic responses.

Finally, platelet RNA uptake may represent a debris cleaning mechanism by which platelets help attenuate and fine tune vascular cell response to stimuli. Previous work has cited the release of caspase-3 protein from HUVECs in microparticles as imperative to cell health, with accumulation of the protein potentially leading to cell death (203). Platelet mRNA uptake from cells may allow cells to respond to stimuli quickly and mitigate adverse off-target effects. Several of our results support this potential functional role. Our studies focusing on the functions associated with each subpopulations' RNA content revealed that, while larger platelets had a more historically hemostatic profile, smaller platelets lacked these hemostatic markers (results which agree with previous work on smaller, older platelet functionality (28, 204-206)). Instead, the small platelet RNA profile was enriched in mRNAs typically associated with vascular cells. Additional experiments focusing on the apoptotic profile of these subpopulations revealed the smaller platelet profile is composed of a number of transcripts associated with various vascular cell apoptotic pathways. *In vitro* analysis revealed that two transcripts in particular, *BIM* and *BAX*, are significantly upregulated in platelets after incubation with endothelial cells. Both *BIM* and *BAX* are pro-apoptotic factors previously associated with platelet clearance and endothelial health (197-199, 201, 207). Finally, our analyses of the coverage of specific targets during sequence mapping as well as the overall fragmentation level of platelet

subpopulations' RNA suggests that the smaller platelet RNA is more fragmented than that of the larger platelet population. The presence of this fragmented mRNA would, further support a role for the platelet as a debris collector, as it would likely be untranslatable and have little impact on protein production (and sequentially on other vascular cells post RNA transfer). The impact that these transcripts may have on the platelet itself (especially on platelet life span) as well as overall vascular health needs to be further analyzed; however, the potential for the platelet to be regulating the vasculature through this "cleaning mechanism" is quite clear. Further experimentation will focus on the functional capacity of donor cells after incubation and interaction with platelets, to determine if platelet uptake affects donor cell protein level and function. Understanding the purpose of platelet RNA uptake and its connections with platelet RNA transfer may elucidate new ways platelets help regulate systemic responses to stimuli. Additionally, elucidating the full scope of platelet transcriptome variability may also have interesting implications for biomarker and therapeutic development.

Strength and Limitations

Uncovering the ability of platelet to uptake RNA from other vascular cells opens a unique and exciting avenue of how vascular homeostasis may be regulated though a transcription-independent and intercellular communication-dependent mechanism. In evaluating this phenomenon, a number of factors were identified

as being beyond the scope of this study. Platelet sorting, though achievable, is a difficult and laborious process; the time requirements of sorting and the fragility of platelets *ex vivo* limits the overall duration of experimentation, while the minimal RNA content of platelets results in very little viable material for analysis. Additionally, our understanding of how brefeldin A impacts the mechanism of platelet RNA uptake is difficult to discern. The impact of brefeldin A on exosome production has previously been evaluated (196); however, exact quantification of the impact on exosome number is generally difficult due to size limitations. Specifically, exosome contribution in co-incubation studies is confounded by the expression of numerous exosome markers on platelets endogenously (data not shown, PlateletWeb). Further study of these issues will require advanced technology to yield more RNA and allow for more in-depth analysis of fragmentation and gene expression, as well as better analytical methods for small particles.

Conclusions

In summary, this study is the first conclusive demonstration of the platelets' ability to take up mRNA from vascular cells and enhances our fundamental understanding of how platelets interact with the vasculature. Our data provides surprising findings that older, smaller platelets contain a unique transcriptome reflective of vascular cells and demonstrates the platelet's capacity for bidirectional horizontal RNA transfer. These findings further clarify previous

observations that platelet subpopulations are distinct, especially in relation to reactivity and disease (205, 208-211), as well as expand the role of platelets in vascular communication and regulation.

CHAPTER 4: DISCUSSION AND FUTURE STEPS

Permissions

Chapter IV contains excerpts from a published manuscript and is included with permission.

- *Clancy L, Beaulieu LM, Tanriverdi K, Freedman JE. (2017).The role of RNA uptake in platelet heterogeneity. Thromb Haemost, 117(5), 948-961*
    - Permission Information: Copyright Permission No 116/06/2017

Chapter IV contains a figure adapted from a previously published figure, included with permission.

- *Clancy L, Freedman JE. (2015).The role of circulating platelet transcripts. J Thromb Haemost, 13 Suppl 1, S33-9*
    - Permission Information: License Number 4158990752847, License Date Jul 30, 2017, Licensed Content John Wiley and Sons

Author Contributions

Thromb Haemost (2017): L.C. performed all experiments and analyses unless noted below. L.C. wrote manuscript. J.E.F. oversaw overall project development and coordination. L.M.B performed initial platelet sorting experiments. K.T. performed high throughput gene expression analyses. All authors commented on the interpretation of results, and reviewed and approved the manuscript.

J Thromb Haemost (2015): LC performed literature reviews and prepared manuscript with oversight and editing provided by JEF.

While the historic importance of platelets to cardiovascular health and disease has been long understood, their relevance to multiple non-vascular fields of human biology was overlooked until recently. Since their discovery in the 1800s, scientific interest in platelets never waned but the research focus was in understanding fundamental hemostasis or the detrimental effect they play in acute cardiovascular disease (CVD). While numerous therapies now exist in regulating the platelet's role in the various forms of CVD, it has only been during the past 50 years that we truly began to delve into the circulatory mechanistic underpinnings. As our understanding of what platelets are and what they can do expanded, the scientific questions surrounding them grew accordingly. A better understanding of how platelets interact, not only in CVD but in immune and non-vascular disease settings may help elucidate how the platelet plays such diverse systemic roles.

It is easy to understand how the platelet's non-hemostatic functions were overlooked. With most cell types, any deviation from their known role or function are most likely attributed to cell self-regulation, through controlled transcription and directed differential gene expression. Whole fields of study now focus on what happens when certain genes are turned on or off in specific cell types and how this impacts not only cell function and development, but disease phenotypes. Without a nucleus, and thus incapable of transcription, it would be easier to assume the platelet's function was straightforward; respond to specific vascular injury, with a pre-determined order of reactions to produce clot formation

and prevention of blood loss. One can easily comprehend how this process may be dysregulated and therefore result in thrombosis formation. To look beyond this simple assumption has required huge leaps in scientific research; just as the original identification of the platelet was hindered by microscopic techniques, so too was our understanding of the platelet limited by molecular biological methods. As more and more sensitive and reliable ways to interrogate cellular content (specifically transcriptome expression) and cellular function have been developed, our ability to look at the platelet in a different capacity has arisen. When we think beyond the original platelet paradigm as static bits of cytoplasm and instead view them in light of their roles in dynamic cellular processes, it becomes evident that, despite their lack of nucleus, platelets conserve the ability to respond to their environments in alternative ways; post transcriptional modifications, translation and post translational regulation all imbue the platelet with the ability to alter their own transcriptome and perhaps their function.

As described, once the connections between platelets and non-vascular systemic responses were made, it became clear that an interrogation of the specific contents within these fragments was needed. Discovery of platelet RNA (along with the platelet's translational capacity) and correlation of specific platelet transcriptomes to relevant disease settings suggested that RNA may play a role in how platelets can operate in such diverse capacities. Additional studies on the importance of RNA in cell-cell communication and the impact this transfer has on cellular function hinted that platelet RNA may serve the same purpose. The

discovery of platelet RNA transfer confirmed this hypothesis. Initial investigation in our lab revealed a number of distinct expression changes in HUVEC cells post incubation with platelets (Appendix B, Table B.1). The easiest results to interpret were those transcripts which corresponded to distinct platelet markers (such as CD40 ligand, P-selectin and GP1BB) which showed a notable increase in expression in HUVECs post incubation with minimal or no basal expression in untreated HUVECs (Appendix B). Other differential expression changes were more difficult to understand. With transcripts that are endogenously highly expressed in HUVECs, it would be difficult to see any changes in expression due to platelet transfer, as the overall impact of transferred material on the total expression level would be minimal (based on the distinctly different amounts of total RNA in HUVECs and platelets). Even if the fold change of expression was significant compared to background HUVEC profiling, HUVEC are capable of full transcriptional regulation and thus these changes could not be attributed to RNA transfer. We observed differential expression within HUVECs stimulated alone, with plasma treatment alone as well as with platelet rich plasma treatment alone, and these changes seemed to be transcript specific. Even in the simulated clot wells (platelet rich plasma with thrombin stimulation), it is difficult to rule out that changes in gene expression are not just caused by platelet-endothelial cell signaling and corresponding transcription upregulation within the cells (though it is of note that there are still distinct changes in HUVEC cells post incubation even with transcription inhibition, again in a transcript specific manner; Appendix

B, Table B.1). The examination of how platelets and HUVECs interact externally is especially important when considering that platelets are specifically designed to interact with vascular cells (through various GPs expression) to induce signaling cascades during normal hemostatic regulation. Despite these issues, understanding which transcripts are affected by endothelial-platelet interaction and potentially identifying those that change due to transfer as opposed to signaling will be central in truly comprehending how platelet and endothelial cells interact on the cellular level.

More interestingly, these initial experiments showed that platelet fractions themselves exhibit distinct expression changes. As expected, a number of transcripts decreased, coinciding with platelet activation and secretion; however, expression of several transcripts increased significantly (Table 3.4). Notably, several of these transcripts were not present in the basal platelet transcriptome. With no ability to perform transcription and an unlikelihood that increases seen were all due to mRNA processing (based on overall total RNA content, extensive fold changes observed and number of genes affected), the source of these new transcripts was unknown. When concurrent data from platelet subpopulation studies suggested that small platelets also contained transcripts of unknown and distinctly non-platelet origin (Figure 3.2, Table 3.1, Appendices C and E), we hypothesized that the origin of these transcripts was platelet RNA uptake from other vascular cells. Previously published studies had suggested that this phenomenon could occur in oncological settings (with tumor specific RNA

associating with the platelet fraction (133-136)) and further analysis here revealed that platelets were indeed capable of taking up endogenous RNA from the vascular system.

The purpose of platelet RNA uptake

The ability of platelets to take up RNA presents more questions when considering how the platelet functions systemically. The circulatory system allows wide platelet distribution and suggests that the platelet may act as a transport vessel throughout the body, picking up and transferring RNAs between cells,. Many recent studies have focused on microvesicles in the circulation and how extracellular RNA not only impacts disease development but may function similarly as communicators across large distances (212-215). Our labs, as well as others, have identified unique extracellular RNA expression profiles that coincide with various disease, phenotype and infectious states (212, 216-218). One question of interest would be; if transfer can occur across distances via microparticles, is there a partially redundant mechanism with platelets? Or, alternatively, are these two systems not redundant but part of one system? As suggested in our studies, it appears possible that microvesicle development and transfer affects platelet RNA uptake (inhibition of exosome release from HUVECs through brefeldin A treatment results in decreased uptake of SELE transcript in endothelial-exposed platelets, Figure 3.15, while incubation of HUVEC-derived microparticles with platelets mimicked co-incubation studies, Figure 3.16).

However, this observation is not true for all transcripts seen increased in platelets post co-incubation and other microvesicle inhibitors have inconsistent effects on platelet RNA uptake. As we discover connections between various diseases and extracellular RNA and already know platelets play a role in similar responses, it is conceivable that platelets alter disease development and response through interaction with extracellular RNA. One such example is in response to infection. Our lab has recently shown the presence of viral miRNAs in circulation (Appendix F) and it is well established that platelets themselves play a role in early detection and response to viral and bacterial infections. Could the mechanism by which platelets help regulate the infectious response involve a form of platelet-microvesicle cross communication? Alternatively, as our results suggest that microvesicle inhibition does not affect uptake of all transcripts equally, there may be an alternative microvesicle-independent mechanism which contributes to RNA uptake and transfer, as has been seen with other studies (123, 219).

The above theory of a platelet based communication system is dependent on the functional capability of the transferred RNA and corresponding translation and protein regulation, by either platelets themselves or by vascular cells; however, it is possible that this may not be the case. There may be no relevant use for the transcripts moving in and out of platelets. Studies do support that transcripts transferred out of platelets to other cells are not only functional but can impact cellular expression (114, 120-125). On the other hand, as discussed further in the next section, preliminary results of different platelet subpopulations'

profiles suggest that the RNA that seems to be picked up from circulation may be fragmented and of minimal quality and, thus, irrelevant for translation. Though the connection between these subpopulation profiles and RNA uptake still needs to be solidified and these studies are only preliminary, it suggests that platelet transfer to cells serves a functional expression-based purpose to recipient cells while uptake may not. It is unknown though, as discussed in Chapter 3, if the purpose of uptake may be to remove these non-functional RNA from the vascular system as a whole, and if the process were inhibited or non-existent, could result in detrimental vascular hemostasis.

The role of platelet RNA uptake in platelet subpopulation transcriptome heterogeneity

As described, platelet subpopulations studies revealed distinct RNA transcriptomes correlating to platelet size. As previous studies revealed mRNA degradation correlated to platelet circulating age (108, 185), this differential expression was originally attributed to mere mRNA breakdown; however, our studies showed that the smaller platelet population contained a much more diverse transcriptome than large platelets, made up of significantly more transcripts with more diverse functional associations (Figure 3.2, Table 3.1, Appendices C and E). Preliminary results examining the quality of the RNA in these subpopulations suggest that while the smaller platelet transcriptome is more diverse, its transcripts may be fragmented and thus irrelevant for translation

(Table 3.3). These findings present an interesting possibility, that the more diverse transcripts within the small platelet population correlating to other vascular cells are merely remnant RNA discarded by vascular cells and removed from the circulation by platelets. This would allow the platelets to act as a unique debris cleaner, clearing the circulation of remnant RNA. Taken with several other conjectures about platelet subpopulations, this could further describe an interesting aspect to platelet biology. It is known that platelets newly derived in circulation tend to be larger in size (28, 186, 187, 205, 220); it is also known that these larger platelets are more functionally hemostatic (28, 204-206, 220), and based on our preliminary results here, more hemostatic at the RNA level . Additionally, these large, more hemostatic platelets have been shown to be increased in patients with CAD (221). One could hypothesize that, over time as these large platelets interact within the circulation, they exchange RNA – picking up debris transcripts and dropping off other transcripts in turn (Figure 4.1*a*). As their time in circulation passes, they become smaller and contain more vascular and apoptosis related RNA and less hemostatic transcripts. This would present a novel way by which platelets can help circulatory hemostasis and, as they are removed from circulation, assist in debris removal.

Figure 4.1: Depiction of potential relevance of RNA uptake on platelet subpopulation transcriptome and functional heterogeneity.

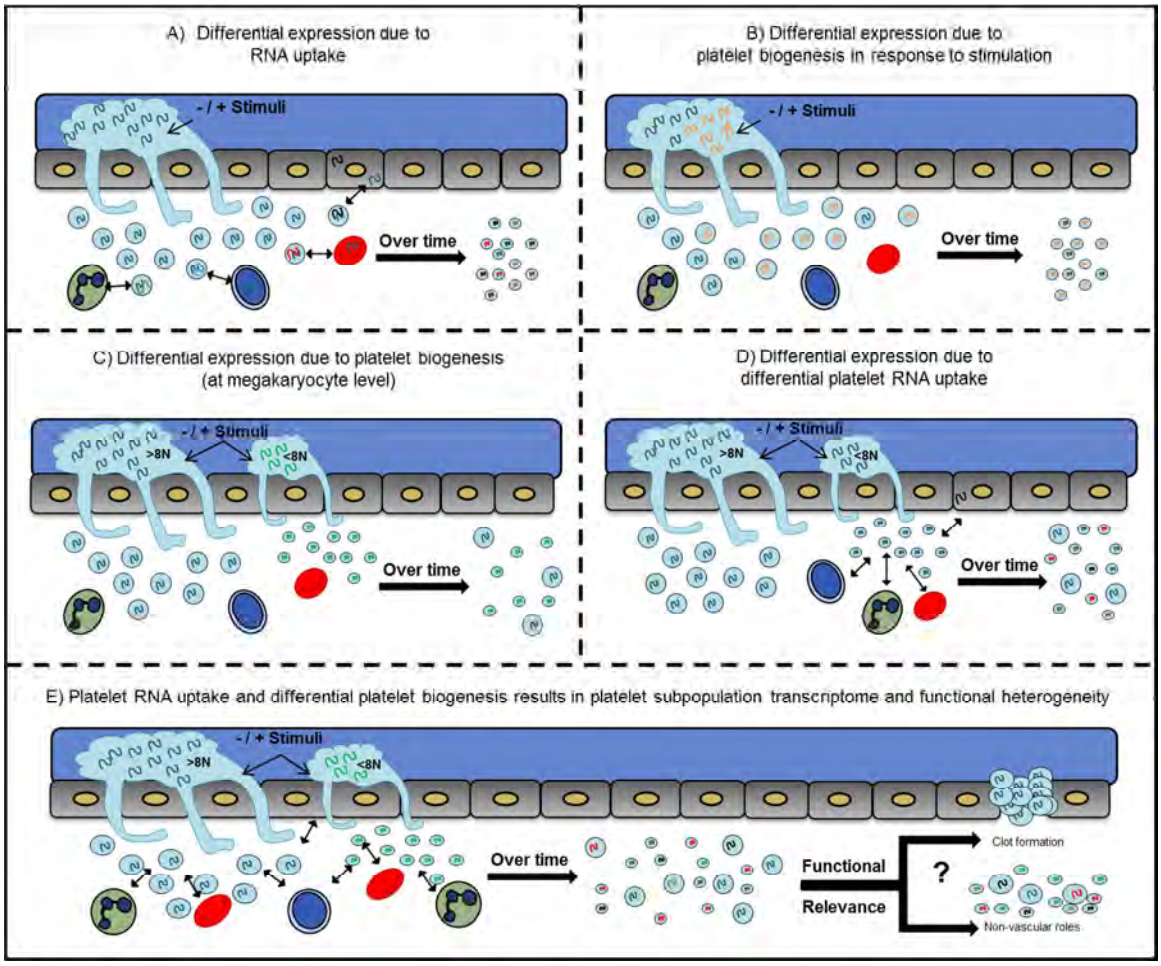

This hypothesis likely only represents one explanation for platelet subpopulation diversity. The idea of platelet size correlating with platelet circulatory time has long been very controversial. While most researchers agree that the newest platelets to enter circulation are larger in size (28, 186, 187, 205, 220) (this has been shown in studies of platelet repopulation after systemic ablation (187)), many disagree on the origin of small platelets (28). There are some studies that support that large platelets become small platelets overtime

(28); there are some that suggest that small and large platelets are actually separately derived from different size megakaryocytes (with smaller megakaryocytes producing smaller platelets) (28); and there are some that assume small platelets merely bleb off larger platelets over time (13). Clarification of the origin of small platelets will have to occur before we can truly understand why their transcriptomes are so diverse. Looking at the results from our transcriptome studies in the setting of bacterial infection and Western diet, it is again clear that the platelet transcriptome is capable of differential expression, with many genes increasing and decreasing in response to inflammatory stimuli. However, with the time scale of observation (weeks) it is possible, and probably more likely, that these transcripts' changes are due to new platelet production by megakaryocytes and differential sorting during production in response to the inflammation as opposed to RNA uptake (Figure 4.1*b*). Indeed, analyses of changing transcripts do not show the unique vascular-related profile seen with small platelets (though since these results are total platelet population results, it would be possible that the profile is there but is not as detectable due to large platelet expression levels).

Additionally, it is possible that the small platelets themselves function in uptake and are not linked to large platelets at all. It could be that large platelets are more hemostatic and act in the traditional role of clotting while small platelets perform the diverse non-vascular roles we have observed. This could mean that small platelets are made with these more non-vascular profiles (though the lack

of these transcripts in megakaryocytes speaks against this) (Figure 4.1*c*) or it could mean that only small platelets perform RNA uptake (Figure 4.1*d*). It would be ideal to sort these populations and then perform *in vitro* clot experiments to see if there is any difference in uptake; however, this experiment would be difficult due to time constraints and the likelihood of platelets being activated post sorting.

An alternative importance to platelet RNA uptake

Even if RNA uptake itself has minimal impact on vascular health, it could create a unique opportunity for therapeutic and diagnostic development. Just as studies of extracellular RNA profiling and disease relevance are quickly expanding, so too could platelet RNA profiling be used in aiding biomarker assessment. Correlating the presence of specific non-platelet derived RNA in isolated platelet fractions to disease states (such as has been shown already in the study of tumor-educated platelets (133-136)), could result in significant biomarker development for a multitude of diseases. Additionally, since platelets are more readily obtained from patients than other cellular samples, they may present a unique method by which to monitor previously difficult to diagnose phenotypes with minimally invasive methods.

Future Steps

It is clear there are many unanswered questions to what platelet RNA changes in various phenotypic and disease settings mean and how to address how platelet RNA impacts both platelet and vascular function. We have observed distinct expression changes with inflammatory stimuli, dependent on time and specific stimuli. Additional analysis of the differential changes in platelets in response to inflammatory stimuli will require repeated tests as well as expansion of comparisons to alternative clinical studies to better visualize results across the human populations. Evaluation of alternative stimuli will help determine how the platelet transcriptome changes broadly in response to inflammation as well as specifically in different phenotypes. Finally, additional timepoint analyses as well as accompanying megakaryocyte analyses will help determine if changes seen are due to differential platelet production or as the result of RNA transfer.

Work still needs to be done to fully understand the platelet's ability to take up RNA, specifically which RNAs are taken up in healthy and disease specific settings. Previously published RNA-sequencing data of HUVECs (222) (Table G.1*c*) as well as RT-qPCR of the our specific HUVECs used in these experiments (Table G.1*a,b*) show that the most expressed transcripts in platelets post HUVEC incubation do not represent the most endogenously expressed transcripts in HUVECs; instead they range in general expression levels or activated expression levels in HUVECs. This suggests that platelet RNA uptake is selective and may be transcript specific, as a bulk transfer would have resulted in the highest expressed HUVEC RNA overexpressed in platelets post transfer.

Furthermore, the specific mechanism by which platelet RNA uptake occurs needs further elucidation; it appears to be complex and may be dependent on the close proximity established *in vitro* and *in vivo* in the vasculature, involve microparticle exchange, and be commensurate on stimulation and time. Additionally, although we previously demonstrated that the amount of RNA transferred to other cells was enough to lead to translation, future studies will demonstrate if the RNA taken up by platelets affects the protein content or cellular function of donor cells, as has been shown with both platelet mRNA and platelet miRNA transfer (122-125) in other groups, or platelets themselves (both in terms of function and clearance). The difficulty in answering these questions lays with the concurrent phenomenon of platelet RNA transfer: elucidating the effects of platelet RNA uptake will first require uncoupling it from platelet RNA transfer to prevent confounding results. Clarifying the complexity of the mechanism of platelet mRNA uptake, and how it is related to the unknown mechanism of platelet mRNA transfer, will shed light on the overall role of platelet RNA transfer and uptake *in vivo*.

Beyond the mechanistic details of what transcripts platelets take up from circulation and how this process occurs, understanding the link between platelet RNA uptake and platelet subpopulation heterogeneity is imperative for elucidating how platelet subpopulations function within the circulation. As described, the small platelet RNA transcriptome is distinctly different than that of the large platelet RNA population, and as the diversity correlates to vascular cell

and apoptosis related profiles, suggests the uptake of RNA from the vasculature. Elucidation of just how these differential expression profiles come to exist will expand our understanding of the heterogeneous platelet profile dramatically. If large platelets become small platelets over time, as some have hypothesized, the presence of these transcripts suggest that all platelets take up RNA over time, leading to a gradual shift in transcriptome over the platelet's circulating life (Figure 4.1*a)*. If small platelets themselves are actually produced through alternative biogenesis (i.e. from different *n* megakaryocytes), it is possible that only this subset is capable of uptake (Figure 4.1*d*), or that these platelets are differentially made to respond differently in circulation (Figure 4.1*c*). As our studies revealed that many aspects of platelet RNA uptake and transfer seem to be transcript specific, it could be that the models of platelet RNA uptake and platelet subpopulation heterogeneity are both complex and multifaceted, and when combined result in a complicated system comprised of elements from all these hypotheses in tandem (Figure 4.1*e*). Either way, understanding how platelets perform RNA uptake and which subsets are capable of transfer (as well as further understanding the specific difference between these subsets) can help us expand our understanding of platelet biology, as well as impact how we use platelets in treatment. For example, if only large platelets perform hemostatically, while small platelets perform non-traditional functions, platelet transfusion treatments could be tailored to the needs of the recipient, allowing for more optimal impact and decreased side effects.

Limitations

As discussed in the previous chapters, a number of limitations exist in our current ability to study the role RNA plays in platelet function and heterogeneity. Because platelets are such unique cells, particularly in size, complexity and function, there is a lack of advanced technology for their proper investigation. Thorough analyses of the effects of stimulation on platelet transcriptomes will require study expansion, both in terms of replicate numbers for *in vivo* modeling as well as additional human clinical data for better comparison studies. Continued interrogation of the mechanics of platelet RNA uptake will require advancements in small particle detection. Platelet subpopulation studies will require improvements in RNA analytics, RT-qPCR and sequencing for low input and low quality samples as well as protocol optimization for maximum platelet output with minimal platelet agitation, allowing for increased RNA output and thus more in-depth analysis and repeated measures. Development of single cell techniques for platelet size particles could thoroughly increase our insight into all these scientific questions.

Concluding Remarks

Based on their historical role in hemostasis alone, platelets are one of the most integral cell types in the body. Their dysregulation leads to some of the most common human diseases but, despite this, there is still much we do not know about platelet function, both in its traditional and alternative roles. Just as the last 150 years focused on regulating the platelet's role in CVD and beginning to determine its mechanistic traits, the next 100 years need to be focused on understanding how the platelet functions at a molecular level. As advances in our ability to interrogate small cell and molecular biology grow, a focus must be placed on utilizing and adapting these technologies to platelet biology. Understanding the role platelet RNA and platelet RNA uptake play in platelet functionality, as well as understanding what platelet RNA can tell us about normal homeostasis, will expand our understanding of cardiovascular and other diseases. As we begin to understand the relevance of platelet RNA and its correlation to platelet subpopulations, we can develop new and potentially more effective methods of adapting the power of platelets for therapeutic and diagnostic purposes.

APPENDIX A: GENE ABBREVIATIONS AND DESCRIPTIONS

Table A.1: Full list of gene names, abbreviations, descriptions and identifiers.
Note: Gene identifier only included for species used in these text.

Gene Symbol	Location (Chapter / Appendix)	Description	Human Gene ID (Entrez)	Mouse Gene ID (Entrez)	Other Gene ID (Accession)
0610010O12Rik	2	RIKEN cDNA 0610010O12 gene		66060	
1100001G20Rik	2	RIKEN cDNA 1100001G20 gene		66107	
1110002L01Rik	2	RIKEN cDNA 1110002L01 gene		100043040	
1110012L19Rik	2	RIKEN cDNA 1110012L19 gene		68618	
1110028F11Rik	2	RIKEN cDNA 1110028F11 gene		68690	
1190002N15Rik	2	RIKEN cDNA 1190002N15 gene		68861	
1700019G17Rik	2	RIKEN cDNA 1700019G17 gene		75541	
1700034H14Rik	2	RIKEN cDNA 1700034H14 gene		67105	
1700034I23Rik	2	RIKEN cDNA 1700034I23 gene		73297	
1810009J06Rik	2	RIKEN cDNA 1810009J06 gene		73626	
2010001M09Rik	2	RIKEN cDNA 2010001M09 gene		69816	
2010107H07Rik	2	RIKEN cDNA 2010107H07 gene		66487	
2310034G01Rik	2	RIKEN cDNA 2310034G01 gene		75579	
2400001E08Rik	2	RIKEN cDNA 2400001E08 gene		66508	
2410018L13Rik	2	RIKEN cDNA 2410018L13 gene		69732	
2810055G20Rik	2	Mir99ahg; Mir99a and Mirlet7c-1 host gene		77994	
2810405K02Rik	2	RIKEN cDNA 2810405K02 gene		66469	
4833413D08Rik	2	RIKEN cDNA 4833413D08 gene		71425	
4921509C19Rik	2	RIKEN cDNA 4921509C19 gene		381393	

4921524J17Rik	2	RIKEN cDNA 4921524J17 gene		66714	
4930433N12Rik	2	RIKEN cDNA 4930433N12 gene		114673	
4930520O04Rik	2	RIKEN cDNA 4930520O04 gene		75116	
4930524N10Rik	2	RIKEN cDNA 4930524N10 gene		75071	
4930562F07Rik	2	RIKEN cDNA 4930562F07 gene		75255	
4933426I21Rik	2	RIKEN cDNA 4933426I21 gene		71163	
5430413K10Rik	2	RIKEN cDNA 5430413K10 gene		433492	
5830417I10Rik	2	RIKEN cDNA 5830417I10 gene		100302730	
5830477G23Rik	2	RIKEN cDNA 5830477G23 gene		76116	
6230400D17Rik	2	RIKEN cDNA 6230400D17 gene		76133	
6530418L21Rik	2	RIKEN cDNA 6530418L21 gene		109050	
6720489N17Rik	2	RIKEN cDNA 6720489N17 gene		211378	
9030624G23Rik	2	RIKEN cDNA 9030624G23 gene		66808	
9330158H04Rik	2	RIKEN cDNA 9330158H04 gene		319472	
A530064D06Rik	2	RIKEN cDNA A530064D06 gene		328830	
A630055G03Rik	2	RIKEN cDNA A630055G03 gene		223970	
A630098A13Rik	2	RIKEN cDNA A630098A13 gene		320913	
AA792892	2	expressed sequence AA792892		100554	
Aadac	2	arylacetamide deacetylase (esterase)		67758	
Acot9	2	acyl-CoA thioesterase 9		56360	
Acp5	2	acid phosphatase 5, tartrate resistant		11433	
Acsf2	2	acyl-CoA synthetase family member 2		264895	
ACTB	3, B, D	actin beta	60	11461	

Aga	2	aspartylglucosaminidase		11593	
Agk	2	acylglycerol kinase		69923	
AGO2 (EIF2C2)	3, B	argonaute 2, RISC catalytic component	27161		
Ahcy	2	S-adenosylhomocysteine hydrolase		269378	
Ahsg	2	alpha-2-HS-glycoprotein		11625	
AI324046	2	expressed sequence AI324046		380795	
AI747699	2	expressed sequence AI747699		381236	
Aif1	2	allograft inflammatory factor 1		11629	
Akr1b10	2	aldo-keto reductase family 1, member B10 (aldose reductase)		67861	
Alb	2	albumin	213	11657	
Ambp	2	alpha 1 microglobulin/bikunin	259	11699	
Angptl3	2	angiopoietin-like 3		30924	
Aph1a	2	anterior pharynx defective 1a homolog (C. elegans)		226548	
Apoa1	2	apolipoprotein A-I		11806	
Apoa2	2	apolipoprotein A-II		11807	
Apoa5	2	apolipoprotein A-V		66113	
Apob	2	apolipoprotein B		238055	
Apoc1	2	apolipoprotein C-I		11812	
Apoc2	2	apolipoprotein C-II		11813	
Apoc3	2	apolipoprotein C-III		11814	
Apoc4	2	apolipoprotein C-IV		11425	
Apoe	2	apolipoprotein E		11816	
Apof	2	apolipoprotein F		103161	
Apoh	2	apolipoprotein H		11818	
Apol10a	2	apolipoprotein L 10a		245282	
Apol9b	2	apolipoprotein L 9b		71898	
ARHGAP18	F	rho GTPase activating protein 18	93663		

Arhgef1	2	Rho guanine nucleotide exchange factor (GEF) 1		16801	
Armc10	2	armadillo repeat containing 10		67211	
ASGR1	3, B, F	asialoglycoprotein receptor 1	432		
Ass1	2	argininosuccinate synthetase 1		11898	
AU019823	2	expressed sequence AU019823		270156	
Azgp1	2	alpha-2-glycoprotein 1, zinc		12007	
B2M	3, B, D	beta-2-microglobulin	567		
B3gnt8	2	UDP-GlcNAc:betaGal beta-1,3-N-acetylglucosaminyltransferase 8		232984	
Bank1	2	B-cell scaffold protein with ankyrin repeats 1		242248	
BAX	3	BCL2 associated X, apoptosis regulator	581		
BC002059	2	cDNA sequence BC002059		213811	
BC003331	2	cDNA sequence BC003331		226499	
BC061237	2	cDNA sequence BC061237		385138	
BC094916	2	cDNA sequence BC094916		545384	
Bckdk	2	branched chain ketoacid dehydrogenase kinase		12041	
BCL2L1	3, B, D	BCL2 like 1	598		
BCL2L11 (BIM)	3	BCL2 like 11	10018		
Bgn	2	biglycan		12111	
Bhmt	2	betaine-homocysteine methyltransferase		12116	
Bin3	2	bridging integrator 3		57784	
blv-miR-B2-5p	F	Bovine leukemia virus (BLV) microRNA B2			MIMAT0025860
C130026I21Rik	2	RIKEN cDNA C130026I21 gene		620078	

C1qb	2	complement component 1, q subcomponent, beta polypeptide		12260	
C3	2	complement component 3		12266	
C330018D20Rik	2	RIKEN cDNA C330018D20 gene		77422	
C87977	2	expressed sequence C87977		97187	
C8b	2	complement component 8, beta polypeptide		110382	
CALR	3, B, F	calreticulin	811		
Car1	2	carbonic anhydrase 1		12346	
Car3	2	carbonic anhydrase 3		12350	
Catsperg1	2	cation channel, sperm-associated, gamma 1		320225	
Cbx6	2	chromobox homolog 6		494448	
CCL17	3, B	C-C motif chemokine ligand 17	6361		
Ccl3 / CCL3	2, 3, B	chemokine (C-C motif) ligand 3	6348	20302	
Ccl6	2	chemokine (C-C motif) ligand 6		20305	
CCL7	3, B, F	C-C motif chemokine ligand 7	6354		
Ccr2	2	chemokine (C-C motif) receptor 2		12772	
CD163	3, B	CD163 molecule	9332		
CD209	3, B	CD209 molecule	30835		
Cd209f	2	CD209f antigen		69142	
Cd2ap	2	CD2-associated protein		12488	
Cd3d/ CD3D	2, 3, B	CD3 antigen, delta polypeptide	915	12500	
Cd3g	2	CD3 antigen, gamma polypeptide		12502	
CD40	3, B, D	CD40 molecule	958		
CD40LG	3, B	CD40 ligand	959		
CD44	3, B	CD44 molecule (Indian blood group)	960		

Cd53 / CD53	2, 3, B	CD53 antigen	963	12508	
Cd5l	2	CD5 antigen-like		11801	
CD63	3, B, F	CD63 molecule	967		
CD69	1	CD69 molecule	969		
Cd79a	2	CD79A antigen (immunoglobulin-associated alpha)		12518	
Cd79b	2	CD79B antigen		15985	
CD81	3, B, F	CD81 molecule	975		
CD86	3, B	CD86 molecule	942		
Cda	2	cytidine deaminase		72269	
Cdkn1a	2	cyclin-dependent kinase inhibitor 1A (P21)		12575	
Cdo1	2	cysteine dioxygenase 1, cytosolic		12583	
CEACAM3	3	carcinoembryonic antigen related cell adhesion molecule 3	1084		
Cenpq	2	centromere protein Q		83815	
Ces3	2	carboxylesterase 1D; carboxylesterase 3		104158	
Cetn4	2	centrin 4		207175	
Cfd	2	complement factor D (adipsin)		11537	
Chchd1	2	coiled-coil-helix-coiled-coil-helix domain containing 1		66121	
CHD9	F	chromo-domain helicase DNA binding protein 9	80205		
Cidec	2	cell death-inducing DFFA-like effector c		14311	
Cldn22	2	claudin 22		75677	
Clec4a3	2	C-type lectin domain family 4, member a3		73149	
Clm3	2	CMRF-35-like molecule 3; cytohesin 3		382551	
Cnn1	2	calponin 1		12797	
Cnn3	2	calponin 3, acidic		71994	
COL18A1	3, B, F	collagen type XVIII alpha 1 chain	80781		

COPA	3, B	coatomer protein complex subunit alpha	1314		
Cops6	2	COP9 (constitutive photomorphogenic) homolog, subunit 6 (Arabidopsis thaliana)		26893	
Cp	2	Ceruloplasmin		12870	
Cpamd8	2	C3 and PZP-like alpha-2-macroglobulin domain-containing protein 8; Mug2, murinoglobulin 2		17837	
CRLS1	3, B	cardiolipin synthase 1	54675		
CRP	3, B, F	C-reactive protein	1401		
Csnk2a1	2	casein kinase 2, alpha 1 polypeptide		12995	
CX3CL1	3, B, F	C-X3-C motif chemokine ligand 1	6376		
CXADR	3, B, F	CXADR, Ig-like cell adhesion molecule	1525		
CXCL1	3, B, F	C-X-C motif chemokine ligand 1	2919		
CXCL12	3, B, F	C-X-C motif chemokine ligand 12	6387		
Cxcl2 / CXCL2	2, 3, B, F	chemokine (C-X-C motif) ligand 2	2920	20310	
CXCL5	3, B	C-X-C motif chemokine ligand 5	6374		
CXCL6	3, B, F	C-X-C motif chemokine ligand 6	6372		
Cyp1a2	2	cytochrome P450, family 1, subfamily a, polypeptide 2		13077	
Cyp2d10	2	cytochrome P450, family 2, subfamily d, polypeptide 10		13101	
Cyp2e1	2	cytochrome P450, family 2, subfamily e, polypeptide 1		13106	
Cyp2f2	2	cytochrome P450, family 2, subfamily f, polypeptide 2		13107	

Cyp3a11	2	cytochrome P450, family 3, subfamily a, polypeptide 11		13112	
Cyp3a44	2	cytochrome P450, family 3, subfamily a, polypeptide 44		337924	
Cyp3a59	2	cytochrome P450, subfamily 3A, polypeptide 59		100041449	
Cyp4a10	2	cytochrome P450, family 4, subfamily a, polypeptide 10		13117	
Cytip	2	cytohesin 1 interacting protein		227929	
D630032N06Rik	2	RIKEN cDNA D630032N06 gene		654810	
Dapl1	2	death associated protein-like 1		76747	
Dcakd	2	dephospho-CoA kinase domain containing		68087	
Ddx28	2	DEAD (Asp-Glu-Ala-Asp) box polypeptide 28		71986	
Defb12	2	defensin beta 12		77674	
Degs1	2	degenerative spermatocyte homolog 1 (Drosophila)		13244	
Diablo	2	diablo homolog (Drosophila)		66593	
DICER1	3, B, F	dicer 1, ribonuclease III	23405		
Dnm3os	2	dynamin 3, opposite strand		474332	
Dock2	2	dedicator of cyto-kinesis 2		94176	
Dppa3	2	developmental pluripotency-associated 3		73708	
Dpy19l3	2	dpy-19-like 3 (C. elegans)		233115	
Dsg1b	2	desmoglein 1 beta		225256	
E030030I06Rik	2	RIKEN cDNA E030030I06 gene		319887	
E330020D12Rik	2	RIKEN cDNA E330020D12 gene		626058	

Ear2	2	eosinophil-associated, ribonuclease A family, member 2		13587	
ebv-miR-BART11-5p	F	Epstein-Barr Virus (EBV) microRNA BART11			MIMAT0003421
ebv-miR-BART19-3p	F	Epstein-Barr Virus (EBV) microRNA BART11			MIMAT0003718
Eif2s1	2	eukaryotic translation initiation factor 2, subunit 1 alpha		13665	
Eif4a3	2	eukaryotic translation initiation factor 4A3		192170	
EIF4G1	3, B, F	eukaryotic translation initiation factor 4 gamma 1	1981		
Eif4h	2	eukaryotic translation initiation factor 4H		22384	
Elovl2	2	elongation of very long chain fatty acids (FEN1/Elo2, SUR4/Elo3, yeast)-like 2		54326	
Emr1	2	EGF-like module-containing mucin-like hormone receptor-like 1; Adgre1; adhesion G protein-coupled receptor E1		13733	
eNOS	1	nitric oxide synthase 3	4846		
EPRS	F	glutamyl-prolyl-tRNA synthetase	2058		
Es1	2	Ces1c, carboxylesterase 1c; esterase 1		13884	
Es31	2	Ces3a, carboxylesterase 3A; esterase 31		382053	
ESAM	3, B	endothelial cell adhesion molecule	90952		
Exosc7	2	exosome component 7		66446	
F2	2	coagulation factor II		14061	

Fabp1	2	fatty acid binding protein 1, liver	2168	14080	
Fabp5	2	fatty acid binding protein 5, epidermal	2171	16592	
Fads1	2	fatty acid desaturase 1		76267	
Fam111a	2	family with sequence similarity 111, member A		107373	
Fam136a	2	family with sequence similarity 136, member A		66488	
Fcer2a	2	Fc receptor, IgE, low affinity II, alpha polypeptide		14128	
Fcf1	2	FCF1 small subunit (SSU) processome component homolog (S. cerevisiae)		73736	
Fcgr3	2	Fc receptor, IgG, low affinity III		14131	
FCN1	3, B	ficolin 1	2219		
Fdps	2	farnesyl diphosphate synthetase		110196	
Fetub	2	fetuin beta		59083	
Fga	2	fibrinogen alpha chain		14161	
Fgb	2	fibrinogen beta chain		110135	
Fgg	2	fibrinogen gamma chain	2266	99571	
Fgl1	2	fibrinogen-like protein 1		234199	
Fkbp4	2	FK506 binding protein 4		14228	
FOLR1	3, B	folate receptor 1	2348		
Fxyd3	2	FXYD domain-containing ion transport regulator 3		17178	
G3bp1	2	Ras-GTPase-activating protein SH3-domain binding protein 1		27041	
GAPDH	3, B, D	glyceraldehyde-3-phosphate dehydrogenase	2597		
Gc	2	group specific component		14473	

Gda	2	guanine deaminase		14544	
Gemin8	2	gem (nuclear organelle) associated protein 8		237221	
Gimap9	2	GTPase, IMAP family member 9		317758	
Gkap1	2	G kinase anchoring protein 1		56278	
Glo1	2	glyoxalase 1		109801	
Gm10029	2	predicted pseudogene 10029		100039532	
Gm10035	2	predicted gene 10035		668178	
Gm10336	2	predicted gene 10336		328186	
Gm10455	2	predicted gene 10455		385277	
Gm10643	2	predicted gene 10643		100038416	
Gm10651	2	predicted pseudogene 10651		100043771	
Gm10767	2	predicted gene 10767		100038538	
Gm10878	2	predicted gene 10878		628268	
Gm10880	2	predicted gene 10880		236047	
Gm10883	2	Igkv8-30; immunoglobulin kappa chain variable 8-30		384419	
Gm10884	2	predicted gene 10884		434040	
Gm10885	2	Ighv8-12; immunoglobulin heavy variable V8-12		780960	
Gm11428	2	predicted gene 11428		100034251	
Gm11710	2	predicted gene 11710		100043123	
Gm11937	2	predicted gene 11937		100041488	
Gm129	2	predicted gene 129		229599	
Gm13034	2	predicted gene 13034		627585	
Gm13139	2	predicted gene 13139		666532	

Gm13212	2	predicted gene 13212		433801	
Gm13213	2	predicted gene 13213		545683	
Gm13931	2	predicted gene 13931		668825	
Gm1418	2	predicted gene 1418		384514	
Gm14420	2	predicted gene 14420		628308	
Gm14851	2	predicted gene 14851		634825	
Gm15210	2	predicted gene 15210		100042069	
Gm1524	2	predicted gene 1524		385253	
Gm15417	2	predicted gene 15417		545539	
Gm16519	2	predicted gene, 16519		546695	
Gm16527	2	predicted gene, 16527		669780	
Gm189	2	predicted gene 189		235952	
Gm2666	2	predicted gene 2666		100040213	
Gm3643	2	predicted gene 3643		100042057	
Gm4459	2	predicted gene 4459		100043472	
Gm4478	2	predicted gene 4478		100043498	
Gm4738	2	predicted gene 4738		13909	
Gm4759	2	GTPase, very large interferon inducible 1 pseudogene		209380	
Gm4889	2	predicted gene 4889		234159	
Gm4943	2	predicted pseudogene 4943		239760	
Gm4964	2	predicted gene 4964		243420	
Gm5081	2	predicted gene 5081		328099	
Gm5154	2	predicted gene 5154		381818	
Gm5168	2	predicted gene 5168		382275	
Gm5292	2	predicted gene 5292		384179	
Gm5321	2	predicted gene 5321		384525	
Gm5331	2	predicted gene 5331		384622	
Gm5413	2	predicted gene 5413		404743	
Gm5416	2	predicted gene 5416		408196	
Gm5431	2	predicted gene 5431		432555	

Gm5476	2	type II keratin Kb17P pseudogene		432985	
Gm5514	2	predicted gene 5514		433229	
Gm5571	2	predicted gene 5571		434025	
Gm5629	2	predicted gene 5629		434609	
Gm5637	2	predicted pseudogene 5637		434782	
Gm5941	2	predicted gene 5941		546347	
Gm5959	2	predicted gene 5959		546638	
Gm5965	2	predicted gene 5965		546672	
Gm6252	2	predicted gene 6252		621699	
Gm6570	2	predicted gene 6570		625281	
Gm6712	2	predicted gene 6712		626854	
Gm6749	2	predicted pseudogene 6749		627371	
Gm6894	2	predicted gene 6894		628541	
Gm6969	2	predicted pseudogene 6969		629383	
Gm6981	2	glyceraldehyde-3-phosphate dehydrogenase pseudogene		629557	
Gm7015	2	predicted gene 7015		629906	
Gm7188	2	predicted gene 7188		636752	
Gm7225	2	predicted gene 7225		637939	
Gm7582	2	predicted gene 7582		665317	
Gm8096	2	3-phosphoglycerate dehydrogenase pseudogene		666422	
Gm8290	2	predicted gene 8290		666790	
Gm8698	2	predicted gene 8698		667550	
Gm8909	2	predicted gene 8909		667977	
Gm8973	2	predicted gene 8973		668092	
Gm8995	2	predicted gene 8995		668139	
Gm9232	2	predicted gene 9232		668544	
Gm9740	2	predicted gene 9740		780938	
Gm9756	2	carboxylesterase 2 pseudogene		667754	
Gm9781	2	predicted gene 9781		100042807	
Gm9803	2	predicted gene 9803		100042179	
Gmeb1	2	glucocorticoid modulatory element binding protein 1		56809	

Gngt2	2	guanine nucleotide binding protein (G protein), gamma transducing activity polypeptide 2		14710	
Gnpda1	2	glucosamine-6-phosphate deaminase 1		26384	
Gnpnat1	2	glucosamine-phosphate N-acetyltransferase 1		54342	
Gnrh1	2	gonadotropin releasing hormone 1		14714	
GP1BB	3, B	glycoprotein Ib platelet beta subunit	2812		
Gpbp1l1	2	GC-rich promoter binding protein 1-like 1		77110	
GPI	3, B	glucose-6-phosphate isomerase	2821		
Gpn2	2	GPN-loop GTPase 2		100210	
Gpnmb	2	glycoprotein (transmembrane) nmb		93695	
Gpr137b-ps	2	G protein-coupled receptor 137B, pseudogene		664862	
Gprasp1	2	G protein-coupled receptor associated sorting protein 1		67298	
Gpx2	2	glutathione peroxidase 2		14776	
Gpx4	2	glutathione peroxidase 4		625249	
Grap	2	GRB2-related adaptor protein		71520	
Gsdmc3	2	gasdermin C3		270328	
Gsta3	2	glutathione S-transferase, alpha 3		14859	
GSTK1	3	glutathione S-transferase kappa 1	373156		
Gstm1	2	glutathione S-transferase, mu 1		14862	
Gstm2	2	glutathione S-transferase, mu 2		14863	
Gtpbp8	2	GTP-binding protein 8 (putative)		66067	

GUK1	3, D	guanylate kinase 1	2987		
H2-DMb1	2	histocompatibility 2, class II, locus Mb1		14999	
H2-Q8	2	histocompatibility 2, Q region locus 8		15019	
H2-T10	2	histocompatibility 2, T region locus 10		15024	
H2-T22	2	histocompatibility 2, T region locus 22		15039	
H3f3a	2	H3 histone, family 3A		15078	
Hamp	2	hepcidin antimicrobial peptide		84506	
Hbq1	2	hemoglobin, theta 1		216635	
hbv-mir-B26-3p-novel	F	Herpes B virus (HBV) microRNA B26			Novel finding
hbv-miR-B26-5p	F	Herpes B virus (HBV) microRNA B26			MIMAT0031771
hbv-miR-B7-5p	F	Herpes B virus (HBV) microRNA B7			MIMAT0031766
hcmv-miR-US25-2-3p	F	Human cytomegalovirus (hCMV) microRNA US25-2			MIMAT0001583
Hdc	2	histidine decarboxylase		15186	
Hebp1	2	heme binding protein 1		15199	
HIF1A	F	hypoxia inducible factor 1 alpha subunit	2091		
Higd1a	2	HIG1 domain family, member 1A		56295	
Hint1	2	histidine triad nucleotide binding protein 1		15254	
Hist1h2ab	2	histone cluster 1, H2ab		319172	
Hist1h3a	2	histone cluster 1, H3a		360198	
Hist1h4b	2	histone cluster 1, H4b		326620	
Hist1h4f	2	histone cluster 1, H4f		319157	
Hist2h2ab	2	histone cluster 2, H2ab		621893	
Hmox1	2	heme oxygenase (decycling) 1		15368	

Hnrpdl	2	heterogeneous nuclear ribonucleoprotein D-like		50926	
Hp	2	haptoglobin		15439	
Hpx	2	hemopexin		15458	
Hrg	2	histidine-rich glycoprotein		94175	
Hrnr	2	hornerin		68723	
hsa-miR-1199-5p	F	human microRNA 1199	102466515		MIMAT0031119
hsa-miR-16-5p	F	human microRNA 16	406950 / 406951		MIMAT0000069
hsa-miR-221-3p	F	human microRNA 221	407006		MIMAT0000278
hsa-miR-2681-3p	F	human microRNA 2681	100616110		MIMAT0013516
hsa-miR-324-3p	F	human microRNA 324	442898		MIMAT0000762
hsa-miR-3663-5p	F	human microRNA 3663	100500893		MIMAT0018084
hsa-miR-4482-5p	F	human microRNA 4482	100616323		MIMAT0019016
hsa-miR-584-5p	F	human microRNA 584	693169		MIMAT0003249
Hsd17b7	2	hydroxysteroid (17-beta) dehydrogenase 7		15490	
Hsp90aa1	2	heat shock protein 90, alpha (cytosolic), class A member 1		15519	
Hspd1	2	heat shock protein 1 (chaperonin)		15510	
hsv1-miR-H1-3p	F	Herpes Simplex Virus 1 (HSV-1) microRNA H1			MIMAT0015220
hsv1-miR-H14-5p	F	Herpes Simplex Virus 1 (HSV-1) microRNA-H14			MIMAT0014691
hsv1-miR-H1-5p	F	Herpes Simplex Virus 1 (HSV-1) microRNA-H1			MIMAT0003744
hsv1-miR-H3-3p	F	Herpes Simplex Virus 1 (HSV-1) microRNA-H3			MIMAT0008400

hsv1-miR-H4-3p	F	Herpes Simplex Virus 1 (HSV-1) microRNA-H4			MIMAT0008402
hsv1-miR-H6-3p	F	Herpes Simplex Virus 1 (HSV-1) microRNA-H6			MIMAT0008404
hvt-miR-H14-3p	F	Herpesvirus of turkeys microRNA-H14			MIMAT0012867
I830127L07Rik	2	RIKEN cDNA I830127L07 gene		546643	
ICAM1	1, 3, B, D, F	intercellular adhesion molecule 1	3383	15894	
Idi2	2	isopentenyl-diphosphate delta isomerase 2		320581	
Ifi203	2	interferon activated gene 203		15950	
Ifi204	2	interferon activated gene 204		15951	
Ifi205	2	interferon activated gene 205		226695	
Ifi27l2a	2	interferon, alpha-inducible protein 27 like 2A		76933	
Ifi30	2	interferon gamma inducible protein 30		65972	
Ifit3	2	interferon-induced protein with tetratricopeptide repeats 3		15959	
Ifitm1/ IFITM1	1, 2, 3, B	interferon induced transmembrane protein 1	8519	68713	
IFITM2	3, B	interferon induced transmembrane protein 2	10581		
IFITM3	3, B, F	interferon induced transmembrane protein 3	10410		
Ifitm6	2	interferon induced transmembrane protein 6		213002	
IFNA1	3, B, F	interferon alpha 1	3439		
IFNB1	3, B	interferon beta 1	3456		
Igh-1b	2	immunoglobulin heavy chain 1b (serum IgG2c)		404711	

Igh-2	2	immunoglobulin heavy chain 2 (serum IgA)		238447	
Igh-3	2	immunoglobulin heavy chain 3 (serum IgG2b)		16016	
Igh-5	2	immunoglobulin heavy chain 5 (delta-like heavy chain)		380797	
Ighg1	2	immunoglobulin heavy constant gamma 1 (G1m marker)		16017	
Ighv1-69	2	immunoglobulin heavy variable V1-69		619833	
Ighv7-2	2	immunoglobulin heavy variable V7-2		780800	
Igkv10-96	2	immunoglobulin kappa chain variable		692165	
Igkv1-117	2	immunoglobulin kappa chain variable 1-117		16098	
Igkv12-44	2	immunoglobulin kappa chain variable 12-44		545851	
Igkv12-46	2	immunoglobulin kappa chain variable 12-46		692245	
Igkv14-111	2	immunoglobulin kappa chain variable 14-111		545847	
Igk-V19-20	2	immunoglobulin kappa chain variable 19 (V19)-20		108024	
Igk-V21-12	2	immunoglobulin kappa chain variable 21 (V21)-12		667914	
Igk-V21-4	2	immunoglobulin kappa chain variable 21 (V21)-4		626347	
Igk-V8-16	2	immunoglobulin kappa chain variable 8 (V8)-16		640340	
Igl-C1	2	immunoglobulin lambda chain, constant region 1		110785	

Igl-C2	2	immunoglobulin lambda chain, constant region 2		110786	
Igl-J1	2	immunoglobulin lambda chain, joining region 1		404737	
Igl-V1	2	immunoglobulin lambda chain, variable 1		16142	
Igl-V2	2	immunoglobulin lambda chain, variable 2		110612	
Ikzf3	2	IKAROS family zinc finger 3		22780	
IL10RA	3, B	interleukin 10 receptor subunit alpha	3587		
IL1b / IL1beta	2, 3, B, D	IL1B; interleukin 1 beta	3553	16176	
IL1R1	1	interleukin 1 receptor, type 1	3554		
Il28b	2	interleukin 28B		338374	
IL2RB	3, B	interleukin 2 receptor subunit beta	3560		
IL5	3, B	interleukin 5	3567		
IL6	1, 3, B, F	interleukin 6	3569		
IL8	3, B, F	C-X-C motif chemokine ligand 8	3576		
iltv-miR-I2	F	Infectious laryngotracheitis virus (ILTV) microRNA-I2			MIMAT0012725
Immp1l	2	IMP1 inner mitochondrial membrane peptidase-like (S. cerevisiae)		66541	
ITGA5	3, B, F	integrin subunit alpha 5	3678		
ITGAE	3, B	integrin subunit alpha E	3682		
ITGAL	3, B	integrin subunit alpha L	3683		
ITGAM	3, B	integrin subunit alpha M	3684		
ITGB7	3, B	integrin subunit beta 7	3695		

Itih4	2	inter alpha-trypsin inhibitor, heavy chain 4		16427	
KIAA0232	3, B, F	KIAA0232	9778		
KIAA1462	3, B, F	JCAD; junctional cadherin 5 associated	57608		
Klhdc5	2	kelch domain containing 5		232539	
Klk1b9	2	kallikrein 1-related peptidase b9		13648	
Klrc1	2	killer cell lectin-like receptor subfamily C, member 1		16641	
Klrc2	2	killer cell lectin-like receptor subfamily C, member 2		16642	
Kmo	2	kynurenine 3-monooxygenase (kynurenine 3-hydroxylase)		98256	
Kng1	2	kininogen 1		16644	
Kng2	2	kininogen 2		385643	
Krt8	2	keratin 8		16691	
Krt81	2	keratin 81		64818	
kshv-miR-K12-10a-5p	F	Kaposi's sarcoma herpesvirus (KSHV) microRNA-K12-10a			MIMAT0015212
kshv-miR-K12-6-5p	F	Kaposi's sarcoma herpesvirus (KSHV) microRNA-K12-6			MIMAT0002188
L2hgdh	2	L-2-hydroxyglutarate dehydrogenase		217666	
LAMP1	3, B	lysosomal associated membrane protein 1	3916		
Lancl3	2	LanC lantibiotic synthetase component C-like 3 (bacterial)		236285	
Lce1c	2	late cornified envelope 1C		73719	
Lce1i	2	late cornified envelope 1I		76585	
LCK	3, B	LCK proto-oncogene, Src family tyrosine kinase	3932		

Lcp1	2	lymphocyte cytosolic protein 1		18826	
LOC100038947	2	signal-regulatory protein beta 1-like		100038947	
LOC100044509	2	similar to transforming growth factor, beta receptor III (betaglycan, 300kDa)		100044509	
LOC100048057	2	hypothetical protein LOC100048057		100048057	
Lrg1	2	leucine-rich alpha-2-glycoprotein 1		76905	
Lsm2	2	LSM2 homolog, U6 small nuclear RNA associated (S. cerevisiae)		27756	
LRP1B	F	LDL receptor related protein 1B	53353		
LSP1	3, B, D	lymphocyte-specific protein 1	4046		
Ly6c1	2	lymphocyte antigen 6 complex, locus C1		17067	
Ly86	2	lymphocyte antigen 86		17084	
Lypla2	2	lysophospholipase 2		26394	
Lyrm7	2	LYR motif containing 7		75530	
Mageb16	2	melanoma antigen family B, 16		71967	
Man1b1	2	mannosidase, alpha, class 1B, member 1		227619	
Manea	2	mannosidase, endo-alpha		242362	
MAP4K4	3, B, F	mitogen-activated protein kinase kinase kinase kinase 4	9448		
Marco	2	macrophage receptor with collagenous structure		17167	
Mat1a	2	methionine adenosyltransferase I, alpha		11720	

mcmv-miR-M01-4-3p	F	Mouse cytomegalovirus (mCMV) microRNA-M01-4			MIMAT0005539
mcmv-miR-M23-2-3p	F	Mouse cytomegalovirus (mCMV) microRNA-M23-2			MIMAT0005545
mcmv-miR-m44-1	F	Mouse cytomegalovirus (mCMV) microRNA-m44-1			MIMAT0005546
mcmv-miR-m59-1	F	Mouse cytomegalovirus (mCMV) microRNA-m59-1			MIMAT0005548
mcmv-miR-m59-2	F	Mouse cytomegalovirus (mCMV) microRNA-m59-2			MIMAT0005549
mdv2-miR-M18-5p	F	Marek's disease virus type 2 (MDV2) microRNA-M18			MIMAT0004458
mdv2-miR-M21-3p	F	Marek's disease virus type 2 (MDV2) microRNA-M21			MIMAT0004464
mdv2-miR-M24-3p	F	Marek's disease virus type 2 (MDV2) microRNA-M24			MIMAT0004468
Me1	2	malic enzyme 1, NADP(+)-dependent, cytosolic		17436	
Med29	2	mediator complex subunit 29		67224	
Med4	2	mediator of RNA polymerase II transcription, subunit 4 homolog (yeast)		67381	
Mettl7b	2	methyltransferase like 7B		71664	
Mfap1a	2	microfibrillar-associated protein 1A		67532	
Mfap5	2	microfibrillar associated protein 5		50530	
Mgp	2	matrix Gla protein		17313	

Mgst1	2	microsomal glutathione S-transferase 1		56615	
MIC1/C18orf8	F	macrophage inhibitory cytokine 1	29919		
miR-10a	1	microRNA 10a	406902		
miR-126-3p	1	microRNA 126	387145		
miR-148a	1	microRNA 148a	406940		
miR-185	1	microRNA 185	406961		
miR-22	1	microRNA 22	407004		
miR-223	1	microRNA 223	723814		
miR-24	1	microRNA 24 (-1/-2)	4077012/ 407013		
miR-27a-3p	B	microRNA 27a	407018		MIMAT0000084
mir31	2	microRNA 31		723895	
miR-320a	1	microRNA 320a	407037		
miR-320b	1	microRNA 320b (-1/-2)	100302117/ 100313769		
miR-423-5p	1	microRNA 423	494335		
miR-490-5p	1	microRNA 490	735279		
mir540	2	microRNA 540		723880	
mir700	2	microRNA 700		735285	
mir713	2	microRNA 713		751548	
MMP2	1	Matrix metallopeptidase 2	4313		
MMP9	3, B	matrix metallopeptidase 9	4318		
Mnd1	2	meiotic nuclear divisions 1 homolog (S. cerevisiae)		76915	
Mnda	2	myeloid cell nuclear differentiation antigen		381308	
Mrgpra5	2	MAS-related GPR, member A5		404235	
MRP-14	1	S100A9; S100 calcium binding protein A9	6280		
Mrpl22	2	mitochondrial ribosomal protein L22		216767	
Mrpl33	2	mitochondrial ribosomal protein L33		66845	

Mrpl42	2	mitochondrial ribosomal protein L42		67270	
Mrps18a	2	mitochondrial ribosomal protein S18A		68565	
Mrps26	2	mitochondrial ribosomal protein S26	64949	99045	
Mrps28	2	mitochondrial ribosomal protein S28		66230	
Mrto4	2	MRT4, mRNA turnover 4, homolog (S. cerevisiae)		69902	
Ms4a6b	2	membrane-spanning 4-domains, subfamily A, member 6B		69774	
Ms4a6c	2	membrane-spanning 4-domains, subfamily A, member 6C		73656	
Mt2	2	metallothionein 2		17750	
Mug1	2	murinoglobulin 1		17836	
Mup3	2	major urinary protein 3		17842	
N6amt2	2	N-6 adenine-specific DNA methyltransferase 2 (putative)		68043	
Naa10	2	N(alpha)-acetyltransferase 10, NatA catalytic subunit Nalpha acetyltransferase 10		56292	
Naa50	2	N(alpha)-acetyltransferase 50, NatE catalytic subunit		72117	
NBEAL2	1	neurobeachin like 2	23218		
Ndufs3	2	NADH dehydrogenase (ubiquinone) Fe-S protein 3		68349	

Nedd9	2	neural precursor cell expressed, developmentally down-regulated gene 9		18003	
Nfil3	2	nuclear factor, interleukin 3, regulated		18030	
NFKB1	3, B	nuclear factor kappa B subunit 1	4790		
NFKBIA	3, B, D, F	NFKB inhibitor alpha	4792	18035	
Nmi	2	N-myc (and STAT) interactor		64685	
Nono	2	non-POU-domain-containing, octamer binding protein		53610	
Npm1	2	nucleophosmin 1		18148	
Npm3-ps1	2	nucleoplasmin 3, pseudogene 1		108176	
Nptxr	2	neuronal pentraxin receptor		73340	
Nr2f6	2	nuclear receptor subfamily 3, group F, member 6	2063	13864	
Nsfl1c	2	NSFL1 (p97) cofactor (p47)		386649	
Nt5c3l	2	5'-nucleotidase, cytosolic III-like		68106	
Nudt21	2	nudix (nucleoside diphosphate linked moiety X)-type motif 21		68219	
Nup62-il4i1	2	Nup62-Il4i1 protein		100328588	
Nutf2	2	nuclear transport factor 2		68051	
Obox2	2	oocyte specific homeobox 2		246792	
Olfr1077-ps1	2	olfactory receptor 1077, pseudogene 1		625853	
Olfr1148	2	olfactory receptor 1148		258220	
Olfr1162	2	olfactory receptor 1162		258105	
Olfr1170	2	olfactory receptor 1170		258525	
Olfr1303	2	olfactory receptor 1303		258397	

Olfr1337	2	olfactory receptor 1337		258306	
Olfr135	2	olfactory receptor 135		258329	
Olfr1371	2	olfactory receptor 1371		276865	
Olfr1418	2	olfactory receptor 1418		258227	
Olfr205	2	olfactory receptor 205		257881	
Olfr224	2	olfactory receptor 224		258198	
Olfr29-ps1	2	olfactory receptor 29, pseudogene 1		29848	
Olfr344	2	olfactory receptor 344		258621	
Olfr399	2	olfactory receptor 399		259006	
Olfr403	2	olfactory receptor 403		404316	
Olfr406-ps	2	olfactory receptor 406, pseudogene		258181	
Olfr441	2	olfactory receptor 441		258649	
Olfr521	2	olfactory receptor 521		258353	
Olfr541	2	olfactory receptor 541		258964	
Olfr57	2	olfactory receptor 57		18357	
Olfr612	2	olfactory receptor 612		545985	
Olfr638	2	olfactory receptor 638		259124	
Olfr744	2	olfactory receptor 744		257884	
Olfr97	2	olfactory receptor 97		258505	
Orm1	2	orosomucoid 1		18405	
Oxct2b	2	3-oxoacid CoA transferase 2B		353371	
PAR1	1	Protease-activated receptor 3; coagulation factor II receptor-like 3	2149	14062	
PAR3	1	Protease-activated receptor 1; coagulation factor II receptor	2151	14064	

Pcdha1	2	protocadherin alpha 1		116731	
Pcdha12	2	protocadherin alpha 12		192164	
Pcdha5	2	protocadherin alpha 5		12941	
Pcdha6	2	protocadherin alpha 6		12937	
Pcdha8	2	protocadherin alpha 8		353235	
Pcdhac2	2	protocadherin alpha subfamily C, 2		353237	
Pcdhga1	2	protocadherin gamma subfamily A, 1		93709	
Pcdhga10	2	protocadherin gamma subfamily A, 10		93722	
Pcdhgb5	2	protocadherin gamma subfamily B, 5		93702	
Pcdhgb7	2	protocadherin gamma subfamily B, 7		93704	
PF4	3, D	platelet factor 4	5196		
Pfkp	2	phosphofructokinase, platelet		56421	
Phb	2	prohibitin		18673	
Phf11	2	Phf11a, PHD finger protein 11		219131	
Phgdh	2	3-phosphoglycerate dehydrogenase		236539	
Pigr	2	polymeric immunoglobulin receptor		18703	
PIK3R1	F	phosphoinositide-3-kinase regulatory subunit 1	5295		
Pip4k2b	2	phosphatidylinositol-5-phosphate 4-kinase, type II, beta		108083	
Plekhf1	2	pleckstrin homology domain containing, family F (with FYVE domain) member 1		72287	
Plg	2	Plasminogen		18815	

Pnp	2	purine-nucleoside phosphorylase		18950	
Polh	2	polymerase (DNA directed), eta (RAD 30 related)		80905	
Polr2c	2	polymerase (RNA) II (DNA directed) polypeptide C		20021	
Polr2k	2	polymerase (RNA) II (DNA directed) polypeptide K		17749	
Polr3g	2	polymerase (RNA) III (DNA directed) polypeptide G		67486	
Pram1	2	PML-RAR alpha-regulated adaptor molecule 1		378460	
Prelp	2	proline arginine-rich end leucine-rich repeat		116847	
Prh1	2	proline rich protein HaeIII subfamily 1		19131	
PRKRA	1	protein activator of interferon induced protein kinase EIF2AK2	8575		
Prp2	2	proline rich protein 2		83380	
Prps1	2	phosphoribosyl pyrophosphate synthetase 1		19139	
prv-miR-LLT3	F	Pseudorabies virus (PRV) microRNA-LLT3			MIMAT0025306
prv-miR-LLT6	F	Pseudorabies virus (PRV) microRNA-LLT6			MIMAT0025309
PSIP1	F	PC4 and SFRS1 interacting protein 1	11168		
Psma4	2	proteasome (prosome, macropain) subunit, alpha type 4		26441	
Psmb3	2	proteasome (prosome, macropain) subunit, beta type 3		26446	

Psmd10	2	proteasome (prosome, macropain) 26S subunit, non-ATPase, 10		53380	
PTGER2	3, B	prostaglandin E receptor 2	5732		
Ptpn5	2	protein tyrosine phosphatase, non-receptor type 5		19259	
Pygl	2	liver glycogen phosphorylase		110095	
Pzp	2	pregnancy zone protein		11287	
Rab5b	2	RAB5B, member RAS oncogene family		19344	
Rai12	2	retinoic acid induced 12		54351	
Rangrf	2	RAN guanine nucleotide release factor		57785	
Rassf4	2	Ras association (RalGDS/AF-6) domain family member 4		213391	
Rbm12b	2	RNA binding motif protein 12B		72397	
RBM26	F	RNA binding motif protein 26	64062		
Rbm4b	2	RNA binding motif protein 4B		66704	
Rbmxrt	2	RNA binding motif protein, X chromosome retrogene		19656	
Rbp2	2	retinol binding protein 2, cellular		19660	
Rbp4	2	retinol binding protein 4, plasma		19662	
Rbpj	2	recombination signal binding protein for immunoglobulin kappa J region		19664	
Rdh7	2	retinol dehydrogenase 7		54150	
Retnla	2	resistin like alpha		57262	

Rgs2	2	regulator of G-protein signaling 2		19735	
Rhox4f	2	reproductive homeobox 4F		636177	
Rhox4g	2	reproductive homeobox 4G		664608	
Rilpl2	2	Rab interacting lysosomal protein-like 2		80291	
rlcv-miR-rL1-14-5p	F	Rhesus lymphocryptovirus microRNA-rL1-14			MIMAT0003444
rlcv-miR-rL1-17-3p	F	Rhesus lymphocryptovirus microRNA-rL1-17			MIMAT0014064
rlcv-miR-rL1-17-5p	F	Rhesus lymphocryptovirus microRNA-rL1-17			MIMAT0019185
rlcv-miR-rL1-29-3p	F	Rhesus lymphocryptovirus microRNA-rL1-29			MIMAT0016953
Rnase4	2	ribonuclease, RNase A family 4		58809	
RNF6	F	ring finger protein 6	6049		
Rnps1	2	ribonucleic acid binding protein S1		19826	
Rnu3a	2	U3A small nuclear RNA		19850	
Rpl18a	2	ribosomal protein L18A		76808	
Rpl21	2	ribosomal protein L21	6144	19933	
Rps24	2	ribosomal protein S24		20088	
Rps25	2	ribosomal protein S25		75617	
Rps27l	2	ribosomal protein S27-like		67941	
Rsph3a	2	radial spoke 3A homolog (Chlamydomonas)		66832	
Rwdd1	2	RWD domain containing 1		66521	
RYR2	3, B	ryanodine receptor 2	6262		
S100a4	2	S100 calcium binding protein A4		20198	

S100a6	2	S100 calcium binding protein A6 (calcyclin)		20200	
S100a8	2	S100 calcium binding protein A8 (calgranulin A)		20201	
S100a9/ S100A9	1, 2, 3, B, D	S100 calcium binding protein A9	6280	20202	
S100B	3, B	S100 calcium binding protein B	6285		
S1pr1	2	sphingosine-1-phosphate receptor 1		13609	
Samhd1	2	SAM domain and HD domain, 1		56045	
Scd1	2	stearoyl-Coenzyme A desaturase 1		20249	
SCGB3A2	F	secretoglobin family 3A member 2	117156		
Sco2	2	SCO cytochrome oxidase deficient homolog 2 (yeast)		100126824	
SELE	3, B, F	selectin E	6401		
SELENBP	3, B, F	SELENBP1; selenium binding protein 1	8991		
Sell	2	selectin, lymphocyte		20343	
SELL	3, B, D	selectin L	6402		
SELP	1, 3, B, D	selectin P	6403		
Serpina1a	2	serine (or cysteine) peptidase inhibitor, clade A, member 1A	5265	20700	
Serpina1b	2	serine (or cysteine) preptidase inhibitor, clade A, member 1B		20701	
Serpina1c	2	serine (or cysteine) peptidase inhibitor, clade A, member 1C		20702	
Serpina1d	2	serine (or cysteine) peptidase inhibitor, clade A, member 1D		20703	
Serpina3i	2	serine (or cysteine) peptidase inhibitor, clade A, member 3I		628900	
Serpina3k	2	serine (or cysteine) peptidase inhibitor, clade A, member 3K		20714	

Serpinb9f	2	serine (or cysteine) peptidase inhibitor, clade B, member 9f		20709	
Serpinc1	2	serine (or cysteine) peptidase inhibitor, clade C (antithrombin), member 1		11905	
Serping1	2	serine (or cysteine) peptidase inhibitor, clade G, member 1		12258	
SELPLG	F	selectin P-ligand	6404		
Sesn3	2	sestrin 3		75747	
Set	2	SET translocation		56086	
Sf3b5	2	splicing factor 3b, subunit 5		66125	
Sfn	2	Stratifin		55948	
Sfpi1	2	SFFV proviral integration 1		20375	
Shc1	2	src homology 2 domain-containing transforming protein C1		20416	
Siglece	2	sialic acid binding Ig-like lectin E		83382	
SIRPA	3, B, F	signal regulatory protein alpha	140885		
Slc9a5	2	solute carrier family 9 (sodium/hydrogen exchanger), member 5		277973	
Slfn1	2	schlafen 1		20555	
Slfn2	2	schlafen 2		20556	
SMC5	F	structural maintenance of chromosomes 5	23137		
Sms	2	spermine synthase		20603	
Snora28	2	small nucleolar RNA, H/ACA box 28		100316932	
Snora41	2	small nucleolar RNA, H/ACA box 41		100217464	
Snora73a	2	small nucleolar RNA, H/ACA box 73a		100306944	
Snora73b	2	small nucleolar RNA, H/ACA box 73b		100306945	

Snord104	2	small nucleolar RNA, C/D box 104		100216537	
Snord35b	2	small nucleolar RNA, C/D box 35B		27212	
Snrpd3	2	small nuclear ribonucleoprotein D3		67332	
Snx20	2	sorting nexin 20		71607	
SOD1	3, B	superoxide dismutase 1	6647		
Spib	2	Spi-B transcription factor (Spi-1/PU.1 related)		272382	
Spic	2	Spi-C transcription factor (Spi-1/PU.1 related)		20728	
Srrm2	2	serine/arginine repetitive matrix 2		75956	
SRSF2IP	F	serine/arginine-rich splicing factor 2, interacting protein	9169		
Srsf3	2	serine/arginine-rich splicing factor 3		20383	
Ssxb1	2	synovial sarcoma, X member B, breakpoint 1		67985	
St3gal6	2	ST3 beta-galactoside alpha-2,3-sialyltransferase 6		54613	
Stap1	2	signal transducing adaptor family member 1		56792	
Stard6	2	StAR-related lipid transfer (START) domain containing 6		170461	
Stfa2l1	2	stefin A2 like 1		268885	
Taar7a	2	trace amine-associated receptor 7A		215856	
Tbc1d22b	2	TBC1 domain family, member 22B		381085	
Tbc1d8b	2	TBC1 domain family, member 8B		245638	
Tcrd-C	2	T-cell receptor delta, constant region		100123473	
Tcrg-C4	2	T-cell receptor gamma, constant 4		107576	

Tfam	2	transcription factor A, mitochondrial		21780	
TGFB1	3, B	transforming growth factor beta 1	7040		
TGFB2	3, B	transforming growth factor beta 2	7042		
Tgfbi	2	transforming growth factor, beta induced		21810	
Thrsp	2	thyroid hormone responsive SPOT14 homolog (Rattus)		21835	
TLR10	3, B	toll like receptor 10	81793		
Tlr13	2	toll-like receptor 13		279572	
Tlr2 / TLR2	1, 3, B, D	toll like receptor 2	7097	24088	
TLR3	3, B, F	toll like receptor 3	7098		
TLR4	3, B, F	toll like receptor 4	7099		
TLR5	3, B	toll like receptor 5	7100		
TLR8	3, B	toll like receptor 8	51311		
TLR9	3, B	toll like receptor 9	54106		
Tmem159	2	transmembrane protein 159		233806	
Tmx2	2	thioredoxin-related transmembrane protein 2		66958	
TNFRSF1B	3, B, F	TNF receptor superfamily member 1B	7133		
TNFSF10	3, B, F	TNF superfamily member 10	8743		
TNFSF11	3, B	TNF superfamily member 11	8600		
TNFSF14	3, B	TNF superfamily member 14	8740		
Trac	2	T cell receptor alpha constant		100101484	
Traj49	2	T cell receptor alpha joining 49		100124339	
Trappc2	2	trafficking protein particle complex 2		66226	
Trav13-3	2	T cell receptor alpha variable region 13-3		432910	
Trbv4	2	T cell receptor beta, variable 10 (variable 4)		100124660	
Trdj1	2	T cell receptor delta joining 1		100115376	

Trdv4	2	T cell receptor delta variable 4		100114901	
Trf	2	transferrin		22041	
Trgj4	2	T cell receptor gamma joining 4		100126434	
Trim12	2	tripartite motif-containing 12		76681	
Trim34	2	tripartite motif-containing 34		94094	
Trim59	2	tripartite motif-containing 59		66949	
Try10	2	trypsin 10		436522	
Tsnax	2	translin-associated factor X		53424	
Ttr	2	transthyretin		22139	
Tyms	2	thymidylate synthase		22171	
U2af1	2	U2 small nuclear ribonucleoprotein auxiliary factor (U2AF) 1		108121	
Ube2n	2	ubiquitin-conjugating enzyme E2N		93765	
Ublcp1	2	ubiquitin-like domain containing CTD phosphatase 1		79560	
Uevld	2	UEV and lactate/malate dehyrogenase domains		54122	
Ugt1a2	2	UDP glucuronosyltransferase 1 family, polypeptide A2		22236	
Ugt1a5	2	UDP glucuronosyltransferase 1 family, polypeptide A5		394433	
Ugt1a6b	2	UDP glucuronosyltransferase 1 family, polypeptide A6B		394435	
Ugt2a2	2	UDP glucuronosyltransferase 2 family, polypeptide A2		552899	

Ugt2b36	2	UDP glucuronosyltransferase 2 family, polypeptide B36		231396	
Ugt2b5	2	UDP glucuronosyltransferase 2 family, polypeptide B5		22238	
UTRN	F	utropin	7402		
VAMP3	3, B	vesicle associated membrane protein 3	9341		
VAMP5	3, B, F	vesicle associated membrane protein 5	10791		
VAMP7	3, B	vesicle associated membrane protein 7	6845		
VAMP8	3, B	vesicle associated membrane protein 8	8673		
Vaultrc5	2	vault RNA component 5		378472	
VCAM1	3, B, F	vascular cell adhesion molecule 1	7412		
VEGFA	1, 3, B, F	vascular endothelial growth factor A	7422		
VEGFB	1, 3, B, F	vascular endothelial growth factor B	7423		
VEGFC	3, B, F	vascular endothelial growth factor C	7424		
VIP	3, B, F	vasoactive intestinal peptide	7432		
Vmn1r175	2	vomeronasal 1 receptor 175		622222	
Vmn1r196	2	vomeronasal 1 receptor 196		100312484	
Vmn1r213	2	vomeronasal 1 receptor 213		171249	
Vmn2r12	2	vomeronasal 2, receptor 12		627569	
Vmn2r66	2	vomeronasal 2, receptor 66		233437	
Vmn2r69	2	vomeronasal 2, receptor 69		330581	
Vmn2r84	2	vomeronasal 2, receptor 84		625068	
Vtn	2	vitronectin	7448	22370	
Wdr53	2	WD repeat domain 53		68980	

X76971	2	cDNA sequence X76971		634322	
ZC3H13	F	zinc finger CCCH-type containing 13	23091		
Zc4h2	2	zinc finger, C4H2 domain containing		245522	
Zcchc17	2	zinc finger, CCHC domain containing 17		619605	
Zcwpw2	2	zinc finger, CW type with PWWP domain 2		100039681	
Zfp422	2	zinc finger protein 422		67255	
Zfp456	2	zinc finger protein 456		408065	
Zfp580	2	zinc finger protein 580		68992	
Zfp59	2	zinc finger protein 59		22717	
Zfp617	2	zinc finger protein 617		170938	
Zfp787	2	zinc finger protein 787		67109	
Zfp825	2	zinc finger protein 825		235956	
Zfp882	2	zinc finger protein 882		382019	
Znrd1	2	zinc ribbon domain containing, 1		66136	
Zswim1	2	zinc finger, SWIM domain containing 1		71971	

APPENDIX B: PLATELET RNA TRANSFER TO CELLS IN *IN VITRO* MODELING SYSTEMS

Permissions

Appendix B contains unpublished data from the Freedman Lab. Figure B.1 and corresponding results taken from unpublished manuscript, without permission required.

- *"Platelet activation and miRNA transfer in the regulation of vascular homeostasis"* Lauren Clancy, Antonina Risitano, Kahraman Tanriverdi, David D. McManus, Jesse W. Rowley, Andrew S. Weyrich, Olga Vitseva, Lea M. Beaulieu, Jeffrey J. Rade and Jane E. Freedman

Author Contributions

A.R. designed and performed experiments, analyzed data, and wrote the manuscript; K.T. designed and performed experiments, analyzed data; D.D.M. and J.J.R. provided the clinical samples and related analysis; J.W.R. performed mouse studies and analyzed data; O.V. and L.C. performed experiments; L.M.B. participated in the design of the adhesion experiment; J.E.F. and A.S.W. designed experiments and edited the manuscript.

Summary

As first described by Risitano et al. and later confirmed by several other labs, platelets are capable of transfer of RNAs to other vascular cells (both mRNAs and miRNAs) with functional consequences on the recipient cells (114, 120-125). Initial studies during this project focused on evaluating the transfer of RNAs from platelets to vascular cells under various stimulatory conditions. Results are included here as the relevance of platelet RNA transfer to the overall phenomenon of platelet RNA communication with vascular cells is evident from our experiments; platelet RNA transfer to cells and RNA uptake from cells work in tandem to create a bidirectional transfer system, the impact of which on vascular health will be determined with further study.

Materials and Methods

Figure B.1

Washed platelets were incubated with 10 μM calcein AM (Life Technologies) for 15 min then resuspended and washed in HBSS (Life Technologies). Subsequently, platelets were stimulated with 0.5U/mL thrombin for 10 minutes. HUVECs were previously cultured on tissue culture treated-glass slides and transfected (using Lipofectamine RNAiMAX technology, according to manufacturer's protocol) with miR-27a-3p mimic, miR-27a-3p inhibitor and relative negative controls (scrambled sequences) without any fluorescent labeling

(Life Technologies). Using a vacuum-based cell adhesion flow chamber (Immunetics, Boston, MA) platelets were passed at a constant rate, for 20 minutes, over HUVECs (24 hours post transfection) pretreated with 0.5U/mL thrombin for 10 minutes as previously described (223). Slides were then analyzed by examined by confocal microscopy (Leica Microsystems and Leica Confocal Software, Exton, PA) and fluorescence quantification was performed by using ImageJ (224). Experimental design mimics that of flow adhesion experiment described in Chapter 3 Materials and Methods, "*Fluorescent RNA transfer in flow adhesion model"* and depicted in Figure 3.12.

Table B.1

Results from Table B.1 match those described in Table 3.4, with methods fully described in Chapter 3, Materials and Methods, "*In Vitro Simulated Clot Experiments".* While Table 3.4 represents platelet fraction results, Table B.1 represents HUVEC fraction results. Some of this data is presented in Table G.1 as well. Full data recorded here to show transcripts of interest for platelet RNA transfer to cells.

Results

Activated endothelial cells internalize platelets under minimal flow conditions

Figure B.1 depicts the transfer of calcein-AM from platelets to HUVECs under flow conditions. In support of previous studies showing platelet binding and internalization of platelets by activated HUVECs, the platelet-derived fluorescence signal is both contained within the HUVEC cells (platelet internalization) and expressed on the cell surface (brighter signals) with as little as 20 minutes exposure. Additionally, during these experiments we investigated the role miR-27a may have on this internalization, as it can regulate vWF expression. HUVECs transfected with miR-27a displayed less fluorescence signal (corresponding to decreased vWF and thus decreased platelet adhesion) compared to control (image quantification showed a 10% decrease). Conversely, the opposite effect is seen with miR-27a inhibitor transfection; miR-27a inhibitor transfection results increased fluorescence expression (15% as compared to controls, corresponding to decreased endogenous miR-27a, increased vWF expression, increased platelet adhesion and thus increased platelet internalization). This supports the internalization of platelets and thus platelet content by endothelial cells, even under the minimal conditions of the flow adhesion model.

Figure B.1: Platelet internalization by endothelial cells. HUVEC-platelet adhesion assay was examined by confocal microscopy. (A) Unlabeled platelets and HUVECs. Scale bar denotes 5 µm for platelets (100X magnification) and 10 µm for HUVECs (40X magnification). (B) HUVECs were transfected with miR-27a mimic, miR-27a inhibitor and related negative controls. Fluorescence, derived from calcein-labeled platelets, is present in the endothelial cytosol and on the cell surface (small brighter dots). Differences in fluorescence intensity and localization are highlighted in the insets. Inset represents magnified region outlined by the yellow box in each image. Scale bar denotes 20 µm; 20X magnification. DIC (Differential Interference Contrast).

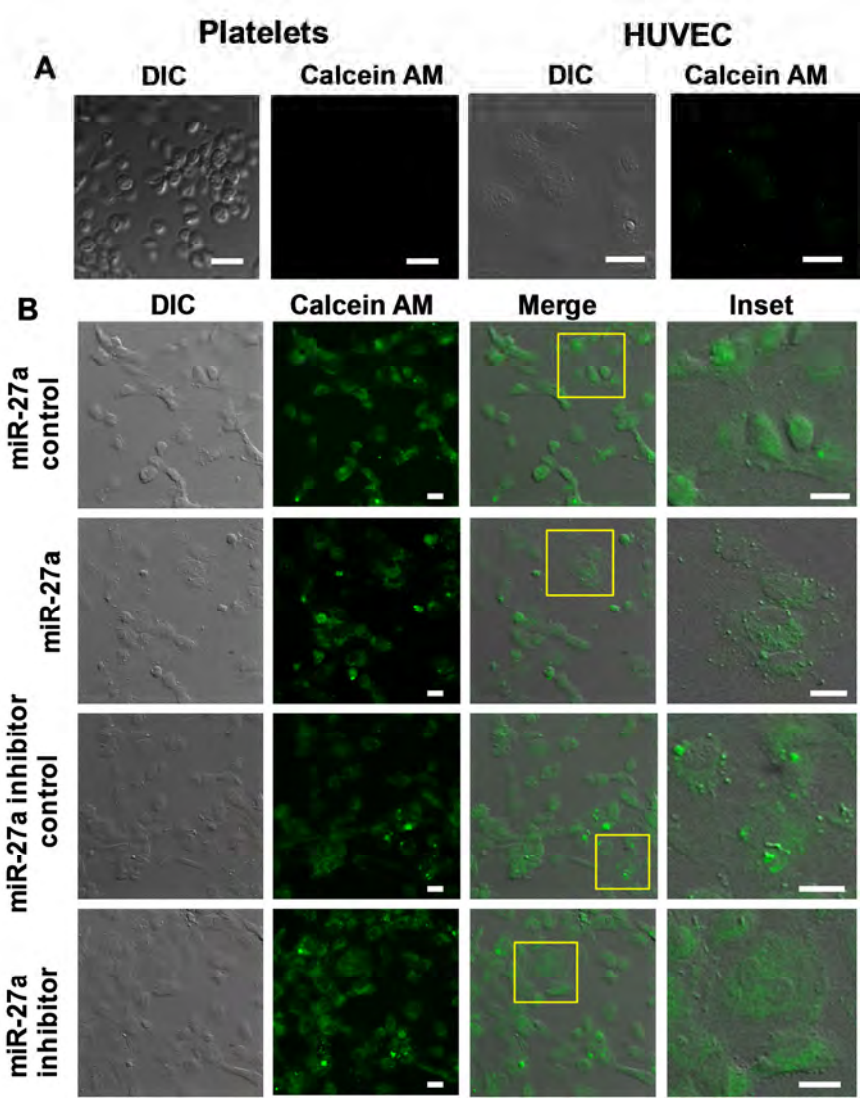

Differential expression of HUVECs post platelet co-incubation suggests transfer of numerous platelet-specific transcripts

Additional studies focused on expression changes in HUVECs post co-incubation with isolated human platelets. We hoped to replicate the results seen by Risitano et al. (114) using human platelets instead of platelet-like particles (PLP) to better estimate the actual transcript changes that may occur *in vivo*. We hypothesized that by evaluating the HUVEC transcriptome post incubation, we could determine a transferred RNA transcriptome as well as correlated the outcomes of this analysis to our expected (but not actual) results from the platelet subpopulations studies. As can be seen, a number of transcript levels changed within HUVECs, though whether this change is stimulation, transcription or platelet dependent seems to be transcript specific (Table B.1). A number of platelet specific markers, particularly CD40LG, P-selectin and GP1BB, transcripts all show increases in HUVEC post incubation, suggesting they correlate to platelet internalization and/or platelet RNA transfer. Other transcript changes will require additional analysis to determine if differential expression is due to platelet RNA transfer, platelet signaling or HUVEC stimulation and mRNA processing.

Table B.1: RT-qPCR results for transcript panel in endothelial cells (HUVECs) post incubation with platelets. Expression fold changes with or without stimulation under normal *in vitro* simulated clot conditions (A) or with pretreatment transcription shutdown in HUVECs through α-amanitin treatment (B). RT-qPCR results were normalized to two housekeeping genes (*CD63* and *CD81*) with HUVEC alone samples set as experimental controls. Red (fold increase) and blue (fold decrease) text coloring denote expression fold changes of interest. Gray color coding denotes $P < 0.05$ (based on a Student's t-test of the replicate $2^{(-\Delta\Delta Ct)}$ values for each gene in the control group and treatment groups) for given value. Legend below table describes sample setup conditions. A) Results represent n=6 experiments. B) Results represent n=3 experiments. (Excerpt of these results presented in Table G.1).

A)	HUVEC Alone	Stimulated HUVEC	Unstimulated HUVEC Post Platelet Incubation	Stimulated HUVEC Post Stimulated Platelet Incubation
ACTB	1	-1.0197	-1.1212	-1.9716
AGO2 (EIF2C2)	1	1.1905	1.1047	1.0765
ASGR1	1	1.2464	-3.0331	-2.3947
B2M	1	1.3725	1.4952	1.6958
BCL2L1	1	-1.0404	1.2447	1.232
CALR	1	-1.015	1.3629	1.3086
CCL17	1	3.2299	-7.3957	-1.4694
CCL3	1	1.0474	30.8217	3.7429
CCL7	1	1.3247	3.0455	2.0097
CD163	1	1.051	1.7062	20.9007
CD209	1	-11.1748	-6.8835	-3.9354
CD3D	1	1.051	1.7062	20.9052
CD40	1	1.1062	1.0383	-1.0744
CD40 LG	1	1.051	1294.6002	**3982.1746**
CD44	1	1.125	1.3539	1.3331
CD53	1	3.0556	**687.6608**	**294.7269**
CD63	1	1.0328	-1.1215	-1.0987
CD81	1	-1.0376	1.1302	1.0993
CD86	1	1.051	4.5961	7.2588
COL18A1	1	1.0427	1.0897	1.3692
COPA	1	1.0924	1.1592	1.2424
CRLS1	1	1.2782	1.1733	1.7428
CRP	1	-1.7252	1.4299	-1.4451
CX3CL1	1	2.5058	2.8626	**5.7266**

CXADR	1	-1.0386	1.0371	1.0066
CXCL1	1	2.1938	8.1581	**17.9698**
CXCL12	1	1.0574	1.7565	2.2814
CXCL2	1	3.7931	6.2366	15.2343
CXCL5	1	1.5499	9.3657	12.9536
CXCL6	1	1.3018	1.8489	3.5899
DICER1	1	-1.1446	1.2915	1.2637
EIF4G1	1	1.1357	1.1905	1.4735
ESAM	1	1.0665	1.1928	1.375
FCN1	1	1.051	**257.2454**	**695.6924**
FOLR1	1	-3.0728	1.3772	-1.0822
GAPDH	1	1.1302	1.2328	1.0563
GP1BB	1	1.0084	**5.0267**	**5.8862**
GPI	1	1.2527	1.0458	1.0492
ICAM1	1	2.4041	3.6179	4.7408
IFITM1	1	-1.1026	-1.1117	-1.0702
IFITM2	1	1.0671	1.3826	1.4347
IFITM3	1	1.1664	1.3856	1.8656
IFNA1	1	1.7806	8.8671	2.7534
IFNB1	1	19.6171	2.3913	13.4521
IL10RA	1	-5.7981	4.4697	-1.6584
IL1beta	1	5.0559	17.4412	11.3618
IL2RB	1	-1.3447	1.219	-1.8047
IL5	1	3.1173	5.1137	9.4402
IL6	1	1.2691	1.4082	2.3907
IL8	1	2.7746	9.616	**31.6084**
ITGA5	1	1.2111	1.3443	1.2841
ITGAE	1	1.0396	-1.5128	11.9228
ITGAL	1	2.6059	**870.3528**	33.2699
ITGAM	1	20.2988	1.8959	15.342
ITGB7	1	12.0804	30.4259	18.1557
KIAA0232	1	-1.1015	1.3689	1.5487
KIAA1462	1	1.1502	1.0647	1.0484
LAMP1	1	-1.0388	1.1552	1.096
LCK	1	1.0723	1.3752	-1.0161

LSP1	1	-1.8727	1.5483	3.0581
MAP4K4	1	1.1246	1.1753	1.4094
MMP9	1	40.6716	5.0022	59.1372
NFKB1	1	1.4177	2.0767	**3.1231**
NFKBIA	1	1.6223	4.9257	7.3516
PTGER2	1	-3.3581	1.3479	4.4997
RYR2	1	1.051	1.7062	2.9843
S100A9	1	3.1385	**12654.4663**	**10065.3338**
S100B	1	1.051	6.4433	87.9429
SELE	1	7.354	18.4109	79.2161
SELENBP	1	-1.091	-1.0949	-2.5136
SELL	1	-1.0773	1.3056	-2.3351
SELP	1	-1.6584	2.5553	3.4953
SIRPA	1	-1.0739	1.3652	1.4739
SOD1	1	-1.035	-1.0232	1.0911
TGFB1	1	1.0551	1.1409	1.0724
TGFB2	1	1.2953	1.5799	2.9009
TLR10	1	1.1747	11.6058	2.8717
TLR2	1	2.9938	2.6005	4.5655
TLR3	1	-1.0572	1.2253	1.425
TLR4	1	-1.0331	1.529	1.6517
TLR5	1	-3.4312	1.2714	-3.2776
TLR8	1	1.051	1.7062	2.9843
TLR9	1	-1.1329	-1.0233	1.2283
TNFRSF1B	1	1.07	1.0277	-2.5518
TNFSF10	1	-1.0035	1.0125	1.0334
TNFSF11	1	-1.4623	-4.693	-4.3661
TNFSF14	1	10.4429	1.7062	2.9843
VAMP3	1	1.0685	1.2486	1.4327
VAMP5	1	1.0032	-1.0534	1.2575
VAMP7	1	-1.0063	1.3657	1.4073
VAMP8	1	1.0622	1.1836	1.4206
VCAM1	1	4.4064	4.1857	9.4458
VEGFA	1	1.1718	**2.2279**	4.5597
VEGFB	1	-1.0576	1.1582	1.5174

VEGFC	1	1.3295	1.5213	1.8612
VIP	1	1.1269	1.3431	2.0989

Platelets	+	+	+	+
Platelet Thrombin Stimulation	-	+	-	+
EC Incubation	-	-	+	+
EC Transcription Shutdown	-	-	-	-
EC Thrombin Stimulation	-	-	-	+

B)

	HUVEC Alone	**Stimulated HUVEC**	**Unstimulated HUVEC Post Platelet Incubation**	**Stimulated HUVEC Post Stimulated Platelet Incubation**
ACTB	1	1.0601	-1.0761	-1.1877
AGO2 (EIF2C2)	1	-1.8677	1.3052	-1.1039
ASGR1	1	-1.0636	1.3645	-6.2191
B2M	1	-1.0687	2.1331	**1.8035**
BCL2L1	1	-1.4957	-1.046	-1.0518
CALR	1	-1.0767	1.179	1.2753
CCL17	1	-1.0237	12.0984	-4.9572
CCL3	1	-1.0228	17.0442	20.6187
CCL7	1	1.1608	1.0418	1.4125
CD163	1	-1.0228	9.5561	2.7164
CD209	1	-1.0228	1.4033	2.7164
CD3D	1	-1.0228	15.3252	27.6313
CD40	1	-1.3567	1.4593	-1.153
CD40 LG	1	-1.0228	5203.3792	676.4863
CD44	1	-1.2037	1.1235	1.2676
CD53	1	-1.0228	**820.8875**	373.8394
CD63	1	-1.2268	1.0035	-1.0599

CD81	1	1.2528	1.0004	1.0713
CD86	1	-1.0228	1.4033	2.7164
COL18A1	1	-1.1222	-1.053	1.1865
COPA	1	-1.1403	1.0528	1.0569
CRLS1	1	-1.0756	1.3501	1.4385
CRP	1	-202.9364	1.6739	-4.9166
CX3CL1	1	-1.4493	1.9653	-1.1286
CXADR	1	-1.3386	-1.2674	-1.0872
CXCL1	1	-2.7425	1.3297	1.5869
CXCL12	1	**-1.7275**	1.1325	-1.1062
CXCL2	1	-4.5639	-2.1235	1.3596
CXCL5	1	-1.2027	7.3623	5.1308
CXCL6	1	-1.0155	1.9935	1.539
DICER1	1	-1.6335	-1.0973	-1.0908
EIF4G1	1	-1.1511	1.0719	1.0521
ESAM	1	-1.1375	-1.0072	1.4959
FCN1	1	-1.0228	198.4575	2.7164
FOLR1	1	-10.6667	-1.018	1.9223
GAPDH	1	-1.059	1.193	1.2349
GP1BB	1	1.123	13.1186	5.6573
GPI	1	1.047	1.2925	1.155
ICAM1	1	-1.5669	1.3233	-1.0825
IFITM1	1	-2.7425	-1.3877	-1.1973
IFITM2	1	1.0622	1.3719	1.4613
IFITM3	1	-1.0297	**1.1681**	1.5931
IFNA1	1	1.2254	4.0384	3.9678
IFNB1	1	-1.0288	-4.368	-2.7301
IL10RA	1	-5.5681	8.2393	15.168
IL1beta	1	12.5778	630.6641	64.3389
IL2RB	1	14.3397	13.7984	2.015
IL5	1	7.4622	13.32	2.7164
IL6	1	-3.1481	-2.9711	1.2978
IL8	1	-1.4783	1.2414	3.0918
ITGA5	1	-1.2034	1.2942	1.2867
ITGAE	1	-1.0857	1.3575	2.4742

ITGAL	1	-1.0228	1752.9844	500.4801
ITGAM	1	-9.7967	1.6048	4.6438
ITGB7	1	4.073	1.5264	4.4965
KIAA0232	1	**-2.8643**	-1.6315	-1.5547
KIAA1462	1	-1.8408	-1.3315	-1.5228
LAMP1	1	-1.2422	-1.0302	1.2044
LCK	1	-1.4037	-3.5985	-1.7437
LSP1	1	-1.3964	**4.3528**	**3.6542**
MAP4K4	1	-1.2553	-1.0763	1.1067
MMP9	1	10.6261	1.4359	3.9312
NFKB1	1	-1.4657	1.2878	1.207
NFKBIA	1	-4.5694	-1.4427	-1.0459
PTGER2	1	-1.0228	11.0449	228.6747
RYR2	1	-1.0228	1.4033	2.7164
S100A9	1	-1.0228	**18042.0499**	19563.48
S100B	1	-1.0228	13.9873	272.7551
SELE	1	-2.6831	2.3852	2.4984
SELENBP	1	-1.1724	-1.0319	-1.008
SELL	1	-1.285	1.1707	1.1727
SELP	1	-1.3416	**4.338**	3.7433
SIRPA	1	-1.2221	-1.0044	1.0852
SOD1	1	-1.1247	-1.0368	1.4196
TGFB1	1	-1.0227	1.0645	-1.0265
TGFB2	1	-1.384	1.1537	1.4572
TLR10	1	1.0248	5.8247	4.2836
TLR2	1	-1.6044	1.3143	-5.8816
TLR3	1	-1.2187	1.3126	1.4144
TLR4	1	-1.8745	-1.151	-1.0423
TLR5	1	1.4175	1.3366	-2.9435
TLR8	1	-1.0228	1.4033	2.7164
TLR9	1	1.0965	1.7337	1.7259
TNFRSF1B	1	-1.0581	-1.0884	-1.2453
TNFSF10	1	-2.0334	-1.6254	-1.4332
TNFSF11	1	-9.3157	-1.0271	-2.5552
TNFSF14	1	10.8385	1.4033	39.895

VAMP3	1	-1.0844	1.2268	1.2652
VAMP5	1	1.0059	-1.0016	1.062
VAMP7	1	-1.1488	1.166	1.1997
VAMP8	1	-1.0432	1.1835	1.1849
VCAM1	1	-2.666	1.3689	-1.1246
VEGFA	1	-2.0494	-1.3374	1.0987
VEGFB	1	-1.068	1.2741	1.4029
VEGFC	1	-1.1601	1.2458	1.2944
VIP	1	-1.1167	1.2831	2.3546

Platelets	+	+	+	+
Platelet Thrombin Stimulation	-	+	-	+
EC Incubation	-	-	+	+
EC Transcription Shutdown	-	-	-	-
EC Thrombin Stimulation	-	-	-	+

APPENDIX C: PLATELET SUBPOPULATION TRANSCRIPTOME RESULTS

Permissions

Appendix C references a table excerpt from a published manuscript, included with permission:

- *Clancy L, Beaulieu LM, Tanriverdi K, Freedman JE. (2017).The role of RNA uptake in platelet heterogeneity. Thromb Haemost, 117(5), 948-961*
    - Permission Information: Copyright Permission No 116/06/2017

Author Contributions

L.C. performed all experiments and analyses unless noted below. L.C. wrote manuscript. J.E.F. oversaw overall project development and coordination. L.M.B performed initial platelet sorting experiments. K.T. performed high throughput gene expression analyses. All authors commented on the interpretation of results, and reviewed and approved the manuscript.

File Information

Cuffdiff expression analysis results of sequencing data for large (Ot7226) versus small (Ot7227) platelets.

File available online at www.thrombosis-online.com

(TH117.5_Clancy_Suppl_Table1)

APPENDIX D: ADDITIONAL STATISTICAL ANALYSES

Post publication, it was suggested that a number of figures from the published manuscript cited in Chapter 3 ("The role of RNA uptake in platelet heterogeneity") should be re-evaluated with non-parametric statistical tests due to non-Gaussian distributions. As these results were already published, the figures and statistics were not altered in the original chapter of this dissertation; however, for clarity, additional statistical tests are included here. It is worth noting that for several studies, non-parametric testing will not accurately determine significance due to sample size.

- Figure 3.2 and Table 3.1: Statistical analyses were performed within DAVID program and therefore not reanalyzed here.
- Figure 3.3:
    - Original Test: Unpaired parametric two-tailed t-test
    - Additional Test: Unpaired Mann-Whitney test
    - Results:

Gene	Original Statistical Results	Additional Statistical Results
ACTB	****p<0.0001	*p=0.0286
B2M	***p=0.0009	*p=0.0286
GAPDH	***p=0.0005	*p=0.0286
BCL2L1	**p=0.0056	*p=0.0286
PF4	**p=0.0012	*p=0.0286
CD40	****p<0.0001	*p=0.0286
SELP	**p=0.0030	*p=0.0286
GUK1	p=0.3012	p=0.4857
LSP1	p=0.2521	p=0.3714
NFKBIA	p=0.1348	p=0.4286
SELL	p=0.3084	p=0.4286

- Figure 3.5:
    - Original Test: Unpaired parametric two-tailed t-test
    - Additional Test: Unpaired Mann-Whitney test
    - Results:

Gene	Original Statistical Results	Additional Statistical Results
Actb	n/a	p>0.9999
Il1b	p=0.0131	p=0.1000
S100a9	p=0.0040	p=0.1000
Tlr2	p=0.0345	p=0.1000
Icam1	p=0.0441	p=0.1000
Nfkbia	P=0.0111	p=0.1000

- Figure 3.6:
    - Original Test: Unpaired parametric ordinary one-way ANOVA
    - Additional Test: Unpaired, non-parametric Kruskal-Wallis test, Dunn's follow up
    - Results

Original Statistical Results	Additional Statistical Results
p=0.0226	p=0.2526

    - Additional Note: Use of a different housekeeping gene (ACTB) for RT-qPCR calculations results in significant findings regardless of statistical method.

Housekeeping Gene	Original Statistical Results	Additional Statistical Results
Actb	p=0.0047	p=0.0361

Actb and *Gapdh* Combined	p=0.0045	p=0.0268

- Figure 3.7:
  - Original Test: Unpaired parametric t test
  - Additional Test: Unpaired, non-parametric Mann-Whitney test
  - Results:

Data Results	Original Statistical Results	Additional Statistical Results
% Events in Platelet Population	p=0.3103	p=0.2857
% CD41+	p=0.8196	p>0.9999
Geometric Mean	p=0.0227	p=0.0556

- Table 3.4: Statistical analyses were performed within the RT^2 Profiler PCR Array Data Analysis tool version 3.5 and therefore not reanalyzed here.

- Figure 3.8:
  - Original Test: Unpaired parametric two-tailed t-test
  - Additional Test: Unpaired non-parametric Mann-Whitney test
  - Results:

Original Statistical Results	Additional Statistical Results
p<0.0001	p=0.1000

- Figure 3.9:
  - Original Test: Parametric ordinary one-way ANOVA

- Additional Test: Unpaired nonparametric Kruskal Wallis with Dunn's follow up
- Results:

	Original Statistical Results	Additional Statistical Results
P value	p<0.0001	p=0.0044
Multiple Comparisons	All individual comparisons significant	All individual comparisons non-significant

- Figure 3.10:
  - Original Test: Multiple unpaired t-tests with discovery determined using original FDR method of Benjamini and Hochberg, Q=1%, each row individually assuming no consistent SD
  - Additional Test: Individual unpaired nonparametric, Mann-Whitney test, two-tailed
  - Results:

	Original Statistical Results	Additional Statistical Results
HUVEC	29 transcripts, p<0.005 12 transcripts, p<0.0001	All 29 transcripts still significant (p=0.0286)
THP1	19 transcripts, p<0.005 12 transcripts, p<0.0001	All 19 transcripts still significant (p=0.0286)

- Table 3.5:
  - Original results match analyses from Figure 3.10. Reanalysis of Figure 3.10 showed all targets still significant, regardless of

statistical test. Therefore no additional analysis of table 3.5 is required.

- Figure 3.13:
  - Original Test: Unpaired parametric ordinary one-way ANOVA
  - Additional Test: Unpaired nonparametric Kruskal-Wallis test with Dunn's follow up
  - Results:

	Original Statistical Results	Additional Statistical Results
p value	p=<0.0001	p=<0.001
Multiple Comparisons	Various significance but all column comparisons of interest significant	All individual comparison still significant except 10' Unstim and 10' Stim to 30' Stim

  - Additional Notes: Data set for Figure 3.13 has a sample size n=20. Though results are not parametric, this sample size should allow for accurate analysis by parametric test.

- Figure 3.15:
  - Original Test: Unpaired parametric ordinary one-way ANOVA
  - Additional Test: Unpaired nonparametric Kruskal-Wallis test with Dunn's follow up
  - Results:

	Original Statistical Results	Additional Statistical Results
p value	p<0.0001	p=0.0092

Multiple comparisons	All column comparisons significant to varying degrees	Individual column comparisons no longer significant except for one

- Figure 3.16:
  - Original Test: Unpaired parametric ordinary one-way ANOVA
  - Additional Test: Unpaired nonparametric Kruskal-Wallis test with Dunn's follow up
  - Results:

	Original Statistical Results	Additional Statistical Results
p value	p=0.0001	p=0.0102
Multiple comparisons	All column comparisons significant to final column	Not all individual column comparisons significant

- Figure 3.17:
  - Original Test: Unpaired parametric two-way ANOVA, α =0.05, with Tukey's multiple comparison follow up
  - Additional Test: Unpaired nonparametric Kruskal-Wallis test with Dunn's follow up, on each gene individually
  - Results:

	Original Statistical Results	Additional Statistical Results
p value	Interaction p=0.0005 Row Factor p<0.0001 Column Factor p<0.0001	BIM p=0.0003 BAX p=0.0001

Multiple comparisons	All control to treatment multiple comparisons significant ($p<0.01$)	Most of individual comparisons not significant

- Figure 3.1, 3.4, 3.11, 3.12, 3.14, Table 3.2, 3.3: Had no associated statistical analyses

APPENDIX E: FUNCTIONAL ANALYSIS OF PLATELET SUBPOPULATION TRANSCRIPTOMES

Permissions

Appendix E is a table excerpt from a published manuscript, included with permission:

- *Clancy L, Beaulieu LM, Tanriverdi K, Freedman JE. (2017).The role of RNA uptake in platelet heterogeneity. Thromb Haemost, 117(5), 948-961*
    - Permission Information: Copyright Permission No 116/06/2017

Author Contributions

L.C. performed all experiments and analyses unless noted below. L.C. wrote manuscript. J.E.F. oversaw overall project development and coordination. L.M.B performed initial platelet sorting experiments. K.T. performed high throughput gene expression analyses. All authors commented on the interpretation of results, and reviewed and approved the manuscript.

Table E.1: DAVID gene ontology (GO) functional analysis of small and large platelet RNA profiles. Listing of associated GO terms and Benjamini corrected *p*-values for small (A) and large (B) platelet RNA profiles. In-depth analysis of biological process (BP) results of DAVID analysis of small and large platelet RNA profiles. Italics denote common processes associated with both populations' RNA.

(A) Small Platelet RNA: DAVID Functional Annotation Chart			
Term	P-Value	Fold Enrichment	Benjamini Corrected P-value
DNA metabolic process	3.05E-05	1.55	5.77E-03
Proteolysis involved in cellular protein catabolic process	2.95E-05	1.50	5.89E-03
Modification-dependent macromolecule catabolic process	3.70E-05	1.50	6.04E-03
Modification-dependent protein catabolic process	3.70E-05	1.50	6.04E-03
tRNA metabolic process	3.40E-05	2.26	6.10E-03
Cellular protein catabolic process	3.62E-05	1.49	6.19E-03
Protein catabolic process	2.94E-05	1.49	6.20E-03
Cell cycle	*4.00E-05*	*1.42*	*6.24E-03*
ncRNA processing	4.22E-05	1.95	6.31E-03
T cell activation	4.77E-05	2.19	6.85E-03
Apoptosis	5.53E-05	1.48	7.63E-03
Programmed cell death	*6.16E-05*	*1.47*	*8.18E-03*
Cellular response to stress	9.57E-05	1.48	1.22E-02
Golgi vesicle transport	*1.03E-04*	*2.10*	*1.27E-02*
Cell death	1.18E-04	1.41	1.40E-02
Mitotic Cell Cycle	1.61E-04	1.59	1.80E-02
Death	1.57E-04	1.40	1.80E-02
Protein modification by small protein conjugation or removal	1.76E-04	1.94	1.90E-02
Ribonucleoprotein complex biogenesis	1.90E-04	1.88	2.00E-02
Chromosome organization	*2.56E-04*	*1.48*	*2.53E-02*
Organelle fission	2.50E-04	1.75	2.54E-02
Protein modification by small protein conjugation	2.84E-04	2.02	2.59E-02
Lymphocyte Apoptosis	2.81E-04	6.22	2.63E-02
Positive regulation of cell death	2.77E-04	1.51	2.66E-02

Positive regulation of programmed cell death	4.06E-04	1.50	3.59E-02
Protein amino acid acetylation	4.27E-04	2.73	3.68E-02
Leukocyte activation	4.54E-04	1.69	3.81E-02
Induction of apoptosis	4.90E-04	1.58	4.02E-02
Induction of programmed cell death	5.30E-04	1.58	4.25E-02
Positive regulation of apoptosis	5.43E-04	1.49	4.25E-02
M phase of mitotic cell cycle	5.79E-04	1.71	4.43E-02
Positive regulation of immune system process	5.92E-04	1.68	4.44E-02
Translation	6.61E-04	1.56	4.84E-02
RNA biosynthetic process	6.98E-04	1.59	5.00E-02
Protein amino acid acylation	7.29E-04	2.52	5.02E-02
B cell apoptosis	7.25E-04	8.89	5.09E-02
Chromatin organization	*8.52E-04*	*1.50*	*5.73E-02*
Histone modification	9.28E-04	1.97	5.80E-02
Ribosome biogenesis	9.28E-04	1.97	5.80E-02
Lymphocyte differentiation	9.17E-04	2.07	5.83E-02
Histone H4 acetylation	9.09E-04	4.00	5.88E-02
Transcription, DNA-dependent	8.95E-04	1.58	5.90E-02
Histone H2A acetylation	1.01E-03	5.18	6.20E-02
Regulation of cell cycle	1.13E-03	1.53	6.66E-02
rRNA processing	1.12E-03	2.13	6.70E-02
Hemopoietic or lymphoid organ development	1.19E-03	1.61	6.88E-02
Leukocyte differentiation	1.27E-03	1.90	7.24E-02
Cell cycle process	*1.34E-03*	*1.38*	*7.47E-02*
Immune system development	1.37E-03	1.58	7.53E-02
Homeostasis of number of cells	1.44E-03	2.04	7.68E-02
Mitosis	1.42E-03	1.66	7.71E-02
Nuclear division	1.42E-03	1.66	7.71E-02
Protein polyubiquitination	1.47E-03	3.42	7.72E-02
Nucleoside metabolic process	1.54E-03	2.36	7.85E-02
Covalent chromatin modification	1.52E-03	1.90	7.86E-02
B cell activation	1.58E-03	2.22	7.91E-02
Hemopoiesis	1.69E-03	1.62	8.32E-02
Cofactor metabolic process	1.83E-03	1.69	8.86E-02
rRNA metabolic process	1.97E-03	2.04	9.15E-02
B cell differentiation	1.92E-03	2.59	9.16E-02

Histone acetylation	1.92E-03	2.59	9.16E-02
RNA modification	1.92E-03	2.59	9.16E-02
Regulation of lymphocyte activation	1.95E-03	1.80	9.18E-02
Chromatin modification	2.04E-03	1.56	9.33E-02
Glycoprotein catabolic process	2.32E-03	3.95	1.04E-01
Transcription from RNA polymerase II promoter	2.56E-03	1.60	1.12E-01
Ribonucleoside monophosphate biosynthetic process	2.60E-03	3.48	1.12E-01
Lymphocyte homeostasis	2.65E-03	3.17	1.12E-01
Positive regulation of ligase activity	2.55E-03	2.19	1.13E-01
Induction of apoptosis by extracellular signals	2.95E-03	1.90	1.23E-01
Protein ubiquitination	3.11E-03	1.87	1.26E-01
Cell activation	3.10E-03	1.52	1.28E-01
Nuclear mRNA splicing, via spliceosome	3.26E-03	1.74	1.31E-01
RNA splicing, via transesterification reactions	3.26E-03	1.74	1.31E-01
RNA splicing, via transesterification reactions with bulged adenosine as nucleophile	3.26E-03	1.74	1.31E-01
I-kappaB kinase/NF-kappaB cascade	3.56E-03	2.26	1.40E-01
Amino acid activation	3.97E-03	2.51	1.53E-01
tRNA aminoacylation	3.97E-03	2.51	1.53E-01
tRNA aminoacylation for protein translation	3.97E-03	2.51	1.53E-01
DNA replication	4.05E-03	1.64	1.54E-01
Oxidoreduction coenzyme metabolic process	4.13E-03	2.39	1.56E-01
Proteasomal protein catabolic process	4.25E-03	1.92	1.56E-01
Proteasomal ubiquitin-dependent protein catabolic process	4.25E-03	1.92	1.56E-01
Attachment of GPI anchor to protein	4.21E-03	6.35	1.57E-01
Ribonucleoside monophosphate metabolic process	4.68E-03	3.20	1.69E-01

Ubiquitin-dependent protein catabolic process	*4.74E-03*	*1.54*	*1.70E-01*
Positive regulation of protein ubiquitination	5.03E-03	2.01	1.77E-01
Leukocyte homeostasis	5.11E-03	2.72	1.78E-01
Cell division	5.34E-03	1.48	1.84E-01
ER to Golgi vesicle-mediated transport	5.53E-03	2.54	1.88E-01
Immune response-regulating cell surface receptor signaling pathway	5.53E-03	2.54	1.88E-01
Lymphocyte proliferation	5.53E-03	2.54	1.88E-01
Regulation of leukocyte activation	5.76E-03	1.66	1.91E-01
Negative regulation of cellular protein metabolic process	5.73E-03	1.63	1.92E-01
Coenzyme metabolic process	6.27E-03	1.68	2.03E-01
T cell homeostasis	6.27E-03	3.39	2.04E-01
Regulation of cell activation	6.82E-03	1.63	2.16E-01
Vesicle-mediated transport	7.17E-03	1.31	2.19E-01
Regulation of protein ubiquitination	7.24E-03	1.87	2.19E-01
Erythrocyte development	7.17E-03	4.44	2.20E-01
Negative regulation of macromolecule metabolic process	7.05E-03	1.27	2.21E-01
Cell proliferation	7.13E-03	1.37	2.21E-01
Erythrocyte maturation	7.67E-03	5.56	2.28E-01
Viral reproductive process	7.85E-03	2.15	2.29E-01
Regulation of ligase activity	7.82E-03	1.98	2.30E-01
Immune response-regulating signal transduction	8.04E-03	2.22	2.30E-01
Leukocyte proliferation	8.04E-03	2.42	2.32E-01
Mononuclear cell proliferation	8.04E-03	2.42	2.32E-01
tRNA processing	9.41E-03	1.99	2.60E-01
Immune response-activating cell surface receptor signaling pathway	9.37E-03	2.51	2.61E-01
Positive regulation of ubiquitin-protein ligase activity	9.94E-03	2.03	2.71E-01
Negative regulation of protein metabolic process	1.01E-02	1.57	2.71E-01
DNA repair	1.09E-02	1.44	2.89E-01

Immune response-activating signal transduction	1.12E-02	2.22	2.93E-01
T cell differentiation	1.20E-02	2.05	3.07E-01
Regulation of protein binding	1.24E-02	2.76	3.14E-01
Activation of caspase activity by cytochrome c	1.26E-02	4.94	3.14E-01
Negative regulation of protein modification process	1.27E-02	1.72	3.15E-01
Heterocycle biosynthetic process	1.25E-02	2.11	3.15E-01
RNA polyadenylation	1.50E-02	3.81	3.54E-01
Neuron apoptosis	1.49E-02	3.27	3.56E-01
Negative regulation of macromolecule biosynthetic process	1.57E-02	1.28	3.67E-01
Negative regulation of protein ubiquitination	1.64E-02	1.92	3.75E-01
M phase	1.63E-02	1.38	3.75E-01
Regulation of cell death	1.72E-02	1.22	3.84E-01
Nucleotide-excision repair	1.74E-02	2.10	3.85E-01
Chromosome segregation	1.71E-02	1.87	3.85E-01
Positive regulation of ubiquitin-protein ligase activity during mitotic cell cycle	1.76E-02	1.96	3.86E-01
Erythrocyte differentiation	1.87E-02	2.27	4.02E-01
Positive regulation of endothelial cell proliferation	2.04E-02	3.56	4.21E-01
Regulation of programmed cell death	2.04E-02	1.22	4.22E-01
Regulation of T cell activation	2.01E-02	1.67	4.23E-01
Regulation of cellular protein metabolic process	2.03E-02	1.29	4.23E-01
Cofactor biosynthetic process	2.19E-02	1.74	4.39E-01
Positive regulation of lymphocyte activation	2.19E-02	1.74	4.39E-01
Fatty acid beta-oxidation using acyl-CoA oxidase	2.18E-02	5.93	4.40E-01
Positive regulation of interleukin-12 production	2.18E-02	5.93	4.40E-01
Mitochondrial membrane organization	2.24E-02	2.50	4.44E-01

Negative regulation of biosynthetic process	2.31E-02	1.26	4.52E-01
Protein folding	2.39E-02	1.51	4.61E-01
Golgi organization	2.45E-02	2.96	4.67E-01
Release of cytochrome c from mitochondria	2.45E-02	2.96	4.67E-01
Regulation of ubiquitin-protein ligase activity during mitotic cell cycle	2.51E-02	1.88	4.72E-01
Viral reproduction	2.51E-02	1.88	4.72E-01
Anaphase-promoting complex-dependent proteasomal ubiquitin-dependent protein catabolic process	2.71E-02	1.91	4.76E-01
Negative regulation of ubiquitin-protein ligase activity during mitotic cell cycle	2.71E-02	1.91	4.76E-01
Regulation of ubiquitin-protein ligase activity	2.57E-02	1.82	4.77E-01
Negative regulation of cellular biosynthetic process	2.70E-02	1.25	4.77E-01
Antigen receptor-mediated signaling pathway	2.67E-02	2.42	4.78E-01
Regulation of apoptosis	2.66E-02	1.21	4.78E-01
B cell homeostasis	2.74E-02	4.04	4.78E-01
mRNA cleavage	2.74E-02	4.04	4.78E-01
mRNA polyadenylation	2.74E-02	4.04	4.78E-01
Regulation of mitochondrial membrane permeability	2.74E-02	4.04	4.78E-01
Chromatin assembly or disassembly	*2.57E-02*	*1.61*	*4.79E-01*
mRNA 3'-end processing	2.70E-02	3.33	4.79E-01
Positive regulation of leukocyte activation	2.65E-02	1.68	4.79E-01
RNA 3'-end processing	2.63E-02	2.63	4.80E-01
T cell proliferation	2.63E-02	2.63	4.80E-01
Protein tetramerization	2.63E-02	2.28	4.81E-01
Positive regulation of caspase activity	2.92E-02	1.96	4.96E-01
Positive regulation of peptidase activity	2.92E-02	1.96	4.96E-01

Ribonucleoside metabolic process	2.92E-02	2.13	4.98E-01
Macromolecular complex subunit organization	*3.01E-02*	*1.21*	*5.04E-01*
Phosphoinositide biosynthetic process	3.06E-02	2.22	5.06E-01
Initiation of viral infection	3.06E-02	2.83	5.08E-01
Vesicle targeting	3.06E-02	2.83	5.08E-01
DNA damage response, signal transduction	3.17E-02	1.78	5.09E-01
Peptide metabolic process	3.14E-02	2.01	5.10E-01
Phosphoinositide metabolic process	3.12E-02	1.83	5.10E-01
GPI anchor biosynthetic process	3.16E-02	2.35	5.10E-01
Negative regulation of translation	3.16E-02	2.35	5.10E-01
DNA catabolic process	3.29E-02	1.93	5.20E-01
Cell cycle phase	*3.31E-02*	*1.29*	*5.20E-01*
Negative regulation of ligase activity	3.40E-02	1.86	5.25E-01
Negative regulation of ubiquitin-protein ligase activity	3.40E-02	1.86	5.25E-01
Positive regulation of protein metabolic process	3.39E-02	1.39	5.27E-01
Positive regulation of filopodium assembly	3.51E-02	5.08	5.34E-01
Regulation of filopodium assembly	3.51E-02	5.08	5.34E-01
Activation of caspase activity	3.56E-02	1.98	5.35E-01
Induction of apoptosis by intracellular signals	3.56E-02	1.98	5.35E-01
Negative regulation of lymphocyte activation	3.56E-02	1.98	5.35E-01
Maintenance of protein location in cell	3.55E-02	2.17	5.37E-01
DNA packaging	*3.66E-02*	*1.60*	*5.44E-01*
Protein kinase cascade	3.79E-02	1.30	5.44E-01
GPI anchor metabolic process	3.71E-02	2.29	5.44E-01
Maintenance of protein location	*3.82E-02*	*2.04*	*5.45E-01*
Negative regulation of cell activation	3.70E-02	1.89	5.45E-01
Glycerophospholipid biosynthetic process	3.78E-02	1.83	5.46E-01

T cell receptor signaling pathway	3.76E-02	2.71	5.47E-01
Monosaccharide metabolic process	3.78E-02	1.40	5.48E-01
Positive regulation of cell activation	*4.04E-02*	*1.60*	*5.64E-01*
Pyridine nucleotide metabolic process	4.08E-02	2.12	5.65E-01
Positive regulation of cytokine production	*4.21E-02*	*1.68*	*5.73E-01*
Negative regulation of immune system process	4.23E-02	1.71	5.73E-01
Lipid modification	4.20E-02	1.80	5.74E-01
Erythrocyte homeostasis	4.34E-02	2.00	5.80E-01
Purine nucleoside monophosphate biosynthetic process	4.38E-02	2.96	5.82E-01
Purine ribonucleoside monophosphate biosynthetic process	4.38E-02	2.96	5.82E-01
Regulation of erythrocyte differentiation	*4.38E-02*	*2.96*	*5.82E-01*
Macromolecular complex assembly	*4.47E-02*	*1.20*	*5.87E-01*
Viral infectious cycle	4.67E-02	2.07	6.01E-01
Regulation of establishment of protein localization	4.97E-02	1.54	6.21E-01
Negative regulation of translational initiation	4.96E-02	3.42	6.22E-01
Negative regulation of leukocyte activation	5.04E-02	1.87	6.24E-01
Regulation of DNA metabolic process	5.10E-02	1.56	6.27E-01
Regulation of protein transport	5.10E-02	1.56	6.27E-01
rRNA modification	5.15E-02	4.44	6.29E-01
Apoptotic mitochondrial changes	5.26E-02	2.29	6.35E-01
Protein amino acid N-linked glycosylation	5.30E-02	2.02	6.36E-01
Myeloid cell differentiation	5.44E-02	1.62	6.44E-01
Regulation of B cell activation	5.50E-02	1.92	6.46E-01
Regulation of caspase activity	5.60E-02	1.69	6.51E-01
Response to cytokine stimulus	5.60E-02	1.69	6.51E-01
Mitochondrion organization	*5.76E-02*	*1.48*	*6.60E-01*
Cellular macromolecular complex subunit organization	*5.93E-02*	*1.27*	*6.67E-01*

Nitrogen compound biosynthetic process	5.91E-02	1.29	6.68E-01
Hexose metabolic process	6.02E-02	1.39	6.71E-01
Glycerolipid biosynthetic process	6.12E-02	1.67	6.74E-01
Spliceosome assembly	6.11E-02	2.22	6.75E-01
Phospholipid biosynthetic process	6.23E-02	1.57	6.79E-01
Nucleobase, nucleoside and nucleotide biosynthetic process	6.35E-02	1.38	6.82E-01
Nucleobase, nucleoside, nucleotide and nucleic acid biosynthetic process	6.35E-02	1.38	6.82E-01
Pseudouridine synthesis	6.34E-02	3.17	6.84E-01
DNA damage response, signal transduction by p53 class mediator	6.43E-02	2.39	6.85E-01
Protein homotetramerization	6.43E-02	2.39	6.85E-01
Negative regulation of alpha-beta T cell proliferation	6.49E-02	6.67	6.87E-01
Purine nucleoside monophosphate metabolic process	6.58E-02	2.67	6.90E-01
Purine ribonucleoside monophosphate metabolic process	6.58E-02	2.67	6.90E-01
Negative regulation of cell cycle	6.67E-02	1.65	6.94E-01
Positive regulation of cellular protein metabolic process	6.71E-02	1.34	6.94E-01
Glycerophospholipid metabolic process	6.79E-02	1.51	6.97E-01
Protein amino acid lipidation	6.86E-02	1.84	6.99E-01
Positive regulation of protein modification process	6.97E-02	1.38	7.03E-01
Establishment of vesicle localization	7.03E-02	2.15	7.05E-01
Positive regulation of B cell activation	7.03E-02	2.15	7.05E-01
Myeloid cell homeostasis	7.09E-02	3.95	7.07E-01
Positive regulation of DNA recombination	7.09E-02	3.95	7.07E-01
Positive regulation of isotype switching	7.09E-02	3.95	7.07E-01
Purine deoxyribonucleotide metabolic process	7.09E-02	3.95	7.07E-01

Regulation of transcription from RNA polymerase III promoter	7.09E-02	3.95	7.07E-01
Regulation of endopeptidase activity	7.25E-02	1.63	7.13E-01
Nicotinamide metabolic process	7.37E-02	2.00	7.18E-01
Nicotinamide nucleotide metabolic process	7.37E-02	2.00	7.18E-01
Regulation of cyclin-dependent protein kinase activity	7.61E-02	1.81	7.28E-01
Proteolysis	7.86E-02	1.13	7.36E-01
Transcription initiation	7.86E-02	1.61	7.38E-01
Positive regulation of T cell activation	8.04E-02	1.64	7.43E-01
Negative regulation of gene expression	8.13E-02	1.20	7.45E-01
Establishment of organelle localization	8.20E-02	1.67	7.47E-01
Alkaloid metabolic process	8.30E-02	1.95	7.50E-01
Regulation of mitotic cell cycle	8.51E-02	1.40	7.53E-01
Maintenance of location in cell	8.41E-02	1.85	7.53E-01
RNA elongation from RNA polymerase II promoter	8.41E-02	1.85	7.53E-01
Nucleosome assembly	*8.50E-02*	*1.59*	*7.54E-01*
Cellular macromolecular complex assembly	*8.48E-02*	*1.26*	*7.55E-01*
Regulation of homeostatic process	*8.60E-02*	*1.48*	*7.55E-01*
Regulation of translation	*8.69E-02*	*1.43*	*7.58E-01*
Positive regulation of macromolecule metabolic process	8.87E-02	1.14	7.62E-01
Regulation of protein modification process	8.87E-02	1.27	7.63E-01
Glucose metabolic process	9.00E-02	1.39	7.66E-01
Hemoglobin metabolic process	9.31E-02	3.56	7.71E-01
RNA methylation	9.31E-02	3.56	7.71E-01
Activation of pro-apoptotic gene products	9.28E-02	2.42	7.71E-01
Nucleotide-excision repair, DNA damage removal	9.28E-02	2.42	7.71E-01
Cellular amide metabolic process	9.25E-02	1.75	7.71E-01

Positive regulation of DNA metabolic process	9.25E-02	1.75	7.71E-01
RNA localization	9.23E-02	1.51	7.72E-01
Regulation of protein localization	9.22E-02	1.42	7.73E-01
Small GTPase mediated signal transduction	9.56E-02	1.25	7.76E-01
Dephosphorylation	9.51E-02	1.39	7.77E-01
Nucleosome organization	*9.56E-02*	*1.53*	*7.77E-01*
Branched chain family amino acid metabolic process	9.65E-02	2.78	7.77E-01
tRNA modification	9.65E-02	2.78	7.77E-01
Purine nucleoside metabolic process	9.97E-02	2.15	7.82E-01
Purine ribonucleoside metabolic process	9.97E-02	2.15	7.82E-01
Ribonucleotide metabolic process	9.91E-02	1.39	7.83E-01
Cellular response to extracellular stimulus	9.95E-02	1.67	7.83E-01
Regulation of peptidase activity	9.89E-02	1.55	7.83E-01
Regulation of peptidase activity	9.89E-02	1.55	7.83E-01
Nucleotide biosynthetic process	9.87E-02	1.34	7.84E-01

(B) Large Platelet RNA: DAVID Functional Annotation Chart			
Term	P-Value	Fold Enrichment	Benjamini Corrected P-value
Cellular macromolecular complex assembly	*1.41E-04*	*2.83*	*2.27E-01*
Protein-DNA complex assembly	6.59E-04	4.68	3.31E-01
Cellular macromolecular complex subunit organization	*5.77E-04*	*2.52*	*4.10E-01*
Chromatin assembly	2.38E-03	4.35	5.81E-01
Nucleosome assembly	*1.94E-03*	*4.50*	*5.89E-01*
Macromolecular complex assembly	*3.65E-03*	*1.85*	*6.15E-01*
Platelet activation	4.36E-03	7.39	6.32E-01
Nucleosome organization	*3.46E-03*	*4.07*	*6.53E-01*
Regulation of translational initiation in response to stress	8.66E-03	20.27	7.06E-01
Response to wounding	8.37E-03	1.87	7.22E-01

DNA packaging	*1.19E-02*	*3.23*	*7.23E-01*
Response to organic substance	9.98E-03	1.71	7.30E-01
Axon ensheathment	1.15E-02	5.63	7.34E-01
Ensheathment of neurons	1.15E-02	5.63	7.34E-01
Macromolecular complex subunit organization	*8.25E-03*	*1.73*	*7.48E-01*
Regulation of translation in response to stress	1.14E-02	17.74	7.53E-01
Chromosome organization	*7.11E-03*	*1.95*	*7.65E-01*
Myelination	8.11E-03	6.22	7.74E-01
Response to bacterium	2.12E-02	2.45	8.05E-01
Blood coagulation	2.08E-02	3.25	8.11E-01
Coagulation	2.08E-02	3.25	8.11E-01
Cell cycle	*2.26E-02*	*1.58*	*8.13E-01*
Cell cycle process	*1.65E-02*	*1.76*	*8.15E-01*
Defense response	2.02E-02	1.69	8.17E-01
Chromatin assembly or disassembly	*1.79E-02*	*2.98*	*8.25E-01*
Wound healing	2.00E-02	2.48	8.27E-01
Regulation of action potential in neuron	2.68E-02	4.38	8.30E-01
Negative regulation of cellular component organization	3.07E-02	2.66	8.32E-01
Regulation of cellular component biogenesis	3.07E-02	2.66	8.32E-01
Response to heat	3.01E-02	4.22	8.35E-01
Protein localization	1.96E-02	1.56	8.36E-01
Hemostasis	2.66E-02	3.07	8.39E-01
Regulation of translation	*2.59E-02*	*2.76*	*8.43E-01*
Carboxylic acid catabolic process	2.99E-02	2.98	8.43E-01
Organic acid catabolic process	2.99E-02	2.98	8.43E-01
Negative regulation of protein complex assembly	3.42E-02	5.56	8.46E-01
Regulation of homeostatic process	*3.35E-02*	*2.90*	*8.48E-01*
Chromatin organization	*2.98E-02*	*1.88*	*8.52E-01*
Positive regulation of tumor necrosis factor production	3.88E-02	9.46	8.66E-01
Regulation of cytokine production	3.79E-02	2.35	8.68E-01

Regulation of cardiac muscle contraction by calcium ion signaling	4.17E-02	47.30	8.71E-01
Regulation of cardiac muscle contraction by regulation of the release of sequestered calcium ion	4.17E-02	47.30	8.71E-01
Release of sequestered calcium ion into cytosol by sarcoplasmic reticulum	4.17E-02	47.30	8.71E-01
Positive regulation of cytokine production	*4.14E-02*	*3.15*	*8.76E-01*
Regulation of protein complex assembly	4.14E-02	3.15	8.76E-01
Cell cycle phase	*5.53E-02*	*1.71*	*9.16E-01*
Response to unfolded protein	6.26E-02	3.33	9.19E-01
Cellular amino acid catabolic process	5.51E-02	3.48	9.20E-01
Regulation of action potential	5.51E-02	3.48	9.20E-01
Membrane organization	6.03E-02	1.74	9.20E-01
Regulation of release of sequestered calcium ion into cytosol by sarcoplasmic reticulum	6.19E-02	31.53	9.21E-01
Response to redox state	6.19E-02	31.53	9.21E-01
Sarcoplasmic reticulum calcium ion transport	6.19E-02	31.53	9.21E-01
Cell cycle arrest	6.65E-02	2.76	9.23E-01
Interphase of mitotic cell cycle	6.65E-02	2.76	9.23E-01
Mitochondrion organization	*7.17E-02*	*2.40*	*9.23E-01*
Regulation of myeloid cell differentiation	6.00E-02	3.38	9.24E-01
Golgi vesicle transport	*5.87E-02*	*2.53*	*9.24E-01*
Interphase	7.33E-02	2.68	9.24E-01
Regulation of translational initiation	5.48E-02	4.61	9.24E-01
Glutamine family amino acid catabolic process	6.55E-02	7.10	9.24E-01
Defense response to bacterium	8.79E-02	2.53	9.25E-01
Protein polymerization	8.40E-02	3.86	9.25E-01
Positive regulation of cell activation	*8.54E-02*	*2.56*	*9.25E-01*
Response to endogenous stimulus	8.70E-02	1.64	9.26E-01
Response to glucose stimulus	6.87E-02	4.20	9.26E-01
Male meiosis	7.14E-02	6.76	9.26E-01

Regulation of cellular protein metabolic process	7.81E-02	1.60	9.27E-01
Regulation of erythrocyte differentiation	*5.42E-02*	*7.88*	*9.27E-01*
Amine catabolic process	8.22E-02	3.03	9.27E-01
Positive regulation of binding	8.22E-02	3.03	9.27E-01
Positive regulation of translation	8.38E-02	6.17	9.27E-01
Microtubule-based movement	9.05E-02	2.51	9.28E-01
Ubiquitin-dependent protein catabolic process	*7.07E-02*	*1.95*	*9.28E-01*
Maintenance of protein location	*8.01E-02*	*3.94*	*9.28E-01*
Response to hexose stimulus	7.62E-02	4.03	9.28E-01
Response to monosaccharide stimulus	7.62E-02	4.03	9.28E-01
Positive regulation of inflammatory response to antigenic stimulus	8.17E-02	23.65	9.29E-01
Regulation of body fluid levels	7.78E-02	2.35	9.29E-01
Glutamine family amino acid metabolic process	9.64E-02	3.64	9.32E-01
Response to temperature stimulus	9.79E-02	2.85	9.32E-01
Programmed cell death	*9.53E-02*	*1.47*	*9.32E-01*
Negative regulation of organelle organization	9.47E-02	2.88	9.34E-01

APPENDIX F: VIRAL MIRNA IN CIRCULATION

Permissions

Appendix F is adapted from an unpublished manuscript, to include supplemental data, included without permission required.

- *"Viral Micro RNAs are Widely Detected in the Human Circulation"* Milka Koupenova, Eric Mick, Heather A. Corkrey, Tianxiao Huan, Lauren Clancy, Ravi Shah, Emelia J. Benjamin, Daniel Levy, Evelyn A. Kurt-Jones, Kahraman Tanriverdi, and Jane E. Freedman

Author Contributions:

M. Koupenova (M.K.) and J.E. Freedman designed, interpreted the results, and wrote this article. M.K. and H. Corkrey (H.C.) conducted the mouse experiments. E. Kurt-Jones provided the viruses and assisted with design of the mouse experiments. E. Mick conducted and provided all statistical analysis with the exception of the analysis related to co-expression and predicted viral miRNA targets which were conducted by T.Huan and provided by D. Levy. K. Tanriverdi ran the quantitative polymerase chain reactions for the human samples and H.C., L. Clancy and M.K. optimized the qPCRs for mouse samples. All authors edited this article.

Summary

MicroRNAs (miRNAs) are small non-coding sequences regulating many processes in humans. Select species of viruses also encode miRNAs to evade host immunity and optimize an efficient viral cycle. We sequenced plasma RNA from 40 participants of the Framingham Heart Study (FHS; visit 8) and, in addition to human miRNAs, identified 19 viral miRNAs from 11 different viruses, most not known to cause productive human infection. To validate this observation, viral miRNA expression was measured in the entire cohort (n=2763) utilizing high-throughput RT-qPCR. Association with concurrently measured inflammatory biomarkers and mRNA by gene array was determined. There were 16 viral miRNA-human mRNA co-expression pairs and an association with inflammatory biomarkers. To validate transfer, expression of viral miRNA was confirmed in murine plasma after infection with two different viruses. In summary, using a large cohort, we report for the first time that miRNAs from viruses are widely detected in the human circulation.

Introduction

As described, microRNAs (miRNAs) are 19 to 24 nucleotide single-stranded noncoding RNA sequences that are present in all multicellular organisms and regulate a vast number of biological processes (225, 226). miRNAs can regulate gene expression by binding to messenger RNA (mRNA) of transcribed genes thereby reducing gene expression. With the exception of the seeded sequence of

~6 nucleotides on the 5' end, miRNAs do not have to align perfectly with the targeted mRNA sequence to achieve their function (226). As a result, one miRNA has the potential to post-transcriptionally regulate up to 300 different mRNA transcripts that may be related to a broad variety of processes (227, 228). Thus, an understanding of the regulatory complexity of miRNAs is central to comprehending wide-ranging biological pathways.

In addition to multicellular organisms, select viruses encode and express miRNAs (228, 229). These select viruses include most DNA viruses from the *Herpesviridae* (230), *Polyomaviridae* and *Adenoviridae* (231) families. Studies have shown that, in target cells, changes in expression of different viral miRNAs may play a role in the regulation of either lytic or latent infection. Whereas most subfamilies of herpesviruses cause a productive infection in single species, some herpesviruses have a broad range of hosts. Herpes infections are characterized by the establishment of a lifelong, dormant state that can periodically reactivate and cause recurrent infection (230).

Herpesviruses are large enveloped viruses that can be categorized into three subfamilies, alpha, beta, and gamma, depending on their viral biology and genome sequence. Alphaherpesviruses such as Herpes simplex viruses (HSV) 1 and 2 have a broad host range, short replicative cycle and establish latent infection in neurons. Betaherpesviruses such as Cytomegaloviruses (CMV) have large genomes that are well adapted to their respective hosts, have a long replicative cycle, and limited host range. Both human (hCMV) and mouse

(mCMV) viruses establish latency in hematopoietic progenitor cells and cause mild symptoms in immunocompetent organisms (228, 232). Gammaherpesviruses have a very restricted host range and are linked to human malignancies. Epstein-Barr virus (EBV) and Kaposi's sarcoma-associated herpesvirus (KSHV) are human gammaherpesviruses and establish latency predominantly in B-cells (233, 234). EBV is associated with Hodgkin's and Burkitt's lymphoma and nasopharyngeal carcinoma, while KSHV causes lymphoma and Kaposi's sarcoma (235, 236). All of these human DNA viruses can generate miRNAs in their host target cells that mediate viral replication and latency; however, the potential chronic expression and overall effect of these viral miRNAs in humans has yet to be established. Conversely, DNA viruses from the papillomavirus and poxvirus families as well as RNA viruses are not currently known to generate viral miRNA. Rather, most of these viruses directly manipulate host miRNA balance in order to regulate their infectious state (228, 237). For instance, RNA viruses such as influenza are not known to code for their own miRNAs but to affect the host's miRNA pool, thereby, regulating its infectious state (238, 239). An exception to this rule may be select RNA retroviruses such as bovine leukemia virus (BLV) that have an RNA genome encoding a conserved cluster of miRNAs (240).

Viruses can increase the inflammatory state of the host beyond the target tissue or cell of replication. How viruses achieve global inflammation is still unclear. In addition, select DNA viruses are known to incorporate into the host

genome, raising the risk for cancer. As part of the NIH Common Fund-sponsored Extracellular RNA Communication Consortium, we previously reported that, in a large observational cohort, plasma contains a broad number of human extracellular RNA including miRNAs (241). Further analysis of the plasma RNA sequencing led to the identification of 19 viral miRNAs from 11 different viruses and these findings were further studied in the entire cohort. Here, we report that viral miRNAs in human plasma associate with advancing age and select inflammatory biomarkers. To establish that viral infection directly leads to plasma viral miRNA expression, we conducted murine studies demonstrating that miRNAs from alpha- and betaherpesviruses are detectable in plasma post-infection.

Materials and Methods

Study cohort

The Framingham Heart Study (FHS) is a community-based, prospective study of cardiovascular disease and its risk factors. Cohorts undergo an examination at the FHS once every ~4-8 years and have been extensively phenotyped over multiple examinations with a wide variety of noninvasive tests. For the present study we used data and plasma samples from the 8th visit of the offspring (and their spouses) of the Original FHS participants (FHS Offspring cohort). The participants have an extraordinary wealth of clinical data available allowing us to examine the relation of disease and risk factors to gene expression. The FHS

protocol was approved by Boston University Medical Center and by UMass Medical School Institutional Review Boards; all participants provided informed consent.

Study design

As previously described, we determined the broadest number of exRNAs in human plasma by performing RNA sequencing on 40 previously stored samples from FHS participants (Offspring Cohort, Visit 8) (212). Full methods were previously published (212). We identified 19 viral miRNAs in plasma samples of 40 participants that were confirmed in the entire FHS cohort (n=2763) by RT-qPCR (see below). Basic characteristics of the full cohort can be found in Table F.1. Summary of the study design and findings can be found in the Graphical abstract.

Table F.1. Characteristics of the FHS Offspring Cohort (Visit 8, N=2763).

Age (years)	66.8±9
Women, n (%)	1499 (54%)
Body Mass Index (BMI)	28.3±5
Systolic BP (SBP)	129±17
Diastolic BP (DBP)	74±10
Hypertension (HT)	661 (24%)
Coronary Heart Disease (CHD)	286 (10%)
Cancer (any)	441 (16%)
Biomarkers	
P-Selectin, ng/ml	41±14
C-Reactive Protein, mg/L	3±7
Tumor Necrosis Factor Receptor II, pg/ml	2687±1123
Intercellular Adhesion Molecule 1, ng/ml	298±102
Interleukin-6, pg/ml	3±3
Monocyte Chemotactic Protein 1, pg/ml	388±141
Osteoprotegerin, pmol/l	5±2

Values are presented as mean ± standard deviation (SD) unless N (%) is indicated.

Biomarker assessment

Biomarker levels were measured in the 2763 participants of the FHS cohort. A detailed description for the detection of circulatory biomarkers has been previously described (242-244). Briefly, P-Selectin, C-reactive protein (CRP) and osteoprotegerin were detected in plasma (243, 244). Levels of Interleukin-6 (IL6), soluble Intercellular Adhesion Molecule 1 (sICAM1), Monocyte Chemotactic Protein 1 (MCP1) and soluble Tumor Necrosis Factor Receptor II (sTNFRII) were measured in serum (243, 244). Biomarker levels are provided in Table F.1.

Plasma RNA isolation (human and mice)

RNA isolation from human plasma was performed as previously described (212). Briefly, RNA samples were isolated from 1 mL plasma using a miRCURY RNA Isolation Kit –Biofluids (Exiqon, Denmark). Murine plasma RNA was isolated from 100 µl of plasma using the miRNeasy Serum/Plasma Kit (Qiagen, Germany). The RNA isolation was carried out via an automated QIAcube system (Qiagen, Germany). RNA samples were eluted in 14 µl and stored at -80°C.

Template Preparation for RNA Sequencing

An Ion Chef System, Ion PI Chip Kit v3 and Hi-Q Chef kits were used for template preparation as previously described (212). The entire procedure was automated using the Ion Chef System. At the end of the template preparation, loaded PI Chips (Life Technologies, USA) were sequenced (212). RNA Sequencing was performed on an Ion Proton System as described (212) using the Ion PI Hi-Q Chef Kit (Life Technologies, USA).

Sequencing Data Analysis Using the Genboree Sequencing Pipeline

Detailed procedures for this analysis using the exceRpt tool available on the Genboree Workbench [http://www.genboree.org/] are published in (212). After alignment to endogenous sequences and removal of all contaminants with endogenous sequences, the software aligned the remaining sequences to exogenous small RNAs. Reads not mapped to any exogenous small RNAs were

aligned again using sRNAbench to the complete set of viral miRNA sequences available in miRBase.

RT-qPCR for viral miRNAs in human plasma

A detailed description of this procedure was previously provided (212). Briefly, reverse transcription was performed using the miScript SYBR Green PCR Kit (Qiagen, Germany). Viral miRNA primers were purchased from Qiagen (MD, USA). Pre-amplification was done using miScript Microfluidics PreAMP Kit (Qiagen, MD, USA). RT-qPCR was resolved by Dynamic Arrays (Fluidigm, CA, USA) using primers designed by Qiagen (Table F.2).

Table F.2: Primers used to screen the FHS cohort by RT-qPCR (related to Table F.6).

Viral miRNA	Sequence	Virus	Company	TaqMan/ SYBR Green
ebv-miR-BART11-5p	CAGTTTGGTG CGCTAGTTG	Epstein-Barr Virus (EBV)	Qiagen	SYBR Green
kshv-miR-K12-10a-5p	GCTTGGGGC GATACCAC	Kaposi's sarcoma herpesvirus (KSHV)	Qiagen	SYBR Green
kshv-miR-K12-6-5p	CAGCACCTAA TCCATCGG	Kaposi's sarcoma herpesvirus (KSHV)	Qiagen	SYBR Green
hbv-miR-B26-5p	TGAGTTCGGG CAGCAG	Herpes B virus (HBV)	Qiagen	SYBR Green
hbv-miR-B7-5p	GGCCTCGGG TTCGCTT	Herpes B virus (HBV)	Qiagen	SYBR Green
mcmv-miR-m59-2	CCCGAAGAG CCCTCACA	Mouse cytomegalovirus (mCMV)	Qiagen	SYBR Green
prv-miR-LLT3	GCACACGCC CCTCTCG	Pseudorabies virus (PRV)	Qiagen	SYBR Green
prv-miR-LLT6	CGTACCGACC CGCCTA	Pseudorabies virus (PRV)	Qiagen	SYBR Green
mdv2-miR-	GTTTTCTCTC	(MDV2)	Qiagen	SYBR Green

M18-5p	AGGCTGGCAT			
blv-miR-B2-5p	ATGACTGAGT GTAGCGC	Bovine leukemia virus (BLV)	Qiagen	SYBR Green
iltv-miR-I2	TGTGCGATAG GAGCCGA	Infectious laryngotracheitis virus (ILTV)	Qiagen	SYBR Green

mRNA expression profiling

Whole blood mRNA expression was measured in 2446 participants in the FHS (Offspring Cohort, Visit 8), using Affymetrix exon array ST 1.0 platform, as previously described (245). This platform included 17,318 mRNA transcripts. A robust multichip analysis (RMA) algorithm was applied using Affymetrix Power Tools (APT) for generation of signal values (i.e., log-2 transformed expression intensity) to yield an initially normalized dataset.

Detection of viral miRNAs in murine plasma

Animals: Twelve-week-old male C57BL/6J mice were obtained from The Jackson Laboratory. All experimental procedures were approved by the Institutional Animal Care and Use Committee at the University of Massachusetts Medical School.

HSV1 Infection, Harvest and qPCR: Twenty mice were inoculated intravenously via the tail vein with either saline or HSV1-KOS at 1 x 10^6 pfu per mouse. Purified HSV1-KOS was provided by Dr. David Knipe (Harvard Medical School). At 24 hours post-inoculation, five mice from each group were euthanized by carbon dioxide asphyxiation and blood was obtained via cardiac puncture. RNA was

isolated as described above and eluted in 14 µl. RNA was normalized to 10 ng per cDNA reaction. cDNA was synthesized using the Universal cDNA Synthesis Kit II (EXIQON, USA) on a Veriti Thermal Cycler (Applied Biosystems, Inc., USA). Plasma cDNA was diluted 1:40 and qPCR was performed on a 7900HT Fast Real-Time PCR System using the ExiLENT SYBR® Green Master Mix and twenty-six MicroRNA LNA™ PCR primer sets for HSV1 (EXIQON, USA, Table F.3).

Table F.3: Primers used for screening viral miRNAs in mice (related to Table F.10).

miRNA	Virus	Company	TaqMan/ SYBR Green	Catalog Number	Assay ID
hsv1-miR-H1-3p	HSV-1	Exiqon	SYBR Green	205826	N/A
hsv1-miR-H3-3p	HSV-1	Exiqon	SYBR Green	205811	N/A
hsv1-miR-H4-3p	HSV-1	Exiqon	SYBR Green	205740	N/A
hsv1-miR-H6-3p	HSV-1	Exiqon	SYBR Green	205796	N/A
hsv1-miR-H14-5p	HSV-1	Exiqon	SYBR Green	205848	N/A
mcmv-miR-m59-1	mCMV	Applied Biosystems	TaqMan	4440885	005484_mat
mcmv-miR-m59-2	mCMV	Applied Biosystems	TaqMan	4440885	006856_mat
mcmv-miR-M01-4-3p	mCMV	Applied Biosystems	TaqMan	4440885	006883_mat
mcmv-miR-M23-2-3p	mCMV	Applied Biosystems	TaqMan	4440885	007525_mat
mcmv-miR-m44-1	mCMV	Applied Biosystems	TaqMan	4440885	466213_mat

mCMV Inoculation, Harvest and qPCR

Twenty mice were inoculated intraperitoneally with either saline or mCMV (Smith Strain) at 1 x 10^5 pfu per mouse. At 24 hours and 7 days post-inoculation, five mice from each group were euthanized by carbon dioxide asphyxiation and blood was obtained via cardiac puncture. RNA was isolated as described above, 3 µl of the total 14µl RNA-eluate was used per cDNA reaction, with the exception of mcmv-miR-m59-1 and mcmv-miR-m59-2 which were normalized to 10 ng of RNA per cDNA reaction. cDNA was synthesized using the TaqMan® MicroRNA Reverse Transcription Kit (Applied Biosystems, USA) and TaqMan™ MicroRNA RT Assays for mCMV (Table S5) (Applied Biosystems, USA). qPCR was performed on a 7900HT Fast Real-Time PCR System using the TaqMan 2X Universal PCR Master Mix II, No AmpErase UNG (Applied Biosystems, USA) and the TaqMan™ MicroRNA TM Assays (Table F.3).

Statistics

All statistical analyses were performed using STATA 13.0. Descriptive statistics are displayed as mean ± SD for continuous variables and count (percentage) for categorical variables. The RT-qPCR results cycle threshold (Ct) values were normalized (ΔCt) by the global mean of expressed results to account for inter-individual sample differences. miRNAs not expressed were assigned a Ct value of 23 (any miRNA giving undetermined values in 23 cycles) to allow for RT-qPCR protocol/machine background. Ordinary least squares linear regression models were used to test for association with the normalized Ct value of each viral

miRNA and each phenotype (i.e. biomarkers, clinical factors, and disease status). The distributions of biomarker assay levels in the restricted sample were not normally distributed and were consequently natural log (ln) transformed for statistical analysis. To account for the number of statistical comparisons conducted, we employed false discovery rate (FDR=5%) correction for the number of phenotypes tested (7 biomarkers and 8 clinical factors, Table F.1) within each of the viral miRNAs.

Viral miRNA - mRNA co-expression analysis

Co-expression analysis was performed only in the FHS participants for whom both viral miRNA and mRNA data were available (N=2395). Two analyses were performed for each viral miRNA-mRNA pair (11 viral miRNA x 17,318 mRNA): 1. *Dichotomous analysis:* coding viral miRNAs as expressed (1) vs. not expressed (0); 2. *Continuous analysis*: analysis included only samples in which viral miRNA were expressed. A linear mixed model implemented in "*lmekin"* function of R (246, 247) was used to model mRNA as a response variable and viral miRNA as an independent variable, adjusting for age, sex, technical covariates for mRNA expression profiling measurements described previously (248), imputed cell counts (248), and family structure. Benjamini-Hochberg methods were used to calculate FDR or Bonferroni-corrected $P<0.05$.)

In silico prediction of viral miRNA targets

Viral miRNA targets were predicted using the VIRmiRNA online database tool (http://crdd.osdd.net/servers/virmirna) by exactly matching the 7mer seeded region of a vmiRNA with the untranslated region and coding region of mRNAs (249).

Results

Identification of viral miRNAs in human plasma

As previously described (18), we performed small RNA sequencing from plasma of 40 FHS participants. After a series of alignments to human miRNA, tRNA, piRNA, and snoRNA, reads that were not mapped to any of these sequence types were then aligned to the available non-human genomes in exceRpt small RNA-seq Pipeline (www.genboree.org, as of 2015). We identified 19 different viral miRNAs from 11 different viruses that had variable expression in the plasma of the 40 participants (Figure F.1; Table F.4; Table F.5).

Figure F.1: Graphic of workflow for viral miRNA study.

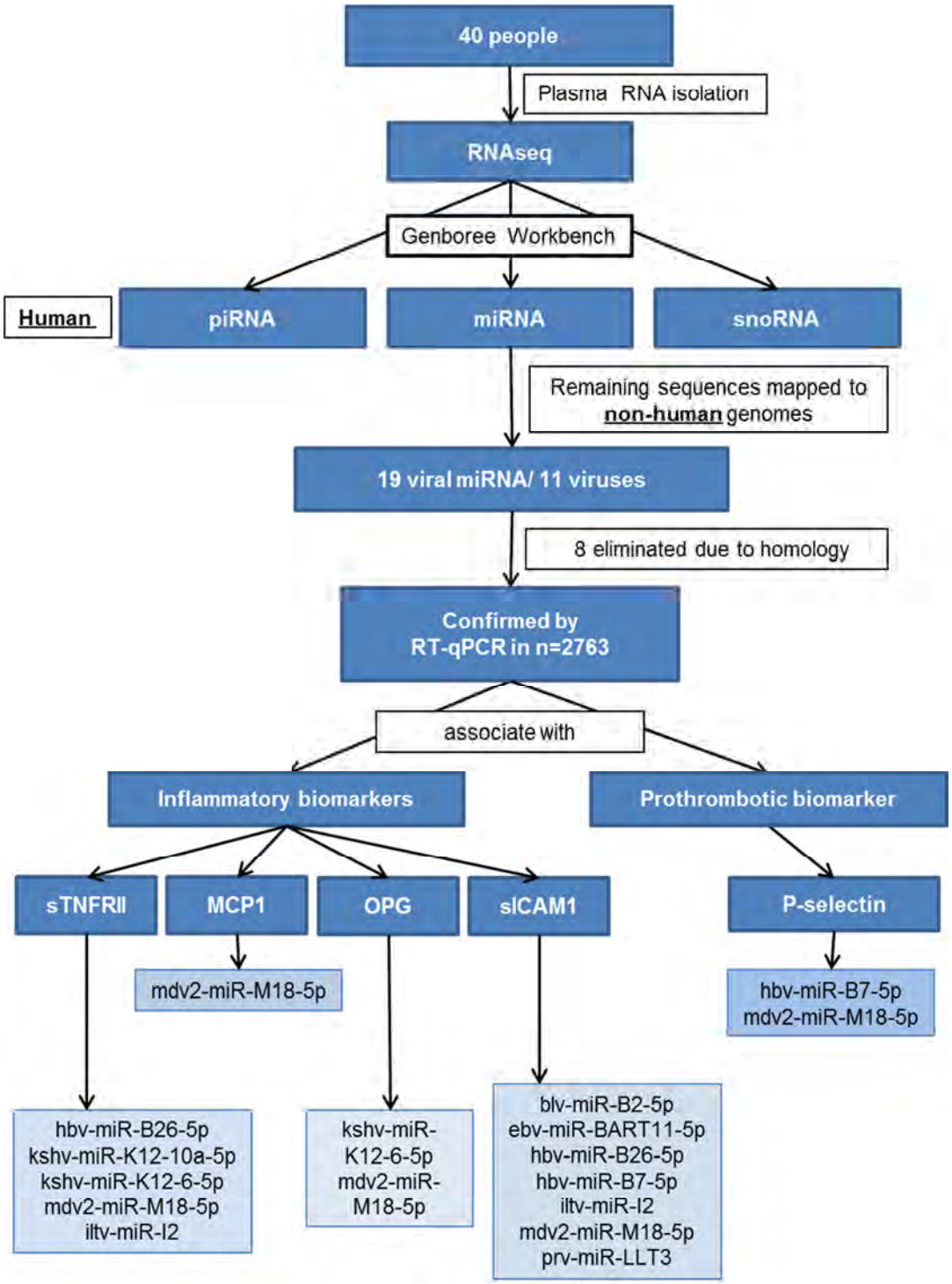

Table F.4: **Viral miRNAs identified by sequencing in the plasma of 40 participants in the FHS (Offspring Cohort, visit 8).**

Viral miRNA	Sequencing		Nucleotide (NT) sequence	Nt #	Homology with other viral miRNA (Score, p-value)	Homology with human miRNA (Score, e-value)
	N	Mean rpm				
ebv-miR-BART11-5p	11	1.56	UCAGACAGUUUG GUGCGCUAGUUG	24	rlcv-miR-rL1-14-5p (70, 1.3)	
kshv-miR-K12-10a-5p	11	2.86	GGCUUGGGGCGA UACCACCACU	22		
kshv-miR-K12-6-5p	12	1.33	CCAGCAGCACCU AAUCCAUCGG	22		hsa-miR-324-3p (60, 9.1)
hcmv-miR-US25-2-3p	40	110.66	AUCCACUUGGAG AGCUCCCGCGGU	24		
hbv-mir-B26-3p-novel	2	2.6	GCGCGCCGGCGG CCCGGGCTCG	22	hbv-miR-B26-5p (64, 4.2)	hsa-miR-1199-5p (65, 3.5)
hbv-miR-B26-5p	6	1.73	UGAGUUCGGGCA GCAGGCGCGU	22		
hbv-miR-B7-5p	4	1.39	UUCUGGGCCUCG GGUUCGCUUC	22		
mcmv-miR-m59-2	9	1.47	CCCGAAGAGCCC UCACAGAGCC	22		
prv-miR-LLT3	30	9	CGCACACGCCCC UCUCGCGCAC	22		
prv-miR-LLT6	8	2.96	CGUACCGACCCG CCUACCAGG	21		
mdv2-miR-M18-5p	7	1.43	UGUUUUCUCUCA GGCUGGCAUUG	23		
mdv2-miR-M21-3p	6	1.24	GAGCACCACGCC GAUGGACGGAGA	24		hsa-miR-3663-5p (61, 7.5)
mdv2-miR-M24-3p	27	6.38	UUAGAUGCCGUC AGGGAAAGAU	22		
rlcv-miR-rL1-17-3p	10	1.51	UGCUUCGCCCUC UCCAUCAUAA	22		hsa-miR-2681-3p (60, 9.1)
rlcv-miR-rL1-17-5p	3	1.14	UGAUGGACAGCG GGGAAGUGCACU	24	hsv1-miR-H1-5p (60, 9.0)	

rlcv-miR-rL1-29-3p	10	1.74	UUUUGUUUGCUUGGGACUGCAG	22	ebv-miR-BART19-3p (91, 0.02)	hsa-miR-584-5p (68, 2.0)
blv-miR-B2-5p	15	3.49	AUGACUGAGUGUAGCGCAGAGA	22		
hvt-miR-H14-3p	4	1.28	AGCUACAUUGCCCGCUGGGUUUC	23		hsa-miR-221-3p (97,0.007) hsa-miR-4482-5p (63, 4.7)
iltv-miR-I2	1	1.34	GGAAGGCUGUGCGAUAGGAGCCGA	24		

*Viral miRNAs with any similarities to host miRNAs or to miRNAs coming from other human viruses were eliminated from all further analysis; similarity scores and p-values were determined using www.mirbase.org with E-value cutoff =10 and maximum number of hits=100; Just “N” in the heather- is the number of people in which a miRNA were detected by sequencing; rpm-reads per million; Nt-nucleotide

Table F.5: Human Herpesvirus family and viruses (in black) that gave rise to the miRNAs detected in the plasma of the FHS participants (Offspring cohort, visit 8); classification and miRNAs (related to Table F.4).

Abbreviation	Other names	Virus type/Family	Host	Mature miRNA (#)	References
HSV1	Herpes Simplex Virus 1; HHV-1	DNA; Alpha Herpesvirus	human	27	PMID:20181707; PMID:22661375; PMID:23512275
HSV2	Herpes Simplex Virus 1; HHV-2	DNA; Alpha Herpesvirus	human	24	PMID:20181707; PMID:19889786
VZV*	Varicella-zoster virus, HHV3	DNA; Alpha Herpesvirus	human	none	PMID:19889786
EBV	Epstein-Barr virus; HHV4	DNA; Gamma Herpesvirus	human	44	PMID:17604727
hCMV	Human cyto-megalovirus; HHV5	DNA; Beta Herpesvirus	human	26	PMID:22013051; PMID:22715351
HHV-6A & 6B	Roseolovirus; HHV6	DNA; Beta Herpesvirus	human	8 (6B)	PMID:22114334
HHV-7	Roseolovirus; HHV7	DNA; Beta Herpesvirus	human	none known	PMID:22114334
KSHV	Kaposi-sarcoma virus; HHV8	DNA; Gamma Herpesvirus	human	28	PMID:22114334
HBV	Herpes B Virus Cercopithecine HV 1	DNA virus; Alpha Herpesvirus	simian zoonotically-human	15	PMID:19144716; PMID:21543500
mCMV	Mouse cytomegalovirus; MuHV-1	DNA; Beta Herpesvirus	murine	29	PMID:17928340; PMID:17942535
PRV	Pseudorabies virus; SuHV-1	DNA; Alpha Herpesvirus	swine	13	PMID:22292087
MDV2	Marek's disease virus, type 2; GaHV-3	DNA; Alpha Herpesvirus	avian (chicken and turkey)	36	PMID: 17459919 PMID:19328516
ILTV	Infectious laryngotracheitis *virus*; GaHV-1	DNA; Alpha Herpesvirus	avian (chicken, turkey and others)	10	PMID:19728068; PMID:19328516
BLV	Bovine leukemia virus	ssRNA-RT; Retroviridae	bovine	10	PMID:23345446 PMID:22308400

*Human HHV3 has no LAT ortholog and it does not encode miRNA and it was not detected in the FHS. Only viruses in black font were detected in the plasma of the FHS participants.

All of the viral miRNAs were products of DNA viruses with the exception of one miRNA that originated from bovine leukemia virus (BLV). BLV is a retrovirus with a single-stranded RNA-RT genome that is able to integrate into the DNA of the B-cell of its host as a DNA intermediate. All miRNAs from DNA viruses came from the *Herpesviridae* family (Table F.4; Table F.5). Four of the viral miRNAs originated from three viruses that use humans as a host (EBV, KSHV, and HCMV). Three viral miRNAs originated from Herpes B Virus, of which the natural host is thought to be macaque monkeys and, though rare in humans, can be fatal. The remaining 12 miRNAs that we identified originated from viruses that are not known to cause any productive infections in humans but, instead, target other animals as hosts. These are swine (PRV, two miRNA), bovine (BLV, one miRNA), avian (MDV2, three miRNA; HVT-1 one miRNA and ILTV-1 one miRNA), mice (mCMV, one miRNA), and simian (HBV, three miRNA; RLCV, three miRNA) viruses (Table F.4; Table F.5). The presence of these miRNAs was confirmed by RT-qPCR in the plasma of FHS participants (Offspring Cohort, Visit 8). The presence of viral miRNAs varied from 2.2% (ebv-miR-BART11-5p) to 99.7% (mdv2-miR-M18-5p) in the entire cohort of 2763 participants (Table F.6).

Table F.6: Viral miRNA expression in the FHS Offspring Cohort (Visit 8, N=2763) confirmed by qPCR.

Viral miRNA	N	%	Ct Values (mean ± SD)
ebv-miR-BART11-5p	60	2.2%	21.3 ±1
kshv-miR-K12-10a-5p	325	11.8%	21.2 ±1
kshv-miR-K12-6-5p	766	27.7%	20.9 ±1
hbv-miR-B26-5p	171	6.2%	21.0 ±1
hbv-miR-B7-5p	101	3.7%	20.9 ±2
mcmv-miR-m59-2	227	8.2%	21.3 ±1
prv-miR-LLT3	80	2.9%	21.3 ±1
prv-miR-LLT6	92	3.3%	21.0 ±1
mdv2-miR-M18-5p	2,754	99.7%	17.7 ±1
blv-miR-B2-5p	66	2.4%	21.3 ±1
iltv-miR-I2	2,641	95.6%	19.7 ±1
hsa-miR-16-5p	*2716*	*98.3%*	*13.5 ±2*

*miRNA levels were determined in the plasma of the participants by quantitative qPCR. Viral miRNAs: hcmv-miR-US25-2-3p and mdv2-miR-M24-3p were detected in less than 0.7% in the plasma of the participants and were omitted from all further analysis. Human miRNA has-mir-16-5p Ct values here are used as a reference to compare host vs. viral miRNA Ct values.

Homology of plasma viral miRNAs with miRNAs originating from host or other viruses

Since the observed broad presence of viral miRNAs in human plasma was unexpected, we wanted to confirm our findings and eliminate any false positive results due to homology between detected miRNAs, host miRNAs and viral miRNAs coming from human viruses. To test similarity of viral miRNA to all known miRNAs, we utilized the mirbase.org search engine and known miRNA sequences (Table F.4). Turkey herpesvirus (HVT) viral miRNA, hvt-miR-H14-3p, was 97% similar to human has-miR-221-3p, and all three Rhesus

lymphocryptovirus (rLCV) simian viral miRNAs were similar to a variable extent to viral miRNA of EBV origin, HSV-1 origin or of human origin. For stringency, we eliminated all viral miRNAs that had any similarities with host or with viral miRNAs that come from viruses that use humans as a host. Two of the miRNAs detected by RT-qPCR in less than 0.7% of the 2763 participants were also eliminated from further analysis. The distribution of the remaining 11 viral miRNAs in the plasma of FHS participants (Offspring Cohort, Visit 8) was confirmed by RT-qPCR as outlined in Table E.6. The characteristics of the participant population in this study are outlined in Table F.1.

Human Plasma Viral miRNA expression associates with circulating inflammatory biomarkers

Many viral infections induce inflammation and/or thrombosis. Thus, we evaluated if any of the plasma viral miRNAs identified associate with circulating inflammatory or pro-thrombotic biomarkers previously measured from the same blood draw used for the viral miRNA measurements. Nine of the 11 viral miRNAs were associated with at least one inflammatory biomarker (Table F.7, Table F.8). Viral miRNA from avian MDV2 virus, mdv2-miR-M18-5p, was associated with all 4 inflammatory biomarkers. Not surprisingly, viral miRNAs originating from Kaposi's sarcoma-associated herpesvirus (kshv-miR-k12-10a-5p, khsv-miR-k12-6-5p) and Herpes B virus (hbv-miR-B26-5p) were associated positively with soluble TNF-alpha receptor II protein presence. In addition, avian viral miRNAs,

iltv-miR-I2 and mdv2-miR-M18-5p, also were associated with elevated sTNFRII presence. Seven out of the 11 viral miRNAs were associated with soluble intercellular adhesion molecule-1 (sICAM-1) and two out of the 11 were associated with reduced levels of osteoprotegerin. Two out of the 11 miRNAs, one originating from Herpes B virus (hbv-miR-B7-5p) and one from Marek's disease virus type 2 (mdv2-miR-m18-5p), associated with changes in pro-thrombotic P-selectin (Table F.7; Table F.8). In this cohort, none of the miRNAs was associated with IL6, C-reactive protein, chronic heart disease (CHD), hypertension, or cancer (Table F.8 and F.9).

Table F.7: Significant association of viral miRNAs with inflammatory and pro-thrombotic biomarkers.

	sICAM1 fold change (95%CI)	**sTNFRII** fold change (95%CI)	**OPG** fold change (95%CI)	**MCP1** fold change (95%CI)	**P-Selectin** fold change (95%CI)
blv-miR-B2-5p	0.97 (0.95 -0.99), p=0.01				
ebv-miR-BART11-5p	0.95 (0.93 -0.98), p=01.0e-04*				
hbv-miR-B26-5p	0.97 (0.94 -1.00), p=0.03	1.05 (1.01 -1.08), p=0.01			
hbv-miR-B7-5p	0.97 (0.95 -1.00), p=0.03				1.03 (1.00 -1.06), p=0.03
iltv-miR-I2	1.05 (1.02 -1.08), p=0.003*	1.04 (1.00 -1.07), p=0.03			
kshv-miR-K12-10a-5p		1.06 (1.02 -1.11), p=0.002*			
kshv-miR-K12-6-5p		1.12 (1.07 -1.18), p=3.6e-06*	0.92 (0.88 -0.96), p=03.0e-04*		
mcmv-miR-m59-2					
mdv2-miR-M18-5p	1.06 (1.04 -1.09), p=6.2e-08*	1.06 (1.04 -1.09), p=1.7e-06*	0.96 (0.93 -0.98), p=03.0e-04*	1.03 (1.00 - 1.05), p=0.02	0.97 (0.95 -1.00), p=0.03
prv-miR-LLT3	0.96 (0.93 -0.98), p=04.0e-04*				
prv-miR-LLT6					

All associations were significant at $p<0.05$. Those surviving corrections for multiple comparisons are marked with *. Full results are available in Table S3.
Fold-change values for quantitative measures are for a 1 SD change in that value. Biomarker values were log-transformed for association analyses; P-selectin- platelet selectin; sTNFRII-soluble tumor necrosis factor alpha receptor II; sICAM1- soluble intercellular adhesion molecule 1; MCP1- Monocyte chemotactic protein 1: OPG-Osteoprotegerin, aka tumor necrosis factor receptor superfamily 11B (TNFRSF11B).

Table F.8: Association analyses for all biomarkers and viral miRNAs (related to Table F.7).

Viral miRNA	P-selectin fold change (95%CI)	CRP fold change (95%CI)	sTNFR II fold change (95%CI)	sICAM-1 fold change (95%CI)	IL6 fold change (95%CI)	MCP1 fold change (95%CI)	OPG fold change (95%CI)
blv-miR-B2-5p	1.02 (0.99 - 1.05), p=0.1	0.99 (0.96 - 1.01), p=0.3	1.02 (0.99 - 1.04), p=0.3	0.97 (0.95 - 0.99), p=0.01	0.98 (0.96 - 1.01), p=0.2	0.99 (0.97 - 1.02), p=0.5	1.00 (0.97 - 1.02), p=0.8
ebv-miR-BART11-5p	1.01 (0.99 - 1.04), p=0.3	0.99 (0.97 - 1.02), p=0.7	1.01 (0.98 - 1.04), p=0.5	0.95 (0.93 - 0.98), p=01.0e-04****	0.98 (0.96 - 1.01), p=0.2	0.99 (0.96 - 1.01), p=0.4	1.00 (0.97 - 1.02), p=0.8
hbv-miR-B26-5p	1.03 (0.99 - 1.06), p=0.1	0.99 (0.96 - 1.02), p=0.6	1.05 (1.01 - 1.08), p=0.01	0.97 (0.94 - 1.00), p=0.03	0.99 (0.96 - 1.02), p=0.7	0.99 (0.96 - 1.02), p=0.4	0.99 (0.96 - 1.02), p=0.6
hbv-miR-B7-5p	1.03 (1.00 - 1.06), p=0.03	0.99 (0.96 - 1.02), p=0.4	1.03 (1.00 - 1.06), p=0.1	0.97 (0.95 - 1.00), p=0.03	0.98 (0.96 - 1.01), p=0.2	1.00 (0.97 - 1.03), p=0.9	0.98 (0.96 - 1.01), p=0.3
iltv-miR-I2	1.02 (0.99 - 1.05), p=0.3	1.02 (0.99 - 1.05), p=0.2	1.04 (1.00 - 1.07), p=0.03	1.05 (1.02 - 1.08), p=0.003****	1.02 (0.99 - 1.05), p=0.2	1.01 (0.98 - 1.04), p=0.7	0.99 (0.96 - 1.02), p=0.6
kshv-miR-K12-10a-5p	1.02 (0.99 - 1.06), p=0.2	1.00 (0.97 - 1.04), p=0.9	1.06 (1.02 - 1.11), p=0.002****	0.98 (0.95 - 1.02), p=0.3	1.00 (0.97 - 1.04), p=0.8	0.98 (0.95 - 1.02), p=0.4	0.98 (0.94 - 1.01), p=0.2
kshv-miR-K12-6-5p	1.00 (0.95 - 1.05), p=0.9	1.01 (0.96 - 1.05), p=0.8	1.12 (1.07 - 1.18), p=3.6e-06****	1.01 (0.96 - 1.05), p=0.8	1.02 (0.98 - 1.07), p=0.3	1.02 (0.98 - 1.07), p=0.3	0.92 (0.88 - 0.96), p=03.0e-04****
mcmv-miR-m59-2	1.03 (1.00 - 1.06), p=0.1	0.99 (0.96 - 1.03), p=0.8	1.02 (0.99 - 1.05), p=0.3	0.97 (0.94 - 1.00), p=0.1	0.99 (0.96 - 1.02), p=0.5	1.01 (0.97 - 1.04), p=0.7	0.98 (0.95 - 1.01), p=0.3
mdv2-miR-M18-	0.97 (0.95 - 1.00),	1.00 (0.98 - 1.02),	1.06 (1.04 - 1.09),	1.06 (1.04 - 1.09),	1.00 (0.98 - 1.03),	1.03 (1.00 - 1.05),	0.96 (0.93 - 0.98),

5p	p=0.03	p=0.9	p=1.7e-06****	p=6.2e-08****	p=0.7	p=0.02	p=03.0e-04****
prv-miR-LLT3	1.02 (1.00 - 1.05), p=0.1	0.99 (0.96 - 1.01), p=0.3	1.01 (0.99 - 1.04), p=0.3	0.96 (0.93 - 0.98), p=04.0e-04****	0.98 (0.96 - 1.00), p=0.1	0.99 (0.97 - 1.02), p=0.5	1.00 (0.98 - 1.03), p=0.9
Prv-miR-LLT6	1.02 (0.99 - 1.05), p=0.1	0.99 (0.97 - 1.02), p=0.6	1.03 (1.00 - 1.05), p=0.1	0.98 (0.95 - 1.00), p=0.1	0.98 (0.96 - 1.01), p=0.2	0.99 (0.96 - 1.02), p=0.4	0.99 (0.97 - 1.02), p=0.6

Fold-change values for quantitative measures are for a 1 SD change in that value. Associations are considered significant at p<0.05. Those surviving corrections for multiple comparisons are marked with ****. Biomarker values were log-transformed for association analyses. Abbreviations: P-selectin- platelet selectin; CRP-C-reactive protein; sTNFRII-soluble Tumor Necrosis Factor Alpha Receptor II; sICAM1- soluble Intercellular Adhesion Molecule 1; IL6-interleukin 6; MCP1- Monocyte Chemotactic Protein 1: OPG- Osteoprotegerin, aka Tumor Necrosis Factor Receptor Superfamily 11B (TNFRSF11B).

Table F.9: Association of viral miRNAs with CHD and cancer (related to Table F.7).

Viral miRNA	Age fold change (95%CI)	Sex (Female) fold change (95%CI)	Hypertension fold change (95%CI)	CHD fold change (95%CI)	Cancer fold change (95%CI)
blv-miR-B2-5p	0.98 (0.96 - 1.01), p=0.2	1.01 (0.96 - 1.06), p=0.7	0.96 (0.91 - 1.02), p=0.2	0.97 (0.90 - 1.05), p=0.5	1.04 (0.98 - 1.11), p=0.2
ebv-miR-BART11-5p	0.99 (0.97 - 1.01), p=0.4	1.02 (0.97 - 1.07), p=0.5	0.97 (0.91 - 1.02), p=0.2	0.99 (0.92 - 1.07), p=0.8	1.03 (0.97 - 1.10), p=0.3
hbv-miR-B26-5p	**0.97 (0.94 - 1.00), p=0.04**	1.04 (0.97 - 1.10), p=0.3	0.96 (0.90 - 1.03), p=0.3	1.00 (0.91 - 1.11), p=0.9	1.03 (0.95 - 1.12), p=0.5
hbv-miR-B7-5p	0.98 (0.95 - 1.00), p=0.1	1.02 (0.97 - 1.07), p=0.4	1.01 (0.95 - 1.07), p=0.9	1.02 (0.94 - 1.11), p=0.7	1.03 (0.96 - 1.11), p=0.4

iltv-miR-I2	0.97 (0.94 - 1.00), p=0.1	1.05 (0.99 - 1.11), p=0.1	0.98 (0.91 - 1.05), p=0.5	0.97 (0.88 - 1.07), p=0.5	0.98 (0.90 - 1.06), p=0.6
kshv-miR-K12-10a-5p	0.97 (0.93 - 1.00), p=0.1	1.02 (0.95 - 1.09), p=0.7	0.96 (0.89 - 1.05), p=0.4	0.96 (0.86 - 1.08), p=0.5	1.08 (0.98 - 1.19), p=0.1
kshv-miR-K12-6-5p	**0.95 (0.91 - 0.99), p=0.01**	1.00 (0.91 - 1.09), p=0.9	0.99 (0.89 - 1.10), p=0.8	0.95 (0.83 - 1.10), p=0.5	0.97 (0.86 - 1.10), p=0.7
mcmv-miR-m59-2	0.98 (0.95 - 1.01), p=0.2	1.03 (0.97 - 1.09), p=0.4	0.96 (0.89 - 1.03), p=0.3	0.97 (0.88 - 1.07), p=0.6	1.07 (0.98 - 1.16), p=0.1
mdv2-miR-M18-5p	**0.97 (0.95 - 1.00), p=0.02**	1.02 (0.98 - 1.07), p=0.3	1.00 (0.95 - 1.05), p=0.9	0.99 (0.92 - 1.07), p=0.8	0.96 (0.91 - 1.03), p=0.3
prv-miR-LLT3	0.98 (0.96 - 1.00), p=0.1	1.03 (0.98 - 1.09), p=0.2	0.98 (0.93 - 1.04), p=0.6	0.96 (0.89 - 1.04), p=0.4	1.05 (0.98 - 1.12), p=0.2
prv-miR-LLT6	0.98 (0.96 - 1.01), p=0.2	1.02 (0.97 - 1.08), p=0.4	0.97 (0.91 - 1.03), p=0.3	0.98 (0.90 - 1.07), p=0.7	1.00 (0.94 - 1.08), p=0.9

Fold-change values for quantitative measures are for a 1 SD change in that value. Associations are considered significant at $p<0.05$. CHD = coronary heart disease

Plasma viral miRNAs modestly associate with age but not with sex

Certain DNA viral infections are known to cause proliferative neoplasms which increase with age. Here, we sought to determine if presence of viral miRNA associates with age and sex. Interestingly, three of the viral miRNAs associated inversely with age (Table F.9). These were hbv-miR-B26-5p, kshv-miR-K12-6-5p and mdv2-miR-M18-5p. None of the viral miRNAs were associated with sex (Table F.9).

Co-expression analysis of plasma viral miRNA and blood cell mRNA transcripts; predicted gene targets

In cells, viral miRNAs target specific mRNAs dependent on their seeded sequence. Since we found viral miRNAs present in plasma we wanted to assess co-expression of plasma viral miRNAs with whole blood derived mRNA transcripts in the same FHS participants. For that purpose we utilized 17,318 whole blood mRNA transcripts from the same FHS participants at the same visit. Using dichotomous analysis we identified three viral miRNA-mRNA pairs (Table F.10). We also performed a continuous analysis for viral miRNA-mRNA pairs. Using Bonferroni corrected $p<0.05$, we identified 13 viral miRNA-mRNA co-expression pairs for genes related to immune response, viral integration, apoptosis, cell mobility and RNA-splicing (Table F.10). To identify possible molecular targets, we used the VIRmiRNA online tool (see Methods) to predict

human gene targets. We identified two target genes for two of the13 viral miRNAs. These were *LRP1B* for blv-miR-B2-5P and *SELPLG* for iltv-miR-I2.

Table F.10: Co-expression of plasma viral miRNA with whole blood mRNA transcripts assessed by using dichotomous or continuous model analysis and a cut off of Bonferroni p <0.05 corrected for all 17,318 transcripts.

Viral miRNA	Human mRNA	Transcript ID	Beta	Correlation p-value	Disease associated with gene target	Function of gene target
mcmv-miR-m59-2*		2340423	0.13	3.44E-07	not known	not known
blv-miR-B2-5p*	LRP1B (LDL receptor related protein 1B)	2578790	0.06	1.64E-06	Endocervical carcinoma	Potential cell surface receptor that binds and internalizes ligands in receptor-mediated endocytosis manner
iltv-miR-I2*	CHD9 (Chromo-domain Helicase DNA Binding Protein 9)	3660858	-0.08	2.53E-06	not known	transcriptional coactivator for PPARA/ binds to A/T-rich DNA
mdv2-miR-M18-5p	SMC5 (Structural Maintenance Of Chromosomes 5)	3174224	0.02	1.67E-07	Viral pneumonia and Cornelia De Lange Syndrome 1	Core component of the SMC5-SMC6 complex, involved in repair of DNA double-strand breaks by homologous recombination ; SMC5-SMC6 may prevent transcription of episomal viral DNA

iltv-miR-I2	SRSF2IP (Serine/Arginine-Rich Splicing Factor 2, Interacting Protein)	3452145	0.02	2.10E-07	Alternative splicing in autism spectrum disorder	Plays a role in pre-mRNA alternative splicing by regulating spliceosome assembly. Related pathways are apoptosis modulation and signaling
mdv2-miR-M18-5p	PIK3R1 (Phosphoinositide-3-Kinase Regulatory Subunit 1)	2813060	0.02	2.67E-07	Short Syndrome and Agammaglobulinemia 7, Autosomal Recessive (severe infections in the first years of life).	Coordinates a diverse range of cell functions including proliferation and survival
mdv2-miR-M18-5p	UTRN (Utropin)	2929168	0.02	4.23E-07	Duchene Muscular Dystrophy ; Becker Muscular Dystrophy	Participates in post-synaptic membrane maintenance and acetylcholine receptor clustering
mdv2-miR-M18-5p	ZC3H13 (Zinc Finger CCCH-Type Containing 13)	3512769	0.02	5.65E-07		Involved in RNA processing and cell cycle as part of the WTAP complex
iltv-miR-I2	RBM26 (RNA Binding Motif Protein 26)	3519119	0.02	7.74E-07		*Involved in nucleic acid binding and n ucleotide binding*
hbv-miR-B26-5p	SCGB3A2 (Secretoglobin Family 3A Member 2)	2834472	-0.22	1.23E-06	Asthma and Asthma Susceptibility	A secreted lung surfactant protein and a downstream target of thyroid

						transcription factor; related pathways are Vesicle-mediated transport and Binding and Uptake of Ligands by Scavenger Receptors
iltv-miR-I2	PSIP1 (PC4 And SFRS1 Interacting Protein 1)	3199790	0.02	1.42E-06	HIV-1	Cellular cofactor for lentiviral integration; Transcriptional coactivator involved in neuroepithelial stem cell differentiation and neurogenesis. Involved in particular in lens epithelial cell gene regulation and stress responses.
kshv-miR-K12-10a-5p	MIC1/C18orf8 (Macrophage Inhibitory Cytokine 1)	3781734	0.07	1.61E-06		Colon cancer associated protein
mdv2-miR-M18-5p	EPRS (Glutamyl-Prolyl-TRNA Synthetase)	2456746	0.02	1.87E-06	Aqueous Misdirection and Separation Anxiety Disorder	Catalyzes the attachment of the cognate amino acid to the corresponding tRNA in a two-step reaction: the amino acid is first activated by ATP to form a covalent intermediate with AMP and is then transferred to the acceptor end of the

						cognate tRNA.
iltv-miR-I2	HIF1A (Hypoxia Inducible Factor 1 Alpha Subunit)	3539070	0.02	2.11E-06	Hypoxia and Retinal Ischemia	Functions as a master transcriptional regulator of the adaptive response to hypoxia. Under hypoxic conditions, activates the transcription of many genes including genes related to glucose metabolism
mdv2-miR-M18-5p	RNF6 (Ring Finger Protein 6)	3506431	0.02	2.38E-06	Esophageal Cancer	Potential tumor suppressor; related pathways are Immune System and Class I MHC mediated antigen processing and presentation
ebv-miR-BART11-5p	ARHGAP18 (Rho GTPase Activating Protein 18)	2973694	0.23	2.74E-06	Penicilliosis	Rho GTPase activating protein that suppresses F-actin polymerization by inhibiting Rho; Regulates cell shape, spreading, and migration

*Only 3 miRNAs-mRNA pairs were significantly co-expressed by dichotomous model; the rest were co-expressed by continuous model.

Viral miRNA presence is detectable post DNA-virus infection in mice

In cells of infected tissues, viral miRNA levels fluctuate as the viral infection switches from lytic to latent; however, there is no uniform consensus whether viral miRNAs are released into the circulation of the host or if they can be detected in plasma. To confirm that viral infections may lead to an increase in viral miRNA balance in the plasma, we infected mice with an alphaherpesvirus (HSV1) or a betaherpesvirus (mCMV). Both infections led to a detectable increase of select miRNAs in the plasma at 24h post infection (Table F.11). Since the alphaherpesvirus infection was only used as a proof of concept, we infected mice intravenously (i.v.) with HSV1 and screened for miRNAs as previously described for cells (229). Although i.v. HSV1 infection is not the physiological route of infection, in certain genetically modified cases it can lead to lethality (250). HSV1 infection led to detectable presence of hsv1-miR-H6-3p and hsv1-mir-H1-3p only in the plasma of the infected mice; no other viral miRNAs tested showed specific detection (Table F.11).

Table F.11: Infections with alpha (HSV1) and beta (mCMV) DNA viruses in mice generates viral miRNA in plasma 24h post infection.

Infection	miRNA	Control (raw Ct)	Virus (Ct)	no cDNA control	NTC	% of mice expressing viral miRNA (n = 5/group)
HSV1	hsv1-miR-H6-3p	u.d	29.9 ± 1	u.d	u.d	80%
	hsv1-miR-H1-3p	u.d	33.9 ± 2	u.d	u.d	80%
	hsv1-miR-H14-5p	u.d	34.10 ± 1	u.d	u.d	40%
	hsv1-miR-H3-3p	35.8 ± 2	35.5 ± 2	u.d	35.2	60%; 40%
	hsv1-miR-H4-3p	u.d	u.d	u.d	u.d	100%
mCMV	mcmv-miR-23-2-3p	u.d	33.2 ± 0.3	u.d	u.d	100%
	mcmv- miR -59-2	39.1 ± 0.5	38.8 ± 0.5	u.d	u.d	80%; 100%
	mcmv- miR -59-1	u.d	u.d	u.d	u.d	100%
	mcmv-miR-M01-4-3p	u.d	u.d	u.d	u.d	100%
	mcmv-miR-m44-1	30.0 ± 0.5	30.0 ± 1.1	u.d	u.d	100%

u.d.-undetermined, i.e. there were no values generated by the qPCR machine generated. The background of the machine for SYBR green is Ct=38 and for Taqman Ct=40. HSV-1 miRNA was measured using SYBR green and 1:40 dilution of RNA (100 µl of plasma, eluted in 14 µl); mCMV miRNA were measured using Taqman primers and 3 µl undiluted RNA (100 µlof plasma, eluted in 14 µl).
"no cDNA" control-negative control run with the RT reaction; includes cDNA synthesis master mix, water, and TaqMan MicroRNA 5X RT Assay, with no RNA added to the well.
"NTC"-no template control-negative control run with the qPCR step; includes TaqMan 2X Universal PCR Master Mix, TaqMan MicroRNA 20X TM Assay, water, with no cDNA added to the well.

Similarly, after intraperitoneal injection with mCMV, a betaherpesvirus, mcmv-miR-m23-3p was detectable only in the plasma of the infected mice (Table F.10). As previously reported (251), mcmv-miR-m59-2 detection by qPCR exhibited

non-specificity in mice, as there was no difference between control and virus-injected mice (Table F.11). Since mice are maintained in pathogen-free conditions, the detection of certain viral miRNAs in the plasma of non-infected mice may be due to primer specificity and/or similarity between the viral miRNA and mouse miRNAs. Taken together, these *in vivo* experiments suggest that viral miRNA can be detected in plasma post infection.

Discussion

MicroRNAs (miRNA) play an important regulatory role in gene expression. Numerous studies have shown that tumor cells can secrete miRNAs in plasma and can affect cells of distant origin. This is the first study to describe the presence of different viral miRNAs in human plasma at steady state. It is important to stress that this study cannot test for infectious profile as a result of miRNA presence and only demonstrates that select viral miRNAs are circulating at the time of participant visit. Though not established from these findings, it is possible that identifying viral miRNAs in human plasma could predict recurrent infection cycles as well as to identify miRNAs that may impact wide-ranging biological processes (252). The genomes of certain viruses are also known to encode miRNAs that may contribute to the regulation of the lytic vs. latent stages of the viral life cycle in their target cell (228). This suggests that establishing the basal human plasma miRNome could both provide insight into disease phenotypes as well as predict recurrent infectious cycles. Using a large cohort of

2763 participants in the FHS and an unbiased sequencing approach, we identified circulating viral miRNAs originating from DNA viruses and one from an RNA-retrovirus. Interestingly, most of the 11 viral miRNAs found in the FHS cohort are expressed during the latent phase of their respective viruses (253-257). The presence of these viral miRNAs in plasma was associated with inflammatory and thrombotic biomarkers. Targeted murine experiments confirmed that viral infections lead to the presence of select viral miRNAs in plasma. Since systemic-wide inflammation beyond the infected tissue during viral infections is poorly understood, circulating miRNAs may provide valuable information about infection progression and control.

In this study, all miRNAs originating from viruses using humans as a host were DNA viruses from the *Herpesviridae* family. Human plasma had detectable miRNAs only for beta and gammaherpesviruses. Our sequencing results showed the presence of hcmv-miR-US25mir-B25-2-3p in the plasma of all 40 participants included in the sequencing evaluation; however, by qPCR we were able to detect this miRNA in less than 0.7% of the entire cohort. The discrepancy between sequencing and RT-qPCR could be due to primer inability to target low levels of the miRNA. Human CMV is a betaherpesvirus that causes a persistent human infection and hcmv-miR-US25-2-3p is known to reduce viral replication by downregulation of host eukaryotic translation initiation factor 4A1 (258). By RT-qPCR we were also able to confirm presence of miRNAs coming from human viruses of the *Gammaherpesvirinae* subfamily (KSHV and EBV). In host cells,

two of the detected KSHV miRNAs are known to regulate cytokine secretion, cell survival, KSHV gene expression (kshv-miR-12-10a-5p) and endothelial cell reprogramming (kshv-miR-12-6-5p) (259-263). Interestingly, in two small cohorts of septic patients plasma (EDTA) levels of different KSHV miRNAs were also elevated, as one of them (kshv-miR-K12-12) exhibited higher levels in patients with African descent (264, 265). EBV, in turn, is a B-cell herpesvirus associated with many diverse B-cell lymphomas. The miRNA detected here, ebv-miR-BART11-5p, targets early B-cell factor 1, which is known to be critical for B-cell germinal center formation (CD40; BCR; PAX5) (266). Other EBV miRNAs have also been detected in plasma of patients with chronic lymphocytic leukemia (CLL) and correlate with shorter survival in two independent small cohorts (267). All miRNAs coming from human viruses associated with inflammatory biomarkers such as sICAM1, sTNFRII and osteoprotegerin.

In addition to viral miRNA originating from human viruses, we also detected two miRNA from HBV. The natural host for HBV is rhesus monkeys and the infection that it causes is mild and self-limiting (253). HBV has also been reported to infect humans zoonotically leading to certain neurological complications (253). HBV miRNAs were first identified in 2011 but their functional target in their natural host or in humans are not well understood. It has been suggested that hbv-miR-7-5p has late expression kinetics in viral replication and may, therefore, be involved in latency (253). Here we report that HBV miRNA present in human plasma associate with the inflammatory biomarkers sTNFRII

and sICAM1 (hbv-mir-B26-5p and hbv-mir-B7-5p) and with the prothrombotic P-selectin (hbv-mir-B7-5p).

In addition, we were able to detect miRNA from viruses that are not known to cause infection in humans. The natural hosts for these viruses are mice and domestic animal species such as chickens, turkey, swine and cattle. There is evidence that murine CMV has the potential to cross over the species barrier with the help of human CMV proteins (232); however, there are no reports on how this crossover may affect humans. Although we were able to detect one mCMV miRNA in the plasma of the FHS participants, this miRNA did not associate with any of the measured inflammatory biomarkers or phenotypical assessments. When it comes to the other viruses targeting domestic animals, three of them are from the *Alphaherpesvirinae* subfamily. For instance, MDV2 (and HVT) is an avian virus that is used for flock vaccination against Marek's disease characterized by T-cell lymphoma (268). Similarly, attenuated forms of the Gallid herpes virus 1 (ILTV) are used to vaccinate against infectious laryngotracheitis in chickens (269). There are no reports in the literature indicating that any of these avian viruses can cross over to humans, although alphaherpesviruses are promiscuous across species. Two of the viral miRNAs detected in the human plasma originate from *Suid herpesvirus 1* (SuHV1, or pseudorabies virus) known to cause Aujeszky's disease in swine (270). Aujeszky's disease is characterized by severe neurological symptoms and death particularly in young animals. The animals that recover can carry the virus latently with reoccurring shedding (270).

SuHV1 is known to be able to cross the species barrier and establish infection in other mammals such as cattle, sheep, dogs and others. Infections in humans are not well documented although there are limited cases in which neutralizing antibodies against the virus were detected in humans (271). In this study we were able to detect two miRNAs in human plasma and one of them associated with soluble ICAM-1. One of the miRNAs detected here came from BLV, a retrovirus using cattle as a host. During its replication BLV goes through a DNA-stage and has the ability to integrate into the host's DNA (272). In humans, antibodies against cattle virus BLV have been detected and elevated presence of BLV-DNA has been described in the epithelium of breast cancer patients (273). It has been postulated that BLV may be transmitted from cattle to humans by eating undercooked meat or drinking raw milk (272). It is unclear how these BLV viral miRNAs appear in human plasma; however, food ingestion or indirect contact may be possible routes of transmission. This study suggests that these viruses may enter human hosts, may sufficiently propagate to generate viral miRNA within the human bloodstream and the presence of these viral miRNAs associates with inflammatory and, in some cases, prothrombotic biomarkers.

Although the data is greatly strengthened by the size of the human population, a limitation of the cohort is the inadequate number of participants with documented oncological conditions, as participants with cancer comprised only 16% of the entire sample. The FHS was originally designed to study cardiovascular disease progression and this limited our ability to detect

associations with cancer or specific type of cancers. The analysis of an oncology-focused cohort for viral miRNA is warranted, particularly because many DNA and some RNA viral infections have been directly or indirectly associated with various types of cancer. There is increasing evidence that hCMV may be involved in the initiation and progression of breast cancer (240). EBV and KSHV are known to induce malignant phenotypes in immunocompromised hosts (233, 236). From the non-human viruses, BLV causes lymphoma in cattle. A recent case control study of 239 donors has shown that the frequency of BLV-DNA in mammary epithelium from women with breast cancer was significantly higher than in normal controls (272). The relationship between DNA viral infections and cancer has long been described in the literature, although the exact mechanisms are still under investigation.

Viral infections and many types of disease are characterized by an increase in inflammation. Regardless of the viral host target, nine of the eleven viral miRNAs that we identified in plasma were associated with at least one inflammatory marker and a number of these markers suggest connections between viral miRNA and disease states. Five of the viral miRNA associated with elevated levels of sTNFRII in plasma. Soluble TNFRII modulates biological functions of TNF-alpha by competing with cell surface receptors. Since TNF-alpha is a primary cytokine and levels fluctuate, levels of sTNFRs show high accuracy in measuring inflammation and prognosis of disease. It has been proposed that sTNFRII levels are a useful quantification of TH1 immune

response. In HIV and sepsis, levels of sTNFRII strongly correlate with progression of disease (274). Seven out of the eleven viral miRNAs also associated with changes in the levels of sICAM-1. sICAM-1 is an intracellular adhesion molecule and is released in plasma with increased inflammation and tissue damage. Circulating levels of sICAM1 have not only been associated with coronary heart and vascular disease but with infectious diseases such as malaria, sepsis, and dengue hemorrhagic fever, with severity of disease (275). Elevated serum levels of sICAM1 have also been associated with immune suppression in patients with chronic liver disease (276) and, in our study, seven out of the 11 viral miRNAs associated with sICAM1. Osteoprotegerin is a member of the tumor necrosis factor receptor superfamily and was initially discovered as a contributor to bone turnover homeostasis (277). Interestingly, patients with multiple myeloma have significantly lower levels of osteoprotegerin (278-280), and viruses such as KSHV are known to modulate osteoprotegerin levels in a COX2-dependent manner (281). Two of the viral miRNAs in this study, kshv-miR-K12-6-5p and mdv2-miR-M18-5p, significantly associated with osteoprotegerin. In summary, the overall presence of viral miRNAs in this human cohort is consistent with increased systemic inflammation.

The presence of viral miRNAs in human plasma has not been previously described in a large cohort and it is unclear what cells and what genes these miRNAs may target. Using whole blood mRNA transcripts measured concurrently with the viral miRNAs, we were able to identify novel co-expression relationships

between seven viral miRNAs and sixteen whole blood mRNAs. Additionally, by utilizing the seven nucleotide seeding sequence of each miRNA, we were able to predict two gene targets for miRNAs originating from non-human viruses, i.e. cattle BLV and avian ILTV. Our findings highlight the need for future molecular studies assessing targets and potential disease-related mechanisms for these plasma miRNAs in humans.

Using an unbiased, non-targeted approach, we were able to identify 19 different known viral miRNAs by sequencing, and we confirmed their presence by RT-qPCR in the plasma of the FHS Offspring Cohort Visit 8. There are, however, certain limitations to our study. First and foremost, we can only identify viral miRNAs that had already been identified and deposited to the Genboree database prior to our analysis. Thus, miRNA from other viruses may also be present but would not have been identified due to limitations in sequence information. In addition, there is a potential for primer cross-reactivity although this is mitigated in our study by the use of RT-qPCR in a very large number of samples to confirm the deep sequencing findings. Another important and related technical limitation is the small size of viral miRNAs and their similarity to host miRNA or to the miRNAs of other human viruses. Because of this concern we omitted hbv-mir-B26-3p-novel, mdv2-miR-M21-3p, rlcv-miR-rL1-17-3p, rlcv-miR-rL1-17-5p, rlcv-miR-rL1-29-3p, and hvt-miR-H14-3p from our full analyses and kept all miRNAs from human viruses. However, this does not necessarily mean that they are not present in the circulation and do not have an association with

inflammation or disease phenotypes. Because the fundamental observation that viral miRNAs are widely distributed in a human population has never been reported, we performed, as a proof of concept, murine viral infections to show presence of viral miRNA in the plasma post infection. However, this system itself presents an additional study limitation as, by design, it is modelling acute viral miRNA infection and does not assess the potential chronic findings associated with the observational cohort. Limitations of the co-expression model analysis have been previously described (282) and further work is necessary to prove mRNA targets, cell of interest and physiological implication for these viral miRNAs. Finally, the FHS Offspring Cohort Visit 8 population is older and of European descent and future ongoing studies in our laboratory are exploring whether these specific findings hold up in a racially and ethnically diverse sample as well as in younger individuals.

In conclusion, this is the first large study to identify expression of viral miRNAs in human plasma originating from viruses that can infect humans as well as animals to which humans are exposed or may consume. These miRNAs, regardless of primary host target, associated with inflammatory and thrombotic biomarkers but did not associate with specific disease phenotypes. Further studies are necessary to include broader, more inclusive populations as well as to understand the mechanistic relationship between plasma viral miRNA, inflammation and cancer.

APPENDIX G: GENE EXPRESSION OF HUMAN UMBILICAL VEIN ENDOTHELIAL CELLS (HUVECs)

Permissions

Appendix G is a table excerpt from a published manuscript, included with permission.

- *Clancy L, Beaulieu LM, Tanriverdi K, Freedman JE. (2017).The role of RNA uptake in platelet heterogeneity. Thromb Haemost, 117(5), 948-961*
    - Permission Information: Copyright Permission No 116/06/2017

Author Contributions

L.C. performed all experiments and analyses unless noted below. L.C. wrote manuscript. J.E.F. oversaw overall project development and coordination. L.M.B performed initial platelet sorting experiments. K.T. performed high throughput gene expression analyses. All authors commented on the interpretation of results, and reviewed and approved the manuscript.

Table G.1: Differential gene expression in HUVECs. RT-qPCR results for genes of interest in HUVECs after platelet incubation under normal *in vitro* simulated clot conditions (A) or with pretreatment transcription shutdown in HUVECs (B). RT-qPCR normalized to two genes, *CD63* and *CD81*, with HUVEC alone samples as experimental controls. Additional table legend below table denotes sample setup conditions. A) Results represent *n*=6 experiments. B) Results represent *n*=3 experiments. C) RNA sequencing of genes of interest from HUVEC RNA profile previously published (222).

A)	ECs Alone	Stimulated Ecs	Unstimulated ECs Post Platelet	Stimulated ECs Post Stimulated
CXADR	1.0	-1.0	1.0	1.0
COL18A1	1.0	1.0	1.1	1.4
SELE	1.0	7.4	18.4	79.2
ICAM1	1.0	2.4	3.6	4.7
ITGA5	1.0	1.2	1.3	1.3
TLR3	1.0	-1.1	1.2	1.4
CXCL1	1.0	2.2	8.2	18.0
CXCL12	1.0	1.1	1.8	2.3
TLR4	1.0	-1.0	1.5	1.7
KIAA1462	1.0	1.2	1.1	1.0
CX3CL1	1.0	2.5	2.9	5.7
IL6	1.0	1.3	1.4	2.4
VCAM1	1.0	4.4	4.2	9.4
CD81	1.0	-1.0	1.1	1.1
CXCL2	1.0	3.8	6.2	15.2
EIF4G1	1.0	1.1	1.2	1.5
TNFSF10	1.0	-1.0	1.0	1.0
CALR	1.0	-1.0	1.4	1.3
ASGR1	1.0	1.2	-3.0	-2.4
VEGFA	1.0	1.2	2.2	4.6
IL8	1.0	2.8	9.6	31.6
SIRPA	1.0	-1.1	1.4	1.5
VEGFB	1.0	-1.1	1.2	1.5
VAMP5	1.0	1.0	-1.1	1.3
VIP	1.0	1.1	1.3	2.1
CRP	1.0	-1.7	1.4	-1.4
IFNA1	1.0	1.8	8.9	2.8
TNFRSF1B	1.0	1.1	1.0	-2.6
CCL7	1.0	1.3	3.0	2.0
NFKBIA	1.0	1.6	4.9	7.4
CD63	1.0	1.0	-1.1	-1.1
SELENBP1	1.0	-1.1	-1.1	-2.5
DICER1	1.0	-1.1	1.3	1.3
KIAA0232	1.0	-1.1	1.4	1.5
IFITM3	1.0	1.2	1.4	1.9
MAP4K4	1.0	1.1	1.2	1.4
CXCL6	1.0	1.3	1.8	3.6
VEGFC	1.0	1.3	1.5	1.9
Platelets	-	-	+	+
Platelet Thrombin Stimulation	-	-	-	+
EC Incubation	+	+	+	+
EC Transcription Shutdown	-	-	-	-
EC Thrombin Stimulation	-	+	-	+

B)	ECs Alone	Stimulated Ecs	Unstimulated ECs Post Platelet	Stimulated ECs Post Stimulated
CXADR	1	1.1	1.1	1.2
COL18A1	1	1.0	1.1	1.3
SELE	1	2.6	6.4	6.7
ICAM1	1	1.0	2.1	1.4
ITGA5	1	1.6	1.6	1.5
TLR3	1	1.7	1.6	1.7
CXCL1	1	2.2	3.6	4.4
CXCL12	1	1.5	2.0	1.6
TLR4	1	1.3	1.6	1.8
KIAA1462	1	1.2	1.4	1.2
CX3CL1	1	1.4	2.8	1.3
IL6	1	2.4	1.1	4.1
VCAM1	1	1.9	3.6	2.4
CD81	1	-1.2	-1.3	-1.2
CXCL2	1	3.2	2.1	6.2
EIF4G1	1	1.3	1.2	1.2
TNFSF10	1	1.4	1.3	1.4
CALR	1	1.1	1.3	1.4
ASGR1	1	1.8	1.5	-5.8
VEGFA	1	1.6	1.5	2.3
IL8	1	2.1	1.8	4.6
SIRPA	1	1.5	1.2	1.3
VEGFB	1	1.3	1.4	1.5
VAMP5	1	1.2	-1.0	1.1
VIP	1	2.2	1.4	2.6
CRP	1	20.3	339.7	41.3
IFNA1	1	1.5	3.3	3.2
TNFRSF1B	1	-1.2	-1.0	-1.2
CCL7	1	-1.4	-1.1	1.2
NFKBIA	1	1.9	3.2	4.4
CD63	1	1.1	1.2	1.2
SELENBP1	1	1.2	1.1	1.2
DICER1	1	1.2	1.5	1.5
KIAA0232	1	1.5	1.8	1.8
IFITM3	1	1.4	1.2	1.6
MAP4K4	1	1.2	1.2	1.4
CXCL6	1	1.2	2.0	1.6
VEGFC	1	1.4	1.4	1.5

Platelets	-	-	+	+
Platelet Thrombin Stimulation	-	-	-	+
EC Incubation	+	+	+	+
EC Transcripton Shutdown	+	+	+	+
EC Thrombin Stimulation	-	+	-	+

C)	RPKM Avg
CXADR	0.7
COL18A1	133.5
SELE	4.4
ICAM1	21.0
ITGA5	404.2
TLR3	0.6
CXCL1	10.8
CXCL12	0.1
TLR4	24.2
KIAA1462	12.4
CX3CL1	1.1
IL6	2.7
VCAM1	12.5
CD81	35.5
CXCL2	4.0
EIF4G1	71.6
TNFSF10	21.6
CALR	925.4
ASGR1	1.2
VEGFA	2.0
IL8	21.3
SIRPA	20.0
VEGFB	28.1
VAMP5	64.8
VIP	1.2
CRP	0.0
IFNA1	0.0
TNFRSF1B	25.7
CCL7	0.7
NFKBIA	23.5
CD63	169.1
SELENBP1	6.0
DICER1	5.5
KIAA0232	6.0
IFITM3	163.2
MAP4K4	45.2
CXCL6	1.0
VEGFC	13.8

REFERENCES

1. Robinson JT, Thorvaldsdottir H, Winckler W, Guttman M, Lander ES, Getz G, et al. Integrative genomics viewer. Nat Biotechnol. 2011 Jan;29(1):24-6.
2. Thorvaldsdottir H, Robinson JT, Mesirov JP. Integrative Genomics Viewer (IGV): high-performance genomics data visualization and exploration. Brief Bioinform. 2013 Mar;14(2):178-92.
3. Clark SR, Ma AC, Tavener SA, McDonald B, Goodarzi Z, Kelly MM, et al. Platelet TLR4 activates neutrophil extracellular traps to ensnare bacteria in septic blood. Nat Med. 2007 Apr;13(4):463-9.
4. Robb-Smith AH. Why the platelets were discovered. Br J Haematol. 1967 Jul;13(4):618-37.
5. Brewer DB. Max Schultze (1865), G. Bizzozero (1882) and the discovery of the platelet. Br J Haematol. 2006 May;133(3):251-8.
6. Michelson AD. Platelets. 3rd ed. London ; Waltham, MA: Academic Press; 2013.
7. Ghoshal K, Bhattacharyya M. Overview of platelet physiology: its hemostatic and nonhemostatic role in disease pathogenesis. ScientificWorldJournal. 2014;2014:781857.
8. Drelich DA, Bray PF. The Traditional Role of Platelets in Hemostasis. In: Kerrigan S, Moran N, editors. The Non-Thrombotic Role of Platelets in Health and Disease. Rijeka: InTech; 2015. p. Ch. 02.
9. Giles C. The platelet count and mean platelet volume. Br J Haematol. 1981 May;48(1):31-7.
10. Nakeff A, Maat B. Separation of megakaryocytes from mouse bone marrow by velocity sedimentation. Blood. 1974 Apr;43(4):591-5.
11. Machlus KR, Italiano JE, Jr. The incredible journey: From megakaryocyte development to platelet formation. J Cell Biol. 2013 Jun 10;201(6):785-96.
12. Italiano JE, Jr., Lecine P, Shivdasani RA, Hartwig JH. Blood platelets are assembled principally at the ends of proplatelet processes produced by differentiated megakaryocytes. J Cell Biol. 1999 Dec 13;147(6):1299-312.
13. Patel SR, Hartwig JH, Italiano JE, Jr. The biogenesis of platelets from megakaryocyte proplatelets. J Clin Invest. 2005 Dec;115(12):3348-54.
14. Schulze H, Korpal M, Hurov J, Kim SW, Zhang J, Cantley LC, et al. Characterization of the megakaryocyte demarcation membrane system and its role in thrombopoiesis. Blood. 2006 May 15;107(10):3868-75.
15. Tablin F, Castro M, Leven RM. Blood platelet formation in vitro. The role of the cytoskeleton in megakaryocyte fragmentation. J Cell Sci. 1990 Sep;97 (Pt 1):59-70.
16. Schwer HD, Lecine P, Tiwari S, Italiano JE, Jr., Hartwig JH, Shivdasani RA. A lineage-restricted and divergent beta-tubulin isoform is essential for the biogenesis, structure and function of blood platelets. Curr Biol. 2001 Apr 17;11(8):579-86.
17. Handagama PJ, Feldman BF, Jain NC, Farver TB, Kono CS. In vitro platelet release by rat megakaryocytes: effect of metabolic inhibitors and cytoskeletal disrupting agents. Am J Vet Res. 1987 Jul;48(7):1142-6.
18. Patel SR, Richardson JL, Schulze H, Kahle E, Galjart N, Drabek K, et al. Differential roles of microtubule assembly and sliding in proplatelet formation by megakaryocytes. Blood. 2005 Dec 15;106(13):4076-85.

19. Richardson JL, Shivdasani RA, Boers C, Hartwig JH, Italiano JE, Jr. Mechanisms of organelle transport and capture along proplatelets during platelet production. Blood. 2005 Dec 15;106(13):4066-75.
20. Cecchetti L, Tolley ND, Michetti N, Bury L, Weyrich AS, Gresele P. Megakaryocytes differentially sort mRNAs for matrix metalloproteinases and their inhibitors into platelets: a mechanism for regulating synthetic events. Blood. 2011 Aug 18;118(7):1903-11.
21. Thon JN, Montalvo A, Patel-Hett S, Devine MT, Richardson JL, Ehrlicher A, et al. Cytoskeletal mechanics of proplatelet maturation and platelet release. J Cell Biol. 2010 Nov 15;191(4):861-74.
22. Hartwig JH, Italiano JE, Jr. Cytoskeletal mechanisms for platelet production. Blood Cells Mol Dis. 2006 Mar-Apr;36(2):99-103.
23. Zhang L, Orban M, Lorenz M, Barocke V, Braun D, Urtz N, et al. A novel role of sphingosine 1-phosphate receptor S1pr1 in mouse thrombopoiesis. J Exp Med. 2012 Nov 19;209(12):2165-81.
24. Schachtner H, Calaminus SD, Sinclair A, Monypenny J, Blundell MP, Leon C, et al. Megakaryocytes assemble podosomes that degrade matrix and protrude through basement membrane. Blood. 2013 Mar 28;121(13):2542-52.
25. Schwertz H, Koster S, Kahr WH, Michetti N, Kraemer BF, Weitz DA, et al. Anucleate platelets generate progeny. Blood. 2010 May 06;115(18):3801-9.
26. Thon JN, Devine MT, Jurak Begonja A, Tibbitts J, Italiano JE, Jr. High-content live-cell imaging assay used to establish mechanism of trastuzumab emtansine (T-DM1)--mediated inhibition of platelet production. Blood. 2012 Sep 06;120(10):1975-84.
27. Thon JN, Macleod H, Begonja AJ, Zhu J, Lee KC, Mogilner A, et al. Microtubule and cortical forces determine platelet size during vascular platelet production. Nat Commun. 2012 May 22;3:852.
28. Martin J, Trowbridge A, European Society of Clinical Investigation. Meeting. Platelet heterogeneity : biology and pathology. London ; New York: Springer-Verlag; 1990.
29. Bath PM, Butterworth RJ. Platelet size: measurement, physiology and vascular disease. Blood Coagul Fibrinolysis. 1996 Mar;7(2):157-61.
30. Kamath S, Blann AD, Lip GY. Platelet activation: assessment and quantification. Eur Heart J. 2001 Sep;22(17):1561-71.
31. Berger JS, Eraso LH, Xie D, Sha D, Mohler ER, 3rd. Mean platelet volume and prevalence of peripheral artery disease, the National Health and Nutrition Examination Survey, 1999-2004. Atherosclerosis. 2010 Dec;213(2):586-91.
32. Chu SG, Becker RC, Berger PB, Bhatt DL, Eikelboom JW, Konkle B, et al. Mean platelet volume as a predictor of cardiovascular risk: a systematic review and meta-analysis. J Thromb Haemost. 2010 Jan;8(1):148-56.
33. Slavka G, Perkmann T, Haslacher H, Greisenegger S, Marsik C, Wagner OF, et al. Mean platelet volume may represent a predictive parameter for overall vascular mortality and ischemic heart disease. Arterioscler Thromb Vasc Biol. 2011 May;31(5):1215-8.
34. Kunicki TJ, Williams SA, Nugent DJ, Yeager M. Mean platelet volume and integrin alleles correlate with levels of integrins alpha(IIb)beta(3) and alpha(2)beta(1) in acute coronary syndrome patients and normal subjects. Arterioscler Thromb Vasc Biol. 2012 Jan;32(1):147-52.

35. Habart D, Cheli Y, Nugent DJ, Ruggeri ZM, Kunicki TJ. Conditional knockout of integrin alpha2beta1 in murine megakaryocytes leads to reduced mean platelet volume. PLoS One. 2013;8(1):e55094.
36. Gieger C, Radhakrishnan A, Cvejic A, Tang W, Porcu E, Pistis G, et al. New gene functions in megakaryopoiesis and platelet formation. Nature. 2011 Nov 30;480(7376):201-8.
37. Lackie JM. A dictionary of biomedicine. 1st ed. Oxford: Oxford University Press; 2010.
38. Jurk K, Kehrel BE. Platelets: physiology and biochemistry. Semin Thromb Hemost. 2005;31(4):381-92.
39. Boilard E, Nigrovic PA, Larabee K, Watts GF, Coblyn JS, Weinblatt ME, et al. Platelets amplify inflammation in arthritis via collagen-dependent microparticle production. Science. 2010 Jan 29;327(5965):580-3.
40. Gasparyan AY, Stavropoulos-Kalinoglou A, Mikhailidis DP, Douglas KM, Kitas GD. Platelet function in rheumatoid arthritis: arthritic and cardiovascular implications. Rheumatol Int. 2011 Feb;31(2):153-64.
41. Knijff-Dutmer EA, Koerts J, Nieuwland R, Kalsbeek-Batenburg EM, van de Laar MA. Elevated levels of platelet microparticles are associated with disease activity in rheumatoid arthritis. Arthritis Rheum. 2002 Jun;46(6):1498-503.
42. Boilard E, Blanco P, Nigrovic PA. Platelets: active players in the pathogenesis of arthritis and SLE. Nat Rev Rheumatol. 2012 Sep;8(9):534-42.
43. Harifi G, Sibilia J. Pathogenic role of platelets in rheumatoid arthritis and systemic autoimmune diseases. Perspectives and therapeutic aspects. Saudi Med J. 2016 Apr;37(4):354-60.
44. Zimmerman GA, Weyrich AS. Immunology. Arsonists in rheumatoid arthritis. Science. 2010 Jan 29;327(5965):528-9.
45. Vieira-de-Abreu A, Campbell RA, Weyrich AS, Zimmerman GA. Platelets: versatile effector cells in hemostasis, inflammation, and the immune continuum. Semin Immunopathol. 2012 Jan;34(1):5-30.
46. Garraud O, Cognasse F. Platelet Toll-like receptor expression: the link between "danger" ligands and inflammation. Inflamm Allergy Drug Targets. 2010 Dec;9(5):322-33.
47. Semple JW, Freedman J. Platelets and innate immunity. Cell Mol Life Sci. 2010 Feb;67(4):499-511.
48. Beaulieu LM, Freedman JE. The role of inflammation in regulating platelet production and function: Toll-like receptors in platelets and megakaryocytes. Thromb Res. 2010 Mar;125(3):205-9.
49. Shiraki R, Inoue N, Kawasaki S, Takei A, Kadotani M, Ohnishi Y, et al. Expression of Toll-like receptors on human platelets. Thromb Res. 2004;113(6):379-85.
50. Andonegui G, Kerfoot SM, McNagny K, Ebbert KV, Patel KD, Kubes P. Platelets express functional Toll-like receptor-4. Blood. 2005 Oct 1;106(7):2417-23.
51. Cognasse F, Hamzeh H, Chavarin P, Acquart S, Genin C, Garraud O. Evidence of Toll-like receptor molecules on human platelets. Immunol Cell Biol. 2005 Apr;83(2):196-8.
52. Aslam R, Speck ER, Kim M, Crow AR, Bang KW, Nestel FP, et al. Platelet Toll-like receptor expression modulates lipopolysaccharide-induced thrombocytopenia and tumor necrosis factor-alpha production in vivo. Blood. 2006 Jan 15;107(2):637-41.

53. Freedman JE, Larson MG, Tanriverdi K, O'Donnell CJ, Morin K, Hakanson AS, et al. Relation of platelet and leukocyte inflammatory transcripts to body mass index in the Framingham heart study. Circulation. 2010 Jul 13;122(2):119-29.
54. Ma AC, Kubes P. Platelets, neutrophils, and neutrophil extracellular traps (NETs) in sepsis. J Thromb Haemost. 2008 Mar;6(3):415-20.
55. Koupenova M, Vitseva O, MacKay CR, Beaulieu LM, Benjamin EJ, Mick E, et al. Platelet-TLR7 mediates host survival and platelet count during viral infection in the absence of platelet-dependent thrombosis. Blood. 2014 Jul 31;124(5):791-802.
56. Cognasse F, Nguyen KA, Damien P, McNicol A, Pozzetto B, Hamzeh-Cognasse H, et al. The Inflammatory Role of Platelets via Their TLRs and Siglec Receptors. Front Immunol. 2015;6:83.
57. Assinger A. Platelets and infection - an emerging role of platelets in viral infection. Front Immunol. 2014;5:649.
58. Zhang G, Han J, Welch EJ, Ye RD, Voyno-Yasenetskaya TA, Malik AB, et al. Lipopolysaccharide stimulates platelet secretion and potentiates platelet aggregation via TLR4/MyD88 and the cGMP-dependent protein kinase pathway. J Immunol. 2009 Jun 15;182(12):7997-8004.
59. McDonald B, Urrutia R, Yipp BG, Jenne CN, Kubes P. Intravascular neutrophil extracellular traps capture bacteria from the bloodstream during sepsis. Cell Host Microbe. 2012 Sep 13;12(3):324-33.
60. Mueller BM, Reisfeld RA, Edgington TS, Ruf W. Expression of tissue factor by melanoma cells promotes efficient hematogenous metastasis. Proc Natl Acad Sci U S A. 1992 Dec 15;89(24):11832-6.
61. Gay LJ, Felding-Habermann B. Contribution of platelets to tumour metastasis. Nat Rev Cancer. 2011 Feb;11(2):123-34.
62. Young A, Chapman O, Connor C, Poole C, Rose P, Kakkar AK. Thrombosis and cancer. Nat Rev Clin Oncol. 2012 Jul 10;9(8):437-49.
63. Menter DG, Tucker SC, Kopetz S, Sood AK, Crissman JD, Honn KV. Platelets and cancer: a casual or causal relationship: revisited. Cancer Metastasis Rev. 2014 Mar;33(1):231-69.
64. Sabrkhany S, Griffioen AW, Oude Egbrink MG. The role of blood platelets in tumor angiogenesis. Biochim Biophys Acta. 2011 Apr;1815(2):189-96.
65. Tesselaar ME, Romijn FP, Van Der Linden IK, Prins FA, Bertina RM, Osanto S. Microparticle-associated tissue factor activity: a link between cancer and thrombosis? J Thromb Haemost. 2007 Mar;5(3):520-7.
66. Sun NC, McAfee WM, Hum GJ, Weiner JM. Hemostatic abnormalities in malignancy, a prospective study of one hundred eight patients. Part I. Coagulation studies. Am J Clin Pathol. 1979 Jan;71(1):10-6.
67. Mohle R, Green D, Moore MA, Nachman RL, Rafii S. Constitutive production and thrombin-induced release of vascular endothelial growth factor by human megakaryocytes and platelets. Proc Natl Acad Sci U S A. 1997 Jan 21;94(2):663-8.
68. Wartiovaara U, Salven P, Mikkola H, Lassila R, Kaukonen J, Joukov V, et al. Peripheral blood platelets express VEGF-C and VEGF which are released during platelet activation. Thromb Haemost. 1998 Jul;80(1):171-5.
69. Heldin CH, Westermark B. Mechanism of action and in vivo role of platelet-derived growth factor. Physiol Rev. 1999 Oct;79(4):1283-316.

70. Heldin CH. Targeting the PDGF signaling pathway in tumor treatment. Cell Commun Signal. 2013;11:97.
71. Pinedo HM, Verheul HM, D'Amato RJ, Folkman J. Involvement of platelets in tumour angiogenesis? Lancet. 1998 Nov 28;352(9142):1775-7.
72. Verheul HM, Pinedo HM. The role of vascular endothelial growth factor (VEGF) in tumor angiogenesis and early clinical development of VEGF-receptor kinase inhibitors. Clin Breast Cancer. 2000 Sep;1 Suppl 1:S80-4.
73. Jain S, Harris J, Ware J. Platelets: linking hemostasis and cancer. Arterioscler Thromb Vasc Biol. 2010 Dec;30(12):2362-7.
74. Ibele GM, Kay NE, Johnson GJ, Jacob HS. Human platelets exert cytotoxic effects on tumor cells. Blood. 1985 May;65(5):1252-5.
75. Jurasz P, Alonso-Escolano D, Radomski MW. Platelet--cancer interactions: mechanisms and pharmacology of tumour cell-induced platelet aggregation. Br J Pharmacol. 2004 Dec;143(7):819-26.
76. Niers TM, Klerk CP, DiNisio M, Van Noorden CJ, Buller HR, Reitsma PH, et al. Mechanisms of heparin induced anti-cancer activity in experimental cancer models. Crit Rev Oncol Hematol. 2007 Mar;61(3):195-207.
77. Wang Y, Zhang H. Platelet-induced inhibition of tumor cell growth. Thromb Res. 2008;123(2):324-30.
78. Zimmerman GA, Weyrich AS. Signal-dependent protein synthesis by activated platelets: new pathways to altered phenotype and function. Arterioscler Thromb Vasc Biol. 2008 Mar;28(3):s17-24.
79. Weyrich AS, Schwertz H, Kraiss LW, Zimmerman GA. Protein synthesis by platelets: historical and new perspectives. J Thromb Haemost. 2009 Feb;7(2):241-6.
80. Rowley JW, Oler AJ, Tolley ND, Hunter BN, Low EN, Nix DA, et al. Genome-wide RNA-seq analysis of human and mouse platelet transcriptomes. Blood. 2011 Oct 6;118(14):e101-11.
81. Bugert P, Dugrillon A, Gunaydin A, Eichler H, Kluter H. Messenger RNA profiling of human platelets by microarray hybridization. Thromb Haemost. 2003 Oct;90(4):738-48.
82. Gnatenko DV, Dunn JJ, McCorkle SR, Weissmann D, Perrotta PL, Bahou WF. Transcript profiling of human platelets using microarray and serial analysis of gene expression. Blood. 2003 Mar 15;101(6):2285-93.
83. Rowley JW, Schwertz H, Weyrich AS. Platelet mRNA: the meaning behind the message. Curr Opin Hematol. 2012 Sep;19(5):385-91.
84. Bray PF, McKenzie SE, Edelstein LC, Nagalla S, Delgrosso K, Ertel A, et al. The complex transcriptional landscape of the anucleate human platelet. BMC Genomics. 2013;14:1.
85. Kissopoulou A, Jonasson J, Lindahl TL, Osman A. Next generation sequencing analysis of human platelet PolyA+ mRNAs and rRNA-depleted total RNA. PLoS One. 2013;8(12):e81809.
86. Ple H, Landry P, Benham A, Coarfa C, Gunaratne PH, Provost P. The repertoire and features of human platelet microRNAs. PLoS One. 2012;7(12):e50746.
87. Huang Y, Shen XJ, Zou Q, Wang SP, Tang SM, Zhang GZ. Biological functions of microRNAs: a review. J Physiol Biochem. 2011 Mar;67(1):129-39.
88. Denis MM, Tolley ND, Bunting M, Schwertz H, Jiang H, Lindemann S, et al. Escaping the nuclear confines: signal-dependent pre-mRNA splicing in anucleate platelets. Cell. 2005 Aug 12;122(3):379-91.

89. Nagalla S, Shaw C, Kong X, Kondkar AA, Edelstein LC, Ma L, et al. Platelet microRNA-mRNA coexpression profiles correlate with platelet reactivity. Blood. 2011 May 12;117(19):5189-97.
90. Landry P, Plante I, Ouellet DL, Perron MP, Rousseau G, Provost P. Existence of a microRNA pathway in anucleate platelets. Nat Struct Mol Biol. 2009 Sep;16(9):961-6.
91. Zampetaki A, Willeit P, Tilling L, Drozdov I, Prokopi M, Renard JM, et al. Prospective study on circulating MicroRNAs and risk of myocardial infarction. J Am Coll Cardiol. 2012 Jul 24;60(4):290-9.
92. Schulte C, Molz S, Appelbaum S, Karakas M, Ojeda F, Lau DM, et al. miRNA-197 and miRNA-223 Predict Cardiovascular Death in a Cohort of Patients with Symptomatic Coronary Artery Disease. PLoS One. 2015;10(12):e0145930.
93. Shi R, Zhou X, Ji WJ, Zhang YY, Ma YQ, Zhang JQ, et al. The Emerging Role of miR-223 in Platelet Reactivity: Implications in Antiplatelet Therapy. Biomed Res Int. 2015;2015:981841.
94. Sunderland N, Skroblin P, Barwari T, Huntley RP, Lu R, Joshi A, et al. MicroRNA Biomarkers and Platelet Reactivity: The Clot Thickens. Circ Res. 2017 Jan 20;120(2):418-35.
95. Darrow AL, Fung-Leung WP, Ye RD, Santulli RJ, Cheung WM, Derian CK, et al. Biological consequences of thrombin receptor deficiency in mice. Thromb Haemost. 1996 Dec;76(6):860-6.
96. Connolly AJ, Ishihara H, Kahn ML, Farese RV, Jr., Coughlin SR. Role of the thrombin receptor in development and evidence for a second receptor. Nature. 1996 Jun 6;381(6582):516-9.
97. Ishihara H, Zeng D, Connolly AJ, Tam C, Coughlin SR. Antibodies to protease-activated receptor 3 inhibit activation of mouse platelets by thrombin. Blood. 1998 Jun 1;91(11):4152-7.
98. Tsakiris DA, Scudder L, Hodivala-Dilke K, Hynes RO, Coller BS. Hemostasis in the mouse (Mus musculus): a review. Thromb Haemost. 1999 Feb;81(2):177-88.
99. Terashita Z, Imura Y, Nishikawa K. Inhibition by CV-3988 of the binding of [3H]-platelet activating factor (PAF) to the platelet. Biochem Pharmacol. 1985 May 1;34(9):1491-5.
100. Simon LM, Edelstein LC, Nagalla S, Woodley AB, Chen ES, Kong X, et al. Human platelet microRNA-mRNA networks associated with age and gender revealed by integrated plateletomics. Blood. 2014 Apr 17;123(16):e37-45.
101. Edelstein LC, Simon LM, Montoya RT, Holinstat M, Chen ES, Bergeron A, et al. Racial differences in human platelet PAR4 reactivity reflect expression of PCTP and miR-376c. Nat Med. 2013 Dec;19(12):1609-16.
102. Lood C, Amisten S, Gullstrand B, Jonsen A, Allhorn M, Truedsson L, et al. Platelet transcriptional profile and protein expression in patients with systemic lupus erythematosus: up-regulation of the type I interferon system is strongly associated with vascular disease. Blood. 2010 Sep 16;116(11):1951-7.
103. Jain S, Kapetanaki MG, Raghavachari N, Woodhouse K, Yu G, Barge S, et al. Expression of regulatory platelet microRNAs in patients with sickle cell disease. PLoS One. 2013;8(4):e60932.
104. Healy AM, Pickard MD, Pradhan AD, Wang Y, Chen Z, Croce K, et al. Platelet expression profiling and clinical validation of myeloid-related protein-14 as a novel determinant of cardiovascular events. Circulation. 2006 May 16;113(19):2278-84.
105. Eicher JD, Wakabayashi Y, Vitseva O, Esa N, Yang Y, Zhu J, et al. Characterization of the platelet transcriptome by RNA sequencing in patients with acute myocardial infarction. Platelets. 2016;27(3):230-9.

106. Gnatenko DV, Zhu W, Xu X, Samuel ET, Monaghan M, Zarrabi MH, et al. Class prediction models of thrombocytosis using genetic biomarkers. Blood. 2010 Jan 7;115(1):7-14.
107. Xu X, Gnatenko DV, Ju J, Hitchcock IS, Martin DW, Zhu W, et al. Systematic analysis of microRNA fingerprints in thrombocythemic platelets using integrated platforms. Blood. 2012 Oct 25;120(17):3575-85.
108. Mills EW, Green R, Ingolia NT. Slowed decay of mRNAs enhances platelet specific translation. Blood. 2017 Apr 27;129(17):e38-e48.
109. Shashkin PN, Brown GT, Ghosh A, Marathe GK, McIntyre TM. Lipopolysaccharide is a direct agonist for platelet RNA splicing. J Immunol. 2008 Sep 1;181(5):3495-502.
110. Lindemann S, Tolley ND, Dixon DA, McIntyre TM, Prescott SM, Zimmerman GA, et al. Activated platelets mediate inflammatory signaling by regulated interleukin 1beta synthesis. J Cell Biol. 2001 Aug 6;154(3):485-90.
111. Brown GT, Narayanan P, Li W, Silverstein RL, McIntyre TM. Lipopolysaccharide stimulates platelets through an IL-1beta autocrine loop. J Immunol. 2013 Nov 15;191(10):5196-203.
112. McRedmond JP, Park SD, Reilly DF, Coppinger JA, Maguire PB, Shields DC, et al. Integration of proteomics and genomics in platelets: a profile of platelet proteins and platelet-specific genes. Mol Cell Proteomics. 2004 Feb;3(2):133-44.
113. Londin ER, Hatzimichael E, Loher P, Edelstein L, Shaw C, Delgrosso K, et al. The human platelet: strong transcriptome correlations among individuals associate weakly with the platelet proteome. Biol Direct. 2014;9:3.
114. Risitano A, Beaulieu LM, Vitseva O, Freedman JE. Platelets and platelet-like particles mediate intercellular RNA transfer. Blood. 2012 Jun 28;119(26):6288-95.
115. Aatonen M, Gronholm M, Siljander PR. Platelet-derived microvesicles: multitalented participants in intercellular communication. Semin Thromb Hemost. 2012 Feb;38(1):102-13.
116. Heijnen HF, Schiel AE, Fijnheer R, Geuze HJ, Sixma JJ. Activated platelets release two types of membrane vesicles: microvesicles by surface shedding and exosomes derived from exocytosis of multivesicular bodies and alpha-granules. Blood. 1999 Dec 1;94(11):3791-9.
117. Montecalvo A, Larregina AT, Shufesky WJ, Stolz DB, Sullivan ML, Karlsson JM, et al. Mechanism of transfer of functional microRNAs between mouse dendritic cells via exosomes. Blood. 2012 Jan 19;119(3):756-66.
118. Valadi H, Ekstrom K, Bossios A, Sjostrand M, Lee JJ, Lotvall JO. Exosome-mediated transfer of mRNAs and microRNAs is a novel mechanism of genetic exchange between cells. Nat Cell Biol. 2007 Jun;9(6):654-9.
119. Wahlgren J, De LKT, Brisslert M, Vaziri Sani F, Telemo E, Sunnerhagen P, et al. Plasma exosomes can deliver exogenous short interfering RNA to monocytes and lymphocytes. Nucleic Acids Res. 2012 Sep 1;40(17):e130.
120. Gidlof O, van der Brug M, Ohman J, Gilje P, Olde B, Wahlestedt C, et al. Platelets activated during myocardial infarction release functional miRNA, which can be taken up by endothelial cells and regulate ICAM1 expression. Blood. 2013 May 9;121(19):3908-17, S1-26.
121. Laffont B, Corduan A, Ple H, Duchez AC, Cloutier N, Boilard E, et al. Activated platelets can deliver mRNA regulatory Ago2*microRNA complexes to endothelial cells via microparticles. Blood. 2013 Jul 11;122(2):253-61.

122. Liang H, Yan X, Pan Y, Wang Y, Wang N, Li L, et al. MicroRNA-223 delivered by platelet-derived microvesicles promotes lung cancer cell invasion via targeting tumor suppressor EPB41L3. Mol Cancer. 2015 Mar 11;14:58.
123. Kirschbaum M, Karimian G, Adelmeijer J, Giepmans BN, Porte RJ, Lisman T. Horizontal RNA transfer mediates platelet-induced hepatocyte proliferation. Blood. 2015 Jun 8.
124. Laffont B, Corduan A, Rousseau M, Duchez AC, Lee CH, Boilard E, et al. Platelet microparticles reprogram macrophage gene expression and function. Thromb Haemost. 2015 Sep 3;115(1).
125. Michael JV, Wurtzel JGT, Mao GF, Rao AK, Kolpakov MA, Sabri A, et al. Platelet microparticles infiltrating solid tumors transfer miRNAs that suppress tumor growth. Blood. 2017 May 12.
126. Takeuchi K, Satoh M, Kuno H, Yoshida T, Kondo H, Takeuchi M. Platelet-like particle formation in the human megakaryoblastic leukaemia cell lines, MEG-01 and MEG-01s. Br J Haematol. 1998 Feb;100(2):436-44.
127. Baj-Krzyworzeka M, Szatanek R, Weglarczyk K, Baran J, Urbanowicz B, Branski P, et al. Tumour-derived microvesicles carry several surface determinants and mRNA of tumour cells and transfer some of these determinants to monocytes. Cancer Immunol Immunother. 2006 Jul;55(7):808-18.
128. Kahr WH, Hinckley J, Li L, Schwertz H, Christensen H, Rowley JW, et al. Mutations in NBEAL2, encoding a BEACH protein, cause gray platelet syndrome. Nat Genet. 2011 Aug;43(8):738-40.
129. Gunay-Aygun M, Falik-Zaccai TC, Vilboux T, Zivony-Elboum Y, Gumruk F, Cetin M, et al. NBEAL2 is mutated in gray platelet syndrome and is required for biogenesis of platelet alpha-granules. Nat Genet. 2011 Jul 17;43(8):732-4.
130. Albers CA, Cvejic A, Favier R, Bouwmans EE, Alessi MC, Bertone P, et al. Exome sequencing identifies NBEAL2 as the causative gene for gray platelet syndrome. Nat Genet. 2011 Jul 17;43(8):735-7.
131. Deppermann C, Cherpokova D, Nurden P, Schulz JN, Thielmann I, Kraft P, et al. Gray platelet syndrome and defective thrombo-inflammation in Nbeal2-deficient mice. J Clin Invest. 2013 Jul 01.
132. Deppermann C, Nurden P, Nurden AT, Nieswandt B, Stegner D. The Nbeal2(-/-) mouse as a model for the gray platelet syndrome. Rare Dis. 2013;1:e26561.
133. Best MG, Sol N, Kooi I, Tannous J, Westerman BA, Rustenburg F, et al. RNA-Seq of Tumor-Educated Platelets Enables Blood-Based Pan-Cancer, Multiclass, and Molecular Pathway Cancer Diagnostics. Cancer Cell. 2015 Nov 9;28(5):666-76.
134. Best MG, Vancura A, Wurdinger T. Platelet RNA as a circulating biomarker trove for cancer diagnostics. J Thromb Haemost. 2017 Jul;15(7):1295-306.
135. Nilsson RJ, Balaj L, Hulleman E, van Rijn S, Pegtel DM, Walraven M, et al. Blood platelets contain tumor-derived RNA biomarkers. Blood. 2011 Sep 29;118(13):3680-3.
136. Sol N, Wurdinger T. Platelet RNA signatures for the detection of cancer. Cancer Metastasis Rev. 2017 Jul 05.
137. Hu CM, Fang RH, Wang KC, Luk BT, Thamphiwatana S, Dehaini D, et al. Nanoparticle biointerfacing by platelet membrane cloaking. Nature. 2015 Oct 1;526(7571):118-21.

138. McManus DD, Beaulieu LM, Mick E, Tanriverdi K, Larson MG, Keaney JF, Jr., et al. Relationship among circulating inflammatory proteins, platelet gene expression, and cardiovascular risk. Arterioscler Thromb Vasc Biol. 2013 Nov;33(11):2666-73.
139. Beaulieu LM, Lin E, Mick E, Koupenova M, Weinberg EO, Kramer CD, et al. Interleukin 1 receptor 1 and interleukin 1beta regulate megakaryocyte maturation, platelet activation, and transcript profile during inflammation in mice and humans. Arterioscler Thromb Vasc Biol. 2014 Mar;34(3):552-64.
140. Blair P, Rex S, Vitseva O, Beaulieu L, Tanriverdi K, Chakrabarti S, et al. Stimulation of Toll-like receptor 2 in human platelets induces a thromboinflammatory response through activation of phosphoinositide 3-kinase. Circ Res. 2009 Feb 13;104(3):346-54.
141. Semple JW, Italiano JE, Jr., Freedman J. Platelets and the immune continuum. Nat Rev Immunol. 2011 Apr;11(4):264-74.
142. Gibson FC, Hong C, Chou HH, Yumoto H, Chen JQ, Lien E, et al. Innate immune recognition of invasive bacteria accelerates atherosclerosis in apolipoprotein E-deficient mice. Circulation. 2004 Jun 8;109(22):2801-6.
143. Hayashi C, Viereck J, Hua N, Phinikaridou A, Madrigal AG, Gibson FC, 3rd, et al. Porphyromonas gingivalis accelerates inflammatory atherosclerosis in the innominate artery of ApoE deficient mice. Atherosclerosis. 2011 Mar;215(1):52-9.
144. Velsko IM, Chukkapalli SS, Rivera MF, Lee JY, Chen H, Zheng D, et al. Active invasion of oral and aortic tissues by Porphyromonas gingivalis in mice causally links periodontitis and atherosclerosis. PLoS One. 2014;9(5):e97811.
145. Haraszthy VI, Zambon JJ, Trevisan M, Zeid M, Genco RJ. Identification of periodontal pathogens in atheromatous plaques. J Periodontol. 2000 Oct;71(10):1554-60.
146. Nakano K, Inaba H, Nomura R, Nemoto H, Takeuchi H, Yoshioka H, et al. Distribution of Porphyromonas gingivalis fimA genotypes in cardiovascular specimens from Japanese patients. Oral Microbiol Immunol. 2008 Apr;23(2):170-2.
147. Yakob M, Soder B, Meurman JH, Jogestrand T, Nowak J, Soder PO. Prevotella nigrescens and Porphyromonas gingivalis are associated with signs of carotid atherosclerosis in subjects with and without periodontitis. J Periodontal Res. 2011 Dec;46(6):749-55.
148. Naiki Y, Sorrentino R, Wong MH, Michelsen KS, Shimada K, Chen S, et al. TLR/MyD88 and liver X receptor alpha signaling pathways reciprocally control Chlamydia pneumoniae-induced acceleration of atherosclerosis. J Immunol. 2008 Nov 15;181(10):7176-85.
149. Player MS, Mainous AG, 3rd, Everett CJ, Diaz VA, Knoll ME, Wright RU. Chlamydia pneumoniae and progression of subclinical atherosclerosis. Eur J Prev Cardiol. 2014 May;21(5):559-65.
150. Sakurai-Komada N, Iso H, Koike KA, Ikeda A, Umesawa M, Ikehara S, et al. Association between Chlamydophila pneumoniae infection and risk of coronary heart disease for Japanese: the JPHC study. Atherosclerosis. 2014 Apr;233(2):338-42.
151. Jha HC, Srivastava P, Divya A, Prasad J, Mittal A. Prevalence of Chlamydophila pneumoniae is higher in aorta and coronary artery than in carotid artery of coronary artery disease patients. APMIS. 2009 Dec;117(12):905-11.
152. Ciervo A, Mancini F, Sale P, Russo A, Cassone A. Real-time polymerase chain reaction and laser capture microdissection: an efficient combination tool for Chlamydophila pneumoniae DNA quantification and localization of infection in atherosclerotic lesions. Int J Immunopathol Pharmacol. 2008 Apr-Jun;21(2):421-8.

153. Go AS, Mozaffarian D, Roger VL, Benjamin EJ, Berry JD, Blaha MJ, et al. Heart disease and stroke statistics--2014 update: a report from the American Heart Association. Circulation. 2014 Jan 21;129(3):e28-e292.
154. Nakashima Y, Plump AS, Raines EW, Breslow JL, Ross R. ApoE-deficient mice develop lesions of all phases of atherosclerosis throughout the arterial tree. Arterioscler Thromb. 1994 Jan;14(1):133-40.
155. Sullivan PM, Mezdour H, Aratani Y, Knouff C, Najib J, Reddick RL, et al. Targeted replacement of the mouse apolipoprotein E gene with the common human APOE3 allele enhances diet-induced hypercholesterolemia and atherosclerosis. J Biol Chem. 1997 Jul 18;272(29):17972-80.
156. Eitzman DT, Westrick RJ, Xu Z, Tyson J, Ginsburg D. Hyperlipidemia promotes thrombosis after injury to atherosclerotic vessels in apolipoprotein E-deficient mice. Arterioscler Thromb Vasc Biol. 2000 Jul;20(7):1831-4.
157. Hayashi C, Gudino CV, Gibson FC, 3rd, Genco CA. Review: Pathogen-induced inflammation at sites distant from oral infection: bacterial persistence and induction of cell-specific innate immune inflammatory pathways. Mol Oral Microbiol. 2010 Oct;25(5):305-16.
158. Kalvegren H, Majeed M, Bengtsson T. Chlamydia pneumoniae binds to platelets and triggers P-selectin expression and aggregation: a causal role in cardiovascular disease? Arterioscler Thromb Vasc Biol. 2003 Sep 1;23(9):1677-83.
159. Kramer CD, Weinberg EO, Gower AC, He X, Mekasha S, Slocum C, et al. Distinct gene signatures in aortic tissue from ApoE-/- mice exposed to pathogens or Western diet. BMC Genomics. 2014;15:1176.
160. Nassar H, Chou H-H, Khlgatian M, Gibson FC, Dyke TEV, Genco CA. Role for Fimbriae and Lysine-Specific Cysteine Proteinase Gingipain K in Expression of Interleukin-8 and Monocyte Chemoattractant Protein in Porphyromonas gingivalis-Infected Endothelial Cells. Infection and Immunity. 2002 January 1, 2002;70(1):268-76.
161. He X, Mekasha S, Mavrogiorgos N, Fitzgerald KA, Lien E, Ingalls RR. Inflammation and fibrosis during Chlamydia pneumoniae infection is regulated by IL-1 and the NLRP3/ASC inflammasome. J Immunol. 2010 May 15;184(10):5743-54.
162. Moustardas P, Kadoglou NP, Katsimpoulas M, Kapelouzou A, Kostomitsopoulos N, Karayannacos PE, et al. The complementary effects of atorvastatin and exercise treatment on the composition and stability of the atherosclerotic plaques in ApoE knockout mice. PLoS One. 2014;9(9):e108240.
163. Irizarry RA, Hobbs B, Collin F, Beazer-Barclay YD, Antonellis KJ, Scherf U, et al. Exploration, normalization, and summaries of high density oligonucleotide array probe level data. Biostatistics. 2003 Apr;4(2):249-64.
164. Gautier L, Cope L, Bolstad BM, Irizarry RA. affy--analysis of Affymetrix GeneChip data at the probe level. Bioinformatics. 2004 Feb 12;20(3):307-15.
165. Dai M, Wang P, Boyd AD, Kostov G, Athey B, Jones EG, et al. Evolving gene/transcript definitions significantly alter the interpretation of GeneChip data. Nucleic Acids Res. 2005;33(20):e175.
166. Brettschneider J, Collin F, Bolstad BM, Speed TP. Quality Assessment for Short Oligonucleotide Microarray Data. Technometrics. [doi: 10.1198/004017008000000334]. 2008 2008/08/01;50(3):241-64.

167. Subramanian A, Tamayo P, Mootha VK, Mukherjee S, Ebert BL, Gillette MA, et al. Gene set enrichment analysis: a knowledge-based approach for interpreting genome-wide expression profiles. Proc Natl Acad Sci U S A. 2005 Oct 25;102(43):15545-50.
168. Database resources of the National Center for Biotechnology Information. Nucleic Acids Res. 2013 Jan;41(Database issue):D8-D20.
169. Subramanian A, Kuehn H, Gould J, Tamayo P, Mesirov JP. GSEA-P: a desktop application for Gene Set Enrichment Analysis. Bioinformatics. 2007 Dec 1;23(23):3251-3.
170. Saeed AI, Sharov V, White J, Li J, Liang W, Bhagabati N, et al. TM4: a free, open-source system for microarray data management and analysis. Biotechniques. 2003 Feb;34(2):374-8.
171. Bertola A, Bonnafous S, Anty R, Patouraux S, Saint-Paul MC, Iannelli A, et al. Hepatic expression patterns of inflammatory and immune response genes associated with obesity and NASH in morbidly obese patients. PLoS One. 2010;5(10):e13577.
172. Scott NJ, Cameron VA, Raudsepp S, Lewis LK, Simpson ER, Richards AM, et al. Generation and characterization of a mouse model of the metabolic syndrome: apolipoprotein E and aromatase double knockout mice. Am J Physiol Endocrinol Metab. 2012 Mar 1;302(5):E576-84.
173. Dhingra R, Gona P, Nam BH, D'Agostino RB, Sr., Wilson PW, Benjamin EJ, et al. C-reactive protein, inflammatory conditions, and cardiovascular disease risk. Am J Med. 2007 Dec;120(12):1054-62.
174. Sarwar N, Butterworth AS, Freitag DF, Gregson J, Willeit P, Gorman DN, et al. Interleukin-6 receptor pathways in coronary heart disease: a collaborative meta-analysis of 82 studies. Lancet. 2012 Mar 31;379(9822):1205-13.
175. Browning LM, Krebs JD, Magee EC, Fruhbeck G, Jebb SA. Circulating markers of inflammation and their link to indices of adiposity. Obes Facts. 2008;1(5):259-65.
176. Cheng C, Tempel D, Den Dekker WK, Haasdijk R, Chrifi I, Bos FL, et al. Ets2 determines the inflammatory state of endothelial cells in advanced atherosclerotic lesions. Circ Res. 2011 Aug 5;109(4):382-95.
177. Nie P, Li D, Hu L, Jin S, Yu Y, Cai Z, et al. Atorvastatin improves plaque stability in ApoE-knockout mice by regulating chemokines and chemokine receptors. PLoS One. 2014;9(5):e97009.
178. Beaulieu LM, Lin E, Morin KM, Tanriverdi K, Freedman JE. Regulatory effects of TLR2 on megakaryocytic cell function. Blood. 2011 Jun 2;117(22):5963-74.
179. Ohki T, Itabashi Y, Kohno T, Yoshizawa A, Nishikubo S, Watanabe S, et al. Detection of periodontal bacteria in thrombi of patients with acute myocardial infarction by polymerase chain reaction. Am Heart J. 2012 Feb;163(2):164-7.
180. Hayashi C, Papadopoulos G, Gudino CV, Weinberg EO, Barth KR, Madrigal AG, et al. Protective role for TLR4 signaling in atherosclerosis progression as revealed by infection with a common oral pathogen. J Immunol. 2012 Oct 1;189(7):3681-8.
181. Li L, Messas E, Batista EL, Jr., Levine RA, Amar S. Porphyromonas gingivalis infection accelerates the progression of atherosclerosis in a heterozygous apolipoprotein E-deficient murine model. Circulation. 2002 Feb 19;105(7):861-7.
182. Moazed TC, Kuo C, Grayston JT, Campbell LA. Murine models of Chlamydia pneumoniae infection and atherosclerosis. J Infect Dis. 1997 Apr;175(4):883-90.

183. Karshovska E, Zhao Z, Blanchet X, Schmitt MM, Bidzhekov K, Soehnlein O, et al. Hyperreactivity of Junctional Adhesion Molecule A-Deficient Platelets Accelerates Atherosclerosis in Hyperlipidemic Mice. Circ Res. 2014 Dec 3.
184. Leslie M. Cell biology. Beyond clotting: the powers of platelets. Science. 2010 Apr 30;328(5978):562-4.
185. Angenieux C, Maitre B, Eckly A, Lanza F, Gachet C, de la Salle H. Time-Dependent Decay of mRNA and Ribosomal RNA during Platelet Aging and Its Correlation with Translation Activity. PLoS One. 2016;11(1):e0148064.
186. Ault KA, Rinder HM, Mitchell J, Carmody MB, Vary CP, Hillman RS. The significance of platelets with increased RNA content (reticulated platelets). A measure of the rate of thrombopoiesis. Am J Clin Pathol. 1992 Dec;98(6):637-46.
187. Harrison P, Robinson MS, Mackie IJ, Machin SJ. Reticulated platelets. Platelets. 1997;8(6):379-83.
188. Hellemans J, Mortier G, De Paepe A, Speleman F, Vandesompele J. qBase relative quantification framework and software for management and automated analysis of real-time quantitative PCR data. Genome Biol. 2007;8(2):R19.
189. Vandesompele J, De Preter K, Pattyn F, Poppe B, Van Roy N, De Paepe A, et al. Accurate normalization of real-time quantitative RT-PCR data by geometric averaging of multiple internal control genes. Genome Biol. 2002 Jun 18;3(7):RESEARCH0034.
190. Lopez-Vilchez I, Diaz-Ricart M, Galan AM, Roque M, Caballo C, Molina P, et al. Internalization of Tissue Factor-Rich Microvesicles by Platelets Occurs Independently of GPIIb-IIIa, and Involves CD36 Receptor, Serotonin Transporter and Cytoskeletal Assembly. J Cell Biochem. 2016 Feb;117(2):448-57.
191. Berg M, Offermanns S, Seifert R, Schultz G. Synthetic lipopeptide Pam3CysSer(Lys)4 is an effective activator of human platelets. Am J Physiol. 1994 Jun;266(6 Pt 1):C1684-91.
192. Rex S, Beaulieu LM, Perlman DH, Vitseva O, Blair PS, McComb ME, et al. Immune versus thrombotic stimulation of platelets differentially regulates signalling pathways, intracellular protein-protein interactions, and alpha-granule release. Thromb Haemost. 2009 Jul;102(1):97-110.
193. Michelson AD, Barnard MR, Hechtman HB, MacGregor H, Connolly RJ, Loscalzo J, et al. In vivo tracking of platelets: circulating degranulated platelets rapidly lose surface P-selectin but continue to circulate and function. Proc Natl Acad Sci U S A. 1996 Oct 15;93(21):11877-82.
194. Hartley PS, Savill J, Brown SB. The death of human platelets during incubation in citrated plasma involves shedding of CD42b and aggregation of dead platelets. Thromb Haemost. 2006 Jan;95(1):100-6.
195. Simak J, Gelderman MP. Cell membrane microparticles in blood and blood products: potentially pathogenic agents and diagnostic markers. Transfus Med Rev. 2006 Jan;20(1):1-26.
196. Mittelbrunn M, Gutierrez-Vazquez C, Villarroya-Beltri C, Gonzalez S, Sanchez-Cabo F, Gonzalez MA, et al. Unidirectional transfer of microRNA-loaded exosomes from T cells to antigen-presenting cells. Nat Commun. 2011;2:282.
197. Kelly PN, White MJ, Goschnick MW, Fairfax KA, Tarlinton DM, Kinkel SA, et al. Individual and overlapping roles of BH3-only proteins Bim and Bad in apoptosis of lymphocytes and platelets and in suppression of thymic lymphoma development. Cell Death Differ. 2010 Oct;17(10):1655-64.

198. Kodama T, Takehara T, Hikita H, Shimizu S, Shigekawa M, Li W, et al. BH3-only activator proteins Bid and Bim are dispensable for Bak/Bax-dependent thrombocyte apoptosis induced by Bcl-xL deficiency: molecular requisites for the mitochondrial pathway to apoptosis in platelets. J Biol Chem. 2011 Apr 22;286(16):13905-13.
199. Koenig MN, Naik E, Rohrbeck L, Herold MJ, Trounson E, Bouillet P, et al. Pro-apoptotic BIM is an essential initiator of physiological endothelial cell death independent of regulation by FOXO3. Cell Death Differ. 2014 Nov;21(11):1687-95.
200. Walsh K, Smith RC, Kim HS. Vascular cell apoptosis in remodeling, restenosis, and plaque rupture. Circ Res. 2000 Aug 4;87(3):184-8.
201. Morrison ME, Palenski TL, Jamali N, Sheibani N, Sorenson CM. Modulation of vascular cell function by bim expression. Int J Cell Biol. 2013;2013:297537.
202. Boyanova D, Nilla S, Birschmann I, Dandekar T, Dittrich M. PlateletWeb: a systems biologic analysis of signaling networks in human platelets. Blood. 2012 Jan 19;119(3):e22-34.
203. Shioiri T, Muroi M, Hatao F, Nishida M, Ogawa T, Mimura Y, et al. Caspase-3 is activated and rapidly released from human umbilical vein endothelial cells in response to lipopolysaccharide. Biochim Biophys Acta. 2009 Oct;1792(10):1011-8.
204. Peng J, Friese P, Heilmann E, George JN, Burstein SA, Dale GL. Aged platelets have an impaired response to thrombin as quantitated by P-selectin expression. Blood. 1994 Jan 1;83(1):161-6.
205. Thompson CB, Jakubowski JA, Quinn PG, Deykin D, Valeri CR. Platelet size and age determine platelet function independently. Blood. 1984 Jun;63(6):1372-5.
206. Hirsh J. Platelet age: its relationship to platelet size, function and metabolism. Br J Haematol. 1972 Sep;23:Suppl:209-14.
207. Qiao J, Liu Y, Li D, Wu Y, Li X, Yao Y, et al. Imbalanced expression of Bcl-xL and Bax in platelets treated with plasma from immune thrombocytopenia. Immunol Res. 2016 Apr;64(2):604-9.
208. Guthikonda S, Alviar CL, Vaduganathan M, Arikan M, Tellez A, DeLao T, et al. Role of reticulated platelets and platelet size heterogeneity on platelet activity after dual antiplatelet therapy with aspirin and clopidogrel in patients with stable coronary artery disease. J Am Coll Cardiol. 2008 Aug 26;52(9):743-9.
209. Guthikonda S, Lev EI, Patel R, DeLao T, Bergeron AL, Dong JF, et al. Reticulated platelets and uninhibited COX-1 and COX-2 decrease the antiplatelet effects of aspirin. J Thromb Haemost. 2007 Mar;5(3):490-6.
210. Kim YG, Suh JW, Yoon CH, Oh IY, Cho YS, Youn TJ, et al. Platelet volume indices are associated with high residual platelet reactivity after antiplatelet therapy in patients undergoing percutaneous coronary intervention. J Atheroscler Thromb. 2014;21(5):445-53.
211. Huczek Z, Filipiak KJ, Kochman J, Michalak M, Roik M, Piatkowski R, et al. Baseline platelet size is increased in patients with acute coronary syndromes developing early stent thrombosis and predicts future residual platelet reactivity. A case-control study. Thromb Res. 2010 May;125(5):406-12.
212. Freedman JE, Gerstein M, Mick E, Rozowsky J, Levy D, Kitchen R, et al. Diverse human extracellular RNAs are widely detected in human plasma. Nat Commun. 2016 Apr 26;7:11106.
213. Ramachandran S, Palanisamy V. Horizontal transfer of RNAs: exosomes as mediators of intercellular communication. Wiley Interdiscip Rev RNA. 2012 Mar-Apr;3(2):286-93.

214. Tetta C, Ghigo E, Silengo L, Deregibus MC, Camussi G. Extracellular vesicles as an emerging mechanism of cell-to-cell communication. Endocrine. 2013 Aug;44(1):11-9.
215. Camussi G, Deregibus MC, Bruno S, Cantaluppi V, Biancone L. Exosomes/microvesicles as a mechanism of cell-to-cell communication. Kidney Int. 2010 Nov;78(9):838-48.
216. Yuan T, Huang X, Woodcock M, Du M, Dittmar R, Wang Y, et al. Plasma extracellular RNA profiles in healthy and cancer patients. Sci Rep. 2016 Jan 20;6:19413.
217. Lugli G, Cohen AM, Bennett DA, Shah RC, Fields CJ, Hernandez AG, et al. Plasma Exosomal miRNAs in Persons with and without Alzheimer Disease: Altered Expression and Prospects for Biomarkers. PLoS One. 2015;10(10):e0139233.
218. Arita T, Ichikawa D, Konishi H, Komatsu S, Shiozaki A, Shoda K, et al. Circulating long non-coding RNAs in plasma of patients with gastric cancer. Anticancer Res. 2013 Aug;33(8):3185-93.
219. Connor Y, Tekleab S, Nandakumar S, Walls C, Tekleab Y, Husain A, et al. Physical nanoscale conduit-mediated communication between tumour cells and the endothelium modulates endothelial phenotype. Nat Commun. 2015 Dec 16;6:8671.
220. Thompson CB, Eaton KA, Princiotta SM, Rushin CA, Valeri CR. Size dependent platelet subpopulations: relationship of platelet volume to ultrastructure, enzymatic activity, and function. Br J Haematol. 1982 Mar;50(3):509-19.
221. Grove EL, Hvas AM, Kristensen SD. Immature platelets in patients with acute coronary syndromes. Thromb Haemost. 2009 Jan;101(1):151-6.
222. Michalik KM, You X, Manavski Y, Doddaballapur A, Zornig M, Braun T, et al. Long noncoding RNA MALAT1 regulates endothelial cell function and vessel growth. Circ Res. 2014 Apr 25;114(9):1389-97.
223. Chakrabarti S, Blair P, Wu C, Freedman JE. Redox state of dipyridamole is a critical determinant for its beneficial antioxidant and antiinflammatory effects. J Cardiovasc Pharmacol. [Research Support, N.I.H., Extramural

Research Support, Non-U.S. Gov't]. 2007 Oct;50(4):449-57.
224. Schneider CA, Rasband WS, Eliceiri KW. NIH Image to ImageJ: 25 years of image analysis. Nat Methods. [Historical Article

Research Support, N.I.H., Extramural]. 2012 Jul;9(7):671-5.
225. Ambros V. The functions of animal microRNAs. Nature. 2004 Sep 16;431(7006):350-5.
226. Zamore PD, Haley B. Ribo-gnome: the big world of small RNAs. Science. 2005 Sep 02;309(5740):1519-24.
227. Bartel DP. MicroRNAs: target recognition and regulatory functions. Cell. 2009 Jan 23;136(2):215-33.
228. Skalsky RL, Cullen BR. Viruses, microRNAs, and host interactions. Annu Rev Microbiol. 2010;64:123-41.
229. Jurak I, Kramer MF, Mellor JC, van Lint AL, Roth FP, Knipe DM, et al. Numerous conserved and divergent microRNAs expressed by herpes simplex viruses 1 and 2. J Virol. 2010 May;84(9):4659-72.
230. Umbach JL, Nagel MA, Cohrs RJ, Gilden DH, Cullen BR. Analysis of human alphaherpesvirus microRNA expression in latently infected human trigeminal ganglia. J Virol. 2009 Oct;83(20):10677-83.

231. Cullen BR. Viruses and microRNAs: RISCy interactions with serious consequences. Genes Dev. 2011 Sep 15;25(18):1881-94.
232. Tang Q, Maul GG. Mouse cytomegalovirus crosses the species barrier with help from a few human cytomegalovirus proteins. J Virol. 2006 Aug;80(15):7510-21.
233. Paschos K, Smith P, Anderton E, Middeldorp JM, White RE, Allday MJ. Epstein-barr virus latency in B cells leads to epigenetic repression and CpG methylation of the tumour suppressor gene Bim. PLoS Pathog. 2009 Jun;5(6):e1000492.
234. Chen L, Lagunoff M. Establishment and maintenance of Kaposi's sarcoma-associated herpesvirus latency in B cells. J Virol. 2005 Nov;79(22):14383-91.
235. Ablashi DV, Chatlynne LG, Whitman JE, Jr., Cesarman E. Spectrum of Kaposi's sarcoma-associated herpesvirus, or human herpesvirus 8, diseases. Clin Microbiol Rev. 2002 Jul;15(3):439-64.
236. Flavell KJ, Murray PG. Hodgkin's disease and the Epstein-Barr virus. Mol Pathol. 2000 Oct;53(5):262-9.
237. Parameswaran P, Sklan E, Wilkins C, Burgon T, Samuel MA, Lu R, et al. Six RNA viruses and forty-one hosts: viral small RNAs and modulation of small RNA repertoires in vertebrate and invertebrate systems. PLoS Pathog. 2010 Feb 12;6(2):e1000764.
238. Makkoch J, Poomipak W, Saengchoowong S, Khongnomnan K, Praianantathavorn K, Jinato T, et al. Human microRNAs profiling in response to influenza A viruses (subtypes pH1N1, H3N2, and H5N1). Exp Biol Med (Maywood). 2016 Feb;241(4):409-20.
239. Song H, Wang Q, Guo Y, Liu S, Song R, Gao X, et al. Microarray analysis of microRNA expression in peripheral blood mononuclear cells of critically ill patients with influenza A (H1N1). BMC Infect Dis. 2013 Jun 03;13:257.
240. Kincaid RP, Burke JM, Sullivan CS. RNA virus microRNA that mimics a B-cell oncomiR. Proc Natl Acad Sci U S A. 2012 Feb 21;109(8):3077-82.
241. Freedman JE, Gerstein M, Mick E, Rozowsky J, Levy D, Kitchen R, et al. Corrigendum: Diverse human extracellular RNAs are widely detected in human plasma. Nat Commun. 2016;7:11902.
242. Koupenova M, Mick E, Mikhalev E, Benjamin EJ, Tanriverdi K, Freedman JE. Sex differences in platelet toll-like receptors and their association with cardiovascular risk factors. Arterioscler Thromb Vasc Biol. 2015 Apr;35(4):1030-7.
243. Dupuis J, Larson MG, Vasan RS, Massaro JM, Wilson PW, Lipinska I, et al. Genome scan of systemic biomarkers of vascular inflammation in the Framingham Heart Study: evidence for susceptibility loci on 1q. Atherosclerosis. 2005 Oct;182(2):307-14.
244. Schnabel R, Larson MG, Dupuis J, Lunetta KL, Lipinska I, Meigs JB, et al. Relations of inflammatory biomarkers and common genetic variants with arterial stiffness and wave reflection. Hypertension. 2008 Jun;51(6):1651-7.
245. Joehanes R, Ying S, Huan T, Johnson AD, Raghavachari N, Wang R, et al. Gene expression signatures of coronary heart disease. Arterioscler Thromb Vasc Biol. 2013 Jun;33(6):1418-26.
246. Almasy L, Blangero J. Multipoint quantitative-trait linkage analysis in general pedigrees. Am J Hum Genet. 1998 May;62(5):1198-211.
247. McManus DD, Rong J, Huan T, Lacey S, Tanriverdi K, Munson PJ, et al. Messenger RNA and MicroRNA transcriptomic signatures of cardiometabolic risk factors. BMC Genomics. 2017 Feb 08;18(1):139.

248. Joehanes R, Zhang X, Huan T, Yao C, Ying SX, Nguyen QT, et al. Integrated genome-wide analysis of expression quantitative trait loci aids interpretation of genomic association studies. Genome Biol. 2017 Jan 25;18(1):16.
249. Qureshi A, Thakur N, Monga I, Thakur A, Kumar M. VIRmiRNA: a comprehensive resource for experimentally validated viral miRNAs and their targets. Database (Oxford). 2014;2014.
250. Parker ZM, Murphy AA, Leib DA. Role of the DNA Sensor STING in Protection from Lethal Infection following Corneal and Intracerebral Challenge with Herpes Simplex Virus 1. J Virol. 2015 Nov;89(21):11080-91.
251. Ostermann E, Tuddenham L, Macquin C, Alsaleh G, Schreiber-Becker J, Tanguy M, et al. Deregulation of type I IFN-dependent genes correlates with increased susceptibility to cytomegalovirus acute infection of dicer mutant mice. PLoS One. 2012;7(8):e43744.
252. Zhang Y, Yang P, Wang XF. Microenvironmental regulation of cancer metastasis by miRNAs. Trends Cell Biol. 2014 Mar;24(3):153-60.
253. Amen MA, Griffiths A. Identification and expression analysis of herpes B virus-encoded small RNAs. J Virol. 2011 Jul;85(14):7296-311.
254. Ziegelbauer JM, Sullivan CS, Ganem D. Tandem array-based expression screens identify host mRNA targets of virus-encoded microRNAs. Nat Genet. 2009 Jan;41(1):130-4.
255. Cloix JF, Crabos M, Grichois ML, Meyer P. An endogenous digitalis-like compound extracted from human urine: biochemical and chemical studies. Can J Physiol Pharmacol. 1987 Aug;65(8):1522-7.
256. Mahjoub N, Dhorne-Pollet S, Fuchs W, Endale Ahanda ML, Lange E, Klupp B, et al. A 2.5-kilobase deletion containing a cluster of nine microRNAs in the latency-associated-transcript locus of the pseudorabies virus affects the host response of porcine trigeminal ganglia during established latency. J Virol. 2015 Jan;89(1):428-42.
257. Ghosh Z, Mallick B, Chakrabarti J. Cellular versus viral microRNAs in host-virus interaction. Nucleic Acids Res. 2009 Mar;37(4):1035-48.
258. Qi M, Qi Y, Ma Y, He R, Ji Y, Sun Z, et al. Over-expression of human cytomegalovirus miR-US25-2-3p downregulates eIF4A1 and inhibits HCMV replication. FEBS Lett. 2013 Jul 11;587(14):2266-71.
259. Qin Z, Jakymiw A, Findlay V, Parsons C. KSHV-Encoded MicroRNAs: Lessons for Viral Cancer Pathogenesis and Emerging Concepts. Int J Cell Biol. 2012;2012:603961.
260. Abend JR, Uldrick T, Ziegelbauer JM. Regulation of tumor necrosis factor-like weak inducer of apoptosis receptor protein (TWEAKR) expression by Kaposi's sarcoma-associated herpesvirus microRNA prevents TWEAK-induced apoptosis and inflammatory cytokine expression. J Virol. 2010 Dec;84(23):12139-51.
261. Qin Z, Freitas E, Sullivan R, Mohan S, Bacelieri R, Branch D, et al. Upregulation of xCT by KSHV-encoded microRNAs facilitates KSHV dissemination and persistence in an environment of oxidative stress. PLoS Pathog. 2010 Jan 29;6(1):e1000742.
262. Umbach JL, Cullen BR. In-depth analysis of Kaposi's sarcoma-associated herpesvirus microRNA expression provides insights into the mammalian microRNA-processing machinery. J Virol. 2010 Jan;84(2):695-703.
263. Hansen A, Henderson S, Lagos D, Nikitenko L, Coulter E, Roberts S, et al. KSHV-encoded miRNAs target MAF to induce endothelial cell reprogramming. Genes Dev. 2010 Jan 15;24(2):195-205.

264. Giza DE, Fuentes-Mattei E, Bullock MD, Tudor S, Goblirsch MJ, Fabbri M, et al. Cellular and viral microRNAs in sepsis: mechanisms of action and clinical applications. Cell Death Differ. 2016 Dec;23(12):1906-18.
265. Tudor S, Giza DE, Lin HY, Fabris L, Yoshiaki K, D'Abundo L, et al. Cellular and Kaposi's sarcoma-associated herpes virus microRNAs in sepsis and surgical trauma. Cell Death Dis. 2014 Dec 04;5:e1559.
266. Ross N, Gandhi MK, Nourse JP. The Epstein-Barr virus microRNA BART11-5p targets the early B-cell transcription factor EBF1. Am J Blood Res. 2013;3(3):210-24.
267. Ferrajoli A, Ivan C, Ciccone M, Shimizu M, Kita Y, Ohtsuka M, et al. Epstein-Barr Virus MicroRNAs are Expressed in Patients with Chronic Lymphocytic Leukemia and Correlate with Overall Survival. EBioMedicine. 2015 Jun;2(6):572-82.
268. Kingham BF, Zelnik V, Kopacek J, Majerciak V, Ney E, Schmidt CJ. The genome of herpesvirus of turkeys: comparative analysis with Marek's disease viruses. J Gen Virol. 2001 May;82(Pt 5):1123-35.
269. Hampl H, Ben-Porat T, Ehrlicher L, Habermehl KO, Kaplan AS. Characterization of the envelope proteins of pseudorabies virus. J Virol. 1984 Nov;52(2):583-90.
270. Tischer BK, Osterrieder N. Herpesviruses--a zoonotic threat? Vet Microbiol. 2010 Jan 27;140(3-4):266-70.
271. Mravak S, Bienzle U, Feldmeier H, Hampl H, Habermehl KO. Pseudorabies in man. Lancet. 1987 Feb 28;1(8531):501-2.
272. Buehring GC, Shen HM, Jensen HM, Jin DL, Hudes M, Block G. Exposure to Bovine Leukemia Virus Is Associated with Breast Cancer: A Case-Control Study. PLoS One. 2015;10(9):e0134304.
273. Buehring GC, Shen HM, Jensen HM, Choi KY, Sun D, Nuovo G. Bovine leukemia virus DNA in human breast tissue. Emerg Infect Dis. 2014 May;20(5):772-82.
274. Diez-Ruiz A, Tilz GP, Zangerle R, Baier-Bitterlich G, Wachter H, Fuchs D. Soluble receptors for tumour necrosis factor in clinical laboratory diagnosis. Eur J Haematol. 1995 Jan;54(1):1-8.
275. Page AV, Liles WC. Biomarkers of endothelial activation/dysfunction in infectious diseases. Virulence. 2013 Aug 15;4(6):507-16.
276. Pirisi M, Vitulli D, Falleti E, Fabris C, Soardo G, Del Forno M, et al. Increased soluble ICAM-1 concentration and impaired delayed-type hypersensitivity skin tests in patients with chronic liver disease. J Clin Pathol. 1997 Jan;50(1):50-3.
277. Goswami S, Sharma-Walia N. Osteoprotegerin rich tumor microenvironment: implications in breast cancer. Oncotarget. 2016 Jul 05;7(27):42777-91.
278. Lipton A, Ali SM, Leitzel K, Chinchilli V, Witters L, Engle L, et al. Serum osteoprotegerin levels in healthy controls and cancer patients. Clin Cancer Res. 2002 Jul;8(7):2306-10.
279. Standal T, Seidel C, Hjertner O, Plesner T, Sanderson RD, Waage A, et al. Osteoprotegerin is bound, internalized, and degraded by multiple myeloma cells. Blood. 2002 Oct 15;100(8):3002-7.
280. Pearse RN, Sordillo EM, Yaccoby S, Wong BR, Liau DF, Colman N, et al. Multiple myeloma disrupts the TRANCE/ osteoprotegerin cytokine axis to trigger bone destruction and promote tumor progression. Proc Natl Acad Sci U S A. 2001 Sep 25;98(20):11581-6.
281. Sharma-Walia N, Paul AG, Bottero V, Sadagopan S, Veettil MV, Kerur N, et al. Kaposi's sarcoma associated herpes virus (KSHV) induced COX-2: a key factor in latency, inflammation, angiogenesis, cell survival and invasion. PLoS Pathog. 2010 Feb 12;6(2):e1000777.

282. Huan T, Rong J, Tanriverdi K, Meng Q, Bhattacharya A, McManus DD, et al. Dissecting the roles of microRNAs in coronary heart disease via integrative genomic analyses. Arterioscler Thromb Vasc Biol. 2015 Apr;35(4):1011-21.